Towards the Design of Carnitine Acyltransferase Inhibitors: Modeling the Conformational Behavior of (*R*)-Carnitine, (*R*)-Acetylcarnitine, Morpholinium rings, and 2-Oxo-1,3,6-dioxazaphosphacinium rings.

Víctor Manuel Rosas-García

Dissertation submitted to the Faculty of
Virginia Polytechnic Institute and State University
in partial fulfillment of the requirements for the degree of

Doctor of Philosophy
in
Chemistry

APPROVED:
Richard D. Gandour
Mark Anderson
David Bevan
Harry Gibson
Thomas Hudliçky
James Tanko

Blacksburg, Virginia

KEYWORDS: carnitine , acylcarnitine , modeling of morpholinium rings , phosphonate , modeling of medium-sized rings , conformational analysis

---

Abstract

Full grid-search semiempirical calculations (AM1 and AM1/COSMO) on zwitterionic acetylcarnitine and carnitine, cationic acetylcholine and choline, and 3-acetoxypropanoate and 3-hydroxypropanoate in the gas phase and solution were performed. The calculated {delta}$H°_{hydr}$ for hydrolyses of acetylcarnitine to carnitine and of acetylcholine to choline show reasonable agreement with the experimental values in unbuffered solution (acetylcarnitine: -4.63 kcal/mol calc. vs. -7.43 kcal/mol exp.; acetylcholine: -3.20 kcal/mol calc. vs. -3.06 kcal/mol exp.) The results suggest that a change in the conformational populations of acetylcarnitine-carnitine upon hydrolysis maintains a nearly constant polarity, which keeps the work of desolvation of the products to a minimum. Acetylcholine-choline and acetoxypropanoate-hydroxypropanoate present a much higher work of desolvation, therefore yielding a lower free enthalpy of hydrolysis. Ab initio calculations at the RHF/6-31G* level for the carnitines and the cholines, and RHF/6-31+G for the propanoates, were done to calibrate the quality of the AM1 results for both the gas phase and in solution. The calculations in the gas phase involved full optimization of the AM1-optimized structures at the RHF/6-31G* level and RHF/6-31+G level, and single points at the MP2//RHF/6-31G* and MP2//RHF/6-31+G level to estimate correlation effects. The ab initio calculations in solution were single points on the AM1-optimized geometries and used the Tomasi solvent model. The ab initio results confirmed the qualitative reliability of the semiempirical results.

The conformational behavior of several 4,4-dimethylmorpholinium rings and 4,4-dimethyl-2-oxo-1,3,6-dioxazaphosphacinium rings was examined by molecular mechanics (AMBER* and AMBER*-GB/SA). The contrast between the behavior of these heterocycles and that of the parent saturated hydrocarbon systems formed a picture of the conformational behavior of these six- and eight-membered heterocycles. Influences of factors such as shortened bond lengths, varied bond angles, presence or absence of lone pairs and substituents, and dipolar alignment are described. Morpholinium rings show increased stabilization of the twist-boat with 1,1,3,3-di*gem* substitution, as compared to the parent cyclohexane systems. In the gas phase, the lowest chair/twist-boat energy gap is found in 2-(hydroxymethyl)-2,4,4-trimethylmorpholinium at 1.14 kcal/mol. The gap in the congruent hydrocarbon system is 5.23 kcal/mol. Differential solvation destabilizes the lowest energy twist-boat found in the gas phase, increasing the energy gap to 2.62 kcal/mol. The lowest chair/twist-boat energy gap in GB/SA water amounts to 1.45 kcal/mol, stabilized by solvation from an initial 2.13 kcal/mol in the gas phase.

In the dioxazaphosphacinium rings, the preferred conformation in the gas phase is the boat-chair (BC) and the populations are conformationally heterogeneous. As substituents approach a 1,1,3,3-di*gem* pattern, the twist-chair (TC) and twist-boat (TB) conformers are stabilized. Solvation favors boat-boat (BB) conformers, with the substituents exerting influence on the conformational preference only to stabilize the TB in two instances ([*cis*-substituted ring] and [disubstituted ring]). Solvation reduces the heterogeneity of the conformational populations.

Modeling of phosphonate moieties required development of molecular mechanics parameters for dimethyl methylphosphonate. Dimethyl methylphosphonate conformations were calculated at the RHF/6-31+G* level. Charges were calculated by the CHelpG scheme. The results were used to generate AMBER* parameters for modeling of alkylphosphonates in the gas phase and in solution. Comparison of the results of our AMBER* parameters against three other common force fields (MM2*, MMX and UFF) showed that AMBER* reproduced better the ab initio results when comparing absolute deviations in bond lengths, bond angles and torsion angles. The modified AMBER* reproduced better than the other three force fields several X-ray geometries of alkylphosphonates.

Part of this work was supported by NIH Grant GM 42016

Table of Contents

Title page	**Towards the Design of Carnitine Acyltransferase Inhibitors: Modeling the Conformational Behavior of (*R*)-Carnitine, (*R*)-Acetylcarnitine, Morpholinium rings, and 2-Oxo-1,3,6-dioxazaphosphacinium rings.**
Dedication	
Acknowledgments	
1	Introduction.
1.1.	Purpose of study.
2	Historical.
2.1.	Introduction.
2.2.	Acyltransferase inhibitors.
2.2.1.	Competitive reversible inhibitors.
2.2.2.	Competitive irreversible inhibitors.
2.2.3.	Noncompetitive reversible inhibitors.
2.2.4.	Noncompetitive irreversible inhibitors.
3	Acetylcarnitine hydrolysis.
3.1.	Review of literature.
3.1.1.	Acylcarnitines in cellular metabolism.
3.1.2.	Thermodynamics of acetylcarnitine hydrolysis.

3.1.2.1. High-energy compounds.
3.1.2.2. Effects of solvation on thermodynamic quantities.
3.1.2.3. Relationship between conformational preference and thermodynamics.
3.2. Results and Discussion.
3.2.1. Conformational analyses in gas phase.
3.2.1.1. Acetylcarnitine vs. carnitine.
3.2.1.2. Acetylcholine vs. choline.
3.2.1.3. Acetoxypropanoate vs. hydroxypropanoate.
3.2.1.4. Carnitines vs. cholines.
3.2.1.5. Carnitines vs. propanoates.
3.2.2. Ab initio results in the gas phase.
3.2.3. Comparison of AM1 vs. ab initio.
3.2.4. Conformational analyses including the effect of solvent.
3.2.4.1. Acetylcarnitine vs. carnitine
3.2.4.2. Acetylcholine vs. choline.
3.2.4.3. Acetoxypropanoate vs. hydroxypropanoate.
3.2.4.4. Carnitines vs. cholines.
3.2.4.5. Carnitines vs. propanoates.
3.2.5. Ab initio results including solvent.
3.2.6. Thermochemical calculations from semiempirical results.
3.2.7. Modeling of tetrahedral intermediate: preliminary results.
4 Effects of heteroatoms on conformational stability.
4.1. General effects of introduction of heteroatoms.
4.2. The anomeric effect.
4.3. The gauche effect.
4.4. Conformational analysis of heterocycles.
4.4.1. Six-membered rings.
4.4.2. Eight-membered rings.
4.5. Conformational analyses of morpholinium rings.
4.5.1. Modeling in the gas phase.
4.5.1.1. Cyclohexanes.
4.5.1.2. Morpholinium rings.
4.5.2. Modeling in GB/SA water.
4.6. Conformational analyses of 2-oxo-1,3,6-dioxazaphosphacinium rings.
4.6.1. Modeling in the gas phase.
4.6.1.1. Cyclooctanes.
4.6.1.2. Dioxazaphosphacinium rings.
4.6.2. Modeling in GB/SA water.
5 Modeling of phosphonates.
5.1. Modeling of phosphorus species.
5.1.1. Ab initio methods.
5.1.2. Semiempirical methods.
5.1.3. Molecular mechanics methods.
5.2. Development of AMBER* parameters for phosphonates.

5.2.1. Calculations on dimethyl methylphosphonate.
5.2.2. Comparison vs. crystal structures.
6 Methods.
6.1. General methods and software.
6.1.1. Molecular mechanics.
6.1.2. Semiempirical calculations.
6.1.3. Ab initio calculations.
6.2. Acetylcarnitine calculations.
6.2.1. Conformational search strategy by molecular mechanics.
6.2.2. Conformational populations.
6.2.3. Semiempirical calculations on carnitines, cholines and propanoates.
6.2.4. Ab initio calculations on carnitines, cholines and propanoates.
6.3. Conformational search in six-membered rings.
6.4. Conformational search and analyses in eight-membered rings.
6.5. AMBER* parametrization of phosphonates.
6.6. Least-squares fit of phosphonate rings to tetrahedral intermediate.
6.7. Hardware.
7 Conclusions.
7.1. Summary
7.2. Future work.
Bibliography
A Naming and numbering scheme for cyclooctane conformers.
A.1. Boat-chair family.
A.2. Chair-chair family.
A.3. Boat-boat family.
B Rules for naming hetero-substituted cyclooctanes.
C Software standards used.
D Chemical files included.
E README: Notes on the creation of a dissertation in ETD-ML.
E.1. ETD-ML source encoding.
E.2. Virtual Reality Modeling Language (VRML).
E.3. Chemical Markup Language (CML).
E.4. Babel, PDB, Chime.
E.5. Reformatting the molecules.
E.6. Footnotes.
E.7. Notes on MOL notation substitution.
E.8. README.TXT: Files in this ETD.
Vita

List of Tables

3.1. Comparison of AM1 vs. 6-31G* calculations on carnitines and cholines in the gas phase.
3.2. Comparison of AM1 vs 6-31+G calculations on propanoates in the gas phase.
3.3. Comparison of AM1 vs. 6-31G* calculations on carnitines and cholines in water.

3.4. Comparison of AM1 vs. 6-31+G calculations on propanoates in water.
3.5. Comparison of {delta}H_{hydr} (kcal/mol) calculated at {epsilon}=78.3 vs. calorimetric values.
3.6. Expectation values for Dipoles ({mu}) and Enthalpies of Solvation ({delta}$H°_{solv}$)
3.7. RMS deviation after least-squares fitting of global minimum of rings to global minimum of intermediate in GB/SA water.
3.8. RMS deviation after least-squares fitting of second most populated conformer of ring to global minimum of intermediate in GB/SA water.
4.1. Comparison of relative energies in the gas phase (kcal/mol) of cyclohexane conformations.
4.2. Comparison of morpholinium vs. dimethylcyclohexane in the gas phase.
4.3. Comparison of energies of trimethylmorpholinium vs. trimethylcyclohexane in the gas phase (kcal/mol).
4.4. Comparison of energies of tetramethylcyclohexane vs. tetramethylmorpholinium in the gas phase (kcal/mol).
4.5. Comparison of energies of ethyltrimethylcyclohexane vs. (hydroxymethyl)trimethylmorpholinium in the gas phase (kcal/mol).
4.6. Conformational and solvation energies (kcal/mol) of dimethylmorpholinium in the gas phase and GB/SA water.
4.7. Conformational and solvation energies (kcal/mol) of trimethylmorpholinium in the gas phase and GB/SA water.
4.8. Conformational and solvation energies (kcal/mol) of tetramethylmorpholinium in the gas phase and GB/SA water.
4.9. Conformational and solvation energies (kcal/mol) of (hydroxymethyl)trimethylmorpholinium in the gas phase and GB/SA water.
4.10. Conformers of cyclooctane within 3.0 kcal/mol of global minima in the gas phase.
4.11. Conformers of tetramethylcyclooctane within 3.0 kcal/mol of global minima in the gas phase.
4.12. Conformers of pentamethylcyclooctane within 3.0 kcal/mol of global minima in the gas phase.
4.13. Conformers of hexamethylcyclooctane within 3.0 kcal/mol of global minima in the gas phase.
4.14. Conformers of dioxazaphosphacinium within 3.0 kcal/mol of global minima in the gas phase.
4.15. Conformers of *cis*-methyl dioxazaphosphacinium within 3.0 kcal/mol of global minimum in the gas phase.
4.16. Conformers of *trans*-methyl dioxazaphosphacinium within 3.0 kcal/mol of global minimum in the gas phase.
4.17. Conformers of dimethyl dioxazaphosphacinium within 3.0 kcal/mol of global minimum in the gas phase.
4.18. Conformers of dioxazaphosphacinium within 3.0 kcal/mol of global minimum in water.
4.19. Conformers of *cis*-methyl dioxazaphosphacinium within 3.0 kcal/mol of global minimum in water.
4.20. Conformers of *trans*-methyl dioxazaphosphacinium within 3.0 kcal/mol of global minimum in water.
4.21. Conformers of dimethyl dioxazaphosphacinium within 3.0 kcal/mol of global minimum in water.
5.1. Predicted bond lengths and angles of dimethyl methylphosphonate.
5.2. RMS fit of molecular mechanics to ab initio geometries.
5.3. Relative conformational energies (kcal/mol)
5.4. Comparison of Molecular Mechanics results vs. X-ray.
5.5. RMS values of MM vs. X-ray including all heavy atoms.
5.6. RMS values of MM vs. X-ray including phosphonate heavy atoms only.

List of Figures

1.1. 4,4-dimethylmorpholinium ring.
1.2. 2,4,4,-trimethyl-2-oxo-1,3,6-dioxazaphosphacinium ring.
2.1. Tetrahedral intermediate for Carnitine-CoA acyl transfer.
2.2. Aminocarnitine.

2.3. Hemiacylcarnitinium moiety.
2.4. 3-hydroxy-5,5-dimethylhexanoic acid.
2.5. 3-amino-5,5-dimethylhexanoic acid.
2.6. 4-hexadecyl-2,4,4-trimethyl-2-oxo-1,3,6-dioxazaphosphacinium bromide.
2.7. 6-(Carboxylatomethyl)-2-(hydroxymethyl)-2,4,4-trimethylmorpholinium.
2.8. Anderson's phosphonate.
2.9. Anderson's phosphate.
3.1. Comparison of free energies of hydrolysis between acetylcarnitine and acetylcholine.
3.2. ``Folded'' conformer of carnitine.
3.3. ``Extended'' conformer of carnitine.
3.4. Hydrolyses of extended and folded conformers.
3.5. Labels for torsion angles used in acetylcarnitine.
3.6. Changes in population and dipole moments upon hydrolysis.
3.7. Differences in the energies of solvation for acetylcarnitine, acetylcholine and 3-acetoxypropanoate.
3.8. Global minimum for (*R,S*) tetrahedral intermediate in GB/SA water.
3.9. 3D Model of the *R,S* tetrahedral intermediate in GB/SA water.
3.10. Global minimum for (*R,R*) tetrahedral intermediate in GB/SA water.
3.11. 3D Model of the *R,R* tetrahedral intermediate in GB/SA water.
3.12. Atom pairs used in the least squares fit between the phosphonate rings and the tetrahedral intermediate.
4.1. Orbital and hyperconjugation description of the anomeric effect.
4.2. **Crown** (D_{4d})
4.3. Chair-chair, **CC** (C_{2v})
4.4. Twist-chair-chair, **TCC** (D_2)
4.5. Twist-chair, **TC** (C_{2v})
4.6. Chair, **C** (C_{2h})
4.7. Boat-chair, **BC** (C_s)
4.8. Twist-boat-chair, **TBC** (C_2)
4.9. Boat-boat, **BB** (D_{2d})
4.10. Twist-boat, **TB** (S_4)
4.11. Boat, **B** (D_{2d})
4.12. Structure of explosive HMX.
4.13. 2-(Hydroxymethyl)-2,4,4-trimethylmorpholinium studied by Savle *et al.*
4.14. Labeling of substituent positions in cyclohexane.
5.1. Fit of AMBER* phosphonate parameters for P-C bond stretch to 6-31+G* curve.
5.2. Fit of AMBER* phosphonate parameters for P-O bond stretch to 6-31+G* curve.
5.3. Fit of AMBER* phosphonate parameters for O-P-O bond angle to 6-31+G* curve.
5.4. Fit of AMBER* phosphonate parameters for C-P=O bond angle to 6-31+G* curve.
5.5. Fit of AMBER* phosphonate parameters for H-C-P=O torsion angle to 6-31+G* curve.
5.6. Fit of AMBER* phosphonate parameters for C-O-P-O torsion angle to 6-31+G* curve.
5.7. Conformers of dimethyl methylphosphonate.
5.8. Comparison of molecular mechanics C-O-P=O torsion profiles vs. ab initio.
5.9. First crystal structure used for comparison (ZAYSIB).

5.10. Additional crystal structures used in the comparison.
A.1. ``Left-oriented" and ``right-oriented" BCs
A.2. Labels for the orientations of substituents in BC
A.3. ``Left-oriented" and ``right-oriented" TBCs
A.4. Labels for the orientations of substituents in TBC
A.5. CC numbering and labeling scheme.
A.6. Crown.
A.7. TCC numbering and labeling scheme.
A.8. TC numbering and labeling scheme.
A.9. C numbering and labeling scheme.
A.10. B numbering and labeling scheme.
A.11. BB numbering and labeling scheme.
A.12. TB numbering and labeling scheme.
B.1. Example conformer.

[Title] [Ded] [Ack] [1] [2] [3] [4] [5] [6] [7] [Bib] [A] [B] [C] [D] [E] [Vita]

Chapter 4. Effects of heteroatoms on conformational stability.

Here follows a general exposition of the changes in conformational behavior induced by the introduction of heteroatoms, according to the following scheme:

- General effects of introduction of heteroatoms.
- The anomeric effect.
- The gauche effect.

4.1. General effects of introduction of heteroatoms.

The first difference between hydrocarbon rings and their hetero-substituted analogs resides in the different bond lengths and bond angles involving the heteroatoms. Shorter distances, such as those of C-N and C-O bonds, increase the van der Waals repulsion among substituents in the ring. Longer distances between substituents, as those provided by C-P and C-S bonds, relieve van der Waals repulsions. Heteroatoms differ from carbon in the number of substituents they can bond to. This difference affects directly the energies of eclipsing interactions within the ring.

Differences in electronegativity introduce dipolar bonds, and the orientation of the resulting dipoles can change the relative stabilities within a series of conformers (*e.g.*, in side-by-side dipoles, antiparallel orientation reduces Coulombic repulsions, yielding a lower energy than a parallel orientation). In general, dipoles interact to yield the smallest possible total dipole. The lowest energy conformers tend to have the smallest dipole moments. [Note.] Polar solvents better stabilize conformers of greater polarity as compared to the least polar ones. Given that the solvation of a molecule depends strongly on its polarity, solvation affects the energy gap between conformations possessing opposing dipoles and the ones containing parallel dipoles, (see p.747 on Eliel, Wilen and Mander's book [Eliel, 1994]). As different atoms have orbitals with different energies, accounting for stereoelectronic factors, such as orbital overlap, can help understand the conformations of heterocycles. The anomeric effect provides the best known case of such an interaction.

Consideration of the lone pairs present on certain heteroatoms requires an interaction model. The debate centers on the best description of the lone pairs density: as unhybridized $n_{\{sigma\}}$ and n_p orbitals, or as sp^3 hybrids. Although equivalent in many respects, the models differ in the directionality of the lone pairs. sp^3-Hybridized orbitals are directionally equivalent, while the unhybridized orbitals are not. Each model requires different spatial dispositions for optimal overlap. Laing has compiled theoretical and experimental evidence [Laing, 1987] supporting the nonequivalence of the lone pairs. Kirby [Kirby, 1983] has discussed the differences that arise between the two models, concluding that both are equivalent energetically speaking, so the choice of a particular description is done better on a *per case* basis.

4.2. The anomeric effect.

This review follows the main lines of a similar one in the book by Juaristi and Cuevas. [Juaristi, 1995] Edward [Edward, 1955] [Chu, 1959] reported on the axial preference of an alkoxy substituent in pyranoses, instead of the equatorial orientation one would expect from comparison with hydrocarbon systems. This behavior received the designation of **anomeric effect**. Later experimental results pointed to the existence of a similar phenomenon in compounds other than sugars, calling this effect the **generalized anomeric effect**. The generalized anomeric effect appears whenever a molecule possesses a fragment with the formula: R-Z-X-Y, where R is an alkyl group or hydrogen, X is an atom of intermediate electronegativity (C, Si, P, S among others), Y is an atom of stronger electronegativity than X (usually O, N or halogen (Hal)) and Z is an atom with lone pairs. By the previous criteria, we can suggest several common molecular fragments expected to show an anomeric effect: **R-O-C-O** , R-O-C-N, R-O-C-S, R-O-C-Hal, R-N-C-O, R-N-C-Hal, **R-S-C-O** , **R-O-P-O** , R-O-P-N and R-O-P-Hal among others.

In addition to the marked axial preference of oxygenated substituents on pyranose rings, some researchers report [Lemieux, 1969] that polar solvents preferentially stabilize the more polar conformer (equatorial). The anomeric effect results in altered bond lengths and bond angles, specifically, the axial bond is shorter than usual, while the equatorial bond is longer. An electronic model, proposed early by Edward [Edward, 1955] suggests that the repulsive interaction between the ring dipole and nearly parallel polar bonds in the equatorial conformer constitute the dominating forces in the preference for the axial position. Juaristi [Juaristi, 1955] has criticized Edward's hypothesis on the grounds that it cannot explain the variations on bond lengths and angles. Juaristi favors a stereoelectronic interpretation suggested by Altona. [Altona, 1963] [Romers, 1969] The stereoelectronic hypothesis attributes the anomeric effect to mixing of the nonbonding electrons on oxygen with the antiperiplanar antibonding {sigma}* orbital in C-Y, involving a stereoelectronic interaction of type n_Z ----> {sigma}$^{*}_{C\text{-}Y}$. Hyperconjugation (no-bond/double-bond resonance) can help us visualize the effect of the electron transfer involved in this interaction. Kirby [Kirby, 1983] expressed this as ``there is a stereoelectronic preference for conformations in which the best donor lone pair is antiperiplanar to the best acceptor bond."

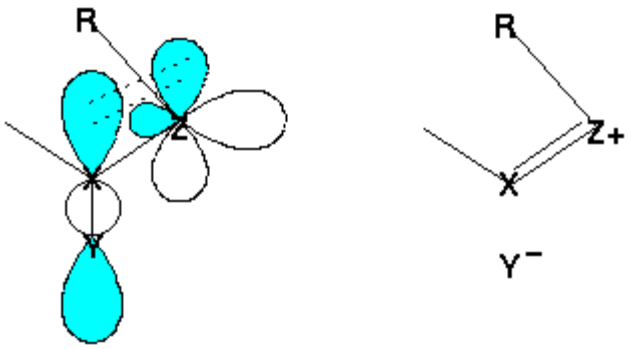

Figure 4.1. Orbital and hyperconjugation description of the anomeric effect.[fig.anomeric.gif, 1.774KB]

4.3. The gauche effect.

Polar factors can markedly bias a conformation, such as in the case of the well-known gauche effect. [Sundaralingam, 1968] The **gauche effect** is the preference, usually 1-2 kcal/mol, that 1,2-disubstituted ethanes show for the *gauche* conformation, as opposed to the *anti* conformation preferred by butane. Wolfe [Wolfe, 1972] has described it as:

> ``(. . .)when electron pairs or polar bonds are placed on adjacent pyramidal atoms, *syn*- or *anti*-periplanar orientations are disfavoured energetically with respect to that structure which contains the maximum number of *gauche* interactions."

Based on steric grounds, the *anti* conformation has greater stability. The gauche effect shows up in molecules containing the unit: X-C-C-Y, where X and Y are groups more electronegative than carbon (N, O or halogen). Wolfe rationalized the gauche effect by postulating that nuclear-electron attraction between X and Y dominated over nuclear-nuclear and electron-electron repulsions. Baddeley preferred to extend Altona's explanation of the anomeric effect, arguing that the gauche effect arises from {sigma} ---> {sigma}* orbital interactions that stabilize the *gauche* conformation. This interaction implies a no-bond/double-bond resonance model. Dionne and St-Jacques [Dionne, 1987] used Baddeley's argument to justify the preference for the twist-boat conformation in 3-substituted-1,5-benzodioxepines in CHF_2Cl. Based on calculated bond paths, Wiberg and Murcko [Wiberg, 1990] have suggested that the gauche effect originates in "bent" bonds, due to the greater electronegativity of the 1,2 substituents. This model implies a destabilization of the *anti* conformer, as opposed to the stabilization of the *gauche* conformer suggested by hyperconjugation.

4.4. Conformational analysis of heterocycles.

4.4.1. Six-membered rings.

The conformational analysis of compounds containing six-membered rings has been a favorite topic for organic research; thus, we have not attempted an exhaustive coverage of the literature. This section only summarizes the background needed for an understanding of the conformational behavior described in this dissertation. The interested reader can find the fundamentals in the excellent textbook by Eliel, Wilen and Mander [Eliel, 1994] while some finer points regarding conformational interconversion between chair and non-chair conformers are covered by Kellie and Riddell, [Kellie 1974] and Anderson. [Anderson, 1974]

We can assign steric energies to any substituent attached to a six-membered ring. These steric energies are usually additive, a scheme that aids in the estimation of conformational stabilities. However, geminal substitution tends to break simple additivity: one group interferes with the free rotation of its geminal neighbor so the optimal conformation of a substituent may change when adding a geminal neighbor.

Weiser *et al.* [Weiser, 1996] employed MM3(92) to study the conformational behavior of polyalkylated cyclohexanes, focusing mostly on how substituents affect the chair/twist-boat energy gap. They determined that

> (. . .) two methyls and two isopropyl groups are sufficient for rendering the twist-boat form the minimum energy conformation (. . .)

and determined *cis,trans,trans*-1,2-diisopropyl-3,4-dimethylcyclohexane; *cis,syn,cis*-1,2-diisopropyl-4,5-dimethylcyclohexane and *cis,syn,cis*-1,4-diisopropyl-2,5-dimethylcyclohexane as the less crowded cyclohexanes that prefer a twist-boat (0.8 kcal/mol lower in energy than the chair).

For geminally substituted cyclohexanes, the magnitudes of the energy gaps calculated by MM3 were: cyclohexane, 6.2 kcal/mol; [Aped, 1992] 1,1-dimethylcyclohexane, 5.7 kcal/mol; 1,1,3,3-tetramethylcyclohexane, 5.0 kcal/mol.

Mursakulov *et al.* [Mursakulov, 1984] used MM2 to study 2-substituted-1,1-dimethylcyclohexanes. They found that *gem* substitution flattens the ring. They also found a ``negligibly small'' amount of twist-boat in 1,1,2-trimethylcyclohexane (4.6 kcal/mol higher in energy than the chair). All these calculations simulated gas phase. Dalling's [Dalling, 1967] NMR results in solution, indicate an appreciable contribution of the twist-boat.

Kolossváry and Guida [Kolossváry, 1993] did a comprehensive conformational search on cyclohexane using MM2*. Some of their results are gathered in the [table below].

Table 4.1. Comparison of relative energies in the gas phase (kcal/mol) of cyclohexane conformations.

Conformation	MM3(92)	MM2*
Chair	0.00	0.00
Twist-boat	6.2	5.35
Boat	n.d. [*]	6.45
Half-chair	n.d. [*]	10.51

Sieburth [Sieburth, 1994] analyzed crystal structures and molecular mechanics evidence on cyclohexene-like cyclohexanes and observed a correlation between the internal bond angles and the preference for a boat over a half-chair. He concluded that partially flattened cyclohexanes prefer a boat conformation when the average value of the internal bond angles approaches 114°. As the same average approaches 117.5°, the half-chair becomes preferred.

4.4.2. Eight-membered rings.

[Note.]

Molecular mechanics calculations in the gas phase show that the conformational hypersurface of cyclooctane has at least ten possible stationary points. [Hendrickson, 1964] [Hendrickson, 1967] [Kolossváry, 1993] We can split these conformers into three families: chair-chair, boat-boat and boat-chair. We depict the conformers of cyclooctane by the usual perspective drawings and by their Weiler plots [Ounsworth, 1987] as Weiler plots are specially clear bidimensional representations of ring conformation. **Weiler plots** depict the internal torsion angles of a ring in the form of a radar plot. We took all the values of the torsions from Hendrickson's paper to use in the ``standard'' Weiler plots. [Hendrickson, 1967]

Chair-chair.

- 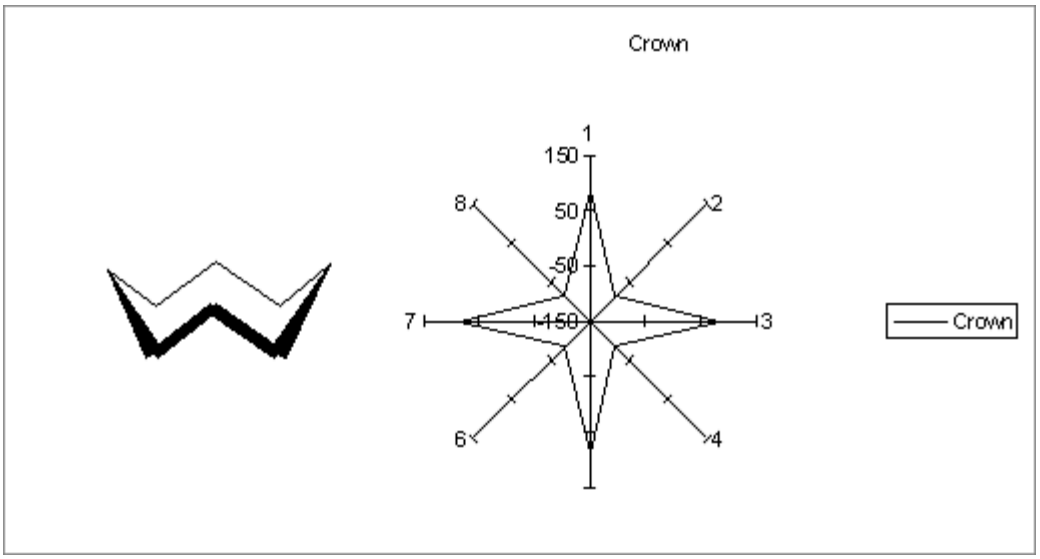

Figure 4.2. Crown (D_{4d}) [fig.crown.gif, 3.852KB]

- 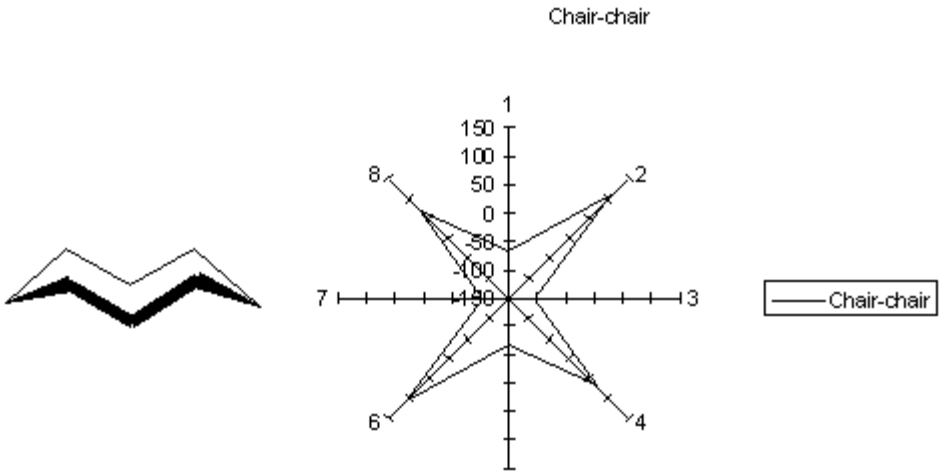

Figure 4.3. Chair-chair, **CC** (C_{2v})[fig.cc.gif, 2.539KB]

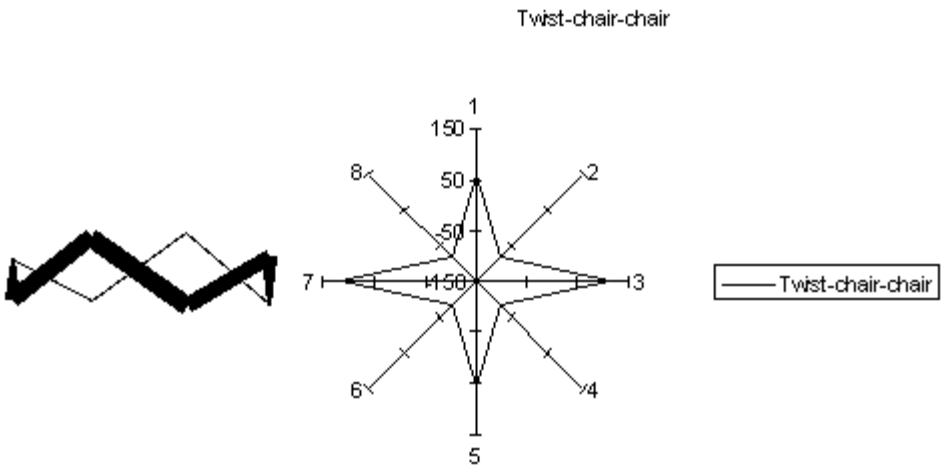

Figure 4.4. Twist-chair-chair, **TCC** (D_2) [fig.tcc.gif, 2.446KB]

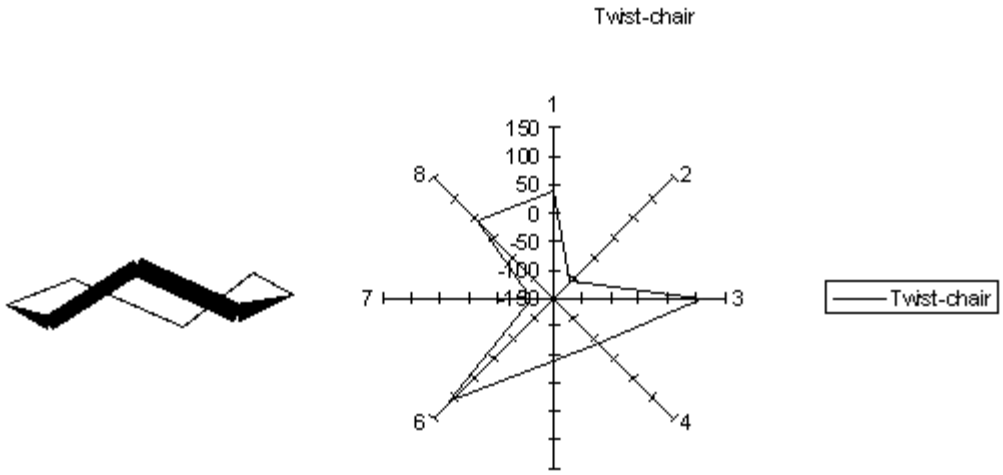

Figure 4.5. Twist-chair, **TC** (C_{2v}) [fig.tc.gif, 2.500KB]

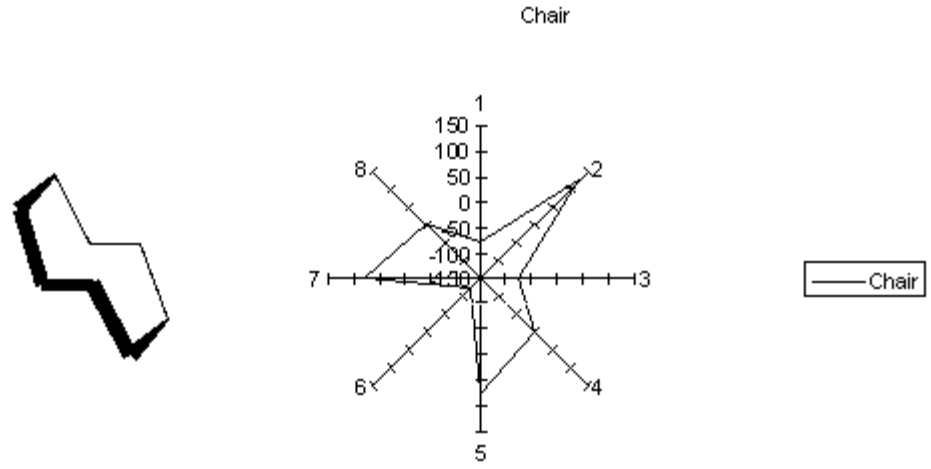

Figure 4.6. Chair, **C** (C_{2h}) [fig.c.gif, 2.416KB]

Boat-chair.

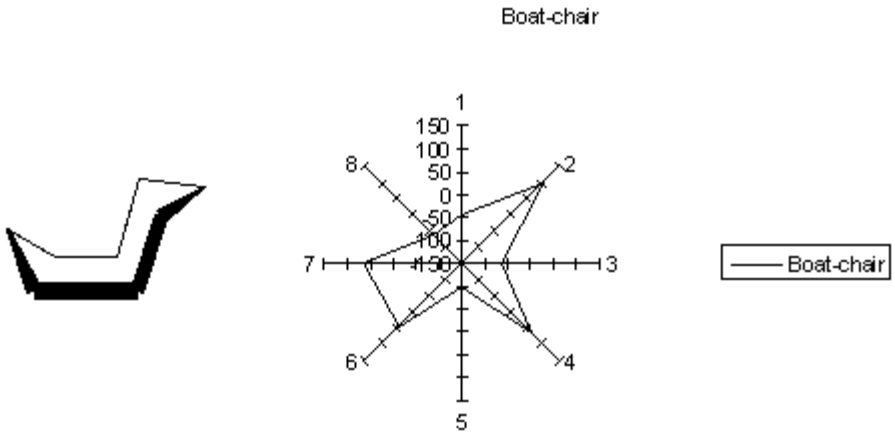

- **Figure 4.7.** Boat-chair, **BC** (C_s) [fig.bc.gif, 2.304KB]

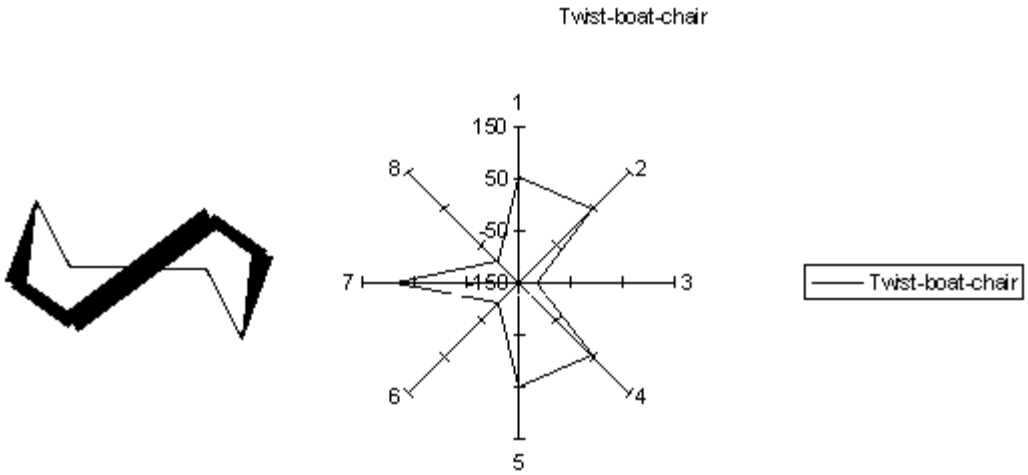

- 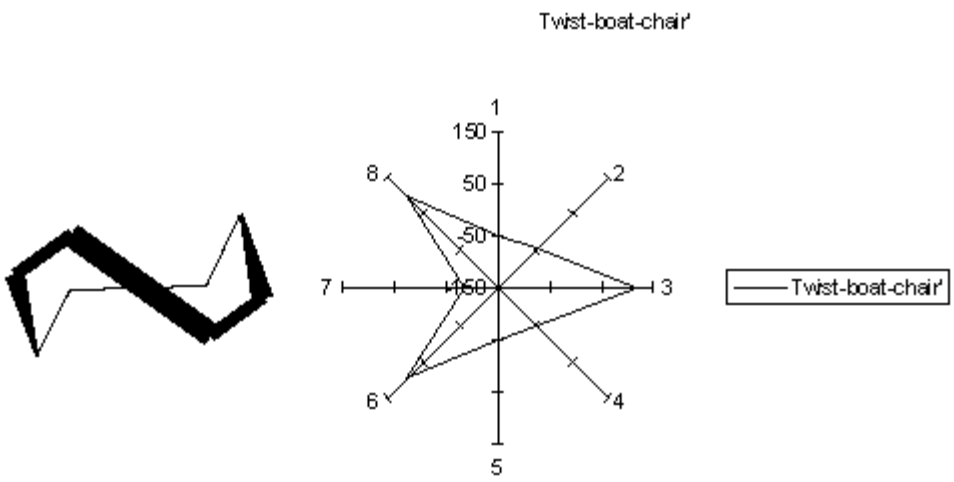

Figure 4.8. Twist-boat-chair, **TBC** (C_2) [fig.tbc1.gif, 2.639KB][fig.tbc-1.gif, 2.601KB]

Boat-boat.

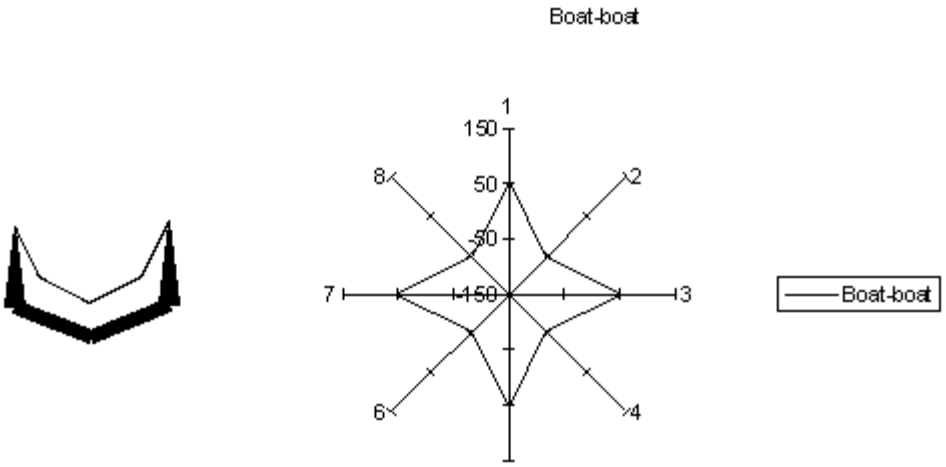

- **Figure 4.9.** Boat-boat, **BB** (D_{2d}) [fig.bb.gif, 2.486KB]

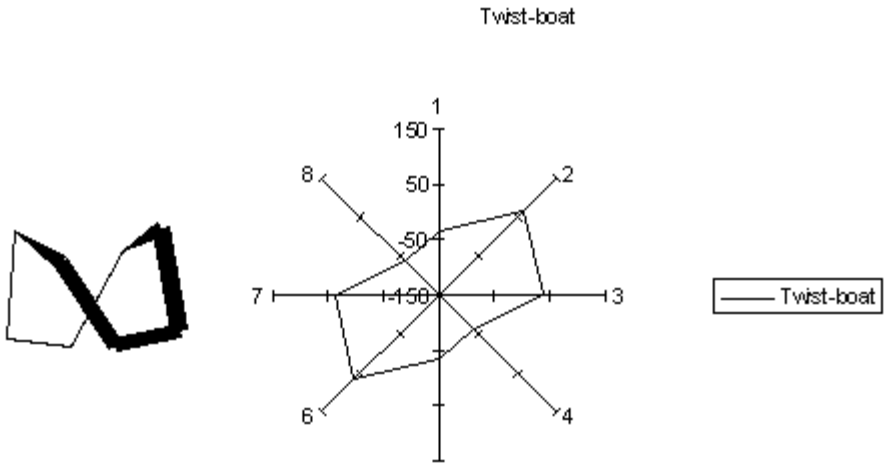

- **Figure 4.10.** Twist-boat, **TB** (S_4) [fig.tb.gif, 2.426KB]

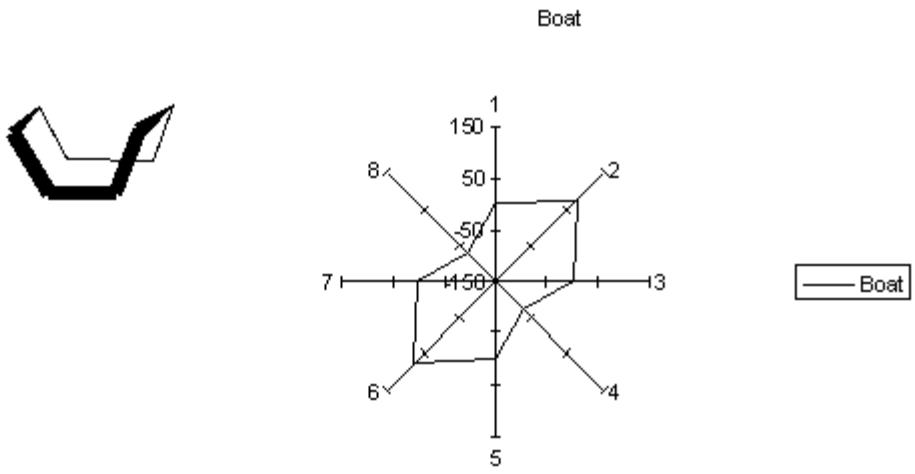

Figure 4.11. Boat, **B** (D_{2d}) [fig.b.gif]

Most calculations indicate BC as the global minimum in cyclooctane. [Bixon, 1967] [Hendrickson, 1967] [Allinger, 1968] [Kolossváry, 1993] This agrees with X-ray structural determinations of substituted cyclooctane rings, where the BC conformation predominates. Wiberg constitutes the exception, [Wiberg, 1965] finding the BC 0.25 kcal/mol higher in energy than the TCC. After reviewing dynamic NMR, X-ray and computational results for cyclooctanes, Anet [Anet, 1974] concluded that

> (. . .) most 'simple' cyclooctanes, including ketones and heterocyclic analogues, exist predominantly in BC conformations.

Reports differ, though, in the energetic ranking of other conformers. The latest results by Kolossváry and Guida, [Kolossváry, 1993] who employed the MM2* [Allinger, 1997] force field, indicated the TCC approximately 1.0 kcal/mol above the BC. Other researchers have reported the TCC form as 1.7 [Hendrickson, 1967], 1.89 [Bixon, 1967], -0.25 [Wiberg, 1965] and 2.20 [Anet, 1971] kcal/mol higher in energy than the BC.

The crown is another conformation thought to be significantly populated in cyclooctane. Again, we find differences in the reported energies relative to the BC: 2.8 [Hendrickson, 1967], 3.62 [Bixon, 1967], 0.26 [Wiberg, 1965] and 2.09 [Anet, 1971] kcal/mol higher in energy than the BC. Kolossváry did not report finding the crown conformer.

Anet and Yavari [Anet, 1972] studied oxocane (fig.oxo.gif, 0.414KB), 1,3-dioxocane (fig.dioxo.gif, 0.411KB), 1,3,6-trioxocane (fig.trioxo.gif, 0.420KB), 1,3,5,7-tetraoxocane (fig.tetraoxo.gif, 0.432KB), by ^{1}H NMR. 1,3-dioxocane showed a single BC conformation, while the two other compounds showed a mixture of two conformations. The authors could not identify positively the conformations, but they argued for a TCC or a crown, in equilibrium with a distorted BC. They reasoned that transannular repulsions between the oxygen atoms would destabilize the BC conformers.

Dale *et al.* [Dale, 1972] studied by ^{1}H NMR the conformational behavior in $CDCl_3$ and $CHFCl_2$ of 1,3,5,7-tetraoxocane, 2,2- or 6,6-disubstituted-1,3,6-trioxocanes and 2,2,6,6-tetrasubstituted-1,3-dioxocanes, including 2,2-dimethyl-1,3-dioxocane (fig.22dioxo.gif, 0.516KB), 6,6-dimethyl-1,3-dioxocane (fig.66dioxo.gif, 0.530KB) and 2,2,6,6-tetramethyl-1,3-dioxocane (fig.2266dioxo.gif, 0.573KB). Their findings led them to conclude that incorporation of a 1,3-dioxa moiety does not suffice to favor the BB over the BC, but geminal substitution at position 6 is also necessary. Geminal substitution on the 2 position had little effect on determining the preferred conformer.

Armarego reviewed extensively the stereochemistry of heterocyclic compounds. [Armarego, 1977] He showed that

oxocanes, in general, prefer a BC conformation, sometimes with substantial amount of the crown. Special substitution patterns, such as in 2,4,6,8-tetrakis(trischloromethyl)-1,3,5,7-tetraoxocane can bias the global minimum to the crown form. Thiocanes also prefer the BC, but the crown form is destabilized, as compared to oxocanes.

Riddell discussed briefly the conformational behavior of eight-membered rings, both saturated and heterocyclic. [Riddell, 1980] Based on X-ray data, he concluded that, in general, heterocyclic eight-membered rings adopt either a crown or a BC conformation. Both conformations are generally regarded as the most populated conformations in cyclooctane.

Moore and Anet reviewed the dynamics of hydrocarbon and heteroatom-substituted eight-membered rings. [Moore, 1984] The BC conformer predominated in oxocane, according to NMR data, although the position of the oxygen was not well-defined, opening the possibility for several BC conformations coexisting in solution. The crown conformer constituted a minor part of the population.

Quin thoroughly reviewed conformational analyses of medium-sized heterocycles. [Quin, 1988] 1,3,6-Dioxaza- and 1,3,6-dioxaphospha-2-oxide phosphocanes preferred to crystallize as crowns. In 2-oxo-1,3,6-trioxaphosphocane a CC conformation predominated at room temperature, as determined by ^{31}P NMR. In 1,3-dioxa-6-thia-2-phosphocane the most abundant conformer was the crown.

In their review of nitrogen heterocycles, Alder and White conclude that azacanes with one nitrogen atom prefer the BC. [Alder, 1988] Nevertheless, additional heteroatoms give rise to a preference for other conformations, such as in the case of the explosive HMX. HMX prefers a CC global minimum.

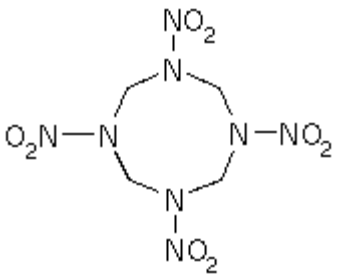

Figure 4.12. Structure of explosive HMX.[fig.hmx.gif, 0.823KB]

Kolossváry and Guida [Kolossváry, 1993] did a comprehensive conformational search on cyclooctane. They reported the energetic ranking as follows: BC, 0.00; TCC, 0.96; CC, 1.14; TBC (minimum), 1.67; TBC (saddle), 2.80; TB, 3.13; BB, 3.56; C, 7.50 kcal/mol.

In summary, eight-membered rings prefer a BC conformer as global minimum, but heteroatom substitution can shift the preference towards a member of the chair-chair family or to a BB conformer.

4.5. Conformational analyses of morpholinium rings.

Previous modeling results from our group [Savle, 1997] on the following compound

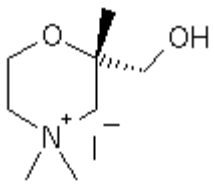

Figure 4.13. 2-(Hydroxymethyl)-2,4,4-trimethylmorpholinium studied by Savle *et al.*[fig.savle97.gif, 0.583KB]

pointed to a predominant chair conformation, the same as in solid state. The calculations also showed that twist-boat conformations accounted for approximately 14% of the total population. To support this finding and to gain a better understanding of the conformational behavior of these rings, we analyzed by computational methods the conformational behavior of:

1. 1,1-dimethylcyclohexane in the gas phase
2. (*R*)-1,1,3-trimethylcyclohexane in the gas phase
3. 1,1,3,3-tetramethylcyclohexane in the gas phase
4. (*R*)-1-ethyl-1,3,3-trimethylcyclohexane in the gas phase

as a reference framework to understand:

1. 4,4-dimethylmorpholinium in the gas phase and in solution
2. (*S*)-2,4,4-trimethylmorpholinium in the gas phase and in solution
3. 2,2,4,4-tetramethylmorpholinium in the gas phase and in solution
4. (*R*)-2-hydroxymethyl-2,4,4-trimethylmorpholinium in the gas phase and in solution

respectively.

4.5.1. Modeling in the gas phase.

We tried to get a complete picture of the energy hypersurface by means of MonteCarlo conformational searches. We chose MonteCarlo instead of Grid Search because the number of torsion angles involved made the Grid Search less efficient. For more details about the procedures, see the Methods section. Conformational energies always refer to the global minimum as 0.00 kcal/mol, unless specified otherwise.

The following figure summarizes the nomenclature we use for cyclohexane conformers:

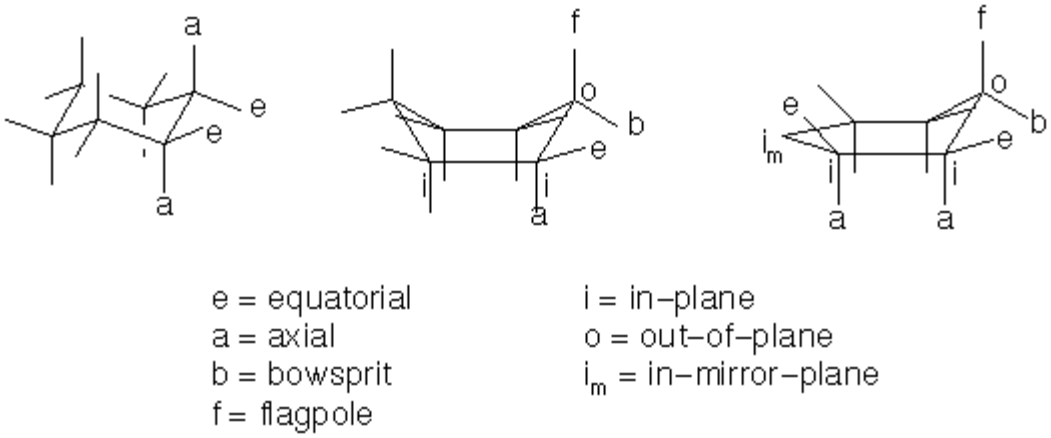

Figure 4.14. Labeling of substituent positions in cyclohexane.[fig.hexConfs.gif, 3.085KB]

4.5.1.1. Cyclohexanes.

1,1-Dimethylcyclohexane yielded five minima: a chair (global minimum) and four twist-boats (pairs at 5.09 and 6.12 kcal/mol). Introducing *gem* substitutents in a chair destabilizes it by worsening 1,3-diaxial interactions, both because of the greater volume of the methyl group and because of **Allinger buttressing**, where an equatorial substituent pushes its axial neighbor into closer proximity with the other 1,3 axial substituents. As the chair constitutes our zero-energy

reference, we can only *deduce* the changes in stability of the chair after analyzing the behavior of other higher-energy conformers.

We find a boat at 6.51 kcal/mol. We observe a smaller chair/boat energy gap than in cyclohexane: 6.95 kcal/mol. This boat has the methyl groups on an in-plane carbon so this increases the strain due to eclipsing interactions with the hydrogens on the adjacent in-plane carbon, and possibly with the hydrogens on the in-plane carbon connected through the out-of-plane carbon. We have now the first indication of a destabilized chair: *if* the increase in 1,3-diaxial strain in the chair is greater than the increase due to 1,2 and 1,3 eclipsing strain, the resulting destabilization of the chair yields a smaller energy-gap. A second boat appears at 9.99, a much greater energy gap than in cyclohexane. This boat has the methyl substituents in bowsprit-flagpole positions. The crowding of a methyl group with the flagpole hydrogen can account for almost 3 kcal/mol of conformational energy.

The hypersurface shows four twist-boats, two enantiomeric pairs at 5.09 and 6.12 kcal/mol. The pair at 5.09 has the *gem* substitution on an in-plane carbon. Again, we find a smaller energy gap than the 5.82 kcal/mol in cyclohexane. We can apply an argument similar to the one used for the boats: a greater destabilization of the chair than of the twist-boat, to explain the reduced gap. The twist-boats at 6.12 have flagpole-flagpole interactions strong enough to destabilize this conformer even more than the chair. Apparently, flagpole-flagpole interactions are at least 2 kcal/mol stronger than the 1,3-diaxial. We can justify this by pointing out that 1,3-diaxial interactions involve mostly changes in torsion angles, while flagpole-flagpole interactions involve compression of bonds. Bonds have usually much stiffer potentials and narrower energy wells than torsions.

Six half-chairs determine three distinguishable barriers to chair/twist-boat interconversion with values of 10.98, 11.91 and 12.12 kcal/mol. All these values are close to the 11.25 kcal/mol found in cyclohexane. Both 1,3-diaxial as well as eclipsing interactions are still at work within the appropriate substitution patterns. On the other hand, flagpole-flagpole interactions are eliminated, because there is only one out-of-plane carbon. This eliminates one of the sources of strong destabilization.

Trimethylcyclohexane shows eight minima: two chairs (0.00 and 3.61 kcal/mol) and six twist-boats. 1,3-Diaxial interactions (worsened by Allinger buttressing) raise the chair to 3.61 kcal/mol. The lowest energy boat appears at 6.68 kcal/mol, slightly higher than the lowest boat in dimethylcyclohexane (6.51), but still lower than the 6.95 kcal/mol in cyclohexane. This boat has 1,3(in-plane) diaxial interactions with one of the *gem* methyls. The third methyl group is in the equatorial orientation on one in-plane carbon. At this energy, this boat splits the twist-boats in two triads. The first three twist-boats have the third methyl group either in bowsprit or in equatorial orientation, thus reducing van der Waals interactions. The other three have the methyl group in flagpole or axial orientation, so van der Waals repulsions increase. This increased repulsion affects the bond angles: when the methyl group is equatorial, the H_{ax}-C-R bond angle approaches 109° very closely. When the same methyl group is axial, the H_{ax}-C-R bond angle approaches 112°, being ``pushed out'' by the bulk of the methyl group. Higher in energy than these twist-boats, we find three boats. All have 1,3-diaxial methyl-methyl interactions, or methyl-hydrogen flagpole interactions.

Trimethylcyclohexane shows four half-chairs, three of them with energies close to the half-chair in cyclohexane: 11.22, 11.57 and 11.83 vs. 11.25. The first two half-chairs show a small energetic difference between the pseudoaxial and pseudoequatorial positions in the half-chair when the *gem* substituents are on the out-of-plane carbon, about 0.35 kcal/mol. The fourth chair has an energy of 17.05, and vibrational analysis characterized it as a higher-order saddle point. This half-chair has 1,3-diaxial methyl-methyl repulsions, justifying its high energy.

1,1,3,3-Tetramethylcyclohexane shows the effects of crowding substituents, now in a 1,1,3,3 di*gem* pattern. We see only one chair as the global minimum. The bond angles indicate strain due to 1,3-diaxial repulsions: the Me_{ax}-C-C angles are 113.3°, compared to the 109.2° of the H_{ax}-C-C angles. The change in the bond angles also affects the torsions according to the equation reported by Romers *et al.* [Romers, 1969]:

```
cos({omega}) = -cos({theta})/(1+cos({theta}))
```

where {omega} is the torsion angle, and {theta} is the adjacent bond angle. Measuring the torsion adjacent to the

113.3° angle yields a value of 46.8°; the value calculated with the equation is 49.1°. We can attribute the deviation to the uncommon steric crowding produced by the 1,1,3,3 di*gem* substitution pattern which induces severe 1,3-diaxial stress.

After the chair, we find four twist-boats in enantiomeric pairs. The first pair shows up at 3.93 kcal/mol and the second at 4.75. Both values, 3.93 and 4.75, are lower than the 5.82 kcal/mol gap in cyclohexane. In the first one, all the methyl groups are on in-plane carbons, the second pair has two methyls in bowsprit-flagpole positions. We infer that the reduction of the gap has to do with the severe strain present in the chair, although the twist-boats have strain as evidenced by the flatter torsions found. The average of the (absolute) values of the torsions in the cyclohexane twist-boat is 42.8°. The same average in tetramethylcyclohexane comes out as 39.8° and 37.3°.

Two boats, corresponding to the two pairs of twist-boats, have energies of 5.23 and 6.57 kcal/mol. Again, the highest energy boat has flagpole-equatorial methyl-methyl interactions, increasing its energy over the boat with axial-axial methyl-methyl interactions.

At first sight, (*R*)-1-ethyl-1,3,3-trimethylcyclohexane shows a very complex energy hypersurface, due to the additional degree of freedom introduced by the ethyl group. We can formally generate this hypersurface by splitting each conformer of 1,1,3,3-tetramethylcyclooctane into a family of three conformers, because of the three positions the ethyl group can take (*g*+, *g*- and *anti*). Closer examination reveals that some families are missing a member, namely, the one with the ethyl group pointing inside the ring.

All the minima within 3.5 kcal/mol above the global minimum are exclusively chairs. The first saddle point comes at 3.72 kcal/mol, and it involves rotation of the ethyl group. After that, we find a series of twist-boats, differing in most cases only in the ethyl torsion. The first ten twist-boats are spread over a range from 4.10 kcal/mol to 4.92 kcal/mol. With an average of 4.52 kcal/mol, the chair/twist-boat energy gap is somewhat greater than the 4.34 kcal/mol in 1,1,3,3-tetramethylcyclohexane, in agreement with a greater strain produced by the ethyl group. The first boat appears at 5.33 kcal, higher than its corresponding conformer in 1,1,3,3-tetramethylcyclohexane at 5.23 kcal/mol. 1,1,3,3-tetramethylcyclohexane has another boat at 6.57 kcal/mol, the corresponding conformer here shows up at 6.77 kcal/mol. The lowest energy chair in 1,1,3,3-tetramethylcyclohexane has an energy of 8.09 kcal/mol; the corresponding stationary point in this molecule is at 8.29.

To summarize, destabilization of the chair plays heavily in the determination of the chair/twist-boat energy gap because of the presence of six 1,3-diaxial interactions in the chair. Geminal substitution increases the diaxial strain due to Allinger buttressing. Flagpole-flagpole interactions in twist-boats account for more of the increase in strain energy than diaxial interactions. Flagpole-flagpole interactions in boats are stronger than both eclipsing and axial interactions on the in-plane carbons. Flagpole-axial interactions dominate the stability of the half-chairs, followed by eclipsing and 1-3 diaxial interactions. Our results agree with those obtained by Weiser *et al.* [Weiser, 1996] who employed the MM3(92) force field. This agreement gives us confidence in the ability of AMBER* to model crowded systems.

Cyclohexanes have helped us develop a picture of the changes in energy and strain due to steric effects. In the following sections we use the insights obtained from the analysis of these hydrocarbons as a framework for the inclusion of steric effects due to heteroatom substitution, dipolar effects and the effects of solvation.

4.5.1.2. Morpholinium rings.

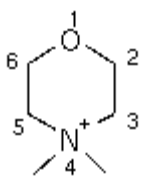

4,4-Dimethylmorpholinium yielded five minima: one chair (global minimum) and four twist-boats grouped in two degenerate pairs with energies equal to 4.51 and 7.12 kcal/mol, respectively. A boat at 5.38 kcal/mol separates these pairs. The other two twist-boats interconvert through a boat at 7.55 kcal/mol. The half-chairs at 10.80

and 11.11 can collapse to the chair or to any of the two twist-boats at 4.51. The half-chair at 10.80 kcal/mol has a plane of symmetry that passes through the N and the O, so it provides a symmetric path for chair-chair interconversion or for the generation of the lowest energy twist-boats. The half-chairs at 11.11 can collapse to any of the lowest energy twist-boats, but they are distorted as compared to the half-chair at 10.80. They represent asymmetric paths for chair-chair interconversion or for the generation of the twist-boats.

Comparing [dimethylcyclohexane vs. 4,4-dimethylmorpholinium], one change is the lowering of the energy of one of the cyclohexane boats, from 9.99 to 5.38 kcal/mol. This corresponds to the boat having the methyl groups in bowsprit-flagpole positions. Crowding with the nearby hydrogen strains the dimethylcyclohexane molecule. Dimethylmorpholinium, having an oxygen atom that eliminates the hydrogen atoms at position 4, relieves that strain. The other boat in dimethylmorpholinium (7.55 kcal/mol) corresponds to the boat at 6.51 kcal/mol in dimethylcyclohexane. These conformers have the methyl substituents on one in-plane carbon. These methyl groups eclipse the adjacent pair of hydrogens so, the greater bulk of the methyl groups, together with the shorter C-N bond, increases the strain by steric hindrance. The asymmetric half-chairs do not have analogs in dimethylcyclohexane, but in the symmetric ones we observe only small changes to lower energies. We can ascribe them to the loss of the hydrogen atoms opposite to the nitrogen, relieving flagpole-flagpole, axial, and eclipsing interactions.

Table 4.2. Comparison of morpholinium vs. dimethylcyclohexane in the gas phase.

Conformer	Dimethylcyclohexane	4,4-Dimethylmorpholinium
chair	0.00	0.00
twist-boat	5.09	4.51
twist-boat	5.09	4.51
twist-boat	6.12	7.12
twist-boat	6.12	7.12
boat	6.51	7.55
boat	9.99	5.38
half-chair	10.98	10.80
half-chair	10.98	NA
half-chair	11.19	11.11
half-chair	11.19	11.11
half-chair	12.12	11.67
half-chair	12.12	NA

Trimethylmorpholinium shows a total of eight minima: two chairs (the global minimum and a chair at 4.73 kcal/mol), and six twist-boats. The global minimum is a chair, followed by a twist boat at 4.49 kcal/mol. This twist-boat has the non-*gem* methyl group in equatorial. The lower destabilization of the global minimum can justify the greater energy gap here. Another chair, now with the non-*gem* methyl group axial, shows up at 4.73 kcal/mol. A combination of increased 1,3-diaxial repulsions due to bulkier groups held closer by the shorter C-N and C-O bonds can explain this higher energy (Let us not forget the lower strain present in the global minimum). The lowest energy boat appears at 7.55 kcal/mol with the non-*gem* methyl in bowsprit and the *gem* substituents on an in-plane carbon. The shape is somewhat distorted from an ideal boat, leaving the equatorial *gem* methyl in an orientation closer to axial and distorting the H_{ax}-C-C angles from the ideal 109.5°, making them as open as 111°. The lowest energy half-chair is at 10.91 kcal/mol. As with dimethylmorpholinium, we find several asymmetric half-chairs. The presence of a boat at

11.68 kcal/mol is very noticeable, as the highest energy boat we have found so far.

Drawing a [comparison of trimethylmorpholinium and trimethylcyclohexane] we see that the second chair is destabilized, going from 3.61 to 4.73 kcal/mol. We can ascribe part of this increased energy gap to a less strained global minimum. From the study of cyclohexanes we learned that 1,3-diaxial interactions could justify the reduced energy gaps found. Since morpholinium compounds lack a pair of hydrogens, that reduces the total number of 1,3-diaxial contacts from six to four, thus reducing the strain introduced by substituents on the ring. A similar observation comes from the boat at 10.09 in trimethylcyclohexane, which goes as low as 5.35 kcal/mol in the trimethylmorpholinium. The loss of flagpole-flagpole crowding helps this lowering of the energy. Additionally, even though this structure does not have any elements of symmetry because of its chirality, the ring conformation is the same as we found in dimethylmorpholinium (with the heteroatoms split by a mirror plane). Given that none of the methyl substituents on the ring have any heteroatoms, the dipolar picture approaches very closely that of dimethylmorpholinium. This results in a reduction of the overall dipole moment due to a symmetric disposition of the dipoles.

Table 4.3. Comparison of energies of trimethylmorpholinium vs. trimethylcyclohexane in the gas phase (kcal/mol).

	Trimethylcyclohexane	Trimethylmorpholinium
Chair	0.00	0.00
Chair	3.61	4.73
Twist-boat	5.10	7.04
Twist-boat	6.14	4.49
Twist-boat	6.28	6.84
Boat	6.68	7.55
Twist-boat	7.44	4.89
Twist-boat	7.63	9.06
Twist-boat	8.53	5.37
Boat	10.09	5.35
Half-chair	11.22	10.91
Half-chair	11.57	11.11
Half-chair	11.83	12.22
Boat	8.76	n.f. [*] [*]
Boat	10.52	n.f. [*]
Boat	10.09	n.f. [*]
Boat	10.52	n.f. [*]
Half-chair	17.05	n.f. [*]
Boat	n.f. [*]	9.41
Boat	n.f. [*]	11.68
Half-chair	n.f. [*]	11.61

The gap between the first twist-boat in trimethylcyclohexane and its chair (5.10 kcal/mol) increases in the morpholinium to 7.04. Flagpole-flagpole hydrogen-hydrogen repulsion can partly justify this result, even more because the non-*gem* methyl in bowsprit forces Allinger buttressing, but examination of the internal angles of the ring reveals that they are distorted, having an average value of 111.9°.

Tetramethylmorpholinium has a two enantiomeric chairs as global minima. These enantiomers arise because the introduction of nitrogen and oxygen into the global minimum in 1,1,3,3-tetramethylcyclohexane eliminates a plane of symmetry. After the chairs we find three enantiomeric pairs of twist-boats. The energies are remarkably low if compared to the other morpholinium rings: 1.25, 1.56 and 3.93 kcal/mol vs. the lowest twist-boat at 4.51 kcal/mol in morpholinium; or the lowest twist-boat in trimethylmorpholinium at 4.49 kcal/mol. Because of the 1,3 substitution pattern, two of the twist-boat pairs have two methyl groups in bowsprit-flagpole orientations. These are the lowest energy pairs. The third pair has all methyl groups on in-plane carbons, and corresponds to the highest energy pair. We indicated above that flagpole-flagpole interactions weighed heavily among the contributions to strain, followed by diaxial and eclipsing. The lowest energy twist-boats have a methyl in flagpole, but they lack the opposite flagpole atom, leaving only 1,3-diaxial and eclipsing repulsions to induce strain. The third twist-boat pair shows flagpole-flagpole H···H contacts, plus 1,3-diaxial Me···Me contacts, therefore increasing the strain.

At 6.69 kcal/mol we find the lowest energy half-chair in all the cases analyzed so far. It shows some distortion from a perfect half-chair, and lacks strong flagpole interactions because of the absence of hydrogens on position 1,4 to the out-of-plane carbon. Higher in energy we see a pair of enantiomeric boats at 6.86 kcal/mol. These have the methyl groups on nitrogen in bowsprit-flagpole, so flagpole-flagpole interactions do not destabilize it. By analyzing the possible permutations of the substituents on the basic boat framework, we realize that another boat, with all four methyl groups on in-plane carbons, is possible. Under the conditions of our minimizations, AMBER* could not find those stationary points in the search, nor refine the gradients under acceptable cutoffs when the structures were generated by hand and increased the number of iterations for the minimization routine (Full Matrix Newton Raphson) to 2000. **This is probably the first indication of a significant shortcoming in this model chemistry.** After this result, we consider that the results obtained at higher energies may be less reliable, so we mention only the presence of three more half-chairs, one of them classified as a multiple maximum by AMBER* although there are no methyl rotations that could justify the additional imaginary frequencies.

We can [contrast tetramethylmorpholinium vs. tetramethylcyclohexane]. About half of the stationary points found in morpholinium have a cyclohexane analog. Most of the conformers lose strain in the morpholinium analog, due to the loss of 1,3-diaxial or flagpole interactions. There are only two cases of more highly strained morpholinium analogs: the boat at 6.57 kcal/mol in the cyclohexane rises to 6.86 kcal/mol in the morpholinium, and the enantiomeric half-chairs that go from 8.25 to 8.73 kcal/mol. Both increases correspond to increased eclipsing interactions brought about by the shorter C-N bonds. The presence of so many conformers without an analog, casts some doubt on the ability of AMBER* to model such **highly crowded, charged** systems.

Table 4.4. Comparison of energies of tetramethylcyclohexane vs. tetramethylmorpholinium in the gas phase (kcal/mol).

Conformer	Tetramethylcyclohexane	Tetramethylmorpholinium
Chair	0.00	0.00
Twist-boat	4.75	1.25 & 1.56
Twist-boat	4.75	1.25 & 1.56
Boat	6.57	6.86
Half-chair	8.09	6.98
Half-chair	8.25	8.73

Half-chair	8.25	8.73
Half-chair	9.60	6.69
Twist-boat	3.93	n.f. [*]
Twist-boat	3.93	n.f. [*]
Boat	5.23	n.f. [*]
Half-chair	14.07	n.f. [*]
Half-chair	14.07	n.f. [*]
Twist-boat	n.f. [*]	3.93
Twist-boat	n.f. [*]	3.93
Half-chair	n.f. [*]	13.32

The introduction of a hydroxymethyl group complicates the hypersurface of the molecule, by adding the degrees of freedom, in the -CH_2-CH_2-O-H fragment. Additionally, the new N-CH-CH_2-OH fragment shows a gauche effect. Given the risks involved in modeling such crowded systems uncovered by the results on tetramethylmorpholinium, we content ourselves with discussing only the lowest energy conformers, namely, those within 3.0 kcal/mol above the global minimum.

In (*R*)-2-hydroxymethyl-2,4,4-trimethylmorpholinium, the global minimum is a chair. Within 3.0 kcal/mol we observe a mixture of chairs and twist-boats. [Comparing ethyltrimethylcyclohexane vs. hydroxymethyl trimethylmorpholinium] shows the effects of polar influences on conformation. These comparisons take into account seven torsions: the six internal torsions of the ring and the torsion of the bond that connects the ethyl group to the ring because we cannot compare the C-C-O-H torsion to the C-C-CH_2-H. The table shows many changes in the energetic ranking of the conformers, the most noticeable of which is the change in global minimum. Both conformations are chairs, but they differ in the orientation of the ethyl/hydroxymethyl substituent. The ethyl prefers an *anti* conformation, while the hydroxymethyl prefers *gauche*. Some conformers show substantial stabilization by the presence of heteroatoms, like in the case of a twist-boat at 7.00 kcal/mol in the cyclohexane. The morpholinium analog has an energy of 2.18 kcal/mol. The gauche effect comes into play here: a *gauche* ethyl group has a much higher energy than a *gauche* hydroxymethyl subject to gauche effect. Most conformers in this morpholinium ring are highly distorted, and the identification of analog pairs was difficult.

Table 4.5. Comparison of energies of ethyltrimethylcyclohexane vs. (hydroxymethyl)trimethylmorpholinium in the gas phase (kcal/mol).

Conformer	Ethyltrimethylcyclohexane	(Hydroxymethyl)trimethylmorpholinium
Chair	0.00	2.19
Chair	0.35	1.77
Chair	0.74	1.60
Chair	0.74	0.81
Chair	1.64	0.00
Twist-boat	4.10	2.20
Twist-boat	4.83	2.13

Twist-boat	5.23	1.14
Twist-boat	5.39	2.71
Twist-boat	7.00	2.18
Twist-boat	n.f. [*]	1.20
Chair	n.f. [*]	2.01
Twist-boat	n.f. [*]	2.35
Chair	n.f. [*]	2.56
Chair	n.f. [*]	2.73

In summary, morpholinium rings follow the same general trends regarding steric interactions uncovered by the study of hydrocarbon systems, but the shorter bond lengths associated with heteroatoms increase steric crowding. In analyzing these conformational energies one has to take into consideration the reduced number of diaxial or flagpole interactions, due to the absence of substituents on atoms like oxygen. Dipole-dipole interactions do not seem to play an important role in the gas phase. We might have pushed AMBER* over its limit of applicability by modeling this highly crowded, charged species.

4.5.2. Modeling in GB/SA water.

MacroModel does not calculate dipole moments, but all calculations including solvent report a ``Solvation'' component. We use this term in lieu of a dipole moment. The table for dimethylmorpholinium in water displays all the minima found including GB/SA water. The [comparison between gas phase and water]

Table 4.6. Conformational and solvation energies (kcal/mol) of dimethylmorpholinium in the gas phase and GB/SA water.

Conformer	Energy in the gas phase	Energy in GB/SA water	{delta}H_{solv}
Chair	0.00	0.00	-56.66
Twist-boat	4.51	4.92	-55.35
Boat	5.38	5.93	-54.91
Twist-boat	7.12	6.66	-57.52
Boat	7.55	7.23	-57.06
Half-chair	10.80	10.66	-56.22
Half-chair	11.11	11.07	-56.47

shows the differences brought about by solvation. The chair is the global minimum, two twist-boats have energies of 4.92 kcal/mol, having increased its energy by 0.41 kcal/mol from the 4.51 it had in the gas phase. The other pair has an energy of 6.66 kcal/mol. Solvation has stabilized these structures by 0.46 kcal/mol from their 7.12 kcal/mol in the gas phase. The energy gap between the twist-boats has decreased from 2.61 kcal/mol to 1.74 kcal/mol. The difference in solvation is 2.17 kcal/mol, which explains, at least qualitatively, the difference. One of the boats, at 5.38 kcal/mol in the gas phase, has an energy of 5.93 in solution. The energetic ranking in solution follows closely that in the gas phase, although the highest energy half-chair (pair) in solution does not show up in the gas phase. The saddle points have

among the highest solvation terms in the set of conformers, to the exception of the first boat. The first boat has the nitrogen and the oxygen in out-of-plane positions; thus they are part of a plane of symmetry of the molecule. This symmetric arrangement makes for a partial cancellation of the dipoles, thereby reducing the overall molecular dipole moment, and yielding the smallest $\{delta\}H_{solv}$.

Trimethylmorpholinium in water shows eight minima, two chairs and six twist-boats. The chairs follow the same energetic ranking as in the gas phase. So do most of the twist-boats. There is only one crossover in the ranking, as the twist-boat at 6.84 kcal/mol in the gas phase increases its energy to 7.54 kcal/mol in water, while the one at 7.04 is lowered to 6.63 kcal/mol by solvation. The solvation terms fit that behavior, given that the twist-boat at 6.63 kcal/mol in water has a solvation term equal to -56.08 kcal/mol, while the destabilized twist-boat has a solvation equal to -53.50. This destabilized twist-boat does not have any elements of symmetry because of its chirality, but the ring conformation is the same as we found in dimethylmorpholinium in solution (with the heteroatoms in out-of-plane positions). Thus the dipolar picture approaches closely that of dimethylmorpholinium. This results in a reduction of the overall dipole moment due to a symmetric disposition of the dipoles and in one of the lowest solvation terms in the table.

Table 4.7. Conformational and solvation energies (kcal/mol) of trimethylmorpholinium in the gas phase and GB/SA water.

Conformer	Energy in the gas phase	Energy in GB/SA water	$\{delta\}H_{solv}$
Chair	0.00	0.00	-55.27
Twist-boat	4.49	4.87	-53.97
Chair	4.73	4.88	-54.98
Twist-boat	4.89	5.36	-53.66
Boat	5.35	5.86	-53.52
Twist-boat	5.37	5.76	-54.12
Twist-boat	6.84	7.54	-53.50
Twist-boat	7.04	6.63	-56.08
Boat	7.55	12.57?	-55.59
Twist-boat	9.06	8.87	-55.59
Boat	9.41	n.f. [*]	----
Half-chair	10.91	10.84, 14.93	-54.76
Half-chair	11.11	n.f. [*]	----
Half-chair	11.61	n.f. [*]	----
Boat	11.68	n.f. [*]	----
Half-chair	12.22	n.f. [*]	----
Boat	n.f. [*]	7.33	-55.54
Half-chair	n.f. [*]	11.15	-55.02
Half-chair	n.f. [*]	18.28	-55.73

In tetramethylmorpholinium, all the stationary points we found had their corresponding structure in the gas phase. They keep the same energetic ranking as in the gas phase. We found two chairs (0.00 kcal/mol) and three pairs of enantiomeric twist-boats. The saddle points, however, deviate from the calculated behavior in the gas phase. One boat and two half-chairs could not be found, despite repeated attempts with increased energy windows (perhaps one more of the difficulties AMBER* has coping with charged, crowded molecules?). The boats have energies of 4.18 and 6.67 kcal/mol and the half-chairs have energies of 6.47 and 9.95 kcal/mol.

Table 4.8. Conformational and solvation energies (kcal/mol) of tetramethylmorpholinium in the gas phase and GB/SA water.

Conformer	Energy in the gas phase	Energy in GB/SA water	{delta}H_{solv}
Chair	0.00	0.00	-53.71
Chair	0.00	0.00	-53.71
Twist-boat	1.25	1.63	-52.40
Twist-boat	1.25	1.63	-52.40
Twist-boat	1.56	2.07	-52.23
Twist-boat	1.56	2.07	-52.23
Twist-boat	3.93	3.67	-54.27
Twist-boat	3.93	3.67	-54.27
Half-chair	6.69	6.47*	-53.57
Boat	6.86	6.67	-53.85
Boat	6.86	6.67*	-53.85
Half-chair	6.98	n.f. [*]	----
Half-chair	8.73	n.f. [*]	----
Half-chair	13.32	n.f. [*]	----

(*R*)-2-Hydroxymethyl-2,4,4-trimethylmorpholinium in water has a chair as the global minimum. The global minimum has the C-C-CH_2-O-H fragment in *g*-,*g*+. There are two chairs within 1 kcal/mol above the global minimum. One differs only in the conformation of the C-C-CH_2-O-H fragment: *g*+,*g*-. The other one is a conformational diastereomer with the ring torsion angles as "mirror images" of those in the global minimum. That chirality, plus that due to the chiral center already present in the molecule, give rise to diastereomers. The O-C-C-C torsion is *anti* in a few high energy (>4.9 kcal/mol) instances. The C-C-O-H torsion prefers a *gauche* conformation, which probably helps hydrogen bonding to the oxygen in the ring. The first conformer with an *anti* C-C-O-H is 3.20 kcal/mol above the global minimum. We cannot see a simple correlation between the solvation energy of the conformer and the torsions in the ring or those of the hydroxymethyl group. We found a total of 43 conformations, as in the gas phase. See appendix for full listing of results

Table 4.9. Conformational and solvation energies (kcal/mol) of (hydroxymethyl)trimethylmorpholinium in the gas phase and GB/SA water.

Conformer	Energy in the gas phase	Energy in GB/SA water	{delta}H_{solv}
Chair	0.00	0.00	-59.59

Chair	0.81	0.81	-56.84
Twist-boat	1.14	2.62	-54.83
Twist-boat	1.20	n.f. [*]	----
Chair	1.60	0.86	-59.57
Chair	1.77	n.f. [*]	----
Chair	2.01	4.42	-52.24
Twist-boat	2.13	1.45	-58.46
Twist-boat	2.18	n.f. [*]	----
Chair	2.19	4.95	-53.66
Twist-boat	2.20	1.79	-58.51
Twist-boat	2.35	1.90	-58.34
Chair	2.63	3.20	-55.44
Twist-boat	2.71	n.f. [*]	----
Chair	2.73		
Twist-boat	3.66	n.f. [*]	----
Twist-boat	3.90	6.63	-53.15
Twist-boat	4.06	4.57	-57.10
Twist-boat	4.11	7.24	-52.68
Twist-boat	4.32	7.88	-52.85
Boat	4.45	n.f. [*]	----

4.6. Conformational analyses of 2-oxo-1,3,6-dioxazaphosphacinium rings.

We analyzed by molecular mechanics the conformational behavior of:

1. Cyclooctane in the gas phase.
2. 1,1,5,5-tetramethylcyclooctane in the gas phase.
3. 1,1,3,5,5-pentamethylcyclooctane in the gas phase.
4. 1,1,3,3,5,5-hexamethylcyclooctane in the gas phase.

as a reference frame to understand:

1. 6,6-dimethyl-2-oxo-1,3,6-dioxazaphosphacinium in the gas phase and in solution.
2. *cis*-4,6,6-Trimethyl-2-oxo-1,3,6-dioxazaphosphacinium in the gas phase and in solution.
3. *trans*-4,6,6-Trimethyl-2-oxo-1,3,6-dioxazaphosphacinium in the gas phase and in solution.
4. 4,4,6,6-Tetramethyl-2-oxo-1,3,6-dioxazaphosphacinium in the gas phase and in solution.

4.6.1. Modeling in the gas phase.

As previously indicated for the six-membered ring molecules, we repeated MonteCarlo runs until the searches converged. For details about the setup, refer to the Methods section. All energies refer to the global minimum as 0.00 kcal/mol unless specified otherwise.

4.6.1.1. Cyclooctanes.

In cyclooctane we find 8 out of the ten conformations normally regarded as stationary points and which we have described previously in the review of the literature. We only miss the crown and the CC. The BC is the global minimum, in agreement with most of the previous determinations. After this, the TCC is the most populated, with an energy of 0.83 kcal/mol in the gas phase. Two kinds of TBC come at 1.77 kcal/mol (minimum) and at 2.88 kcal/mol (saddle). The TB shows up at 3.63 kcal/mol, a BB at 4.86, a C at 7.76. The TC is at 8.47 and the B at 10.55 kcal/mol. The AMBER* ordering agrees fairly well with that of Kolossváry and Guida [Kolossváry, 1993] giving us confidence in the ability of AMBER* to model these rings.

Table 4.10. Conformers of cyclooctane within 3.0 kcal/mol of global minima in the gas phase.

Conformer	Structure	AMBER* (kcal/mol)	MM2* (kcal/mol)
BC	 bc.wrl, 9.668KB	0.00	0.00
TCC	 tcc1.wrl, 9.651KB	0.83	0.96
TCC'	 tcc1.wrl, 9.651KB	0.83	0.96
TBC	 tbc1.wrl, 9.649KB	1.77	1.67
TBC'	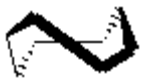 tbc2.wrl, 9.654KB	1.77	1.67
TBC	 tbc3.wrl, 9.667KB	2.88	2.80
TBC'	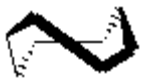 tbc4.wrl, 9.667KB	2.88	2.80

In 1,1,5,5-tetramethylcyclooctane the BCs are global minima with the methyl groups in positions 2 and 6. The introduction of two 1,5-*gem*-dimethyl groups lowers the symmetry, so we describe two different, enantiomeric BCs. See the [appendix] for a full description of the naming and numbering system used for *all* conformers. After the BC follows a lowered TCC (0.39 kcal/mol, possibly an indication of a destabilized BC) with methyl groups in 1,5. Now the TCC is followed by a 1,5 TB, not a TBC as in cyclooctane. The 1,5 TB is now only 0.45 kcal/mol higher in energy than the BC, as does the 3,7 TB, instead of the 3.63 kcal/mol it showed in cyclooctane. The 2,6 and 4,8 BB have an energy gap of 0.84, much smaller than 4.86 the BB showed in cyclooctane. A 1,5 CC appears at 1.12 kcal/mol. On the other hand, the 1,5 TBC has increased to 2.17 kcal/mol from the original 1.77 in cyclooctane.

Table 4.11. Conformers of tetramethylcyclooctane within 3.0 kcal/mol of global minima in the gas phase.

Conformer	Structure	AMBER* (kcal/mol)
2,2,6,6-BC	 bc14O.wrl, 14.058KB	0.00
2,2,6,6-BC'	 bc24O.wrl, 14.074KB	0.00
1,1,5,5-TCC	 tcc14O.wrl, 14.027KB	0.39
1,1,5,5-TCC'	 tcc24O.wrl, 14.082KB	0.39
1,1,5,5-TB	 tb14O.wrl, 14.069KB	0.45
1,1,5,5-TB'	 tb24O.wrl, 14.143KB	0.45
2,2,6,6-BB	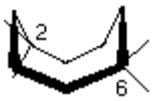 bb14O.wrl 14.000KB	0.84
2,2,6,6-BB'	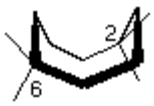 bb24O.wrl, 14.195KB	0.84
1,1,5,5-CC	 cc4O.wrl, 14.201KB	1.12
1,1,5,5-TBC	 tbc14O.wrl, 14.084KB	2.17
1,1,5,5-TBC'	 tbc24O.wrl, 14.084KB	2.17

In 1,1,3,5,5-pentamethylcyclooctane the global minimum is formed by a pair of enantiomeric BCs, followed at 0.43 kcal/mol by two enantiomeric TCCs. The barrier for TCC-TCC' interconversion is very low, 1.49 kcal/mol (CC). We then find a set of TBs at 1.55 and 1.59 kcal/mol, two BCs and two TBCs. These results continue the pattern started with 1,1,5,5-tetramethylcyclooctane: the BCs prefer to carry the *gem* substituents in positions 2 and 6 (sometimes 4

and 8), while the methyl group prefers positions 4*e* and, sometimes, 2*e*. Only in high energy cases we find the substituents in positions 1, 3 or 7. Apparently, this positions suffer strong axial-axial or flagpole-axial interactions. The TCC carries the substituents on positions 1, 3 and 5; as the CC does. Positions 2, 3, 6 and 7 are subject to stronger axial-axial repulsions. [Note]

Table 4.12. Conformers of pentamethylcyclooctane within 3.0 kcal/mol of global minima in the gas phase.

Conformer	Structure	Energy (kcal/mol)
2,2,4,6,6-BC	 bc15O.wrl, 15.236KB	0.00
2,2,4,6,6-BC'	 bc25O.wrl, 15.183KB	0.00
1,1,3,5,5-TCC	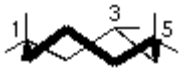 tcc15O.wrl, 15.302KB	0.43
1,1,3,5,5-TCC'	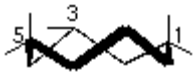 tcc25O.wrl, 15.238KB	0.43
1,1,3,5,5-CC	 cc5O.wrl, 15.181KB	1.49
2,2,4,6,6-TB	 tb15O.wrl, 15.190KB	1.55
2,2,4,6,6-TB'	 tb25O.wrl, 15.177KB	1.55
1,1,3,5,5-TB	 tb35O.wrl, 15.126KB	1.59
1,1,3,5,5-TB'	 tb45O.wrl, 15.168KB	1.59
2,4,4,8,8-BC		1.65

	 bc35O.wrl, 15.291KB	
2,4,4,8,8-BC'	 bc45O.wrl, 15.037KB	1.65
1,1,5,5,7-TBC	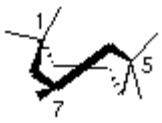 tbc15O.wrl, 15.276KB	1.92
1,1,5,5,7-TBC'	 tbc25O.wrl, 15.220KB	1.92
2,4,4,8,8-BC	 bc55O.wrl, 15.179KB	2.09
2,4,4,8,8-BC'	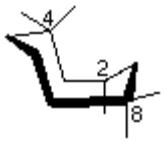 bc65O.wrl, 15.200KB	2.09
2,2,4,6,6-BB	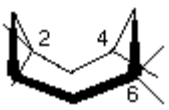 bb5O.wrl, 15.165KB	2.34
1,1,3,5,5-TBC	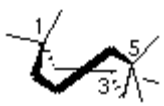 tbc35O.wrl, 15.116KB	2.61
1,1,3,5,5-TBC'	 tbc45O.wrl, 15.141KB	2.61

The TB has a slight preference by 2,4 and 6 closely followed by 1,3 and 5. The single methyl group prefers the equatorial orientation in all cases and only in higher energy structures, (> 5.5 kcal/mol) do we find it in axial. TBC prefers a pattern 1,3,5, although a 2,6,8 pattern is also possible (2,2,6,6,8*e*). A saddle TBC shows a 2,2,4*e*,6,6 pattern. We did not name structures higher than 8.35 kcal/mol. Most of them show great distorsion, and neither by use of the Weiler plots nor direct examination of the structure could we assign them a name. We think it better to assign them a number, rather than trying to force a fit into our preconceived notions. We shall look back on them only if needed to understand the behavior of the systems that concern us.

1,1,3,3,5,5-Hexamethylcyclooctane shows a pair of TBs as global minima. The interconversion barrier, through a BB,

is 0.82 kcal/mol. The BCs are now 1.21 kcal/mol higher in energy than the TBs. The TB prefers to carry its substituents in positions 2,4 and 6. The BC prefers positions 2,4, and 8; and 2,4, and 6. The TBC at 5.99 kcal/mol, prefers substitution on carbons 2,4 and 8. The conformational picture is somewhat simpler than that of 1,1,3,5,5-pentamethylcyclooctane because 1,1,3,3,5,5-hexamethylcyclooctane does not have an equatorial/axial option available as in the pentamethyl substituted ring. As we examine conformations higher in energy, we find many highly distorted structures difficult to name. The distortions seem to depend heavily on the number of substituents so, at present, we cannot see any trends emerging from the ordering of these conformers.

Table 4.13. Conformers of hexamethylcyclooctane within 3.0 kcal/mol of global minima in the gas phase.

Conformer	Structure	Energy (kcal/mol)
1,1,3,3,5,5-TB	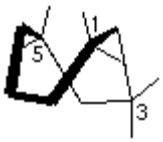 tb16O.wrl, 16.172KB	0.00
1,1,3,3,5,5-TB'	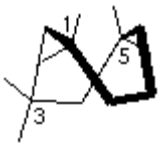 tb26O.wrl, 16.226KB	0.00
2,2,4,4,8,8-BB	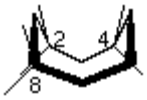 bb6O.wrl, 16.350KB	0.82
2,2,4,4,8,8-BC	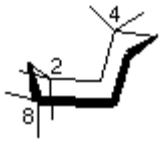 bc16O.wrl, 16.189KB	1.21
2,2,4,4,8,8-BC'	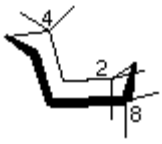 bc26O.wrl, 16.221KB	1.21

BCs accomodate substituents preferentially on an equatorial 2,4,6 pattern; a 2,4,8 pattern introduces more strain than a 2,4,6. Substituents on atom 1 can orient either as bowsprit or flagpole. The flagpole orientation suffers close contacts with the axial substituents on atoms 4 and 6. Axial substituents on atoms 2, 3, 7 and 8 produce strong axial-axial interactions among themselves. The most sterically unhindered positions are 1*b* and *equatorial* 2, 3, 4, 5, 6, 7 and 8. A 1,3,5 pattern becomes highly strained when adding *gem* substituents: in tetramethylcyclooctane, the 1,5 is 5.27 kcal/mol higher in energy than the 2,6; in pentamethylcyclooctane, the 1,3,5 pattern is 5.42 kcal/mol higher in energy than the 2,4,6 and 3.77 kcal/mol higher than the 2,4,8. We could not find this pattern in hexamethylcyclooctane.

TBs prefer a 2,4,6 pattern over a 1,3,5. Because of the high symmetry of the conformation, all the positions have similar steric hindrances. We see that in tetramethylcyclooctane the lowest energy TB is a 1,5; in pentamethylcyclooctane the preferred TB is a 2,4,6 followed closely by a 1,3,5 (0.4 kcal/mol gap); while in hexamethylcyclooctane the lowest TB is a 2,4,6. The TB/BC energy gap starts at 3.63 kcal/mol in cyclooctane, in tetramethylcyclooctane is only 0.45 kcal/mol; increases to 1.55 kcal/mol in pentamethylcyclooctane and becomes -1.21 kcal/mol in hexamethylcyclooctane. The best explanation for the decrease in the TB/BC gap when going from cyclooctane to tetramethylcyclooctane consists of destabilization of the BC. This argument also explains the increase

in energy in the TBC conformers.

The TBCs prefer positions 1,3,5 for the substituents. Positions 2,3,6 and 7 generate some axial-flagpole repulsions with the flagpoles on carbons 1 and 4. The bowsprit orientations on atoms 1 and 5 present little steric hindrance, because they are directed away from the ring, so the justification for the preference on these positions becomes clear. The smallest TBC/BC energy gap in cyclooctane is 1.77 kcal/mol. This increases to 2.17 kcal/mol in tetramethylcyclooctane, goes down to 1.92 kcal/mol in pentamethylcyclooctane and then increases to 4.78 kcal/mol in hexamethylcyclooctane.

To summarize, the conformations of substituted cyclooctanes are very sensitive to the positioning of the substituents on the ring. As the conformation of the ring skeleton becomes less symmetric, the sensitivity to positioning of the substituents increases, *e. g.*, the BC and TBC are more sensitive to the position of the substituents than the TCC or the C. More extended conformers, like the C or the TC, are less affected than more crowded conformers, like the TB or BB. As the number of *gem* substituent groups increases, the TB/BC energy gap tends to decrease until, with three *gem* dimethyl groups in a 1,3,5 pattern, the stabilities switch and the TB becomes the global minimum.

The positions with least steric hindrance are: 2, 4, 6 in the BC (the absence of 8 is an artifact of the rules used to name the conformers); 1 and 5, followed by 3, in the TCC; 2 and 6 in the TBC, although 1 and 5 are not much more hindered; all the positions in the TB are nearly equivalent in terms of steric hindrance; the TC prefers 1 and 3 (5 and 7 are equivalent to 1 and 3 respectively).

4.6.1.2. Dioxazaphosphacinium rings.

The conformational search on the unsubstituted phosphonate ring in the gas phase 6,6-dimethyl-2-oxo-1,3,6-dioxazaphosphacinium showed that the global minimum is a pair of enantiomeric BCs with the nitrogen on position 2 and the phosphorus on 6. [Note.] The more voluminous methyl group, compared to the *oxo* oxygen, prefers the least hindered equatorial position, as one would expect. Putting the methyl groups in any other position carries a very high energetic cost: the 1*b*,5,5 BC increases the energy 7.52 kcal/mol, 2*a*,6,6 increases the energy to 10.12 kcal/mol, while a 3*e*,7,7 pattern raises the energy to 11.18 kcal/mol. In these three cases, unfavorable 1,3-diaxial interactions are responsible for most of the increase in energy. We could not find examples of BCs with a 1*f*,5,5 or a 3*a*,7,7 substitution pattern.

As in the cyclooctanes, we found a minimum TBC and a saddle point TBC. The TBC (min) has an energy of 2.37 kcal/mol, compared to the 2.17 kcal/mol in tetramethylcyclooctane. The TBC (saddle) has an energy of 6.70 kcal/mol, compared to the 6.33 kcal/mol in tetramethylcyclooctane.

Two other conformers have energies within 3.0 kcal/mol above the global minimum: TB (pair at 2.55) and TC (2.75). This differs appreciably from tetramethylcyclooctane, which shows the TB at 0.45 and the TC at 4.42 kcal/mol.

Table 4.14. Conformers of dioxazaphosphacinium within 3.0 kcal/mol of global minima in the gas phase.

Conformer	Structure	Energy (kcal/mol)
2,2,6,6-BC	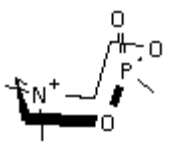 bc1P2.wrl, 13.665KB	0.00
2,2,6,6-BC'		0.00

	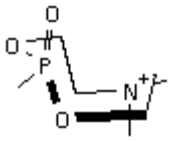 bc2P2.wrl, 13.653KB	
2,2,6,6-TBC	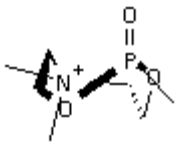 tbc2P2.wrl, 13.697KB	2.37
2,2,6,6-TBC'	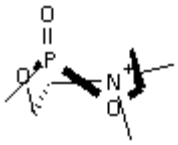 tbc1P2.wrl, 13.678KB	2.37
1,1,5,5-TB	 tb1P2.wrl, 13.780KB	2.55
1,1,5,5-TB'	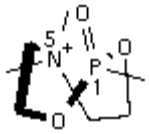 tb2P2.wrl, 13.732KB	2.55
3,3,7,7-TC	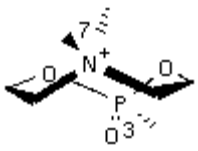 tcP2.wrl, 13.635KB	2.75

cis-4,6,6-Trimethyl-2-oxo-1,3,6-dioxazaphosphacinium in the gas phase also shows a BC as the global minimum, but its conformational heterogeneity is much lower than that of the unsubstituted ring. Pentamethylcyclooctane has BCs as global minima, but the similarity ends there. Pentamethylcyclooctane shows a TCC at 0.43 kcal/mol (a reduced TCC/BC gap that we previously ascribed to destabilization of the BC), while this phosphorus ring has its lowest TCC at 5.59 kcal/mol. The CC originally at 1.49 kcal/mol in pentamethyl, now appears at 5.70 kcal/mol. The first TB in pentamethyl has increased from 1.55 to 4.10 kcal/mol. The second TB has gone from 1.59 to 5.59 kcal/mol. The TBC starting at 1.92 is now 4.94 kcal/mol above the global minimum.

Table 4.15. Conformers of *cis*-methyl dioxazaphosphacinium within 3.0 kcal/mol of global minimum in the gas phase.

Conformer	Structure	Energy (kcal/mol)
2,2,4,6,6-BC'	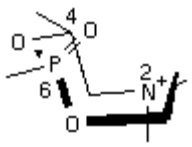 bcP3.wrl, 14.873KB	0.00

1,3,3,7,7-TC	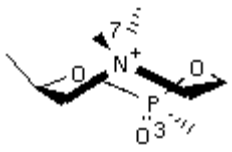 tcP3.wrl, 14.910KB	2.89

trans-4,6,6-Trimethyl-2-oxo-1,3,6-dioxazaphosphacinium in the gas phase shows a distorted TBC as the global minimum. Its conformational heterogeneity is much higher than that of the *cis* ring: the *cis* ring has only two conformers within 3.0 kcal/mol above the global minimum (inclusive), while the *trans* ring has seven. Both have fewer conformers than pentamethylcyclooctane, which has eight pairs of conformational enantiomers and two saddle points, all within 3.0 kcal/mol above the global minimum (inclusive). We find a BC (0.20 kcal/mol), two TCs (1.43 and 2.49), two TBs (1.50 and 2.84 kcal/mol) and another TBC (2.01 kcal/mol).

Table 4.16. Conformers of *trans*-methyl dioxazaphosphacinium within 3.0 kcal/mol of global minimum in the gas phase.

Conformer	Structure	Energy (kcal/mol)
2,2,4,6,6-TBC	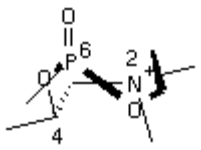 tbc1P4.wrl, 14.853KB	0.00
2,2,6,6,8-BC	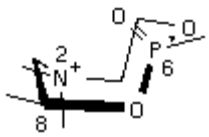 bcP4.wrl, 14.860KB	0.20
1,3,3,7,7-TC	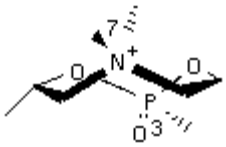 tc1P4.wrl, 14.841KB	1.43
1,1,3,5,5-TB	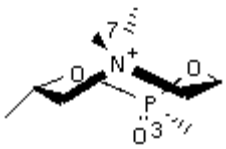 tb1P4.wrl, 14.814KB	1.50
2,2,6,6,8-TBC	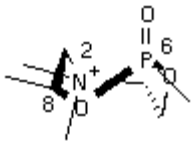 tbc2P4.wrl, 14.857KB	2.01
3,3,5,7,7-TC	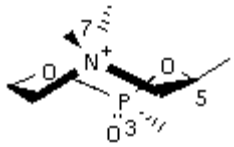 tc2P4.wrl, 14.813KB	2.49
1,1,3,5,5-TB'	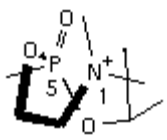	2.84

	tb2P4.wrl, 14.881KB	

The results in the gas phase for 4,4,6,6-tetramethyl-2-oxo-1,3,6-dioxazaphosphacinium show a mixture of conformers. Five conformers show up within 3.0 kcal/mol above the global minimum. Now the global minimum is a TC, followed closely (0.58 kcal/mol) by a BC. In hexamethylcyclooctane, the global minimum is a TB, and the first TC has an energy of 7.26 kcal/mol. The first TB in this phosphonate ring appears at 2.58 kcal/mol and follows a TBC at 2.62, completing all the conformations within 3.0 kcal/mol.

Table 4.17. Conformers of dimethyl dioxazaphosphacinium within 3.0 kcal/mol of global minimum in the gas phase.

Conformer	Structure	Energy (kcal/mol)
1,1,3,3,7,7-TC	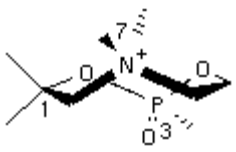 tcP5.wrl, 15.871KB	0.00
2,2,6,6,8,8-BC	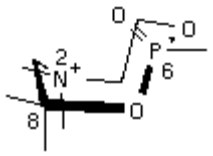 bc1P5.wrl, 15.785KB	0.58
2,2,4,4,6,6-BC'	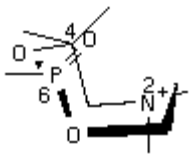 bc2P5.wrl, 15.646KB	1.71
3,3,5,5,7,7-TB	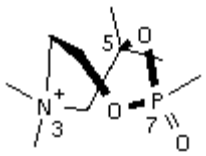 tb1P5.wrl, 15.871KB	2.58
1,1,3,3,5,5-TB	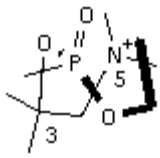 tb2P5.wrl, 15.844KB	2.61
2,2,6,6,8,8-TBC	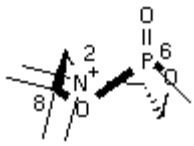 tbcP5.wrl, 15.826KB	2.62

4.6.2. Modeling in GB/SA water.

The conformational search for the 6,6-dimethyl-2-oxo-1,3,6-dioxazaphosphacinium in water showed that the global minimum is a degenerate pair of BBs. These are followed by a degenerate pair of BC conformers, at 2.52 kcal/mol. All the other conformers are higher than 3.0 kcal/mol. The P-O bonds are longer than C-C bonds (1.59Å vs. 1.54Å), so this helps the relief of strain. The steric requirements of the oxygens and of the methyl groups are the same in both cases.

The dipole moments measured by Dale [Dale, 1972] could fit both a BC or a BB, but he could not define unambiguously the positions of the oxygens. In the BBs, the oxygens could have taken positions 1,3 or 1,7; leaving the *gem*-dimethyls in positions 2,6. Our results agree with Dale's: in the BBs, the oxygens take positions 1,3 and 1,7 and the *gem* groups (dimethyl and methyl-oxo) are in 2,6. In the BCs at 2.52 kcal/mol (the only ones significantly populated at room temperature) the oxygens occupy positions 5,7 and the *gem* groups take 2,6.

Table 4.18. Conformers of dioxazaphosphacinium within 3.0 kcal/mol of global minimum in water.

Conformer	Structure	Energy (kcal/mol)
2,2,6,6-BB	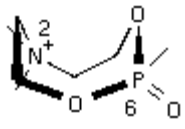 bb1PW2.wrl, 13.903KB	0.00
4,4,8,8-BB	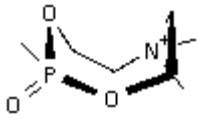 bb2PW2.wrl, 13.751KB	0.00
2,2,6,6-BC	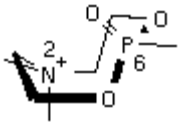 bc1PW2.wrl, 13.695KB	2.52
2,2,6,6-BC'	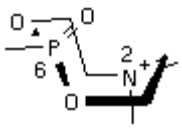 bc2PW2.wrl, 13.702KB	2.52

cis-4,6,6-Trimethyl-2-oxo-1,3,6-dioxazaphosphacinium in water shows a TB' as the global minimum. It is closely followed (0.19 kcal/mol) by a BC. The enantiomeric conformer TB appears at 1.71 kcal/mol, and the last conformer within 3.0 kcal/mol is a BC. The second BC is not the conformational enantiomer of the one at 0.19 kcal/mol.

Table 4.19. Conformers of *cis*-methyl dioxazaphosphacinium within 3.0 kcal/mol of global minimum in water.

Conformer	Structure	Energy (kcal/mol)
1,1,3,5,5-TB'	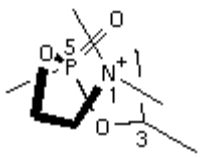 tbPW3.wrl, 14.900KB	0.00
2,2,4,6,6-BC'	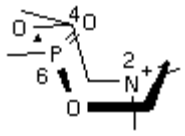 bc1PW3.wrl, 14.847KB	0.19
4,4,6,8,8-BB	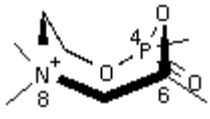 bbPW3.wrl, 14.764KB	1.71
2,2,4,6,6-BC		2.84

	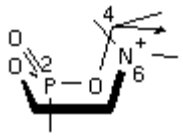 bc2PW3.wrl, 14.796KB	

trans-4,6,6-Trimethyl-2-oxo-1,3,6-dioxazaphosphacinium in water shows a BB as the global minimum another BB is at 0.49 kcal/mol. The oxygens prefer positions 1,7 and 5,7; and the *gem* groups (Me, Me and Me, oxo) are in 4,8 and 2,6. A series of BCs show up in the region from 0.89 to 4.81 kcal/mol. The BCs have 2, 4, 6 as the preferred substitution sites. There are no TBCs lower than 5.4 kcal/mol.

Table 4.20. Conformers of *trans*-methyl dioxazaphosphacinium within 3.0 kcal/mol of global minimum in water.

Conformer	Structure	Energy (kcal/mol)
4,4,6,8,8-BB	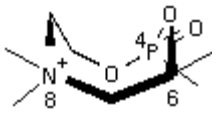 bb1PW4.wrl, 14.854KB	0.00
2,2,6,6,8-BB	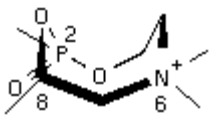 bb2PW4.wrl, 14.818KB	0.49
2,2,4,6,6-BC'	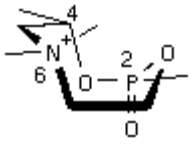 bc1PW4.wrl, 14.860KB	0.89
2,2,6,6,8-BC	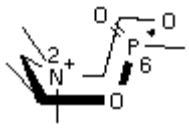 bc2PW4.wrl, 14.924KB	2.98

The results in water for 4,4,6,6-tetramethyl-2-oxo-1,3,6-dioxazaphosphacinium show TB (global minimum) and TB' (1.47 kcal/mol) as the only conformers within the 3.0 kcal/mol window. We could not characterize the lowest energy structure as either a minimum or as a saddle point. We attribute that to the different gradient-calculation algorithms used in the minimization routine and the vibrational frequencies routine. The higher gradient calculated by the frequencies routine terminated the calculation every time we attempted to characterize the stationary point. The energy minimization yielded a gradient well below 0.05 and we did not find any eclipsing methyl groups, nor torsions with values approaching 0° that could make it a saddle point, so we designate it as a minimum. We believe this intuitive supplementation of the results of this model chemistry is justified, because not including the global minimum could render our reasoning without a good foundation.

Table 4.21. Conformers of dimethyl dioxazaphosphacinium within 3.0 kcal/mol of global minimum in water.

Conformer	Structure	Energy (kcal/mol)
1,1,5,5,7,7-TB'	 tb1PW5.wrl, 15.969KB	0.00

1,1,5,5,7,7-TB	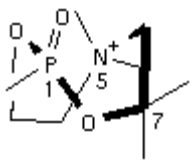 tb2PW5.wrl, 15.815KB	1.47

This ring shows conformational homogeneity, with only two conformers within 3.0 kcal/mol above the global minimum (inclusive).

Now we can compare our results to those by Dale. [Dale, 1972] Dale found that 6,6-disubstituted-1,3-dioxocanes prefer BB as the global minimum. The unsubstituted dioxazaphosphacinium ring prefers BB *in solution*, but in the gas phase it prefers BC. The *cis*-substituted ring prefers a TB in solution and a BC in the gas phase; the *trans*-substituted ring has a BB in solution and a TBC in the gas phase; while the dimethyl substituted ring prefers a TB in solution and a TC in the gas phase. Solvation plays heavily in determining the preferred conformation: the unsubstituted ring global minimum in the gas phase (BC) is destabilized in solution by 2.52 kcal/mol. The *cis*-substituted ring BC in the gas phase is destabilized by 0.19 kcal/mol. In the *trans*-substituted ring, the gas-phase TBC could not be found in solution. The gas-phase TC found for the dimethyl-substituted ring, shows up 7.51 kcal/mol higher than the global minimum in solution. Dale's finding of a BB as minimum, could be due to a true BB minimum, such as in *trans*-methyl dimethyldioxazaphosphacinium, or to a pair of rapidly interconverting TBs, which could be the case in the dimethyl substituted ring, although the searches we performed did not find the saddle point for such a transformation.

(footnotes)

[*F.PERRIN95*]	However, Perrin [Perrin, 1995] has shown two counterexamples to the commonly accepted assertion that the conformer with the *largest* dipole moment is always the *least* stable.
[*MM2MAC*]	MM2* is the modification of the MM2 force field included in the package MacroModel.
[*ND*]	*not determined
[*F.EIGHTNAME*]	We discuss the behavior of eight-membered heterocycles by using cyclooctane as a reference structure. A note on nomenclature is in order: Hendrickson developed the most generally employed nomenclature for cyclooctane conformations. [Hendrickson, 1964] His system visualizes the conformations of cyclooctane as formed by cyclohexane components. Anet [Anet, 1974] prefers the scheme suggested by Roberts [Anderson, 1969] because Hendrickson's scheme leaves the S_4 conformer without an appropriate name. For that reason, we prefer Roberts's naming scheme throughout this dissertation. The naming of the S_4 conformer is the only difference between Hendrickson's and Roberts's schemes.
[*F.ARTIFACT1*]	The absence of substitution patterns in carbons 4 and 8 may well be an artifact of the [procedure to name the conformers].
[*F.DALE72*]	The results reported by Dale *et al.* [Dale, 1972] show that 6,6-disubstituted-1,3-dioxocanes prefer the BB as the global minimum. Given the close analogy of this skeleton to that of 6,6-dimethyl-2-oxo-1,3,6-dioxazaphosphacinium, we wonder what are the reasons for this discrepancy. We defer this until we discuss the effects of solvation on the conformations of this ring. Dale carried out his determinations in $CDCl_3$ and $CHFCl_2$. Our results including water solvation *may* compare better.

Dedication

A mis padres, que me enseñaron el buen camino.

> ``(. . .)I had an extreme desire to acquire instruction. But so soon as I had achieved the entire course of study at the close of which one is usually received into the ranks of the learned, I entirely changed my opinion. For I found myself embarrassed with so many doubts and errors that it seemed to me that the effort to instruct myself had no effect other than the increasing discovery of my own ignorance."
>
> Rene Descartes, *Discourse on the Method, ed. James Fieser (Internet Release, 1996)*

[Title] [Ded] [Ack] [1] [2] [3] [4] [5] [6] [7] [Bib] [A] [B] [C] [D] [E] [Vita]

Acknowledgments

I want to thank many people: first comes Rich, who provided guidance and taught me the intellectual habits that make a good scientist. Also my friends from Baton Rouge, especially Guillermo (G-man) and Renee Morales, for all the fun we had together and for their support. Here at Virginia Tech I cannot forget Brett Kite, for providing an always challenging environment; Alex Lostetter, Dan Lough and the people in the Newman Communities (LSU and Va Tech) for helping me keep my sanity. I thank Ms. Paige Phillips for her friendship and support, and for all those discussions about chemistry.

I extend my appreciation also to my professors back in UANL (Monterrey), especially Alejandro García, Celso Rodríguez and Ricardo Flores for their exhaustive teaching and for encouraging me to pursue advanced studies.

Quentin MacDonald (Columbia Univ.) provided invaluable help by teaching me the how-to of parameter development for molecular mechanics force fields. The Computing Center at Virginia Tech gave me a generous allocation of CPU time in the IBM SP2 and SMP machines. Without these contributions, many of my calculations would have been impossible.

I thank Jan Labanowski (Ohio Supercomputer Center) for his excellent job running the Computational Chemistry List (CCL) and the members of the CCL for the high quality of their discussions about computational chemistry. Interacting with them has been (and still is) a great educational experience.

Steve Young from MDL Information Systems, Inc. provided a free copy of the software used for the chemical drawings in this dissertation (ISIS/Draw v.1.2).

This has been a time of growth and change, and many people, too numerous to list here, have influenced my life. To those that go unmentioned, I express my deepest thanks. Rest assured that the seed you planted in me will not be lost.

Chapter 1. Introduction.

This research attempted to determine the conformational behavior of several building blocks employed in our group for the design of enzymatic inhibitors. To this effect, this dissertation covers three main projects:

1. A computational study of the energetics of the hydrolysis of acetylcarnitine, accounting for the effects of changes in the predominant conformation due to solvation.
2. Effect of substitution on the conformational behavior of 4,4-dimethylmorpholinium rings, studied by computational techniques.

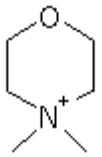

Figure 1.1. 4,4-dimethylmorpholinium ring.[fig.morph.gif, 0.44k]

3. Development of parameters for AMBER* force field, and modeling of the conformational behavior of 4,4-dimethyl-2-oxo-1,3,6-dioxazaphosphacinium rings.

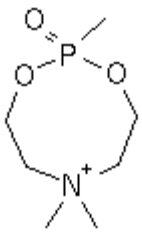

Figure 1.2. 2,4,4,-trimethyl-2-oxo-1,3,6-dioxazaphosphacinium ring.[fig.phosp.gif, 0.591KB]

1.1. Purpose of study.

Our group designs and synthesizes transition-structure analogs (TSA) as inhibitors for carnitine acetyl-, octanoyl- and palmitoyltransferases (CAT, COT and, CPT-I and CPT-II). Normally the designer of an inhibitor tries to imitate the geometry of the transition structure [Wolfenden, 1969] for the reaction catalyzed by the enzyme. Ideally, knowing the shape of the active site in an enzyme would enable us to design strong inhibitors. Presently, we only know the aminoacid sequences for CAT, COT, CPT-I and CPT-II, but their tertiary structures remain unknown. Until the resolution of the tertiary structures, only indirect methods can yield information about the shape of the active site. Knowledge of the preferred conformations adopted by TSAs, together with their measured inhibitory potency, can shed some light on the shape of the active site of these enzymes.

Inhibitors for CAT, COT and CPT can help us understand the role of each carnitine acyltransferase in the cell. Such understanding will help us in the design of potentially therapeutic compounds for diseases like diabetes and myocardial ischemia.

As the costs of experimentation and waste disposal continue to increase, it is imperative to find more efficient ways to choose targets for synthesis, especially those compounds with a greater chance of success as inhibitors. Computer

modeling allows us to examine many compounds before choosing a target. The question then becomes: are there any modeling methods refined to the point they can yield reliable results for charged species? In particular, modeling of species with charges such as morpholinium, and zwitterions as that of carnitine in solution is difficult. [Note.] We need, however, such modeling to understand the conformational preferences of the reactants --acetylcarnitine, carnitine-- and the enzymic reaction intermediate to achieve a more rational design of inhibitors. As several of our inhibitors include phosphonate substructures, we require methods able to deal with them. Such methods are not widely available; modeling of phosphonates has certainly lagged behind that of more popular phosphorus species, such as phosphates.

For these purposes we want to assess the ability of current state-of-the-art computational methods to model the compounds of our concern. We put particular emphasis on the inclusion of solvent effects, so we want to see the abilities of methods such as COSMO to reproduce properties such as dipole moments and heats of formation in solution. As we need to consider hundreds of conformations and configurations in crowded, charged species, optimization of computer resources is essential. We therefore need to evaluate the applicability of ab initio, semiempirical and molecular mechanics methods so that we spend a minimum of resources without undermining the quality of the predictions.

Among the problems we face are: the high free energy of hydrolysis of acetylcarnitine, which qualifies it as a high-energy molecule. This high energy has remained unexplained for about three decades. [Friedman, 1955] The conformational dynamics of six- and eight-membered heterocycles are still imperfectly understood. [Eliel, 1994] All these pieces of information can help us understand the mode of action of the inhibitors already available to us.

We can take two approaches to deal with modeling:

1. As a tool oriented to engineering of results, meaning that achieving experimental accuracy is the most important matter, even though the methods may not have full theoretical justification.
2. As a research tool, where the theoretical basis of the method can provide insight on the mechanisms underlying the phenomenon of interest, even if the approximation to experiment is only qualitative.

In general, molecular modelers use a combination of the two approaches, and it would be difficult to find examples of ``pure'' techniques, (techniques that adhere strictly to only one approach). Regardless of the ``purity'' of the technique employed, if we can model experimental results, we can gain confidence on the predictions generated for systems that have not been tested yet. How closely should the modeling results approach the experimental results to render the modeling as reliable? This is a somewhat subjective matter, as there are no hard guidelines to make such a decision.

(footnotes)

[*F.SOLVATION*] Cramer and Truhlar [Cramer, 1995] have reviewed the performance of several solvation models and critically analyzed their implementations. One of their conclusions is that few software packages take into account both the contributions of charge and of multipolar moments, such as dipole, quadrupole, octapole and hexadecapole moments.

Chapter 2. Historical.

2.1. Introduction.

This review reproduces the latest advances in the design of carnitine acyltransferase inhibitors, and provides only the background necessary for a fruitful discussion of the conformational behavior of the inhibitors mentioned below.

2.2. Acyltransferase inhibitors.

One common strategy to design enzymatic inhibitors is to use transition-structure-analog theory [Wolfenden, 1969] to design a compound that the enzyme can recognize. Binding of the following tetrahedral intermediate is commonly considered important in the transfer of acyl groups to CoA:

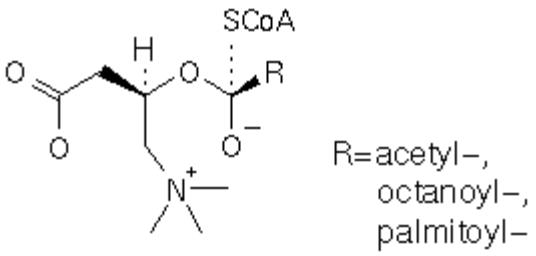

Figure 2.1. Tetrahedral intermediate for Carnitine-CoA acyl transfer. [fig.gandour93.gif, 1.231KB]

We can classify enzymatic inhibitors according to their observed effects on enzymatic activity (reversible or irreversible) or by their mechanism of action (competitive or noncompetitive). Irreversible inhibitors eliminate enzymatic activity in such a way that the enzyme does not recover its original activity. Reversible inhibitors allow the recovery of catalytic activity after elimination of the inhibitor. Competitive inhibitors bind to the active site instead of the substrate, while noncompetitive inhibitors do not attach themselves to the active site, so the substrate can still bind to the enzyme. Thus we have four main types of enzymatic inhibitors:

1. Competitive reversible
2. Competitive irreversible
3. Noncompetitive reversible
4. Noncompetitive irreversible

Competitive carnitine analogs constitute our primary concern, but we include summaries of the other types for the sake of completeness. We offer only a brief description of each, as Colucci and Gandour [Colucci, 1988] have reviewed extensively CAT inhibitors.

2.2.1. Competitive reversible inhibitors.

(*S*)-Carnitine and (*S*)-acetylcarnitine inhibit competitively pigeon CAT. [Tipton, 1969] Tipton and Chase justified the recognition of the *S* isomers by postulating a two-point recognition site that binds only to carboxylate and ammonium. CATs extracted from bovine heart, pig heart and mouse-liver peroxisomes discriminated substantially between the (*R*) and the (*S*) isomers. The authors postulated a more restricted two-point recognition site, or a three-point recognition site for these CATs.

Aminocarnitine

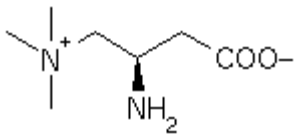

Figure 2.2. Aminocarnitine.[fig.aminocarn.gif, 0.595KB.]

is a weak reversible competitive inhibitor for CAT, although it inhibits strongly both CPT-I and CPT-II. [Kanamaru, 1985] [Jenkins, 1985] [Jenkins, 1986] Due to the isosteric relationship to carnitine, *N*-Acylated derivatives of racemic aminocarnitine can also inhibit reversibly carnitine acyltransferases, as shown by the great inhibitory potency of D,L-acetylaminocarnitine. [Jenkins, 1985] (*R*)-acetylaminocarnitine --named ``emeriamine'' because it was isolated from a culture filtrate of *Emericella quadrilineata*-- showed even stronger inhibitory action than the racemic compound. [Shinagawa, 1987]

Gandour *et al.* [Gandour, 1986] [Gandour, 1992] showed good inhibition of CAT by hemiacylcarnitinium (HAC). Later, the same authors [Gandour, 1988] [Gandour, 1993] demonstrated the strong activity of hemipalmitoylcarnitinium (HPC) as a competitive inhibitor of CPT-I. HAC inhibits CAT, but not CPT. HPC inhibits CPT, but not CAT. It seemed that CPT requires a long chain for proper recognition of the substrate. These differences in the specificity of the inhibitors allowed for a partial mapping of the topographies of the active sites in both enzymes. The design of all these inhibitors relied on making them analogs of the [tetrahedral intermediate] mentioned previously by means of restricting the conformations with a morpholinium moiety:

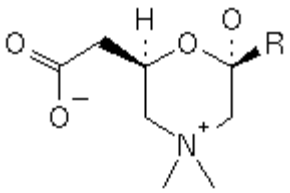

Figure 2.3. Hemiacylcarnitinium moiety. [fig.HAC.gif, 0.740KB]

The morpholinium ring locks the N-CH_2-CH-OH(Ac) torsion of the carnitine backbone in the *gauche* conformation. The authors stated the difficulty of excluding selective binding of the open form of the hemiacetal, but "presumably" hemiacylcarnitiniums bind as cyclic structures. NMR did not detect any open form of the compound in solution.

Saeed *et al.* [Saeed, 1993] showed that 3-hydroxy-5,5-dimethylhexanoic acid

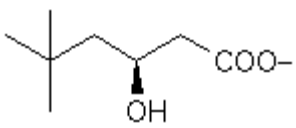

Figure 2.4. 3-hydroxy-5,5-dimethylhexanoic acid. [fig.saeed93.gif, 0.581KB]

competitively inhibited CAT, CPT-I and CPT-II, indicating that these enzymes require a positively charged center to show catalysis. Saeed *et al.* [Saeed, 1994] later reported the inhibitory properties of 3-amino-5,5-dimethylhexanoic acid.

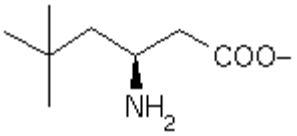

Figure 2.5. 3-amino-5,5-dimethylhexanoic acid.[fig.saeed94.gif, 0.585KB]

Both 3-hydroxy- and 3-amino-5,5-dimethylhexanoic acid are alternative substrates for CAT.

Gandour's group evaluated Protein Kinase C, COT and CPT inhibitors based on a 2-oxo-1,3,6-dioxazaphosphacinium moiety. [Kumaravel, 1994]

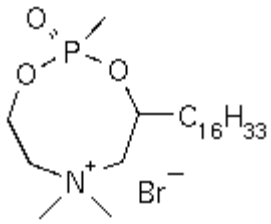

Figure 2.6. 4-hexadecyl-2,4,4-trimethyl-2-oxo-1,3,6-dioxazaphosphacinium bromide.[fig.kumaravel94.gif, 0.743KB]

The authors tested racemic mixtures (2*S*, 4*S*)/(2*R*, 4*R*) and (2*S*, 4*R*)/(2*R*, 4*S*) and found they inhibited COT and CPT-II moderately.

Gandour's group also reported several CAT inhibitors incorporating a methylenecarboxylate substructure on a morpholinium ring. [Sun, 1995]

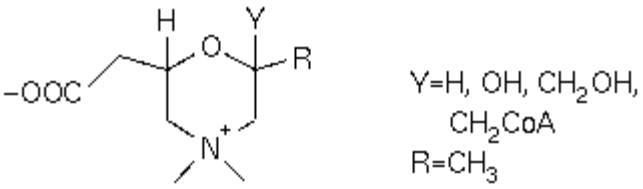

Figure 2.7. 6-(Carboxylatomethyl)-2-(hydroxymethyl)-2,4,4-trimethylmorpholinium.[fig.sun95.gif, 1.157KB]

All four stereoisomers were evaluated for inhibitory activity and the authors concluded that ``CAT recognizes both configurations at C2 and C6 in the analogues."

Anderson *et al.* [Anderson, 1995] reported on the potency of a series of CPT-I inhibitors based on a phosphonate moiety designed by transition-structure-analog theory.

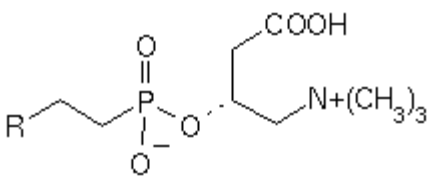

Figure 2.8. Anderson's phosphonate.[fig.anderson951.gif, 0.842KB]

This compound showed appreciable inhibitory activity. After trying systematic structural variations, they found that the following phosphate:

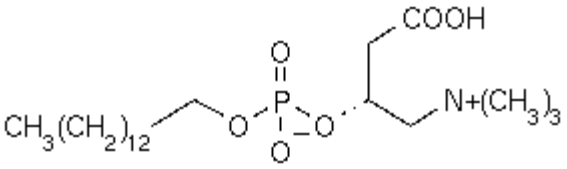

Figure 2.9. Anderson's phosphate.[fig.anderson952.gif, 0.980KB]

inhibited to a level comparable to the phosphonate. Both the phosphonate and the phosphate could show similar detergency, thus explaining the similar inhibition. The authors discarded such an explanation due to the stronger inhibition shown by the *R* enantiomers when compared to the *S* enantiomers.

2.2.2. Competitive irreversible inhibitors.

We can visualize the enzyme and the substrates as part of a ternary complex. **Bisubstrate inhibitors** resemble the spatial disposition of the substrates, leaving the enzyme as the "third" component. One of the earliest examples of a bisubstrate inhibitor is *S*-carboxymethyl-CoA-(*R*)-carnitine ester, reported by Chase and Tubbs. Bromoacetyl-CoA and bromoacetyl-(*R*)-carnitine are also bisubstrate inhibitors for CAT. [Chase, 1969]

Fritz and Schultz [Fritz, 1965] reported inhibition of CAT by *p*-hydroxymercuribenzoate (HMB) at a concentration of 2.6 {micro}M. Such inhibition was prevented or *partially* reversed by addition of acetyl-CoA, which suggested to these authors that HMB may bind to the active site.

Several groups have reported compounds possessing inhibitory activity towards carnitine acyltransferases. Etomoxir (2-[6-(4-chlorophenoxy)hexyl]oxirane-2-carboxylate) is an irreversible inhibitor of CPT-I. [Eistetter, 1982] Tetradecylglycidate (TDGA) is also an oxirane-based irreversible competitive inhibitor of CPT-I. [Tutwiler, 1985]

Another competitive inhibitor is methoxycarbonylCoA disulfide, [Venkatraghavan, 1983] which modifies selectively a sulfhydryl group in the active site. Dithioerythritol or thiocholine can partially reverse its action.

2.2.3. Noncompetitive reversible inhibitors.

5,5'-Dithiobis(2-nitrobenzoic acid) (DTNB), reacts with sulfhydryl groups in a non-specific way. It inhibits pig heart CAT [Fritz, 1963] and pigeon breast CAT. [Venkatraghavan, 1983] Because this reagent forms disulfide linkages, adding a disulfide exchange reagent such as dithiothreitol, dithioerythritol or thiocholine can restore enzymatic activity.

Derrick and Ramsay [Derrick, 1989] showed that malonylCoA is a reversible inhibitor of peroxisomal CPT-I, but does not show competitive behavior. These authors estimated that peroxisomal palmitoyltransferase activity constituted up to 20% of the peroxisomal + overt-mitochondrial pool in fed-rat liver. A concentration lower than 10{micro}M of malonyl-CoA was enough to show 90% inhibition of the peroxisomal palmitoyltranferase.

2.2.4. Noncompetitive irreversible inhibitors.

Fritz and Schultz [Fritz, 1969] reported the inhibitory activity of $ZnCl_2$, $HgCl_2$, *N*-ethylmaleimide and iodoacetamide.

Addition of ethanethiol prevented or partially reversed $HgCl_2$ inhibition. The authors did not cite the values of K_i for these compounds.

[Title] [Ded] [Ack] [1] [2] [3] [4] [5] [6] [7] [Bib] [A] [B] [C] [D] [E] [Vita]

Chapter 3. Acetylcarnitine hydrolysis.

3.1. Review of literature.

3.1.1. Acylcarnitines in cellular metabolism.

Carnitine transports long-chain fatty acids across the mitochondrial membrane; thus, it is essential for lipid metabolism. Bieber reviewed the metabolic roles of acylcarnitine. [Bieber, 1992] In microsomes and peroxisomes, carnitine transports medium-chain fatty acids into the cytosol. Non-Insulin-Dependent Diabetes (NIDD) and myocardial ischemia are among the diseases thought to bear a relationship to carnitine. Carnitine abounds in semen, although the reason for its presence remains a matter of speculation.

CAT catalyzes the acetylation of carnitine. [Colucci, 1988] Acetylated carnitine has a large group-transfer potential, which makes it an active form of acetate that the mitochondria can use efficiently for oxidation. A carrier of acetyl groups is necessary, because the inner mitochondrial membrane is impermeable to Coenzyme A (CoA) and AcetylCoenzyme A (AcCoA).

There are (at least) two kinds of CPT, usually designated as CPT-I and CPT-II. CPT-I resides inside the inner mitochondrial membrane, while CPT-II is attached to the outside of the outer mitochondrial membrane. MalonylCoA, CPT-I and fatty acylCoA form part of a mechanism that regulates glucose levels. Inhibition of CPT-I by high malonylCoA levels suppresses fatty acid synthesis and oxidation in the liver, while a high level of fatty acylCoA lowers malonylCoA levels. Thus, CPT inhibitors are potential therapeutic agents for diabetes.

COT is the long-chain carnitine acyltransferase on peroxisomes. Peroxisomes have the ability to oxidize fatty acids. COT is likely the enzyme responsible for forming carnitine esters of aromatic and branched alkyl acids, which form in the metabolism of drugs.

3.1.2. Thermodynamics of acetylcarnitine hydrolysis.

3.1.2.1. High-energy compounds.

The high energy of hydrolysis of acetylcarnitine places it in the ``energy-rich'' category, like ATP, but the body does not use acetylcarnitine for energy storage. Two basic questions are:

1. How does acetylcarnitine store chemical energy?
2. Why the need for such a high energy?

In this work we shall address mostly the first question, but first a note on terminology: we use the definition of **energy-rich compound** (also called ``high-energy'' compound) suggested by Jencks: [Jencks, 1960]

> ``(. . .)an ``energy-rich'' compound is one which will react, *under physiological conditions*, with a substance that is commonly present in the environment, to liberate a large amount of free energy.''

A free energy of hydrolysis is ``high-energy'' if it releases more than -7.0 kcal/mol, according to Jencks. In addition to ATP, other biomolecules qualify as energy-rich compounds.

Burton [Burton, 1954] measured the free energy of hydrolysis of the thioester bond in AcCoA, reaching a value close to -8 kcal/mol. Burton noticed that this high free energy of hydrolysis puts AcCoA in the same category of ``high-

energy molecule" as ATP. Later, after determining the free energy of hydrolysis of thiol esters and aminoacid esters, Jencks *et al.* [Jencks, 1960] concluded that both qualified as energy-rich compounds. Thiol esters had a free energy of hydrolysis of approx. -7.7 kcal/mol. They reported that, in general, the difference in free energies of hydrolyses between oxygen esters and thiol esters, was approx. 2.5 kcal/mol. This lower value of free energy of hydrolysis placed the oxygen esters outside the energy-rich range. Aminoacids seemed a special case, given that hydrolysis of glycine ethyl ester to the dissociated acid (zwitterionic form) had a free energy change of -8.4 kcal/mol *at pH=7.0*. As a comparison, hydrolysis of glycine ethyl ester to the undissociated acid yielded a free energy change of -1.97 kcal/mol, very similar to that of ethyl acetate. Jencks ascribed the high free energy of hydrolysis of glycine ethyl ester to a destabilizing effect of the positively charged ammonium group, rather than to the high acidity of glycine.

The first indication of the high-energy status of acetylcarnitine came from Friedman and Fraenkel [Friedman, 1955] who reported on the ability of acetylcarnitine to transfer an acetyl group to CoA. They studied the effects of added carnitine on the enzymatic acetylation of *p*-aminobenzoic acid. Carnitine inhibited the acetylation reaction, while neither the zwitterion of glycine, choline or {beta}-hydroxybutyrate showed any inhibitory activity. Acetylcarnitine reversed the inhibition produced by carnitine, while an equivalent amount of acetate added to a carnitine-inhibited system failed to restore enzymatic activity. A few years later, Fritz *et al.* [Fritz, 1963] were the first to measure the high free energy change in the hydrolysis of acetylcarnitine. They reported a value of -7.9 kcal/mol at pH=7.0. This value changed little when using chains longer than acetyl. Acetylcarnitine participated in an acetyl group exchange equilibrium with AcCoA, with an equilibrium constant approximately equal 0.6. Their results indicated that acetylcarnitine required a free carboxylate group to show activity and they postulated anchimeric assistance of the carboxylate (fig.fritz63.gif, 2.362KB) as a step in the acetyl hydrolysis.

Müller and Strack [Müller, 1973] determined the enthalpies of hydrolysis of a series of acylcarnitines, acetylcholine [see figure], glycine methyl ester and acetyl-{beta}-methylcholine by microcalorimetry. Their results show that the enthalpic term contributes the most to the free energy of hydrolysis. For the acylcarnitines, the entropic term is relatively small and invariant with chain length. Glycine methyl ester, acetyl-{beta}-methylcholine, and acetylcarnitine methyl ester had less negative enthalpies of hydrolysis than acetylcarnitine, at pH=7.0, by about 2 kcal/mol.

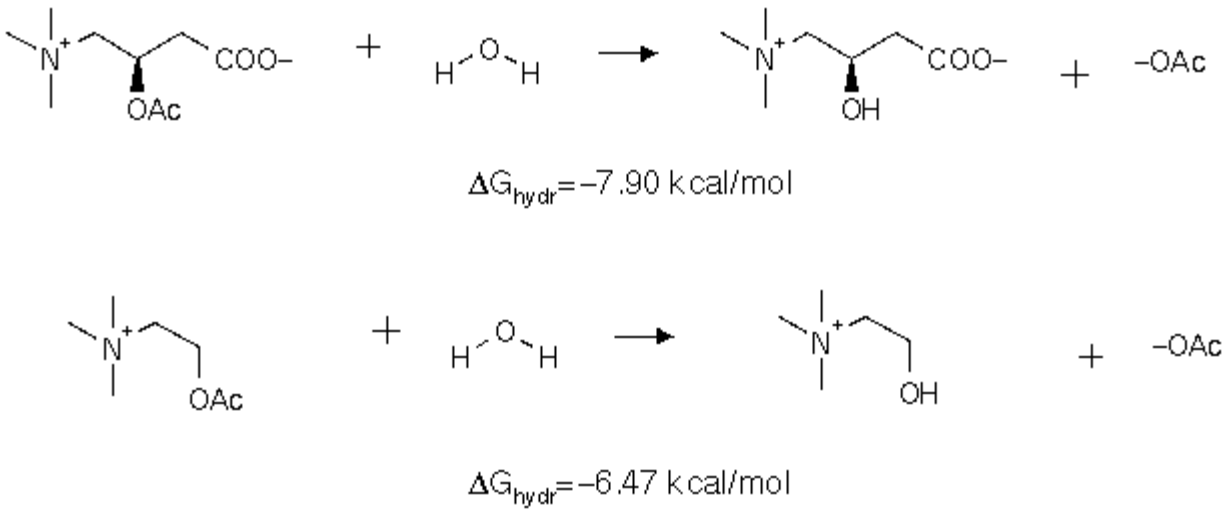

Figure 3.1. Comparison of free energies of hydrolysis between acetylcarnitine and acetylcholine.[fig.hydrolysis2.gif, 2.714KB]

The previous values were determined at buffered pH=7.0. For the process at pH=4.0 (producing HOAc instead of $^{-}$OAc), the values are -4.63 kcal/mol for acetylcarnitine, and -3.20 kcal/mol for acetylcholine. The difference (1.43 kcal/mol) does not depend on pH.

Pierlik and Guynn [Pierlik, 1975] compared the group-transfer potential of acetylcarnitine and acetylcholine under physiological conditions. They found the free energy of hydrolysis of acetylcarnitine only 1.21 kcal/mol more negative

than that for the hydrolysis of acetylcholine: -8.20 kcal/mol for acetylcarnitine vs. -6.99 kcal/mol for acetylcholine.

3.1.2.2. Effects of solvation on thermodynamic quantities.

George *et al.* [George, 1970] called attention to solvation effects in the hydrolysis of ATP. Their work remarked the influence of differential solvation between reactants and products as a ``(. . .) major factor contributing to the thermodynamic reactivity (. . .)". They found that, as the charge increased, water solvation could stabilize multiply charged species such as phosphates, compensating for the increased electrostatic repulsion of the multiple negative charges present in such anions as pyrophosphate, tripolyphosphate, and glucose-6-phosphate.

Wolfenden discussed a similar question about the contributions of solvent effects in group-transfer potentials of uncharged species, mostly of mixed anhydrides of phosphoric and carboxylic acids, [Wolfenden, 1989] as well as carbohydrates. [Wolfenden, 1988] He pointed to the role of solvation energy of the products as a driving force for the reaction when he inquired ``(. . .)whether the large negative change in free energy, that normally accompanies conversion of mixed phosphoric-carboxylic anhydrides to the products of their hydrolysis in dilute aqueous solution, may depend on differences in free energy of solvation between the reactants and the products." One of his findings was that ``(. . .)the uncharged products of hydrolysis of acetyl dimethyl phosphate are solvated much more strongly by water than are the reactants."

Hayes *et al.* [Hayes, 1978] did ab initio calculations on hydrolytic reactions of several high-energy molecules. Their results, which included ``a crude reaction field solvent model", pointed out that the greatest contributions to the energies of hydrolysis came from the relative solvation energies of reactants and products. The relative solvation energies were ``by far the most important factors in determining the energies", especially in those cases of greatest importance in energy storage and transduction, namely,

```
ATP --> ADP + orthophosphate
```

and

```
phosphocreatine + ADP --> creatine + ATP
```

Marsh *et al.* [Marsh, 1980] applied ab initio methods together with molecular mechanics to the study of AMP derivatives. The greater exothermicity of 3',5'-cyclic AMP vs. trimethylene phosphate was attributed to: strain due to *trans* fusion in 3',5'-cyclic AMP (4-5 kcal/mol), an unfavorable O-C-C-O interaction relieved by ring opening (1-2 kcal/mol, because the interaction depends on the solvent), and 1-2 kcal/mol ascribable to differential solvation between reactants and products.

3.1.2.3. Relationship between conformational preference and thermodynamics.

Colucci *et al.* [Colucci, 1986] conducted NMR measurements in D_2O and MM2 calculations that showed that, upon hydrolysis, the predominant conformation of the carnitine skeleton changes from ``folded" to ``extended". The N-CH_2-CH-OH(Ac) torsion angle remained *g*- throughout.

3.2. Results and Discussion.

The carnitine backbone can present two major conformations:

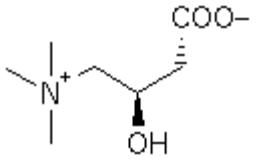

Figure 3.2. ``Folded'' conformer of carnitine.[fig.folded.gif, 0.510KB]

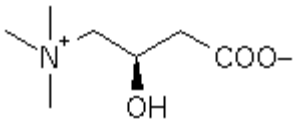

Figure 3.3. ``Extended'' conformer of carnitine.[fig.extended.gif, 0.608KB]

We can break down the process of hydrolysis to that of individual conformers:

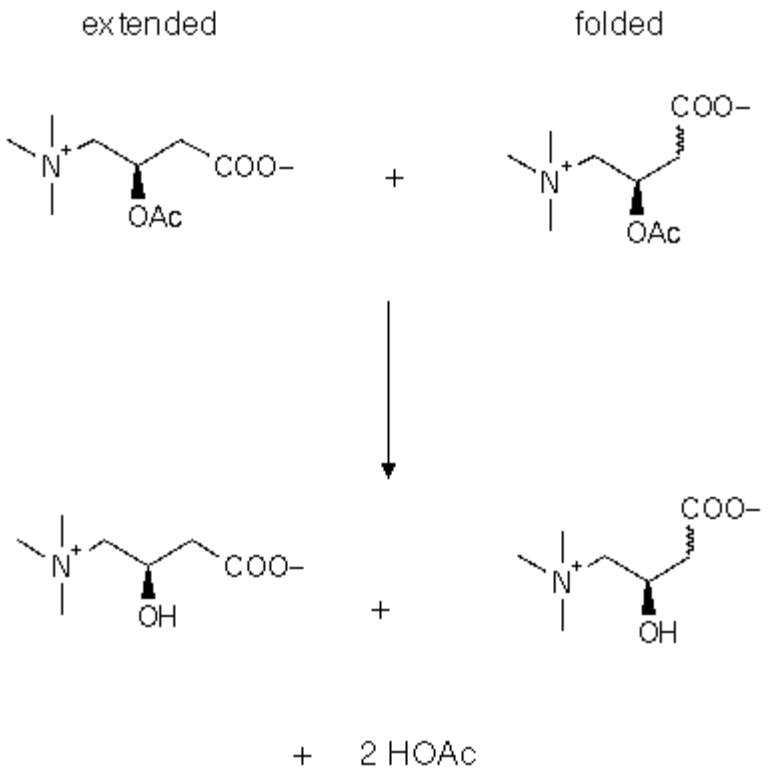

Figure 3.4. Hydrolyses of extended and folded conformers.[fig.hydrolysis1.gif, 2.491KB]

In general, the ratios extended:folded before and after hydrolysis are not the same.

We studied the thermodynamics of acetylcarnitine hydrolysis by semiempirical and ab initio methods both in the gas phase and solvent.

3.2.1. Conformational analyses in gas phase.

We calculated the enthalpies of formation and dipole moments of acetylcarnitine, carnitine, acetylcholine, choline, 3-acetoxypropanoate and 3-hydroxypropanoate in gas phase (see tables). We justified our use of enthalpies instead of free energies on the results reported by Müller and Strack. [See review of literature.]

- Acetylcarnitine in gas phase.
- Carnitine in gas phase.
- Acetylcholine in gas phase.
- Choline in gas phase.
- 3-Acetoxypropanoate in gas phase.
- 3-Hydroxypropanoate in gas phase.

The labels for torsion angles in the tables are as follows:

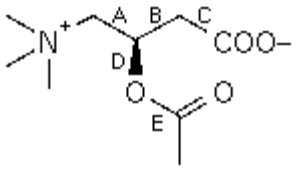

Figure 3.5. Labels for torsion angles used in acetylcarnitine.[fig.torsions.gif, 0.731KB]

A

$N\text{-}CH_2$ - CH-OH(Ac)

B

$CH_2\text{-}CH$ - CH_2COO^-

C

C-C - $C(O)\text{-}O^-$

D

$CH_2\text{-}CH$ - O-H(Ac)

E

C-O - $C(O)\text{-}CH_3$

The hydrolyses of acetylcholine to choline and of 3-acetoxypropanoate to 3-hydroxypropanoate constituted our reference points.

Acetylcholine and choline cannot show an extended or a folded conformation because they lack the methylenecarboxylate group, so they helped us assess the importance of the gauche effect [(see section below)] [Sundaralingam, 1968] [Wiberg, 1990] and of the CH_2-CH-O-H(Ac) torsion in the energetics of the hydrolysis. The propanoates can show folded and extended conformations, but are not affected by the gauche effect.

3.2.1.1. Acetylcarnitine vs. carnitine.

Anti conformers of $N\text{-}CH_2$-CH-OH(Ac) account for nearly 50% of the population of acetylcarnitine but only 1% for carnitine. The CH_2-CH-CH_2-COO^- torsion angle always prefers *gauche* + (*g*+) in carnitine and *gauche* - (*g*-) in acetylcarnitine, so folded conformations comprise 100% of the populations. We can explain this preference by Coulombic attraction between the negatively charged carboxylate and the positively charged tetramethylammonium moiety: the *gauche* conformation allows the closest approach of the charged centers.

Given that the distance between the charged centers does not change much because the conformation is always folded, we expect only a small change in the dipole moment when hydrolyzing acetylcarnitine to carnitine (the dipole moments depend on charge separation). The results of the calculations confirm this suspicion; the global minimum in acetylcarnitine has a dipole moment of 12.15 D, and the global minimum in carnitine a dipole moment of 12.74 D. The hydroxyl group in carnitine could hydrogen bond to the carboxylate. A distance of 2.1 Å separates a carboxylate oxygen from the hydroxylic proton. This indicates a weak hydrogen bond.

3.2.1.2. Acetylcholine vs. choline.

The calculations reproduce the gauche effect: in both cases, the N-CH_2 - CH-OH(Ac) torsion angle prefers a *gauche* conformation. The *gauche*/*anti* energy gap in choline is 1.76 kcal/mol, but in acetylcholine is only 0.28 kcal/mol. Conformers with the N-CH_2 - CH-OH(Ac) torsion angle as *anti* make up about 15% of the population in acetylcholine compared to the 0.01% in choline. Differences in the inductive effects of a hydroxylic oxygen vs. an ester oxygen might explain the difference, given that the gauche effect relates to the electronegativity of the atoms X and Y that form the fragment X-C-C-Y. Conjugation of the ester oxygen with the carbonyl group can decrease the inductive effect exerted on the carbon. Such effect does not appear in the hydroxylic oxygen.

The dipole moments have a good correlation with stability: in both cases the global minimum has the lowest dipole moment, 5.9 D in acetycholine and 2.34 D in choline.

3.2.1.3. Acetoxypropanoate vs. hydroxypropanoate.

Acetoxypropanoate prefers a folded conformation [Note.] in gas phase. This means that torsion B prefers a *gauche* conformation, but this should not be construed as an example of gauche effect because carboxylates do not have an inductive effect strong enough to cause gauche effect. [Juaristi, 1995] 3-Hydroxypropanoate shows equal proportions of *g*+ and *anti*. Hydrogen bonding between the carboxylate and the hydroxyl group seems to favor the *anti* conformation. The expected dipole moment decreases from 6.8 D to 5.4 D upon hydrolysis.

Steric effects and dipole moment reduction seem to control the conformational preference: the bulkiest groups (acetoxy and carboxylate) stay *anti* to each other, and the global minimum has the lowest dipole moment in acetoxypropanoate, 6.8 D and one of the lowest in hydroxypropanoate, 5.4 D.

3.2.1.4. Carnitines vs. cholines.

The N-CH_2-CH-OH(Ac) torsion is *anti* in 15% of the population of acetylcholine, while this conformation makes up approx. 50% of the population in acetylcarnitine. Torsion angles CH_2-CH-O-H(Ac) and C-O-C(O)-CH_3 show parallel behavior: CH_2-CH-O-H(Ac) prefers *g*, although in acetylcarnitine nearly 35% of the conformers have this torsion as *anti*. C-O-C(O)-CH_3 prefers *syn* (*s*) in all cases.

For carnitine vs. choline we observe no major differences in the preferred conformations: N-CH_2-CH-OH(Ac) prefers *gauche*, although carnitine shows 1% of *anti* vs. the 0.01% for choline. CH_2-CH-O-H(Ac) always prefers the *anti*.

3.2.1.5. Carnitines vs. propanoates.

Acetylcarnitine has 100% of the population folded, acetoxypropanoate has 92% folded. Torsion CH_2-CH-O-H(Ac) shows some variation, mostly because of the presence of several *anti* torsion angles in acetylcarnitine. Torsion angle C-O-C(O)-CH_3 shows opposite behavior in the two molecules: E prefers *s* in acetylcarnitine and *anti* in

acetoxypropanoate. However, the global minima have the ``same" conformation, as long as all the torsions in acetoxypropanoate have a corresponding torsion in acetylcarnitine.

In carnitine, 99% of the population is folded, vs. only 51% in hydroxypropanoate.

3.2.2. Ab initio results in the gas phase.

We calculated the predominant conformations, found by AM1, at the RHF/6-31G* level of theory for both the zwitterions and the cations. Calculations for the anions used the 6-31+G basis set. We conducted full optimizations in the gas phase (see tables). In the following tables, the conformer designated as "1" is the global minimum by AM1, and "2" is the conformer next in energy above the global minimum. [Table AM1 vs 6-31G* (gas)]

Table 3.1. Comparison of AM1 vs. 6-31G* calculations on carnitines and cholines in the gas phase.

Compound	{delta}E AM1 (kcal/mol)	{delta}E HF/6-31G* (kcal/mol)	{delta}E MP2 (kcal/mol)	{mu} AM1 (D)	{mu} HF/6-31G* (D)	{mu} MP2 (D)
Acetylcarnitine 1	0.00	0.00	0.00	12.15	10.72	10.72
Acetylcarnitine 2	0.20	-0.66	0.86	12.66	12.81	12.81
Carnitine 1	0.00	0.00	0.00	12.74	12.22	12.22
Carnitine 2	0.94	-0.86	-0.50	13.42	12.54	12.54
Acetylcholine 1	0.00	0.00	0.00	5.92	6.16	6.16
Acetylcholine 2	0.45	0.55	1.83	6.20	6.95	6.95
Choline 1	0.00	0.00	0.00	2.34	1.86	1.86
Choline 2	4.89	4.46	5.76	4.10	3.64	3.64

3.2.3. Comparison of AM1 vs. ab initio.

We observe several differences between the ab initio and the semiempirical results. The acetylcarnitine global minimum by AM1 is a local minimum in the HF/6-31G* hypersurface, but the inclusion of electronic correlation reverses the effect. The dipole moments calculated by HF/6-31G* follow the same trend as those calculated by AM1. Most of the ab initio dipole moments approach closely the values obtained by AM1, with one exception (Acetylcarnitine 1), where the ab initio value is nearly 1.4 D lower than the semiempirical. The difference may be due to the lack of geometric optimization, meaning that we do not have a stationary point on the HF/6-31G* hypersurface, or probably due to the adjustment in the number of surface points included in the calculation. For more details, [refer to the Methods section].

Table 3.2. Comparison of AM1 vs 6-31+G calculations on propanoates in the gas phase.

Compound	{delta}E AM1 (kcal/mol)	{delta}E HF/6-31+G (kcal/mol)	{delta}E MP2 (kcal/mol)	{mu} AM1 (D)	{mu} HF/6-31+G* (D)	{mu} MP2 (D)
Acetoxypropanoate 1	0.00	0.00	0.00	6.68	8.41	8.41

Acetoxypropanoate 2	0.24	0.00	0.00	6.64	8.41	8.41
Hydroxypropanoate 1	0.00	0.00	0.00	5.37	5.82	5.82
Hydroxypropanoate 2	0.01	0.00	0.00	5.37	5.82	5.82

The table shows that in the anions, correlation effects [Note.] do not exert a great influence. Given that we did not use succesively higher levels of theory in the ab initio calculations to assess convergence, we cannot guarantee that correlation effects are not likely to change with higher levels of theory. More importantly to us, we observe that the trends of the MP2 calculations are the same as that of HF. We notice that the same geometries that AM1 calculated as different in energy, are degenerate by ab initio. This may be a reflection of the numerous convergence problems found when using AM1 on these anions.

3.2.4. Conformational analyses including the effect of solvent.

We calculated the enthalpies of formation and dipole moments of acetylcarnitine, carnitine, acetylcholine, choline, 3-acetoxypropanoate and 3-hydroxypropanoate including the effect of solvent. We used full optimization in MOPAC93 using the COSMO solvent model, while the ab initio calculations involved single points at the RHF/6-31G* level of theory employing the solvent model developed by Tomasi. [Miertus, 1982], [Miertus, 1981]

The following tables gather the semiempirical results:

- Acetylcarnitine in water.
- Carnitine in water.
- Acetylcholine in water.
- Choline in water.
- 3-Acetoxypropanoate in water.
- 3-Hydroxypropanoate in water.

3.2.4.1. Acetylcarnitine vs. carnitine

The N-CH_2-CH-OH(Ac) torsion remains fairly constant, although we still see a slight favoring of the *anti* conformation in acetylcarnitine: conformers with the N-CH_2-CH-OH(Ac) torsion angle *anti* make up almost 9% of the population in aceytlcarnitine, while in carnitine they account for less than 4%.

Regarding the CH_2-CH-CH_2-COO^-, the extended conformation constitutes 39% of the population, almost as much as the 43% of the folded. In carnitine we see the situation reversed, with the extended predominating over the folded (61% vs. 27% respectively). Differences in solvation can explain this reversal, as solvation differences relate to polarity: as the distance between the charged centers in the molecule differs between the folded and the extended, we expect the calculated dipole moments to differ as well. In acetylcarnitine, the folded has a dipole moment of 26.67 D vs. the 29.90 D of the extended. In carnitine, the folded conformation has a dipole moment of 23.89 D vs. the 29.17 D of the extended.

There is little support for hydrogen bonding between the carboxylate and the hydroxyl groups in carnitine. In the global minimum (extended conformer), the carboxylic oxygen closest to the hydroxylic proton is 3.8 Å away from it. The only conformer showing a O-H···O distance adequate for hydrogen bonding (2.8 Å) accounts for < 4% of the population.

3.2.4.2. Acetylcholine vs. choline.

Anti conformers of N-CH_2-CH_2-OH(Ac) make up about 4% of the population in acetylcholine. In choline, these conformers account for more than 9% of the population. Differential solvation might hold the key to this reversal in the conformational preference: the global minimum in acetylcholine (N-CH_2-CH-OAc *g*-) has a dipole moment of 10.85 D, while the *anti* conformation of N-CH_2-CH-OAc has a dipole moment of 9.24 D, a difference of 1.6 D. In choline, on the other hand, the global minimum (N-CH_2-CH-OH *g*-) has a dipole moment of 5.25 D, while the *anti* conformer has a dipole moment of 5.07 D. The difference is now less than 0.2 D. We can see that solvation stabilizes the choline conformers to an almost equal extent, while in acetylcholine, the lower polarity of the *anti*-containing conformer increases the energy gap, by solvating more the global minimum.

3.2.4.3. Acetoxypropanoate vs. hydroxypropanoate.

The H-C-C-COO- torsion prefers *g*-, although the *anti* and the *g*+ each make up about 12% of the population. The C-C-C(O)-O- torsion does not change much upon hydrolysis, although hydroxypropanoate shows a much lower percentage of *g*+. The H-C-O-H(Ac) torsion prefers *anti* in both cases. Acetoxypropanoate in solution differs from gas phase by a greater stabilization of *anti* conformations in torsions CH_2-CH-CH_2-COO^-, CH_2-CH-O-H(Ac) and C-O-C(O)-CH_3. *Anti* conformers of these torsion angles have the highest dipole moments in the gas phase (10 >{mu}< 14), so solvation reduces the energy gap to the point that the global minimum in solution accounts only for 0.06% of the population in the gas phase. The population of 3-hydroxypropanoate in solution differs from that in the gas phase because of a lower presence of the extended conformer. The dipole moment decreases from 16.07 D in acetoxypropanoate to 8.93 D in hydroxypropanoate.

3.2.4.4. Carnitines vs. cholines.

Both acetylcarnitine and acetylcholine show gauche effects in the N-CH_2-CH-OAc torsion. The CH_2-CH-O-Ac torsion angle is *g*- in both global minima, but in acetylcarnitine it shows a greater population of *anti*. The CH-O-C(O)-CH_3 torsion angle is *syn*, with only one high energy conformer in acetylcarnitine that shows it in *anti*. The main difference between carnitine and choline is due to the chirality of carnitine: the N-CH_2-CH-OH(Ac) torsion angle prefers the *g*- over the *g*+, while choline shows equal populations of *g*+ and *g*-. The CH_2-CH-O-H torsion angle is always *anti* in choline, but it prefers *g*- in carnitine.

3.2.4.5. Carnitines vs. propanoates.

In general, the carnitines show a greater proportion of *anti* torsions than the propanoates. The conformer that corresponds to the global minimum in acetoxypropanoate, accounts for 0.01% of the population in acetylcarnitine. *Anti* torsion CH_2-CH-CH_2COO^- comprises 50% of the population in acetylcarnitine, 60% in carnitine, 23% in acetoxypropanoate and 48% in hydroxypropanoate.

3.2.5. Ab initio results including solvent.

We compare AM1/COSMO vs. 6-31G*/Tomasi in the following [table]

Table 3.3. Comparison of AM1 vs. 6-31G* calculations on carnitines and cholines in water.

Compound	{delta}E AM1/COSMO	{delta}E 6-31G*/Tomasi	{mu} AM1/COSMO	{mu} 6-31G*/Tomasi
Acetylcarnitine folded	0.00	0.00	26.7	26.7
Acetylcarnitine extended	0.10	5.24	29.9	29.5
Carnitine extended	0.00	0.00	29.2	28.9
Carnitine folded	0.60	-4.63	23.9	23.6
Acetylcholine 1	0.00	0.00	10.9	10.4
Acetylcholine 2	0.15	2.05	9.4	9.0
Choline 1	0.00	0.00	5.3	5.0
Choline 2	0.94	0.82	5.1	4.7

[table]

Table 3.4. Comparison of AM1 vs. 6-31+G calculations on propanoates in water.

Compound	{delta}E AM1/COSMO	{delta}E 6-31+G/Tomasi	{mu} AM1/COSMO	{mu} 6-31+G/Tomasi
Acetoxypropanoate 1	0.00	0.00	17.4	18.65
Acetoxypropanoate 2	0.18	0.90	14.65	15.67
Hydroxypropanoate 1	0.00	0.00	9.2	9.92
Hydroxypropanoate 2	0.10	1.51	9.1	9.81

The 6-31G* calculations were single points on the geometries optimized by AM1/COSMO. We wanted to assess the ability of the combination AM1/COSMO to reproduce the change in dipole moment when going from gas phase to solution. The [gas phase results] indicate the need for inclusion of correlation effects. We found such optimization prohibitively long, and the full conformational search by ab initio is at present beyond the computational resources available to us.

3.2.6. Thermochemical calculations from semiempirical results.

We can calculate the expected enthalpies of hydrolysis. (See [table.])

Table 3.5. Comparison of {delta}H_{hydr} (kcal/mol) calculated at {epsilon}=78.3 vs. calorimetric values.

Compound	AM1	Exp. unbuffered H_2O	Exp. buffered pH=7.0
Acetylcarnitine	-7.43	[-4.63]	[-14.67]
Acetylcholine	-3.06	[-3.20]	[-13.00]

Acetoxypropanoate	-4.02	n.a.	n.a.

From the previous table, we observe that the semiempirical results for the carnitines agree moderately well with the experimental values in unbuffered solution. The results for the cholines show good agreement with the experimental values.

The expectation values for both dipole moments and solvation energies, calculated by using Boltzmann's equation are displayed in the following [table].

Table 3.6. Expectation values for Dipoles ({mu}) and Enthalpies of Solvation ({delta}$H°_{solv}$)

Compound	**{mu} (D)**	**{delta}$H°_{solv}$ (kcal/mol)**
Acetylcarnitine	27.90	-64.76
Carnitine	27.12	-62.35
Acetylcholine	9.89	-59.30
Choline	4.79 [2.65 exp.]	-54.87
Acetoxypropanoate	16.07	-94.54
Hydroxypropanoate	8.93	-90.06
Acetic acid	6.40	-17.02 [-12.7 exp.]
Water	2.22	-9.22 [-9.98 exp.]

The variation in the enthalpies of solvation parallels that in the dipole moments: a smaller decrease in dipole moment upon hydrolysis (0.78 D for acetylcarnitine vs. 5.1 D for acetylcholine and 7.1 D in acetoxypropanoate) corresponds to a smaller decrease in enthalpy of solvation (-2.41 kcal/mol in acetylcarnitine vs. -4.43 kcal/mol for acetylcholine and -4.48 kcal/mol in acetoxypropanoate).

The calculated **Boltzmann factors (F)** for the conformers indicate that the N-CH_2-CH-OH(Ac) torsion prefers *g*- (>90%) for both acetylcarnitine and carnitine, thus we focus mostly on the CH_2-CH-CH_2-COO^- torsion: AM1 shows that in acetylcarnitine 37% of the population is extended, and 41% of the population is folded. The values for carnitine are 57% extended and 18% folded. As acetylcarnitine loses its acetyl group through hydrolysis, the carnitine backbone goes from folded to extended. Such conformational change implies a change in the dipole moment, reflected by the AM1 calculations. The expectation values for the dipole moments of these compounds are gathered in the [table]

We can highlight the results stated above for acetylcarnitine in the following figure:

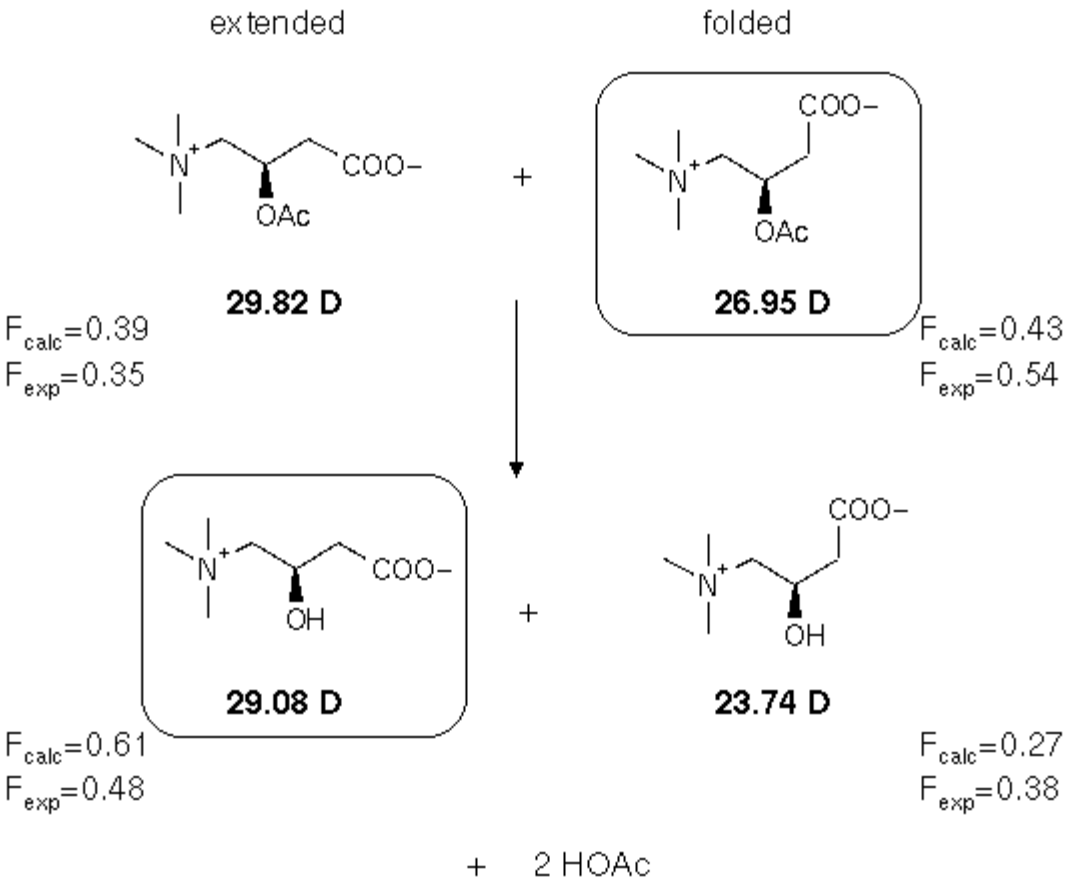

Figure 3.6. Changes in population and dipole moments upon hydrolysis.[fig.highlight.gif, 4.852KB]

We cannot draw a similar figure for acetylcholine and 3-acetoxypropanoate because of the lack of the methylenecarboxylate group, but we present the differences in expectation values for the enthalpies of solvation of the three acetates in the following figure:

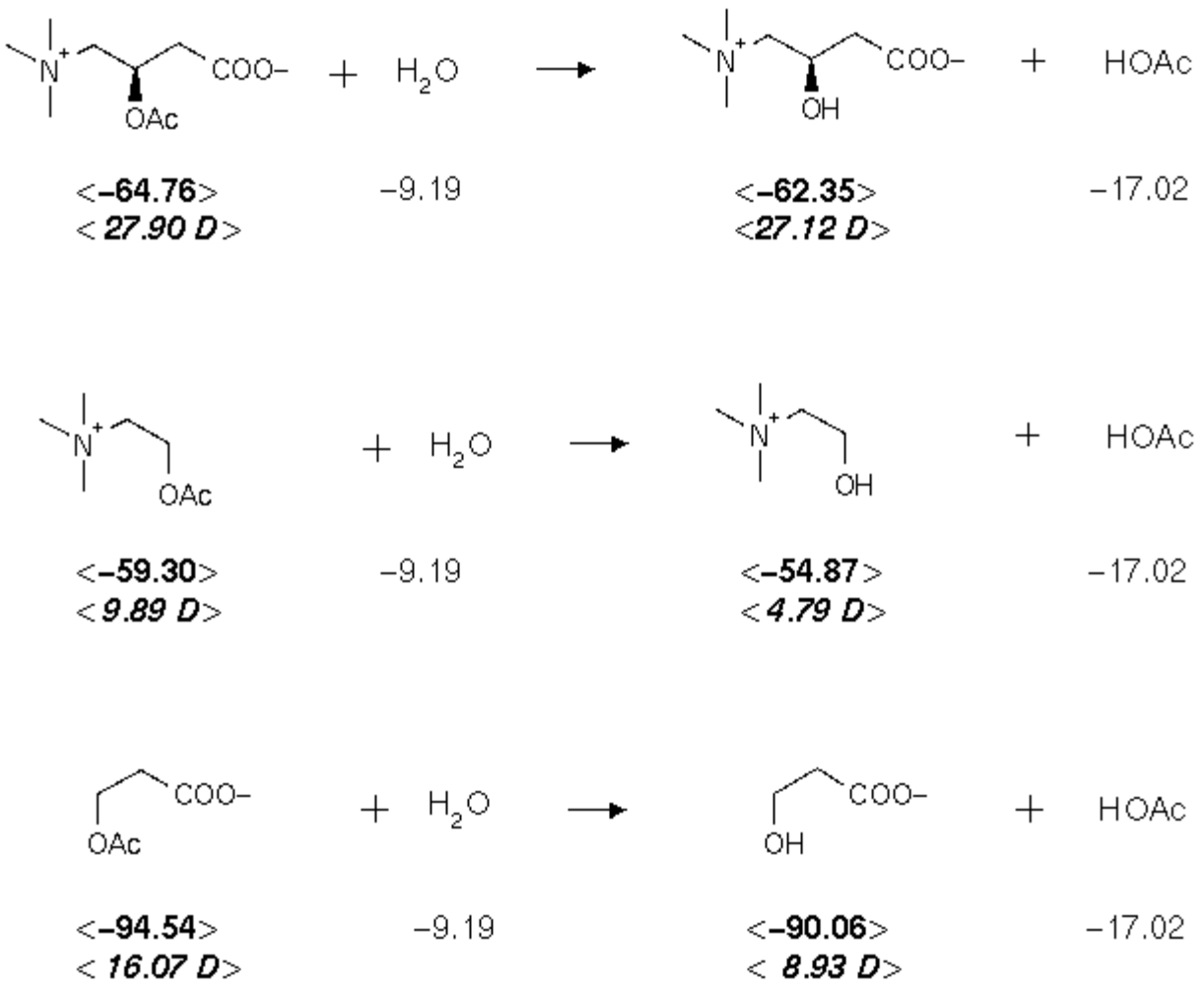

Figure 3.7. Differences in the energies of solvation for acetylcarnitine, acetylcholine and 3-acetoxypropanoate.[fig.solvation.gif, 4.823KB]

The values between brackets are expectation values calculated using the complete Boltzmann populations. The upper values are enthalpies of hydration in kcal/mol, while the lower values are the expectation values for the dipole moments in Debyes.

We see that the dipole moment stays nearly constant for the carnitines (change <0.8 D). For the cholines, the dipole moment suffers a reduction of about 5.0 D, while for the propanoates the dipole reduction amounts to approximately 7.0 D. These lower polarities in choline and hydroxypropanoate imply an additional work (of desolvation) that consumes part of the free energy available from these reactions. Change in free energy measures the work obtainable from a process; thus, *the hydrolysis of acetylcholine yields a lower available work than that of acetylcarnitine because part of the free energy change in acetylcholine hydrolysis is spent desolvating the product (lower polarity choline).* We could apply a similar argument to acetoxypropanoate, but we cannot compare against experiment due to lack of experimental data.

Summary : Changes in polarity coupled to conformational changes can influence deeply the thermodynamics of reactions through differential solvation. Electroneutrality does not guarantee small solvation effects. Calculations have to account for the presence of charged centers, together with the influence in molecular polarity that such centers exert, to understand correctly the thermodynamics of charged systems.

3.2.7. Modeling of tetrahedral intermediate: preliminary results.

We modeled the tetrahedral intermediate suggested by Gandour [Gandour, 1985] to see the geometry of the preferred conformation. Because the attack of the sulfide on the carbonyl group generates a chiral center, we considered both diastereomers generated by the (*R*) configuration of carnitine (*R,R*) and (*R,S*) in GB/SA water. These results are preliminary, because we looked only for the global minimum, not concerning ourselves with finding all the conformers within 3.0 kcal/mol.

The conformational searches yielded the following global minima:

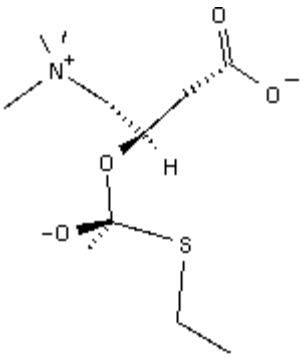

Figure 3.8. Global minimum for (*R,S*) tetrahedral intermediate in GB/SA water.[fig.RSWat.gif, 0.807KB]

RSWat.wrl, 16.938KB

Figure 3.9. 3D Model of the *R,S* tetrahedral intermediate in GB/SA water.[RSWat.wrl, 16.938KB]

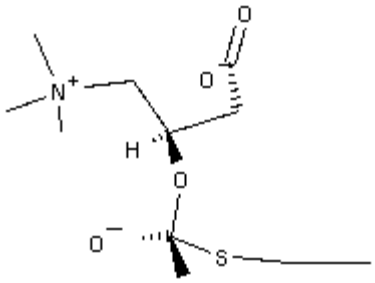

Figure 3.10. Global minimum for (*R,R*) tetrahedral intermediate in GB/SA water.[fig.RRWat.gif, 0.801KB]

RRWat.wrl, 17.048KB

Figure 3.11. 3D Model of the *R,R* tetrahedral intermediate in GB/SA water.[RRWat.wrl, 17.048KB]

We then determined the RMS deviations after least-squares fit to the global minima obtained from the [conformational searches for the phosphonate rings]. The results are displayed in the table below:

Table 3.7. RMS deviation after least-squares fitting of global minimum of rings to global minimum of intermediate in GB/SA water.

Diastereomer	**Unsubstituted ring.**	***Cis*-substituted ring.**	***Trans*-substituted ring.**	**Dimethyl substituted ring.**
R,S	0.438, 0.685	0.384, 0.809	0.767, 0.822	0.322, 0.834
R,R	0.619, 0.600	0.716, 0.548	0.931, 1.017	0.731, 0.537

The first value in each cell corresponds to the fitting of the *oxo* oxygen on the phosphorus to the negatively charged

oxygen (for the *R,S* isomer) or the methyl group on the TI (for the *R,R* isomer) in the tetrahedral intermediate. The second value corresponds to the matching of the *oxo* oxygen on the phosphorus to the sulfur atom in the intermediate (for both diastereomers). This is equivalent to saying that both halves of the ring compounds were used in the fit. The atoms used were:

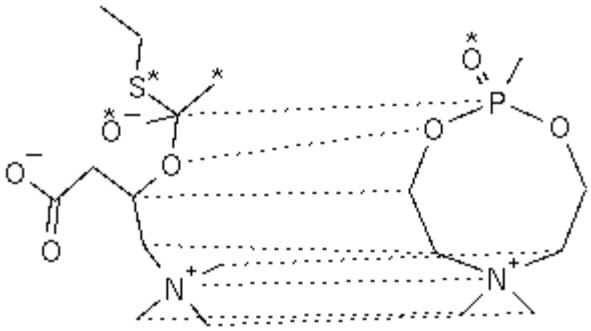

Figure 3.12. Atom pairs used in the least squares fit between the phosphonate rings and the tetrahedral intermediate.[fig.fitTI.gif, 1.511KB]

The *oxo* oxygen on the phosphorus could be matched to any of the atoms marked with asterisks. For more details, see the [Methods] section.

The greater RMS values obtained when matching oxygen to sulfur atom should not be discarded offhand. S-C bonds (1.85 Å) are longer than C=O bonds (1.46 Å), so the difference influences significantly the final RMS value.

The following table displays the RMS values for the second most populated conformation in GB/SA water and the global minimum of the TI. The first value in each cell corresponds to the fitting of the *oxo* oxygen on the phosphorus to the methyl group on the TI, unless specified otherwise. The second value on each cell corresponds to the matching of the *oxo* oxygen on the phosphorus to the sulfur atom in the intermediate (in all cases).

Table 3.8. RMS deviation after least-squares fitting of second most populated conformer of ring to global minimum of intermediate in GB/SA water.

Diastereomer	**Unsubstituted ring.**	***Cis*-substituted ring.**	***Trans*-substituted ring.**	**Dimethyl substituted ring.**
R,S	0.471, 0.630	0.740, 0.935	0.388, 0.747	1.201, 1.032
R,R	0.975, 1.009	0.975, 1.011	0.652, 0.577	1.097, 1.092

To give us an idea of the best possible fit, we did a least-squares fitting of the tetrahedral center in the intermediate to dimethyl methylphosphonate. If we match the *oxo* group on phosphorus to the negatively charged oxygen in the intermediate, the RMS value is 0.227. If we match the *oxo* oxygen to the sulfur atom on the intermediate, the RMS value is 0.203. We note that the conformation around the tetrahedral center matched the [*g*+,*a*] conformer of dimethyl methylphosphonate, which is not a stationary point either by ab initio, or by AMBER*. The fit included only the heavy atoms around the phosphorus, not including the carbons attached to the oxygens.

(footnotes)

[*F.TORSION*] We defined torsion angle B in the propanoates as H-C-C-COO^-, taking the pro-R hydrogen. We did this to keep consistency with the terms ``folded'' and ``extended'', and to yield an easier comparison of the torsions between different compounds.

[*F.CORREL*] The Hartree-Fock approximation does not include the Coulombic repulsion between the electrons of different spins. The Coulombic repulsion of the electrons makes the motions of the electrons depend on one another (``correlates'' the motions). Inclusion of electronic correlation requires schemes that consider configuration interaction. For more details on the procedures, see the book by Szabo and Ostlund [Szabo, 1996].

[Title] [Ded] [Ack] [1] [2] [3] [4] [5] [6] [7] [Bib] [A] [B] [C] [D] [E] [Vita]

Chapter 5. Modeling of phosphonates.

5.1. Modeling of phosphorus species.

Many researchers have tried conformational analysis of phosphorus species by computational means, and they have used the full range of computational approaches: molecular mechanics, semiempirical and ab initio. The following sections review the diverse attempts at modeling molecules containing phosphorus (V). This review emphasizes mostly those efforts to *develop* modeling methods for phosphorus, as opposed to the *application* of methods already developed.

5.1.1. Ab initio methods.

Ewig and van Wazer calculated phosphinic, phosphonic and phosphoric acids using STO-3G, 3-21G and 4-31G basis sets with *d* functions added on phosphorus. [Ewig, 1985] Later, the same authors studied methyl phosphinate, dimethyl phosphonate and trimethyl phosphate [Van Wazer, 1986] employing STO-3G, 3-21G and 4-31G with *d* functions on phosphorus.

Denmark and Cramer studied *P*-allylphosphonic diamide the RHF/3-21G(*) level. [Denmark, 1990] They found good agreement with data from X-ray for both bond lengths and bond angles, but they point out that inclusion of polarization functions would correct for possible structural artifacts, such as an artificially planar nitrogen attached to the phosphorus.

Thatcher and Campbell recommend 3-21+G(*) basis set for modeling of phosphates and phosphonates, based on the need for *d* orbitals and diffuse functions to describe properly the electronic density. [Thatcher, 1993]

Liang *et al.* used 3-21G*, 6-31G* and 6-31+G* basis sets to calculate geometries of dimethyl phosphate and methylpropyl phosphate anions. [Liang, 1993] They showed that **3-21G*** (this basis set includes *d* orbitals for first and second row atoms) overestimates some bond lengths and the vibrational frequencies agree only qualitatively with those determined by 6-31G* and 6-31+G* basis sets. Their basis set of choice was 6-31G*, given the excellent agreement between its results and those of 6-31+G*, although they did not compare the quality of the charges.

Cramer *et al.* studied phosphorus (V)-substituted methyl anions with full geometry optimization using 3-21G(*). [Cramer, 1994] They preferred **3-21G(*)** (this basis set contains a set of six *d* orbitals for second row atoms but no *d* orbitals for first row atoms) because of the computational costs involved in using more extended basis sets, although they stressed the qualitative validity of the hypersurfaces calculated.

Landin *et al.* [Landin, 1986] studied dimethyl phosphate anion and 2-ammonioethanol at the Hartree-Fock level using 3-21G, and 3-21G(*) basis sets for full geometry optimization, followed by single point calculations with 6-31G* and 6-31+G* basis sets. The most stable conformation had both O-CH_3 in syn-clinal (+sc) orientation. They reported differences in the charges calculated with 6-31G* and 6-31+G* basis sets, with the phosphorus atom suffering the greatest change in the charge when including polarization functions.

5.1.2. Semiempirical methods.

Gorenstein *et al.* modeled phosphate esters at the CNDO/2 level including *d* orbitals. The results compared favorably to those of a PCILO calculation, and to an ab initio calculation using a minimal Slater-type orbital basis set without *d* orbitals. [Gorenstein, 1976] They compared their calculated bond distances and bond angles against X-ray data and found good agreement. Based on Gorenstein's conclusions, Van der Veken and Herman reported conformational analysis of dimethyl methylphosphonate at the CNDO/2 level including *d* orbitals. [van der Veken, 1977]

Koch and Anders compared MP2(full)/6-31+G*//MP2(full)/6-31+G*, MNDO and PM3 calculations on lithiophosphonates. [Koch, 1995] PM3 reproduced well the energetic ranking of the conformers produced by ab initio, while MNDO failed. The suitability of PM3 to model organolithium species was confirmed, but it underestimated the bond lengths around the phosphorus atom.

Landin *et al.* [Landin, 1995] found PM3 inadequate to model dimethyl phosphate anion, a result of an underestimation of dipole-dipole interactions which in turn, related to an underestimation of charge separation by the PM3 Hamiltonian. A Fourier analysis of the coefficients for the C-O-P=O torsion indicated that the coefficient associated with the anomeric effect was less important than the one associated with the dipole-dipole interactions, although none could be neglected due to a third coefficient that coupled both effects.

5.1.3. Molecular mechanics methods.

Plyamovatyi *et al.* modeled dimethyl phosphate anion by a molecular mechanics scheme that emphasized interactions between unshared electron pairs. The results of their suggested molecular mechanics scheme reproduced the global minimum determined experimentally better than an ab initio calculation using the STO-3G basis set. [Plyamovatyi, 1977a], [Plyamovatyi, 1977b], [Plyamovatyi, 1990], [Plyamovatyi, 1993]

Weiner *et al.* developed a molecular mechanics force field (AMBER) that could model phosphates. [Weiner, 1986] The molecular mechanics parameters were determined by fitting them to experimental geometries. The starting points were experimentally-determined force constants (from IR and Raman) and bond angles (from X-ray).

Mikolajczyk *et al.* studied 2-phosphoryl and 2-thiophosphoryl-1,3-heteroanes by molecular mechanics. [Mikolajczyk, 1989] The potential energy function included nonbonded interactions, torsional energy, angle deformations and lone pair interactions. They concluded that hyperconjugation did not play an important role in determining the conformational stabilities of 2-substituted-1,3-dithianes

Fox, Bowen, and Allinger extended their MM3 force field to include alkylphosphines. [Fox, 1992] As starting points for their parametrization, they used structural parameters from electron diffraction and microwave spectroscopy. The resulting parameters modeled structures, vibrational spectra, moments of inertia and dipole moments fairly accurately.

Jin, Benesch, and Weaver developed MM2 parameters for modeling of lipids (MM2(Lipid) force field) by taking structures of phospholipids calculated by AM1. [Jin, 1994] They observed good agreement between their results and those obtained by Ewig and Van Wazer using ab initio approaches. [Ewig, 1985] [Van Wazer, 1986] They showed, however, that AM1 overestimated the barriers to rotation. This overestimation reduced the reliability of their torsional parameters.

5.2. Development of AMBER* parameters for phosphonates.

We suggest three levels of molecular properties that molecular mechanics (MM) should reproduce:

1. Atomic connectivities.
2. Torsion angles.
3. Energetic ranking of conformers.

If we want to believe the result of any computation, we need to ensure that it can reproduce accurately bond lengths and bond angles, otherwise we can discard its results offhand. The accurate reproduction of torsion angles implies a good representation of the intramolecular interactions, such as van der Waals repulsions and electrostatic effects, just to mention the most important. A correct ranking of the conformers means a proper accounting of the relative weights that correspond to the intramolecular forces. From these criteria, we can propose three ways to measure how well MM reproduces molecular properties:

1. Absolute differences in bond lengths and angles between the MM values and the reference values.
2. RMS deviation after least-squares fit of the MM geometry to the reference geometry.
3. Comparison of MM conformational energies against reference energies.

As reference values one can take either experimental information (X-ray data) or high level ab initio calculations. In the particular case of the energetic ranking of the conformers, one is usually limited to high level ab initio calculations, given the experimental difficulties involved in determining conformational populations in the gas phase. To see the details of the development process see the [corresponding subsection in Methods].

5.2.1. Calculations on dimethyl methylphosphonate.

The following figures show the molecular mechanics curves with the best fit to the ab initio curves.

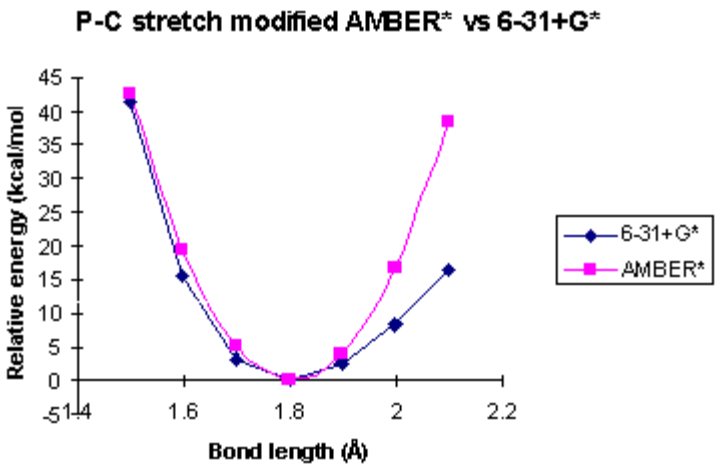

Figure 5.1. Fit of AMBER* phosphonate parameters for P-C bond stretch to 6-31+G* curve.[fig.pc.gif, 3.795KB]

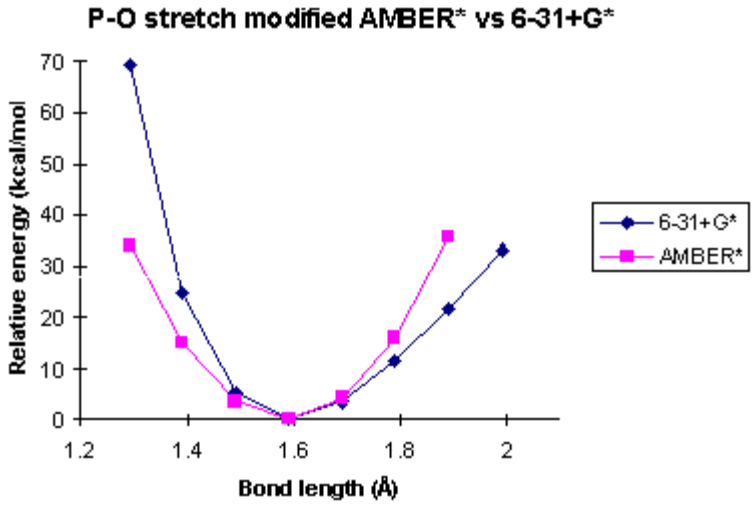

Figure 5.2. Fit of AMBER* phosphonate parameters for P-O bond stretch to 6-31+G* curve.[fig.po.gif, 3.817KB]

We took the P=O bond length from the ab initio results. The starting point for the fitting of the stretching force constant was the one found for the phosphonate P=O bond.

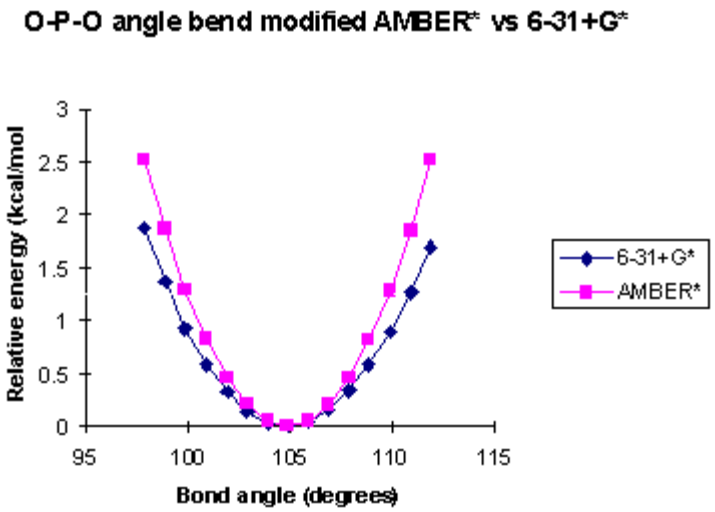

Figure 5.3. Fit of AMBER* phosphonate parameters for O-P-O bond angle to 6-31+G* curve.[fig.opo.gif, 3.991KB]

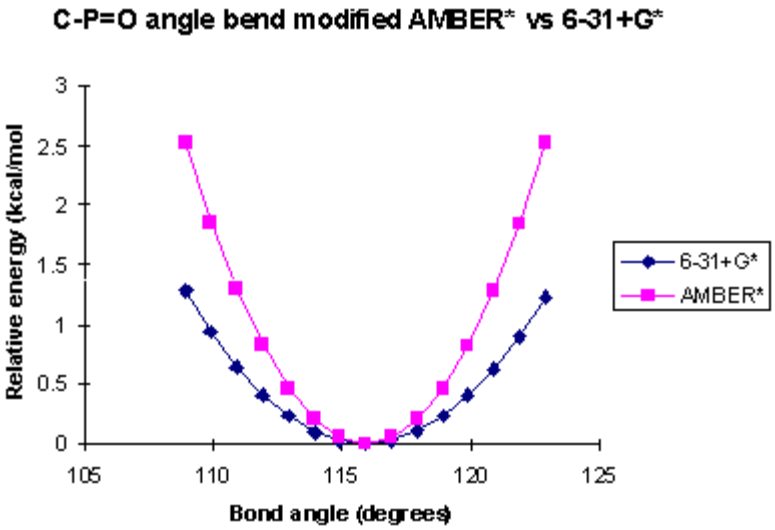

Figure 5.4. Fit of AMBER* phosphonate parameters for C-P=O bond angle to 6-31+G* curve.[fig.cp2o.gif, 4.142KB]

Dimethyl methylphosphonate has a total of six bond angles around the phosphorus: C-P=O, O-P-O, 2 O-P=O and 2 C-P-O. We included parameters only for C-P=O and O-P-O because adding parameters for the other bond angles gave rise to erratic behavior in the calculated geometries. Cross-coupling of the bond angle terms may be part of the reason. The simple functions used in AMBER* may not represent adequately such coupling.

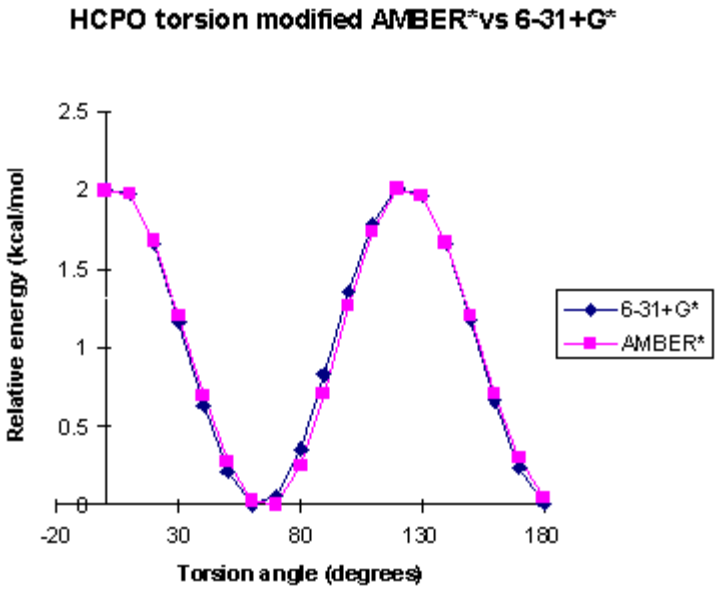

Figure 5.5. Fit of AMBER* phosphonate parameters for H-C-P=O torsion angle to 6-31+G* curve.[fig.hcpo.gif, 4.349KB]

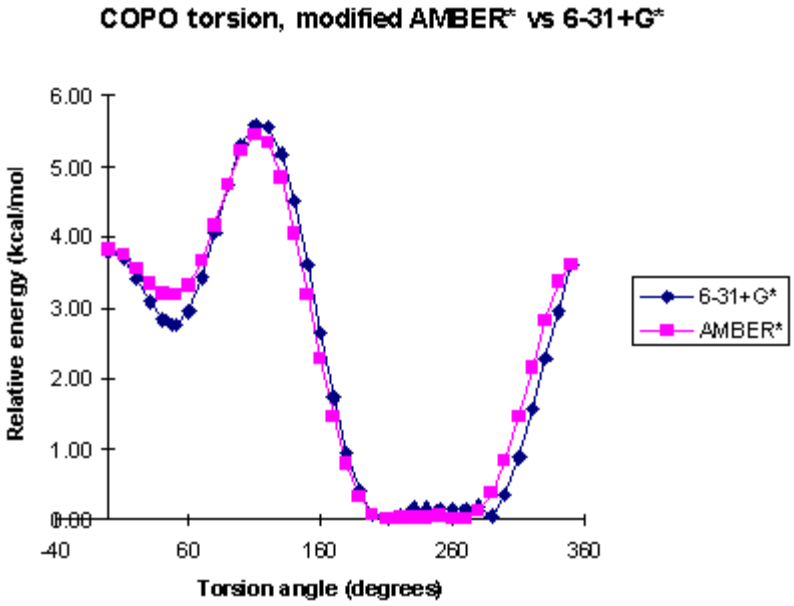

Figure 5.6. Fit of AMBER* phosphonate parameters for C-O-P-O torsion angle to 6-31+G* curve.[fig.copo.gif, 4.789KB]

The AMBER* H-C-P=O torsion potential very closely matches the ab initio curve. The C-O-P-O torsion potential from AMBER* has problems reproducing the very flat part of the ab initio] potential where the C-O bond eclipses the P=O bond. It also introduces an error close to 0.5 kcal/mol in the energy of the minima where the C-O bond is *gauche* to the singly bonded oxygens.

The results in [the table] show that our AMBER* parameters reproduce ab initio bond lengths with a maximum deviation of 0.002 Å, and bond angles with a maximum deviation of 1.1°. MM2* has maximum deviations of 0.037Å and 10.9° respectively. MMX shows maximum deviations of 0.062Å and 8.9°, while the maximum errors in UFF

predictions amounted to 0.111Å and 6.4° respectively. MM2* and MMX overestimated the P-C bond length, with values greater than 1.83Å. The prediction of UFF was as good as ours (1.799Å vs. 1.797Å). MM2*, MMX and UFF overestimated the P-O bond length, with MM2* getting the closest value (1.605Å) to the ab initio (1.590Å). Our parameters predicted 1.588Å. The smallest error by MM2*, MMX and UFF in the P=O length predictions was 0.02Å. Our modified AMBER* matched the ab initio result within 0.001 Å. In the predictions of the bond angles our modified AMBER* correctly reproduced all the ab initio trends, while MM2 and UFF predict standard tetrahedral angles, with little correlation to the ab initio results. MMX did remarkably well, predicting correctly the trends and most values, although the O-P-O angle resembles more a phosphine-like C-P-C angle. For the full listing of the predicted values for the different bond lengths and angles used in the evaluation, see the [table of predicted bond lengths and angles] for dimethyl methylphosphonate.

Table 5.1. Predicted bond lengths and angles of dimethyl methylphosphonate.

	6-31+G*	AMBER* {epsilon}=1.0	MM2*	MMX	UFF
P-C	1.798	1.797	1.835	1.860	1.799
P-O	1.590	1.588	1.605	1.622	1.701
P=O	1.455	1.455	1.470	1.479	1.510
O-P-O	104.8	105.1	107.8	96.7	109.1
O=P-C	115.9	116.3	105.8	114.3	109.5
O-P-C	104.3	105.2	115.2	109.2	109.1
O=P-O	113.3	112.1	106.1	113.1	110.1

The RMS deviations in the least-squares fits do not reveal major differences in the quality of the predictions. Our AMBER* parameters performed *marginally better* than the other force fields. AMBER* yields RMS values between 0.10 and 0.15, while the other force fields produced values between 0.10 and 0.25, but the difference is probably not significant. See the table of RMS fits of molecular mechanics to ab initio geometries for a full comparison of the RMS values produced by all the force fields.

Table 5.2. RMS fit of molecular mechanics to ab initio geometries.

	AMBER* {epsilon}=1.0	**MM2***	**MMX**	**UFF**
g-,g-	0.140	0.187	0.111	0.669
g+,g+	0.141	0.187	0.104	0.169
g-,g+	0.135	0.240	0.250	0.174
g-,a	0.102	0.192	0.129	0.166
a,g+	0.102	0.192	0.128	0.160

Ab initio reveals only five minima in the conformational hypersurface of dimethyl methylphosphonate. (Our repeated attempts to locate the missing four conformers failed, when all our input structures collapsed to conformers already found.) The table of relative conformational energies shows that AMBER* using constant dielectric closely reproduces the energetic ranking of the minima found by ab initio. The greatest error resides in the energies of the *g*-, *a* and *a*, *g*+ conformers, which AMBER* predicts 0.4 kcal/mol higher than ab initio. AMBER* found two more saddle points than ab initio. We believe this is a manifestation of the less-than-perfect match of our parameters to the ab initio results. [Note.]

The results [tabulated], refer to the following conformers:

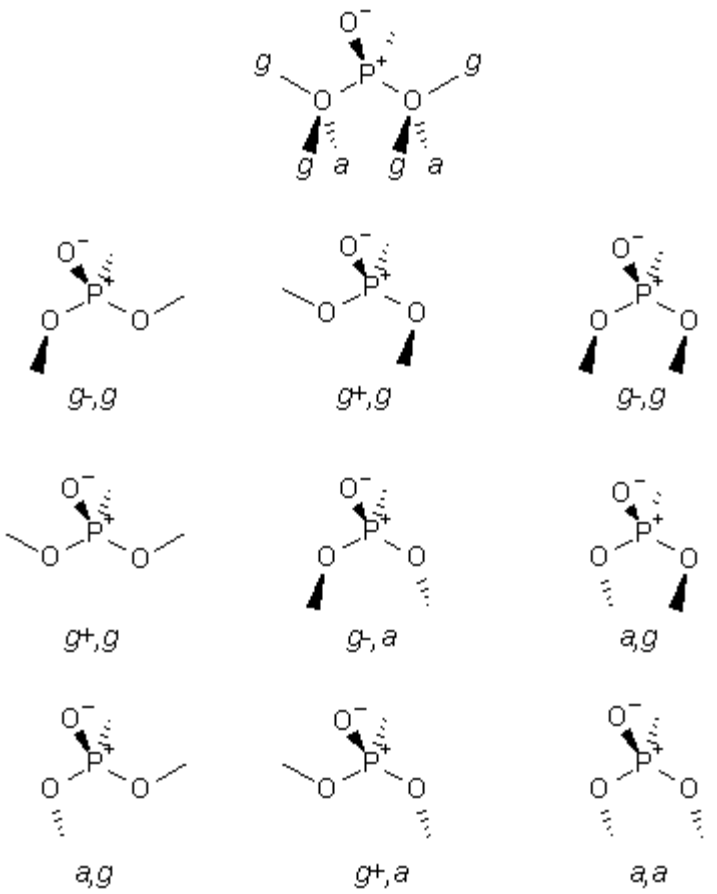

Figure 5.7. Conformers of dimethyl methylphosphonate.[fig.confs.gif, 4.000KB]

Table 5.3. Relative conformational energies (kcal/mol)

	6-31+G*	AMBER* {epsilon}=1.0	AMBER*(default)	MM2*	MMX	UFF
g-,g-	0.00	0.00	0.08	2.01	0.00	0.00
g+,g+	0.00	0.00	0.08	2.01	0.00	0.00
g-,g+	0.14	0.12	n.f. [*]	4.07	0.68	0.11
g+,g-	n.f. [*]	0.16 [*]	0.00	4.70	0.46	n.f. [*]
g-,a	2.75	3.17	2.15	0.00	0.39	7.58
a,g+	2.75	3.17	2.15	0.00	0.38	7.58
a,g-	n.f. [*]	n.f. [*]	1.99	2.32	0.64	n.f. [*]
g+,a	n.f. [*]	n.f. [*]	1.99	2.32	0.61	n.f. [*]
a,a	n.f. [*]	7.41 [*]	6.86	3.70	n.f. [*]	n.f. [*]

MM2* found degenerate pairs, but its energetic ranking differs from that by ab initio. MM2* finds *g-,a* and *a,g+* as global minima. MMX found the same global minima as ab initio and nearly degenerate pairs of conformers, but the conformational energies span a narrow range. The hypersurface is, thus, very flat. The hypersurface contains two

minima not found by ab initio. UFF found the same global minima as ab initio and the energetic ranking is qualitatively the same, but the conformational energies are much higher than the ab initio predictions. We looked repeatedly for the *g*+,*g*- conformer without success.

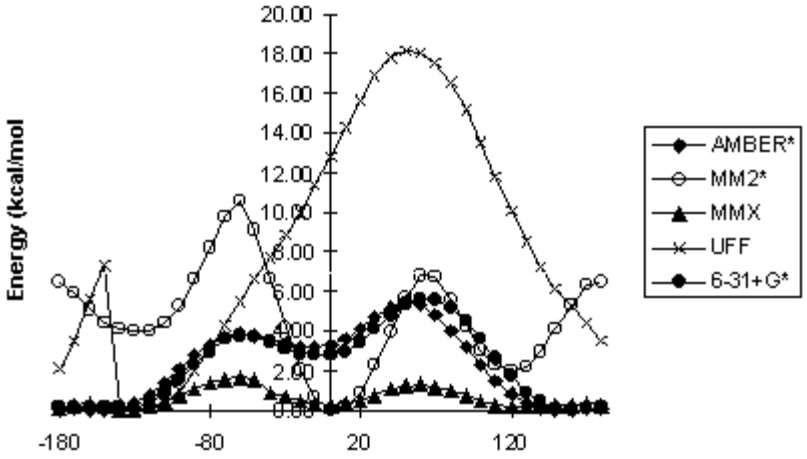

Figure 5.8. Comparison of molecular mechanics C-O-P=O torsion profiles vs. ab initio.[fig.profile.gif, 4.658KB]

Our computational results agree with the experimental work by Katolichenko *et al.* [Katolichenko, 1973] who used IR spectroscopy and measurements of dipole moments, and detected two major conformers: gauche-trans (*a*,*g*- and *g*+,*a* by our notation) and gauche-gauche (*g*+,*g*+, *g*-,*g*+, *g*+,*g*-, and *g*-,*g*+). They deduced the presence of the gauche-trans by elimination of other conformers due to dipole moment considerations. The difference in energy found between the gauche-trans and the gauche-gauche was less than 0.5 kcal/mol.

5.2.2. Comparison vs. crystal structures.

After developing the parameters, we tested them against our molecule of interest and several crystal structures to see how well could they reproduce results in the condensed phase. The structures were retrieved from the Cambridge Crystallographic Data File (CCDF) [Allen, 1977] and their codenames are: ZAYSIB (zaysib.wrl, 13.587KB), [Kumaravel, 1995] CEGXUH (cegxuh.wrl, 15.784KB), [Day, 1984] FELSOE (felsoe.wrl, 23.386KB), [Nastopoulos, 1987] DUKSOR (duksor.wrl, 15.993KB) and [Bentrude, 1986] DUMLEC (dumlec.wrl, 26.911KB). [Dyrbusch, 1986] We looked for structural variety, always accounting for the limitations of our parameters:

- No P-C(sp^2) fragments.
- No P-C(*sp*) fragments.
- No P-O-C(*sp*).
- No charges on the oxygens.

We chose only one structure from several reported by Nastopoulos [Nastopoulos, 1987] because including several molecules of the same structural type could bias the evaluation by giving a greater relative weight to a particular kind of functionality.

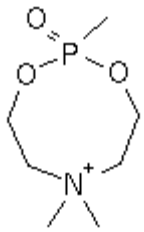

Figure 5.9. First crystal structure used for comparison (ZAYSIB).[fig.phosp.gif, 0.591KB]

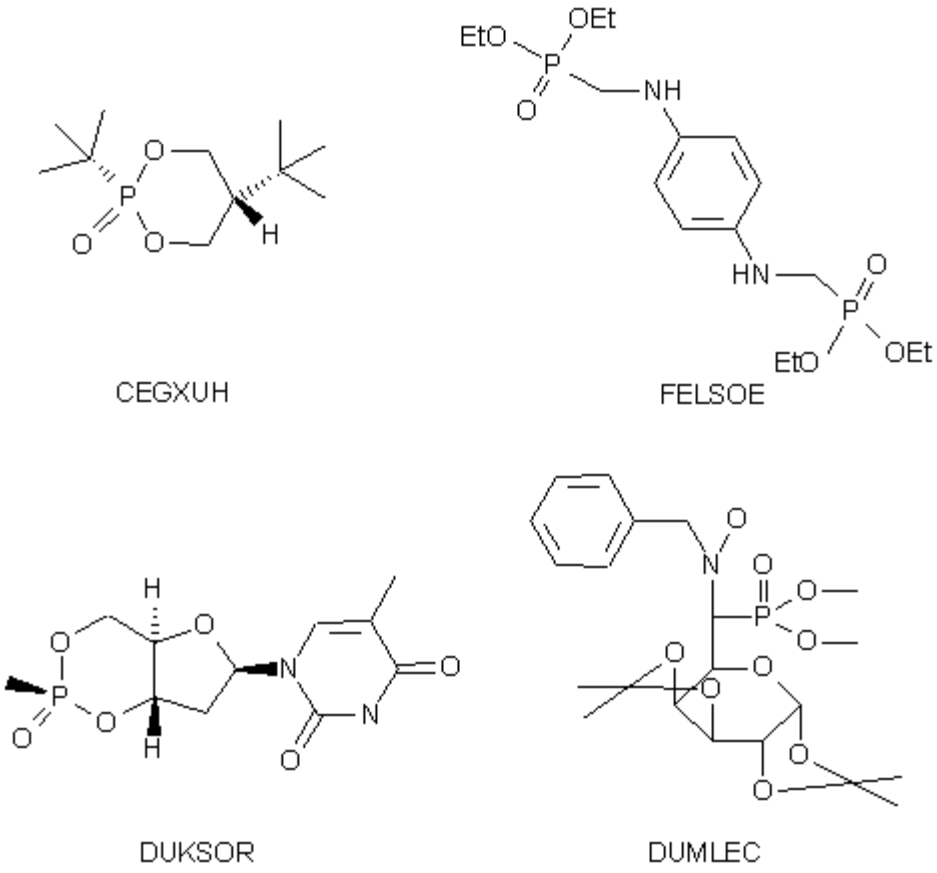

Figure 5.10. Additional crystal structures used in the comparison.[fig.crystals.gif, 4.624KB]

The [table of molecular mechanics vs. X-ray] displays the results of the tests against crystal structures.

Table 5.4. Comparison of Molecular Mechanics results vs. X-ray.

	X-ray	6-31+G*	AMBER* {epsilon}=1.0	MM2*	MMX	UFF
P-C	1.797	1.798	1.798	1.833	1.869	1.830
P-O	1.574	1.590	1.592	1.592	1.620	1.707
P=O	1.461	1.455	1.455	1.466	1.479	1.512
O-P-O	104.2	104.8	103.7	100.3	98.7	109.6

O=P-C	114.8	115.9	117.9	108.5	114.3	109.5
O-P-C	106.2	104.3	106.5	114.4	108.7	110.1
O=P-O	112.7	113.3	110.6	109.4	112.6	108.7

We observe the same trends as from the comparison against ab initio. Ab initio does show some discrepancies with the crystal structures. Two of the most intriguing are the longer P-O bond predicted by ab initio (1.590Å ab initio vs. 1.574Å X-ray), and the shorter P=O bond (1.455Å ab initio vs. 1.461Å X-ray). We can only suggest a few reasons for these differences: a) correlation effects not included in the calculations, b) crystal packing forces affecting the experimental values or c) a combination of a) and b). Regarding the inclusion of correlation, calculations by Koch and Anders [Koch, 1995] on methylphosphonic acid at the HF/6-31+G* and MP2/6-31+G* levels show that electronic correlation *increases* both bond lengths: P=O (1.460Å by HF to 1.494Å by MP2) and P-O (1.596Å by HF to 1.629Å by MP2) so we find it difficult to justify the differences on these grounds. [Note.] Crystal packing forces become unlikely candidates after realizing that all the molecules used for testing crystallize in different systems. AMBER* reproduces fairly closely the deficiencies shown by HF/6-31+G* in the predicted bond lengths (maximum deviation of 0.018Å) and in the bond angles (maximum deviation of 3.1°). MM2* overestimates the P-C and P-O bond lengths by 0.035Å at the most, while the greatest deviation from the experimental bond angles amounts to 8°. MMX fits well the angles, but it overestimates P-C and P-O lengths by as much as 0.07Å. UFF has the greatest errors in bond lengths (maximum deviation of 0.13Å) and has little predictive value for the angles, as they cluster around 109.5°.

Table 5.5. RMS values of MM vs. X-ray including all heavy atoms.

	ZAYSIB	**CEGXUH**	**FELSOE**	**DUKSOR**	**DUMLEC**
Gas phase					
AMBER*	0.603	0.241	0.602	0.862	0.445
MM2*	0.167	0.416	0.602	0.631	0.446
MMX	0.086	0.013	0.034	0.713	0.056
Water					
AMBER*	0.086	0.474	0.476	0.656	0.502
MM2*	0.160	0.417	0.557	0.575	0.433
MMX	0.084	0.013	0.032	0.681	0.284

The RMS values including all heavy atoms show that MMX yields best fits both in the gas phase and in water. AMBER* produces a low RMS value only for ZAYSIB in water, but we note that some torsion angles far from the phosphonate group change after minimization. MM2* yields RMS values close to those by AMBER*. Differences in torsion angles dominate RMS values, so changes in torsion angles not controlled by our parameters can give a wrong idea of the quality of the fit.

Table 5.6. RMS values of MM vs. X-ray including phosphonate heavy atoms only.

	ZAYSIB	**CEGXUH**	**FELSOE**	**DUKSOR**	**DUMLEC**
Gas phase					
AMBER*	0.445	0.240	0.176	0.039	0.347
MM2*	0.170	0.287	0.182	0.094	0.286

MMX	0.097	0.262	0.150	0.058	0.213
Water					
AMBER*	0.078	0.281	0.157	0.046	0.280
MM2*	0.159	0.294	0.186	0.099	0.280
MMX	0.087	0.011	0.013	0.055	0.251

If we include only the phosphonate atoms, we observe a much improved fit in the AMBER* results for water. MM2* has values slightly higher than those by AMBER* both in the gas phase and water. MMX consistently yields very low RMS values in the gas phase and water.

The low RMS values obtained by MMX are misleading because MMX provides a very flat hypersurface, as evidenced in the [table] and in the [profiles]. This means that the starting geometry changes very little.

(footnotes)

[*F.SADDLE*] Saddle point.

[*NF*] *not found

[*F.ARTIFACT2*] We want to illustrate the importance of dealing properly with the electrostatics: use of the default (distance-dependent) dielectric treatment of electrostatics, completely scrambles the energetic ranking of the conformers, *e.g.*, the global minima have now a relative energy of 0.08 kcal/mol, the minimum found at 0.14 kcal/mol by ab initio is found at 0.12 kcal/mol by the constant dielectric treatment, while the distance-dependent failed to find it as a stationary point. Two structures that are not part of the hypersurface (a,g- and g+,a) either by ab initio or AMBER* with constant dielectric, were found by the distance-dependent dielectric treatment at 1.99 kcal/mol. A constant dielectric was the proper choice to develop the parameters because the ab initio results were calculated assuming a vacuum, so the dielectric permittivity of the medium stayed constant. In the version of AMBER included in MacroModel, [Weiner, 1986] the parameters fit *experimental* values so the authors found that a distance-dependent dielectric gave a better fit because of its emulation of polarization effects.

[*F.ARTIFACT3*] MP2 is known to overestimate corrections in bond lengths when the basis set used is too small [Szabo, 1996] and the effect is more pronounced on multiply bonded species. One could expect, then, to see a greater increase in the P=O length than in the P-O length. The P=O bond increases 0.034Å, while the P-O increases 0.033Å. Most likely, only a calculation using a larger basis set (and probably more terms in the Møller-Plesset expansion) can settle the issue of the appropriateness of the basis set used.

Chapter 6. Methods.

6.1. General methods and software.

6.1.1. Molecular mechanics.

We employed the package MacroModel v.5.0 for Silicon Graphics workstations. All the conformational searches used the AMBER* force field and MonteCarlo sampling routine with Normal setup and Full Matrix Newton Raphson (FMNR) minimization with line search disabled. All the stationary points obtained were characterized as minima or saddle points by using the MTEST utility (calculation of vibrational frequencies) available in MacroModel. All the saddle points showed only one imaginary frequency and the minima had only real frequencies.

FMNR with line search disabled requires substantial storage resources and accumulates many structures with high gradients which render them meaningless chemically; however, the author opted for this algorithm due to its extreme speed (even when including solvent effects) and because of the *good ability of the algorithm to find saddle points*. Polak-Ribiere Conjugate Gradient (PRCG) and Oren-Spedicato Variable Metric (OSVM) are not likely to converge to saddle points. TCNG can converge to saddle points, but its speed makes it less convenient than FMNR, while Steepest Descent (SD) is a mediocre gradient minimizer. SD requires a postprocessing step of the structures it generates by some algorithm able to reduce the gradients under acceptable cutoffs. For a better discussion of the relative merits of the different minimization algorithms available in MacroModel, see the MacroModel Manual. The spurious structures are easily filtered out by cutting and pasting only the structures with gradients <0.05.

The AMBER* calculations in water used the GB/SA solvent model. In all cases we calculated the vibrational frequencies of the conformations to characterize them as minima or as saddle points. The morpholinium rings and the cyclohexanes used the default distance-dependent dielectric.

When using PCMODEL [v.4.0] we used all the default settings. When including the effect of water the dielectric constant was set to 78.3. PCMODEL uses the MMX force field. We also used PCMODEL as a front end for MOPAC 6.0 and MOPAC93. [Gajewski, 1991]

6.1.2. Semiempirical calculations.

We used MOPAC 6.0 [Stewart, 1990] and MOPAC93 for the semiempirical calculations. We chose AM1 as the Hamiltonian in all cases. The solvent model COSMO [Klamt, 1993] employed a dielectric constant of 78.3. All the structures were minimized (sometimes requiring an Intrinsic Reaction Coordinate calculation) until a vibrational analysis showed absence of imaginary frequencies. The optimizations in the gas phase used the Broyden-Fletcher-Golfarb-Shannon (BFGS) minimization routine, reducing all the gradient norms under 0.01. The minimizations in solution benefitted from using Eigenvector Following (EF), to lower all the gradient norms under 0.3.

6.1.3. Ab initio calculations.

All the ab initio computations were done using Gaussian94 [Gaussian, Inc.] In those cases where the structure corresponded to a stationary point, the vibrational frequencies were calculated to confirm the absence of imaginary frequencies, for the minima, or the presence of just one imaginary frequency, for the saddle points. We chose single points for the carnitine calculations after finding out that full optimization including solvent effects was prohibitively expensive, and only a supercomputer could tackle such calculations.

6.2. Acetylcarnitine calculations.

6.2.1. Conformational search strategy by molecular mechanics.

We performed a grid search with the following guidelines:

1. We allowed three initial values, 60°, -60° and 180° (*g*+, *g*- and *a* respectively) for the following torsions: N-CH_2-CH-OH(Ac), CH_2-CH-CH_2COO^-, and CH_2-CH-O-H(Ac)
2. We used initial values of 0° and 180° (*s* and *a* conformations) for the CH-O-C(O)-CH_3torsion angle.
3. We used initial values of 90° and 180° for the CH-CH_2-C(O)-O^- torsion angle
4. No initial values were given to torsions containing symmetric tops, like those for methyl groups and $(CH_3)_3N^+$-CH_2, but they were left free for optimization.

The previous conditions yielded 108 conformers for acetylcarnitine, 54 for carnitine, 27 for acetylcholine and 9 for choline. All input geometries were fully optimized in the gas phase (AM1) and with solvent (AM1/COSMO). We also calculated water and acetic acid.

6.2.2. Conformational populations.

Boltzmann factors (F) were calculated by the following formula:
F(c)=exp(-{delta}H_f/RT)/{sigma}i(exp(-{delta}H_f/RT))
where:

F(c)
Boltzmann factor corresponding to conformer c
{delta}H_f
Heat of formation,
R
Gas constant
T
Temperature.

Heats of formation that included the contributions of individual conformers were calculated with the following equation:
{delta}H_{ftot} = {sigma}i (F(c))({delta}H*f*(c_i))
where:

{delta}H_{ftot}
Heat of formation over all conformers
F(c_i)
Boltzmann factor for conformer i
{delta}H*f*(c_i)
Heat of formation for conformer i

6.2.3. Semiempirical calculations on carnitines, cholines and propanoates.

The first route card we tried was:

```
AM1 NOXYZ NOINTER PRECISE
```

but the most effective route card used for the carnitines in the gas phase was:

```
AM1 NOINTER T=3600.00 EF LET DDMIN=0.0
```

The cholines required a different route card:

```
AM1 CHARGE=+1 GNORM=0.01 GEO-OK EF LET DDMIN=0.0 NOINTER T=3600.00
```

The acetoxypropanoates used:

```
AM1 CHARGE=-1 GEO-OK GNORM=0.5 NOXYZ NOINTER NOLOG T=3600.00 XYZ
```

The hydroxypropanoates used:

```
AM1 CHARGE=-1 GNORM=0.5 T=3600.00 GEO-OK NOXYZ NOINTER NOLOG
```

The inclusion of solvent required the following route card for carnitines:

```
AM1 NOINTER T=3600.00 EPS=78.3 PRECISE EF LET DDMIN=0.0
```

while the carnitines needed more care with the gradient norm:

```
AM1 T=3600.00 EF LET DDMIN=0.0 EPS=78.3 GNORM=0.01 NOINTER PRECISE
```

The acetylcholines used:

```
AM1 CHARGE=+1 GNORM=0.01 GEO-OK EF LET DDMIN=0.0 EPS=78.3 NOINTER T=3600.00
```

and the cholines:

```
AM1 CHARGE=+1 GNORM=0.01 GEO-OK EPS=78.3 EF LET DDMIN=0.0 NOINTER T=3600.00
```

The propanoates used:

```
AM1 CHARGE=-1 EPS=78.3 GNORM=0.5 NOXYZ NOINTER NOLOG T=3600.00
```

The hydroxypropanoates used:

```
AM1 CHARGE=-1 EPS=78.3 T=3600.00 GNORM=0.5 NOXYZ NOINTER NOLOG
```

To simplify, a general route card would be:

```
AM1 CHARGE=(charge) EPS=78.3 EF LET DDMIN=0.0 T=(time) PRECISE + GNORM=X.XXXX GEO-OK NOXYZ
NOINTER NOLOG XYZ
```

AM1 CHARGE=(charge) EPS=78.3
Specify Hamiltonian, charge on the system and solvent dielectric constant.

EF LET DDMIN=0.0 T=(time)
Minimization options: eigenvector following, let the heat of formation increase, take the smallest possible step for the trust radius. Specify a time long enough to complete the optimization.

PRECISE
(optional) Tighten up criteria in case the final gradients are >2.0. Adjust (time) appropriately. Sometimes (not

always) MOPAC prints out a message to indicate this keyword is needed.

GNORM=X.XXXX

(optional) Tighten up the gradient norm criterion to finish the minimization to <X.XXXX (0.01 < X.XXXX < 2.0). Use this keyword in case PRECISE is unable to reduce the gradients <2.0.

GEO-OK

(optional) Some distorted input geometries may require this keyword. MOPAC prints out a message whenever this keyword is needed.

NOXYZ NOINTER NOLOG

(preferred) Keywords to reduce the size of the output files: do not print cartesian coordinates, do not print interatomic distances, suppress log trail if possible.

XYZ

(optional) Last resort for difficult minimization cases: perform optimization in cartesian coordinates.

6.2.4. Ab initio calculations on carnitines, cholines and propanoates.

In gas phase, the output geometries after full optimization by AM1 were used as input for Gaussian94. We used the following route card:

```
#rhf 6-31G* opt freq scf=direct maxdisk=10000000 geom=(nodistance, noangle)
```

for the carnitines and the cholines. For the propanoates we used:

```
#rhf 6-31+G opt freq scf=direct maxdisk=10000000 geom=(nodistance, noangle)
```

notice that the only difference resides in the choice of basis set. The MP2 calculations had the following route cards:

```
#rhf mp2 6-31g* scf=direct maxdisk=10000000 geom=(nodistance, noangle)
```

for the carnitines and the cholines, and

```
#rhf mp2 6-31+g scf=direct maxdisk=10000000 geom=(nodistance, noangle)
```

for the propanoates.

In solvent, the output geometries after full optimization by AM1/COSMO ({epsilon}=78.3) were used as input for single point calculations including the Tomasi solvent model. The route card was:

```
#rhf 6-31G* scrf=Tomasi scf=direct maxdisk=10000000 geom=(noangle, nodistance)
```

for the carnitines and the cholines. The propanoates used:

```
#rhf 6-31+G scrf=Tomasi scf=direct maxdisk=10000000 geom=(noangle, nodistance)
```

Again, the only difference resides in the choice of basis set. The acetylcarnitines used `78.3 100`, the carnitines used `78.3 200`, the acetylcholines used `78.5 128`, the cholines used `78.3 200`, the acetoxypropanoates and hydroxypropanoates used `78.3 128`. The value `78.5` for the acetylcholines was the product of attempts at eliminating oscillatory behavior of the wavefunction. The choice of the number of points per sphere was governed by the possibility to achieve convergence in the wavefunction. In every case we started with the default value of ``200'' and reduced the number of points until the program could achieve self-consistency. According to the Gaussian94 manual, the number of points per sphere has to be a number in the series #points = $2(n^2)$ where ``n'' is a positive integer.

6.3. Conformational search in six-membered rings.

An average of 15,000 structures were generated for each compound to achieve convergence. The criterion for convergence was that one 2,000-structure run failed to generate any new conformers after examination of a minimum of 10,000 structures. The energy window was 35.8 kcal/mol above the global minimum (150 kJ/mol). The default distance-dependent dielectric constant was used for the calculations in the gas phase.

6.4. Conformational search and analyses in eight-membered rings.

For the eight-membered rings, an average of 130,000 structures for each compound were generated and minimized until convergence was achieved. The criterion for convergence was that one 15,000-structure run failed to produce any new conformers after examination of a minimum of 100,000 structures. All the calculations in the gas phase were done specifying constant dielectric treatment of the electrostatics, instead of the default distance-dependent dielectrics.

The conformations were named by comparing the structures to perspective drawings of cyclooctane conformers. In difficult cases (distorted structures), recourse to Weiler plots usually afforded a fast identification of the conformer.

6.5. AMBER* parametrization of phosphonates.

We followed the procedure described by Hopfinger and Pearlstein. [Hopfinger, 1984] All the points for the parametrization of dimethylmethylphosphonate were calculated at the RHF/6-31+G* level of theory. 6-31G* can easily match the 6-31+G* geometries, the reason for the choice of 6-31+G* was our desire to generate high-quality charges for the inclusion of solvation effects. Landin *et al.* [Landin, 1995] found appreciable differences in the charges calculated by 6-31G* and 6-31+G* in their calculations. We calculated seven points, taken at 0.1 Å steps, for each of the P-C, and P-O bonds stretchings. For the C-P=O, and O-P-O bond angles, we calculated 15 points with 1° separation. The H-C-P=O and C-O-P-O torsions each required 36 points, at 10° steps, to parametrize the full rotation. We used the optimized values of the bond lengths and angles as first guesses for the parameters. The parameters were then adjusted by trial and error, judging "by eye" the best fit to the ab initio curves.

In the evaluation of the RMS fits, we used the least-squares fit utility provided in each MM program. Only heavy atoms were included in the fitting. We used the program Babel v.1.1 [Babel, v.1.1] for the translation of structures between the different file formats required by each program.

Cerius^2 v.2.0, which employs the Universal Force Field (UFF) [Castonguay, 1992] [Rappé, 1992] [Rappé, 1993] was used only for comparison purposes in the calculations on dimethyl methylphosphonate. We set the phosphorus atom type to P_3+5, disabled "Automatic Atom Typing". Enabled "Update Charges" by the QEq charge equilibration scheme [Rappé, 1991] every 50 iterations. Selected "Grid Search" varying both C-O-P=O torsions from -150° to 130° with 30° steps, minimizing each conformer. We disabled restraining of the torsions and kept unique conformers within 100.00 kcal/mol above the current minimum.

6.6. Least-squares fit of phosphonate rings to tetrahedral intermediate.

First, we fit only the N-C-C-O atom pairs, to determine the atoms that corresponded best to the *oxo* on the phosphorus, and the corresponding methyl groups on the quaternary nitrogens. After that, we repeated the least-squares fitting including all the atoms pairs described in the [figure].

6.7. Hardware.

PCMODEL v.4.0, MacroModel v.5.0, Cerius^2 v.2.0, MOPAC 6.0 and MOPAC93 ran on a Silicon Graphics Indigo^2 Extreme with 96 MB of RAM, R4400 CPU and R4010 FPU, under IRIX 5.3. Gaussian94 (serial version) ran on an IBM SP2 equipped with 14 nodes, 128 MB/node of RAM and 2 GB/node of scratch space, running under AIX 3.2/4.0

and LoadLeveler as a batch process controller.

[Title] [Ded] [Ack] [1] [2] [3] [4] [5] [6] [7] [Bib] [A] [B] [C] [D] [E] [Vita]

Chapter 7. Conclusions.

7.1. Summary

One goal of our research is determine what are the conformations and configurations of the tetrahedral intermediates in carnitine acyl transfers. So far, the approach has been experimental, by designing conformationally constrained analogues of the tetrahedral intermediates. To make the approach cost-effective, we need reliable modeling methods to guide the choice of the next generation of inhibitors. The modeling methods developed in this dissertation fulfill that need for the most part.

This dissertation addressed two additional questions:

- Why does acetylcarnitine have such a high free energy of hydrolysis?
- What are the conformations of our heterocyclic moieties that could best fit the tetrahedral intermediate for acetylcarnitine-CoA exchange?

Acetylcarnitine reaches its high energy of hydrolysis by drawing from the solvation energy. The coupling between solvation energy, dipole moment and conformational change, supplies the necessary energy from the solvation term to yield a free energy of hydrolysis that compares to that of AcCoA. The high-energy status of acylcarnitine makes possible an exchange equilibrium with CoA (K_{eq} = 0.6), that minimizes the energy consumed by processes other than the transport through the cell membrane.

From the preliminary results for the modeling of the tetrahedral intermediate, [shown in the table in chapter 3,] we see the RMS fits of the dioxazaphosphacinium rings to the intermediate. The most promising candidates are both boat-boat conformers that correspond to the *R,S* diastereomer of the tetrahedral intermediate. The *cis*-substituted ring and the dimethyl-substituted ring yield the closest fit to the *R,S* tetrahedral intermediate. These fits should be considered as one parameter in a quantitative structure-activity relationship for the inhibitory potency of the inhibitors already developed by our group. This will help in the prediction of the next generation of inhibitors. The morpholinium rings should receive a similar treatment.

- Upon hydrolysis, the zwitterion of acetylcarnitine keeps a nearly constant dipole moment thanks to the influence of conformational flexibility on the positioning of the charged centers. This keeps the solvation energy nearly constant, leaving more chemical energy available to be released.
- Conformational change can act as a mechanism for the storage of chemical energy.
- In morpholinium rings, the conformational preference in aqueous media obeys more the increased steric interactions due to the shorter C-N and C-O bonds than the differences in dipole moment.
- *Gem* substitution in morpholinium rings can help control the relative stabilities of the chair and the twist-boat.
- Addition of substituents in a 1,1,3,3-di*gem* pattern on dioxazaphosphacinium rings can favor a twist-boat global minimum over a boat-chair conformation.
- Differences in polarity in dioxazaphosphacinium rings override steric effects, when methyl groups are involved, in determining the preferred conformation in aqueous solution.
- We have developed parameters for accurate modeling of neutral dialkyl alkylphosphonates by molecular mechanics (AMBER*). We used three measures of the goodness of fit when testing against ab initio results and crystal structures, and found our parameters more reliable than other commonly used force fields (MM2*, MMX and UFF)

7.2. Future work.

Based on the results obtained from the acetylcarnitine hydrolysis, the aqueous modeling of the heterocycles including a methylenecarboxylate should pay attention to the influence of the dipole moments. In the dioxazaphosphacinium rings,

there will be two sources of polarity: the dipoles due to the C-O-P=O torsions, and the dipole due to the zwitterion. How will the conformational preference of the rings be affected by the presence of the zwitterion?. Answering such question will require careful attention to the charge set used in the calculation. It may be desirable to determine a new charge set for the methylenecarboxylate-substituted ring, at the HF/6-31+G* level of theory using the CHelpG scheme, to ensure that the charge set found in this dissertation is still applicable (see the file BondPC.txt for the output from the CHelpG calculation). After all, changing from a cation to a neutral species will likely affect the charge distribution in the molecule. In addition, unless newer versions of MacroModel provide utilities for the calculation of the dipole moment, it will be necessary to supplement the MacroModel results with some other modeling package. Single-point calculations on the AMBER*-optimized geometries, using the AM1 Hamiltonian in MOPAC93, would provide an appropriate starting point.

- Improved modeling of the transition structure for the acetyl exchange between acetylcarnitine and CoA by:
    1. Modeling by semiempirical (or ab initio) methods, including a solvent model.
    2. Determination of molecular mechanics parameters specific to the sulfur found in the molecule (from ab initio).
    3. Molecular mechanics modeling including longer chains in place of the acetyl group.
- Modeling of the morpholinium rings including a methylenecarboxylate, both in the gas phase and solution.
- Modeling of the phosphonate rings including a methylenecarboxylate, both in the gas phase and solution.

[Title] [Ded] [Ack] [1] [2] [3] [4] [5] [6] [7] [Bib] [A] [B] [C] [D] [E] [Vita]

Bibliography

Alder, R. W.; White, J. M. *Conformational Analysis of Medium-Sized Rings;* Glass, R. S.; VCH Publishers, Inc.: New York, 1988, 97-150

Allen, F. H.; Bellard, S.; Brice, M .D.; Cartwright, B. A.; Doubleday, A.; Higgs, H.; Hummelink, T.; Hummelink-Peters, B. G.; Kennard, O.; Motherwell, W. D. S.; Rodgers, J. R.; Watson, D. G. *Acta Crystallogr., Sect. B* 1977, B35, 2331-2339

Allinger, N. L.; Hirsch, J. A.; Miller, M.; Tyminski, J. J.; van Catledge, F. A. *J. Am. Chem. Soc.* 1968, 90, 1199-1210

Allinger, N. L.; Yuh, Y. H.; Lii, J.-J. *J. Am. Chem. Soc.* 1977, 99, 8127-8134

Altona, C.; Knobler, C.; Romers, C. *Acta Crystallogr.* 1963, 16, 1217-1225

Anderson, J. E.; Glazer, E. D.; Griffith, D. L.; Knorr, R.; Roberts, J. D. *J. Am. Chem. Soc.* 1969, 91, 1386-1395

Anderson, J. E. *Topics in Current Chemistry. Dynamic Chemistry;* Springer-Verlag: Berlin, 1974, 139-168

Anderson, R. C.; Balestra, M.; Bell, P. A.; Deems, R. O.; Fillers, W. S.; Foley, J. E.; Fraser, J. D.; Mann, W. R.; Rudin, M.; Vilhauer, E. B. *J. Med. Chem.* 1995, 38, 3448-3450

Anet, F. A. L; Anet, R. *Det. Org. Struct. Phys. Methods;* 1971, 5 344-420

Anet, F. A. L; Degen, P. J. *J. Am. Chem. Soc.* 1972, 94, 1390-1392

Anet, F. A. L. *Topics in Current Chemistry. Dynamic Chemistry;* Springer-Verlag: Berlin, 1974, 169-220

Aped, P.; Allinger, N. L. *J. Am. Chem. Soc.* 1992, 114, 1-16

Armarego, W. L. F. *Stereochemistry of Heterocyclic Compounds;* Taylor, E. C.; Weisberger, A. John Wiley & Sons: New York, 1977

Walters, P.; Stahl, M. *Babel, v.1.1* University of Arizona, Tucson, AZ 85721, 1994

Ben-Naim, A. *Solvation Thermodynamics* Plenum Press: New York, 1987, p 81

Bentrude, W. G.; Sopchik, A. E.; Bajwa, G. S.; Setzer, W. N.; Sheldrick, W. S. *Acta Crystallogr., Sect. C* 1986, C42, 1027-1029

Bieber, L. L.; Dai, G.; Chung, C. *Current Concepts in Carnitine Research* A. Lee Carter; CRC Press: Boca Raton, 1992, 7-18

Bixon, M. Lifson, S. *Tetrahedron* 1967, 23, 769-784

Burton, K. *Biochem. J.* 1954, 59, 44-46

Castonguay, L. A.; Rappé, A. K. *J. Am. Chem. Soc.* 1992, 114, 5832-5842

Colucci, W. J.; Gandour, R. D.; Mooberry, E. A. *J. Am. Chem. Soc.* 1986, 108, 7141-7147

Colucci, W. J.; Gandour, R. D. *Bioorg. Chem.* 1988, 16, 307-334

Chase, J. F. A.; Tubbs, P. K. *Biochem. J.* 1969, 111, 225-235

Chu, N.-J. *Ph.D. Thesis;* University of Ottawa 1959

Cramer, C. J.; Denmark, S. E.; Miller, P. C.; Dorow, R. L.; Swiss, K. A.; Wilson, S. R. *J. Am. Chem. Soc.* 1994, 116, 2437-2447

Cramer, C. J.; Truhlar, D. G. *Reviews in Computational Chemistry;* Lipkowitz, K. B.; Boyd, D. B; VCH Publishers: New York, 1995, 1-72

Dale, J.; Ekeland, T.; Krane, J. *J. Am. Chem. Soc.* 1972, 94, 1389-1390

Dalling, D. K.; Grant, D. M. *J. Am. Chem. Soc.* 1967, 89, 6612-6622

Day, R. O.; Bentrude, W. G.; Yee, K. C.; Setzer, W. N.; Dieters, J. A.; Holmes, R. R. *J. Am. Chem. Soc.* 1984, 106, 103-106

Denmark, S. E.; Cramer, C. J. *J. Org. Chem.* 1990, 55, 1806-1813

Derrick, J. P.; Ramsay, R. R. *Biochem. J.* 1989, 262, 801-806

Dionne, P.; St-Jacques, M. *J. Am. Chem. Soc.* 1987, 109, 2616-2623

Dyrbusch, M.; Egert, E. *Acta Crystallogr., Sect. C* 1986, C42, 1235-1237

Edward, J. T. *Chem. Ind.* 1955, 1102-1104

Eliel, E. L.; Wilen, S. H.; Mander, L. N. *Stereochemistry of organic compounds;* Wiley-Interscience: New York, 1994

Eistetter, K.; Wolf, H. P. O. *J. Med. Chem.* 1982, 25, 109-113

Ewig, C. S.; Van Wazer, J. R. *J. Am. Chem. Soc.* 1985, 107, 1965-1971

Fox, P. C.; Bowen, J. P.; Allinger, N. L. *J. Am. Chem. Soc.* 1992, 114, 8536-8544

Friedman, S.; Fraenkel, G. *Arch. Bioch. Biophys.* 1955, 59, 491-501

Fritz, I. B.; Schultz, S. K.; Srere, P. A. *J. Biol. Chem.* 1963, 238, 2509-2517

Fritz, I. B.; Schultz, S. K.; *J. Biol. Chem.* 1965, 240, 2188-2192

Gajewski, J. J. Gilbert, K. E. McKelvey, J. *Adv. Mol. Mod.;* Liotta, D.; JAI Press, Inc.: Greenwich, 2, 1990, 65-92

Gandour, R. D.; Colucci, W. J.; Fronczek, F. R. *Bioorg. Chem.* 1985, 13, 197-208

Gandour, R. D.; Colucci, W. J.; Stelly, T. C.; Brady, P. S.; Brady, L. J. *Biochem. Biophys. Res. Commun.* 1986, 138, 735-741

Gandour, R. D.; Colucci, W. J.; Stelly, T. C.; Brady, P. S.; Brady, L. J. *Arch. Bioch. Biophys.* 1988, 267, 515-520

Gandour, R. D.; Blackwell, M.; Colucci, W. J.; Chung, C.; Bieber, L.; Ramsay, R. R.; Brass, E. P.; Fronczek, F. R. *J. Org. Chem.* 1992, 57, 3426-3431

Gandour, R. D.; Leung, O.-T.; Greway, A. T.; Ramsay, R. R.; Bhaird, N. N.; Fronczek, F. R.; Bellard, B. M.; Kumaravel, G. *J. Med. Chem.* 1993, 36, 237-248

Gaussian 94, Revision C.2, Frisch, M. J.; Trucks, G. W.; Schlegel, H. B.; Gill, P. M. W.; Johnson, B. G.; Robb, M. A.; Cheeseman, J. R.; Keith, T.; Petersson, G. A.; Montgomery, J. A.; Raghavachari, K.; Al-Laham, M. A.; Zakrzewski,

V. G.; Ortiz, J. V.; Foresman, J. B.; Cioslowski, J.; Stefanov, B. B.; Nanayakkara, A.; Challacombe, M.; Peng, C. Y.; Ayala, P. Y.; Chen, W.; Wong, M. W.; Andres, J. L.; Replogle, E. S.; Gomperts, R.; Martin, R. L.; Fox, D. J.; Binkley, J. S.; Defrees, D. J.; Baker, J.; Stewart, J. P.; Head-Gordon, M.; Gonzalez, C.; Pople, J. A. Gaussian, Inc., Pittsburgh PA, 1995

George, P.; Witonsky, R. J.; Trachtman, M.; Wu, C.; Dorwart, W.; Richman, L.; Richman, W.; Shuryah, F.; Lentz, B. *Biochim. Biophys. Acta* 1970, 223, 1-15

Hayes, D. M.; Kenyon, G. L.; Kollman, P. A. *J. Am. Chem. Soc.* 1978, 100, 4331-4340

Hendrickson, J. B. *J. Am. Chem. Soc.* 1964, 86, 4854-4866

Hendrickson, J. B. *J. Am. Chem. Soc.* 1967, 89, 7036-7043

Hopfinger, A. J.; Pearlstein, R. A. *J. Comput. Chem.* 1984, 5, 486-499

Jencks, W. P.; Cordes, S.; Carriuolo, J. *J. Biol. Chem.* 1960, 235, 3608-3614

Jenkins, D. L.; Griffith, O. W. *J. Biol. Chem.* 1985, 260, 14748-14755

Jenkins, D. L.; Griffith, O. W. *Proc. Natl. Acad. Sci. U.S.A.* 1986, 83, 290-294

Jin, A. Y.; Benesch, L. A.; Weaver, D. F. *Can. J. Chem.* 1994, 72, 1596-1604

Stewart, J. J. P. *MOPAC: a General Molecular Orbital Package* Quant. Chem. Prog. Exch. 1990 10:86

Juaristi, E.; Cuevas, G. *The Anomeric Effect* CRC Press: Boca Raton, 1995

Kanamaru, T.; Shinagawa, S.; Asai, M.; Okazaki, H.; Sugiyama, Y.; Fujita, T.; Iwatsuka, H.; Yoneda, M. *Life Sci.* 1985, 30, 217-223

Katolichenko, V. I.; Egorov, Y. P.; Boronikov, Y. Y.; Golik, G. A. *Zh. Obshch. Khim.* 1973, 43, 2475-2490

Kellie, G. M.; Riddell, F. G. *Topics in Stereochemistry;* Eliel, E. L. Allinger, N. L. John Wiley & Sons: New York, 8, 1974, 225-270

Kirby, A. J. *The Anomeric Effect and Related Stereoelectronic Effects at Oxygen;* Springer Verlag: Berlin, 1983, p 77

Klamt, A. Shüürman, G. *J. Chem. Soc. Perkin Trans. 2* 1993, 799-805

Koch, R.; Anders, E. *J. Org. Chem.* 1995, 60, 5861-5866

Kolossváry, I. Guida, W. C. *J. Am. Chem. Soc.* 1993, 115, 2107-2119

Kumaravel, G.; a' Bhaírd, N. N.; Fronczek, F. R.; Ramsay, R. R.; Ashendel, C. L.; Gandour, R. D. *Bioorg. Med. Chem. Lett.* 1994, 4, 883-886

Kumaravel, G.; Gandour, R. D.; *Acta Crystallogr., Sect. C* 1995, C51, 1919-1921

Laing, M. *J. Chem. Ed.* 1987, 64, 124-128

Landin, J.; Pascher, I.; Cremer, D. *J. Phys. Chem.* 1995, 99, 4471-4485

Lemieux, R. U.; Pavia, A. A.; Martin, J. C.; Watanabe, K. A. *Can. J. Chem.* 1969, 47, 4427-4439

Liang, C.; Ewig, C. S.; Stouch, T. R.; Hagler, A. T. *J. Am. Chem. Soc.* 1993, 115, 1537-1545

Marsh, F. J.; Weiner, P.; Douglas, J. E.; Kollman, P. A.; Kenyon, G. L.; Gerlt, J. A. *J. Am. Chem. Soc.* 1980, 102, 1660-1665

Maurel, P.; Galzigna, L. *Biophys. J.* 1971, 11, 550-557

Miertus, S.; Scrocco, E.; Tomasi, J. *Chem. Phys.* 1981, 55, 117-129

Miertus, S.; Tomasi, J. *Chem. Phys.* 1982, 65, 239-245

Müller, D. M.; Strack, E. *Hoppe-Seyler's Z. Physiol. Chem.* 1973, 354, 1091-1096

Mursakulov, I. G.; Svyatkin, V. A; Samoshin, V. V.; Palyulin, V. A.; Zefirov, N. S. *Zh. Org. Khim.* 1984, 20, 80-88

PCMODEL v.4.0 Serena Software, IN

Perrin, C. L.; Young, D. B. *Tet. Lett.* 1995, 36, 7185-7188

Pierlik, J. R.; Guynn, R. W. *J. Biol. Chem.* 1975, 250, 4445-4450

Riddell, F. G. *The Conformational Analysis of Heterocyclic Compounds;* Academic Press: London, 1980

Thatcher, G. R. J.; Campbell, A. S. *J. Org. Chem.* 1993, 58, 2272-2281

Tutwiler, G. F.; Brentzel, H. J.; Kiorpes, T. C. *Proc. Soc. Exp. Biol. Med.* 1985, 178, 288-296

Moore, J. A.; Anet, F. A. L. *Comprehensive Heterocyclic Chemistry;* Katritzki, A. R.; Rees, C. W. Pergamon Press Ltd.: Oxford, 1984, 697-707

Gorenstein, D. G.; Kar, D.; Luxon, B. A.; Momii, R. K. *J. Am. Chem. Soc.* 1976, 98, 1668-1673

van der Veken, B. J.; Herman, M. A. *J. Mol. Struct.* 1977, 42, 161-170

Mikolajczyk, M.; Graczyk, P.; Kabachnik, M. I.; Baranov, A. P. *J. Org. Chem.* 1989, 54, 2859-2861

Nastopoulos, V.; Germain, G.; Kallistis, J.; Voliotis, S. *Acta Crystallogr., Sect. C* 1987, C43, 245-249

Ounsworth, J. P.; Weiler, L. *J. Chem. Ed.* 1987, 64, 568-572

Plyamovatyi, A. Kh.; Dashevskii, V. G.; Kabachnik, M. I. *Dokl. Akad. Nauk SSSR* 1977, 234, 1100-1103

Plyamovatyi, A. Kh.; Dashevskii, V. G.; Kabachnik, M. I. *Dokl. Akad. Nauk SSSR* 1977, 235, 124-127

Plyamovatyi, A. Kh.; Vandyukova, I. I.; Shagidullin, R. R.; Vizel, A. O. *Izv. Akad. Nauk SSSR, Ser. Khim.* 1990, 1577-1584

Plyamovatyi, A. Kh.; Vandyukova, I. I.; Shagidullin, R. R.; *Zhur. Obshch. Khim.* 1994, 64, 232-235

Quin, L. D. *Conformational Analysis of Medium-Sized Heterocycles;* Glass, R. S.; VCH Publishers, Inc.: New York, 1988, 181-216

Rappé, A. K.; Goddard-III, W. A. *J. Phys. Chem.* 1991, 95, 3358-3363

Rappé, A. K.; Casewit, C. J.; Colwell, K. S.; Goddard-III, W. A.; Skiff, W. M. *J. Am. Chem. Soc.* 1992, 114, 10024-10035

Rappé, A. K.; Colwell, K. S. *Inorg. Chem.* 1993, 32, 3438-3450

Romers, C.; Altona, C.; Buys, H. R.; Havinga, E. *Topics in Stereochemistry;* E. L. Eliel; N. L. Allinger; Wiley-Interscience: New York, 4 1969, 39-97

Saeed, A.; McMillin, J. B.; Wolkowicz, P. E.; Brouillette, W. J. *Arch. Biochem. Biophys.* 1993, 305, 307-312

Saeed, A.; McMillin, J. B.; Wolkowicz, P. E.; Brouillette, W. J. *J. Med. Chem.* 1994, 37, 3247-3251

Savle, P. S.; Medhekar, R. A.; Kelley, E. L.; May, J. G.; Watkins, S. F.; Fronzcek, F. R.; Quinn, D. M.; Gandour, R. D. *Chem. Res. Toxicol.* in press.

Shinagawa, S.; Kanamaru, T.; Harada, S.; Asai, M.; Okazaki, H. *J. Med. Chem.* 1987, 30, 1458-1463

Sieburth, S. McN. *J. Chem. Soc., Chem. Commun.* 1994, 1663-1664

Sun, G.; Savle, P. S.; Gandour, R. D.; a' Bhaird, N. N.; Ramsay, R. R.; Fronczek, F. R. *J. Org. Chem.* 1995, 60, 6688-6695

Sundaralingam, M. *Nature* 1968, 217, 35-37

Szabo, A.; Ostlund, N. S. *Modern Quantum Chemistry: Introduction to Advanced Electronic Structure Theory;* Dover Publications, Inc.: Mineola, NY, 1996 370-378

Tipton, K. F.; Chase, J. F. A.; *Biochem. J.* 1969, 115, 517-521

Van Wazer, J. R.; Ewig, C. S. *J. Am. Chem. Soc.* 1986, 108, 4354-4360

Venkatraghavan, V.; Smith, D. J. *Arch. Biochem. Biophys.* 1983, 220, 193-199

Weiner, S. J.; Kollman, P. A.; Nguyen, D. T.; Case, D. A. *J. Comp. Chem.* 1986, 7, 230-252

Weiser, J.; Golan, O.; Fitjer, L.; Biali, S. E. *J. Org. Chem.* 1996, 61, 8277-8284

Wiberg, K. B. *J. Am. Chem. Soc.* 1965, 87, 1070-1078

Wiberg, K. B.; Murcko, M. A.; Laidig, K. E.; MacDougall, P. J. *J. Phys. Chem.* 1990, 94, 6956-6959

Wilson, B.; Georgiadis, R.; Bartmess, J. E. *J. Am. Chem. Soc.* 1991, 113, 1762-1766

Wolfe, S.; *Acc. Chem. Res.* 1972, 5, 102-111

Wolfenden, R. *Nature* 1969, 223, 704-705

Wolfenden, R.; Liang, Y.-L. *J. Biol. Chem.* 1988, 263, 8022-8026

Wolfenden, R.; Liang, Y.-L. *Bioorg. Chem.* 1989, 17, 486-489

[Title] [Ded] [Ack] [1] [2] [3] [4] [5] [6] [7] [Bib] [A] [B] [C] [D] [E] [Vita]

Appendix A. Naming and numbering scheme for cyclooctane conformers.

A.1. Boat-chair family.

We have tried to keep the scheme simple and, primarily, to make it easy to draw a particular conformer from the name. BC has a C_s point group. In general, as soon as substituents are introduced in the ring, the point group becomes C_1 unless the substituents happen to lie in the carbons split by the mirror plane that defines C_s symmetry. Thus, in the general case, we can distinguish two enantiomeric BC conformers, one \ ``left-oriented" and one ``right-oriented"

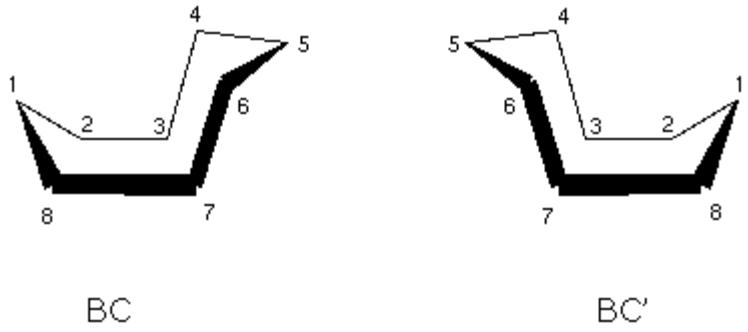

Figure A.1. ``Left-oriented" and ``right-oriented" BCs[fig.chiralBCs.gif, 1.640KB]

We denote the ``left-oriented" version by BC, while the ``right-oriented" is BC'. The numbers on the carbons follow a specular relationship to the numbers in the conformational enantiomer.

To name a particular conformer, we keep the numbering fixed. We do follow the chemical convention of always trying to assign the lowest possible numbers, within the constraint that the positions of fixed number positions. Thus, if the substitution pattern allows it, the choice between BC and BC' depends on which one yields the lowest numbers. We define completely the position of a substituent by choosing the appropriate letter among the following:

e
: equatorial

a
: axial

b
: bowsprit

f
: flagpole

i
: isoclinal

according to the following scheme (we have left some of the positions unlabeled for the sake of clarity in the drawing):

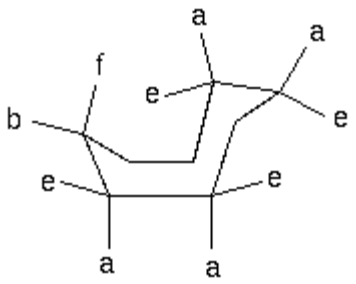

Figure A.2. Labels for the orientations of substituents in BC[fig.BCtags.gif, 0.939KB]

The point group of TBC is C_2. This is a disymmetric group and allows for chiral shapes. We can therefore distinguish two conformers, one ``twisted to the right" and one ``twisted to the left". We designate the one ``twisted to the left" as TBC, and the ``twisted to the right" as TBC'. See the scheme:

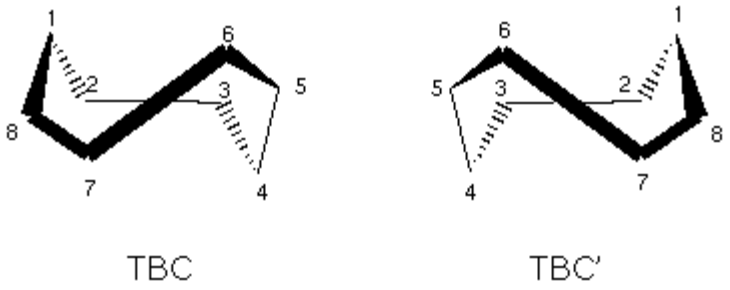

Figure A.3. ``Left-oriented" and ``right-oriented" TBCs[fig.chiralTBCs.gif, 1.689KB]

The labels for the orientation are as follows:

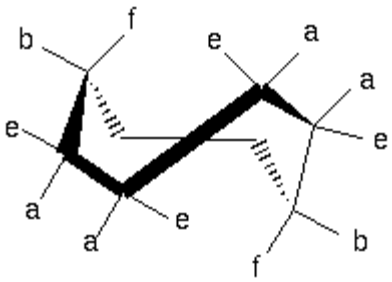

Figure A.4. Labels for the orientations of substituents in TBC[fig.TBCtags.gif, 1.257KB]

A.2. Chair-chair family.

The CC has a C_{2v} point group. Its shape is slightly elliptical (when seen from the z axis). It has four sets of **isochronous** carbons (same NMR signal by symmetry). C_{2v} is not a chiral point group so we only have:

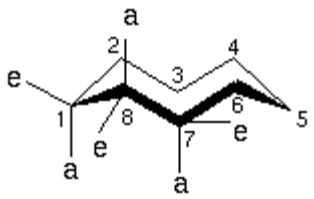

Figure A.5. CC numbering and labeling scheme.[fig.CCtags.gif, 0.846KB]

The numbering starts on one carbon along the major axis of the ellipse.

The Crown is a very high-symmetry conformer, with a D_{4d} point group. All the carbons are undistinguishable by symmetry operations so the choice of any particular carbon to start the numbering is immaterial. The Crown is actually a special case of the CC , but we give the numbering and labels for substituents for the sake of completeness. The introduction of substituents is bound to perturb the high symmetry of the molecule, rendering it as a CC. We do not have any examples of crowns in our results, and we do not find any crown conformers among substituted cyclooctanes, although some authors have referred to CCs as crowns in the past.

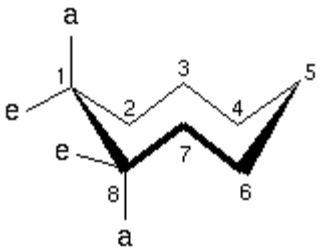

Figure A.6. Crown.[fig.crowntags.gif, 0.941KB]

The TCC has a D_2 point group. This is a disymmetric group, so we find two enantiomers. The numbering and the names follow this scheme:

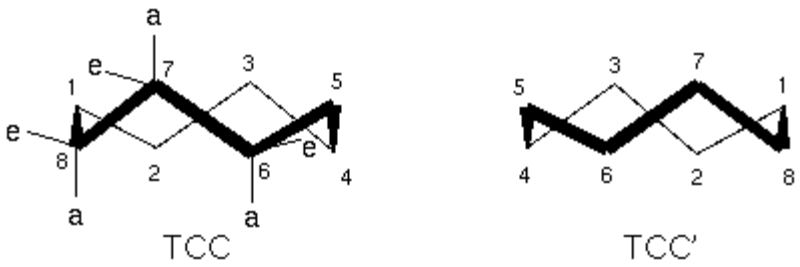

Figure A.7. TCC numbering and labeling scheme.[fig.TCCtags.gif, 1.751KB]

The TC has a C_{2h} point group. The numbering and the names follow this scheme:

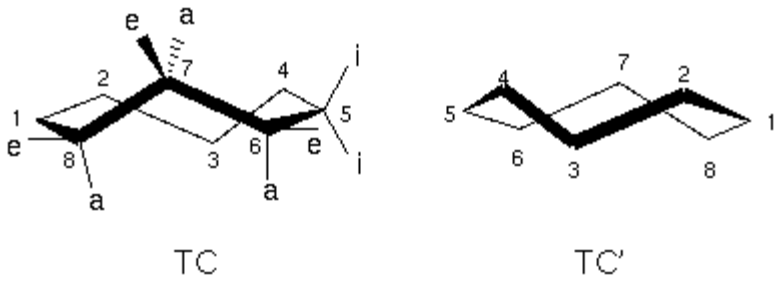

Figure A.8. TC numbering and labeling scheme.[fig.TCtags.gif, 1.593KB]

The C has a C_{2h} point group. The numbering and labeling are as follows:

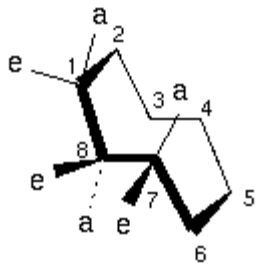

Figure A.9. C numbering and labeling scheme.[fig.Ctags.gif, 0.971KB]

A.3. Boat-boat family.

Boat.

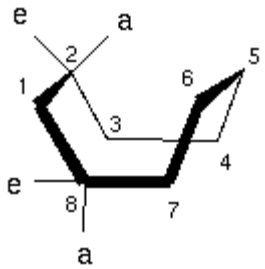

Figure A.10. B numbering and labeling scheme.[fig.Btags.gif, 0.944KB]

Boat-boat.

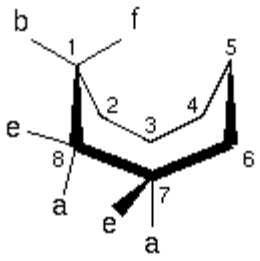

Figure A.11. BB numbering and labeling scheme.[fig.BBtags.gif, 0.997KB]

Twist-boat.

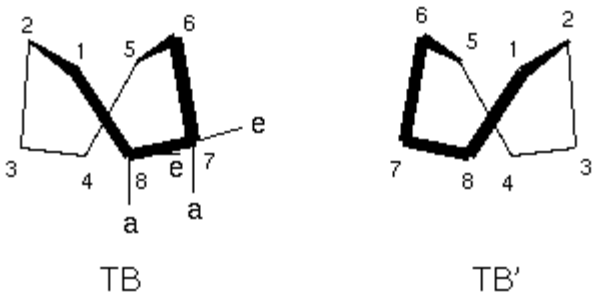

Figure A.12. TB numbering and labeling scheme.[fig.TBtags.gif, 1.700KB]

[Title] [Ded] [Ack] [1] [2] [3] [4] [5] [6] [7] [Bib] [A] [B] [C] [D] [E] [Vita]

Appendix B. Rules for naming hetero-substituted cyclooctanes.

- Keep the numberings assigned to the conformations of cyclooctane fixed.
- Keep the orientation descriptors, such as equatorial and axial, assigned to the conformations of cyclooctane fixed.
- Find out the numbers that correspond to the heteroatoms *within* the ring.
- In case there is more than one way to read the numbers that correspond to the heteroatoms, *e. g.* 2*P*-6*N* in BC vs. 4*N*-8*P* in BC', choose the locant set that assigns the lowest numbers.
- If the numbers are the same and they just switch positions, *e. g.*, 1*N*-5*P* in TBC vs. 1*P*-5*N* in TBC', the atom with the highest priority by Cahn-Ingold-Prelog rules gets the lowest number.
- If it is not clear which locant set assigns the lowest numbers *e.g.*, 1,4,5,6 or 1,2,7,8 then the locant set that assigns the lowest number to the highest priority atom (CIP rules) is chosen. In the previous locant sets, if the highest priority atom can be either 2 or 4, then the locant set 1,2,7,8 should be chosen, despite the 7,8 being higher than 5 and 6.
- Read the numbers that correspond to the substituents *on* the ring.
- List the substituents on the ring preceded by the numbers and an appropriate prefix to indicate the number of times the substituent appears.
- Attach to the numbers the abbreviation of the appropriate orientational descriptor.
- For substituents on isoclinal positions, specify the *R* or *S* configuration of the atom.

By the previous rules the name for the following conformer:

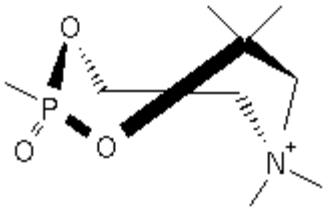

Figure B.1. Example conformer.[fig.example.gif, 0.827KB]

is 1,1,5*e*,8,8-pentamethyl-5*a*-oxo-1*N*-4,6-di*O*-5*P*-TBC.

[Title] [Ded] [Ack] [1] [2] [3] [4] [5] [6] [7] [Bib] [A] [B] [C] [D] [E] [Vita]

Appendix C. Software standards used.

This document is encoded in Electronic Theses and Dissertations Markup Language (ETDML) using etd.dtd v.1.1. Non-ASCII characters are encoded in Unicode v.2.0. All the figures are GIF87a (Data type: unsigned char, Dimension order: interleaved, Color model: color index, Coordinate space: upper-left, Minimum: 0, Maximum: 255). The virtual reality models (*.wrl files) are encoded in VRML 1.0.

The SGML parser used to check this document was "nsgmls" included as part of the package SP v.1.0.1 by James Clark. The word processor was "jot", a utility provided in IRIX 5.3. ISIS/Draw v.1.2 was used for all the chemical drawings. The figures were generated either by using the ``snapshot" utility provided in IRIX 5.3 to make a *.rgb image file, which was later converted to GIF87a by ``movieconvert", another image processing utility provided in IRIX 5.3; or by saving the image as a Microsoft *.bmp file, which was later converted to GIF87a by LView for Windows v.3.1. The *.wrl files were generated by saving the molecule in PDB format from MacroModel, and then translating with the program pdb2vrml using the "-stick" flag. All the conversions between chemical file formats were done using Babel v.1.1.

Mention of a given program or brand name does not imply endorsement by Virginia Polytechnic Institute and State University or any of its departments.

[Title] [Ded] [Ack] [1] [2] [3] [4] [5] [6] [7] [Bib] [A] [B] [C] [D] [E] [Vita]

Appendix D. Chemical files included.

For each VRML model I have included the corresponding file in PDB format (found in the PDB directory). I have also included all the consolidated output files from the conformational searches in macromodel format.

[Title] [Ded] [Ack] [1] [2] [3] [4] [5] [6] [7] [Bib] [A] [B] [C] [D] [E] [Vita]

Appendix E. README: Notes on the creation of a dissertation in ETD-ML.

E.1. ETD-ML source encoding.

This the first ETD-ML ETD ever to be submitted. As a hint for future ETD-ML authors, we have made the encoding for this ETD available in its source format.

- ETD-ML source

The whole document is structured, with left-indentation corresponding to the logical subdivisions:

```
No spaces for a chapter,
    4 spaces for a section,
        8 spaces (tab) for a subsection,
            12 spaces (tab + 4) for a block and
                16 spaces (2 tabs) for a subblock.
```

Links, floating matter, footnotes and tables are not indented. That is to allow an easier construction of a list of tables and list of figures by a reformatter (so far, I am the "reformatter" for those lists, I use the UNIX command "grep" and pipe the output to a file, so I have to keep all the text of the captions in the same line).

Greek letters are symbolyzed by their "{name}" to allow them to show up in the HTML version (there is no provision for greek characters in HTML 2.0). The "{name}" should be substituted by the Unicode number. Note: micro and mu are expressed by the same greek letter, but micro is a prefix in the SI system, while mu may have many other meanings. I considered them as separate entities to allow for a "smart" reformatter or search engine that could take that into account.

The entities chemname, casnum and chemform are included only to help in the search of chemical names, Chemical Abstracts Registry Numbers and chemical formulas, respectively.

E.2. Virtual Reality Modeling Language (VRML).

The three dimensional figures are VRML 1.0 models. The way to incorporate them into a formatted document depends on the technology available and the effect desired by the formatter. VRML figures can be shown as hyperlinks (in HTML) by means of an anchored reference, such as:

```
<a href="carnitine/fig.RSWat.gif">(caption text)</a>
```

This is what I did in the HTML version of my dissertation, because of the computational overhead involved in loading and displaying literally hundreds of little VRML viewers in the same page. Anyway, the VRML models are still encoded as:

```
<mm entity=VR.name>(caption text)</mm>
```

so the reformatter has to make the decision about displaying them as an anchored reference or as an embedded VRML viewer window, e.g., a smart reformatter could choose to display some of the 3D models as anchored references and embed the others.

The virtual reality viewer can also be embedded in a HTML homepage by means of the following code:

```
<embed border=0 type="x-world/x-vrml" src="file.wrl" align=abscenter width=300 height=300>
(caption text)
</embed>
```

It is strongly recommended that the "type" parameter be present. This helps the browser correctly handle the rendering of the image. In the future, it may be necessary to change the x-world/x-vrml type to the definitive MIME type declaration (probably "world/vrml"). So far, "x-world/x-vrml" is an experimental MIME type (thus the "x-" prefix), although it is recognized by most browsers.

These VRML files were succesfully viewed using CosmoPlayer and Live3D. PDB files can be converted to VRML using the script pdb2vrml, available from:

- http://www.pc.chemie.th-darmstadt.de/vrml/pdb2vrml.html

E.3. Chemical Markup Language (CML).

Markup coding of chemical information is still in its infancy. There is a beginning in CML v.1.0 (Chemical Markup Language). You can find all there is to know about CML at (as of June, 1997):

- http://www.venus.co.uk/omf/cml-1.0/intro.html

If the URL doesn't work, a Web search specifying "Chemical Markup Language" or "Open Molecule Foundation" should yield some relevant hits.

Attempting a "merge" of CML coding into ETD-ML coding was beyond the resources (mostly time) available to this writer, although it is clearly the best way to go. Future customizations of the ETD-ML for chemistry should allow for elements encoded in CML. Anyway, since so far there is no accepted standard format for encoding molecular structures I decided to store the structures as VRML models and in PDB format. The PDB format files are not referred to *at any point* in the text of the dissertation, they are kept only because they are the actual results obtained from the modeling and, therefore, contain more chemical information than VRML files. PDB is not even a de facto standard, but it is widely used and it is better than XYZ coordinates because it preserves the connectivities between the atoms (XYZ readers have to make educated guesses about how atoms are connected and about the bond orders).

E.4. Babel, PDB, Chime.

It is possible to use Babel, together with the PDB files and a Netscape plug-in called Chime (available without cost from MDL, Inc.), to yield a fancier rendering of the molecules. Use Babel to transform the PDB files to MDL's MOL format and embed the images in a HTML page using the following code:

```
    <embed border=0 type="chemical/x-mdl-molfile" src="file.mol" align=abscenter width=150
height=150>
    (caption text)
    </embed>
```

This will result in a figure containing a 2D projection of the 3D structure. Clicking on the right button of the mouse will bring up the option of 3D rendering. It also allows for real-time rotation, rendering as wires, ball and stick, sticks, VDW spheres and others. I have included the MDL molfiles. They have the extension ".mol". Chime can be downloaded from:

- http://www.mdli.com/chemscape/chime/chime.html

Chime can identify and render many other chemical types, such as: PDB, XYZ, MOPAC and Gaussian input, MDL's molfile and rxnfile, and EMBL nucleotide format. Only the MDL molfile format will yield the switchable 2D<->3D view. [Note.]

BTW, Babel can be downloaded from the software archives of the Computational Chemistry Mailing List at:

- ftp://ccl.osc.edu/pub/chemistry/software/

looking under the appropriate operating system.

E.5. Reformatting the molecules.

If a reformatter decides to use XYZ files to visualize the molecules (after converting the PDB files to XYZ format), there is a Java applet developed by Sun Microsystems named XYZApp.class (downloadable from http://java.sun.com) that can do the job, although the rendering is somewhat primitive.

A minimum code to embed XYZApp.class in a HTML document is:

```
<applet code=XYZApp.class width=300 height=300>
<param name=model value=file.xyz>
</applet>
```

It is necessary to have Matrix3D.class to be able to run XYZApp.class.

E.6. Footnotes.

All the footnotes are referred to as "Note."s. It would be desirable to have a reformatter that used more standard designations: superscript arabic numbers (Journal of American Chemical Society-style), or a standard sequence of characters (such as the ones specified in the journals "Science" or the "Proceedings of the National Academy of Sciences of the USA")

E.7. Notes on MOL notation substitution.

The following table contains only GIF images and VRML models. Substituting the extension "mol" instead of the "wrl" will access the MDL molfiles, displayable with Chime. It will also be necessary to move the *.mol files out of the MOL directory.In that case, the GIF images will be unnecessary, because molfiles in Chime yield both 2D and 3d views. This is likely to require human intervention, because a reformating script would have to be *really* smart to accomodate all these changes. The caption is all in one line to make it easier to use a utility like "grep" when gathering a "List of Tables." [See table.]

E.8. README.TXT: Files in this ETD.

```
Rosas.tar.gz can be gunzipped to yield a tarred file that contains all
the files of my dissertation.  When untarred, the whole thing takes about
6.5MB.  The following is a list of all the files included (total of 457,
not including directories):

The version of gzip was 1.2.4.

dissertation:
total 1166
-rw-r--r--    1 rosas    user       320242 Jul  3 17:30 diss.etd
-rw-r--r--    1 rosas    user          243 Jun 17 13:16 README.TXT
drwxr-xr-x    4 rosas    user         1024 Jun 17 11:17 carnitine
drwxr-xr-x    3 rosas    user          512 Jun 17 11:09 cyclohexane
drwxr-xr-x    5 rosas    user         3072 Jun 17 11:04 cyclooctane
-rw-r--r--    1 rosas    user        13594 Mar 11 03:09 etd.dtd
drwxr-xr-x    4 rosas    user          512 Jun 17 11:31 methylphosp
drwxr-xr-x    3 rosas    user          512 Jun 17 11:10 morpholinium
drwxr-xr-x    5 rosas    user         3072 Jun 17 11:21 phosphacinium
drwxr-xr-x    2 rosas    user         1024 Jun 17 11:26 reviews

dissertation/carnitine:
total 247
drwxr-xr-x    2 rosas    user          512 Jun 17 11:17 MOL
drwxr-xr-x    2 rosas    user          512 Jun 17 11:17 PDB
```

```
-rw-r--r--    1 rosas    user       16959 May 17 11:46 RRGas.wrl
-rw-r--r--    1 rosas    user       17048 May 17 11:47 RRWat.wrl
-rw-r--r--    1 rosas    user       17017 May 17 11:48 RSGas.wrl
-rw-r--r--    1 rosas    user       16938 May 17 11:51 RSWat.wrl
-rw-r--r--    1 rosas    user        1967 May  1 12:32 TableAcCarnAM1Gas.html
-rw-r--r--    1 rosas    user        4961 May  1 12:33 TableAcCarnAM1Wat.html
-rw-r--r--    1 rosas    user        1781 May  1 12:33 TableAcCholAM1Gas.html
-rw-r--r--    1 rosas    user        2935 May  1 12:34 TableAcCholAM1Wat.html
-rw-r--r--    1 rosas    user        1949 May  1 12:34 TableCarnAM1Gas.html
-rw-r--r--    1 rosas    user        3251 May  1 12:34 TableCarnAM1Wat.html
-rw-r--r--    1 rosas    user        1203 May  1 12:34 TableCholAM1Gas.html
-rw-r--r--    1 rosas    user        1172 May  1 12:35 TableCholAM1Wat.html
-rw-r--r--    1 rosas    user        4805 May  1 12:36 TableOAcPrAM1Gas.html
-rw-r--r--    1 rosas    user        3950 May  1 12:36 TableOAcPrAM1Wat.html
-rw-r--r--    1 rosas    user        3356 May  1 12:37 TableOHPrAM1Gas.html
-rw-r--r--    1 rosas    user        2896 May  1 12:37 TableOHPrAM1Wat.html
-rw-r--r--    1 rosas    user         801 May 17 11:29 fig.RRWat.gif
-rw-r--r--    1 rosas    user         807 May 17 11:36 fig.RSWat.gif
-rw-r--r--    1 rosas    user         608 Feb  8 23:41 fig.extended.gif
-rw-r--r--    1 rosas    user        1511 May 18 12:47 fig.fitTI.gif
-rw-r--r--    1 rosas    user         510 May 22 14:17 fig.folded.gif
-rw-r--r--    1 rosas    user        4852 Apr  1 00:25 fig.highlight.gif
-rw-r--r--    1 rosas    user        2491 Apr  1 12:51 fig.hydrolysis1.gif
-rw-r--r--    1 rosas    user        4823 Apr  3 18:56 fig.solvation.gif
-rw-r--r--    1 rosas    user         731 May  5 21:15 fig.torsions.gif

dissertation/carnitine/MOL:
total 24
-rw-r--r--    1 rosas    user        2679 May 27 13:56 RRGas.mol
-rw-r--r--    1 rosas    user        2679 May 27 13:56 RRWat.mol
-rw-r--r--    1 rosas    user        2679 May 27 13:56 RSGas.mol
-rw-r--r--    1 rosas    user        2679 May 27 13:56 RSWat.mol

dissertation/carnitine/PDB:
total 40
-rw-r--r--    1 rosas    user        4620 May 17 11:41 RRGas.pdb
-rw-r--r--    1 rosas    user        4620 May 17 11:41 RRWat.pdb
-rw-r--r--    1 rosas    user        4620 May 17 11:41 RSGas.pdb
-rw-r--r--    1 rosas    user        4620 May 17 11:42 RSWat.pdb

dissertation/cyclohexane:
total 68
drwxr-xr-x    2 rosas    user         512 Jun 17 11:10 MOD
-rw-r--r--    1 rosas    user        1545 Jan 30 14:16 TableCyclohGas.html
-rw-r--r--    1 rosas    user        3660 May  1 13:49 TableDiMeCyclohGas.html
-rw-r--r--    1 rosas    user       15426 May  1 14:11 TableEtTriMeCyclohGas.html
-rw-r--r--    1 rosas    user        3913 May  1 14:03 TableTetraMeCyclohGas.html
-rw-r--r--    1 rosas    user        4378 May  1 14:02 TableTriMeCyclohGas.html
-rw-r--r--    1 rosas    user        3085 Mar  8 23:56 fig.hexConfs.gif

dissertation/cyclohexane/MOD:
total 813
-rw-r--r--    1 rosas    user        9431 Jun 17 11:09 CyclohexGas.out
-rw-r--r--    1 rosas    user       37811 Jun 17 11:09 DiMeCyclohexGas.out
-rw-r--r--    1 rosas    user       51129 Jun 17 11:09 TetMeCyclohexGas.out
-rw-r--r--    1 rosas    user       70920 Jun 17 11:09 TriMeCyclohexGas.out
-rw-r--r--    1 rosas    user      246240 Jun 17 11:09 TriMeEtCyclohexGas.out

dissertation/cyclooctane:
total 1331
drwxr-xr-x    2 rosas    user         512 Jun 17 11:04 MOD
drwxr-xr-x    2 rosas    user         512 Jun 17 10:02 MOL
drwxr-xr-x    2 rosas    user        1024 Jun 17 10:02 PDB
-rw-r--r--    1 rosas    user       10455 May  1 14:28 Table4MeCyclooctGas.html
-rw-r--r--    1 rosas    user       27249 May  1 14:28 Table5MeCyclooctGas.html
-rw-r--r--    1 rosas    user       19927 May 15 11:11 Table6MeCyclooctGas.html
-rw-r--r--    1 rosas    user        6936 May  1 14:30 TableCycloctGas.html
-rw-r--r--    1 rosas    user       14000 May 15 15:18 bb14O.wrl
-rw-r--r--    1 rosas    user       14195 May 15 15:31 bb24O.wrl
-rw-r--r--    1 rosas    user       15165 May 16 15:18 bb5O.wrl
-rw-r--r--    1 rosas    user       16350 May 16 22:21 bb6O.wrl
-rw-r--r--    1 rosas    user        9668 May 15 14:02 bc.wrl
-rw-r--r--    1 rosas    user       14058 May 15 15:17 bc14O.wrl
-rw-r--r--    1 rosas    user       15236 May 16 15:26 bc15O.wrl
-rw-r--r--    1 rosas    user       16189 May 16 22:29 bc16O.wrl
-rw-r--r--    1 rosas    user       14074 May 15 15:22 bc24O.wrl
-rw-r--r--    1 rosas    user       15183 May 16 15:27 bc25O.wrl
-rw-r--r--    1 rosas    user       16221 May 16 22:24 bc26O.wrl
-rw-r--r--    1 rosas    user       15291 May 16 15:37 bc35O.wrl
-rw-r--r--    1 rosas    user       15037 May 16 15:39 bc45O.wrl
-rw-r--r--    1 rosas    user       15179 May 16 15:43 bc55O.wrl
```

```
-rw-r--r--    1 rosas    user       15200 May 16 15:44 bc65O.wrl
-rw-r--r--    1 rosas    user       14201 May 15 15:33 cc4O.wrl
-rw-r--r--    1 rosas    user       15181 May 16 15:32 cc5O.wrl
-rw-r--r--    1 rosas    user         997 Mar 12 14:05 fig.BBtags.gif
-rw-r--r--    1 rosas    user         939 Mar 12 02:34 fig.BCtags.gif
-rw-r--r--    1 rosas    user         944 Mar 12 13:59 fig.Btags.gif
-rw-r--r--    1 rosas    user         846 Mar 12 12:30 fig.CCtags.gif
-rw-r--r--    1 rosas    user         971 Mar 12 13:48 fig.Ctags.gif
-rw-r--r--    1 rosas    user        1257 Mar 12 11:37 fig.TBCtags.gif
-rw-r--r--    1 rosas    user        1700 Mar 12 16:24 fig.TBtags.gif
-rw-r--r--    1 rosas    user        1751 Mar 12 12:46 fig.TCCtags.gif
-rw-r--r--    1 rosas    user        1593 Jun 13 15:25 fig.TCtags.gif
-rw-r--r--    1 rosas    user         430 May 14 21:50 fig.bb14O.gif
-rw-r--r--    1 rosas    user         435 May 14 21:49 fig.bb24O.gif
-rw-r--r--    1 rosas    user         489 May 15 11:04 fig.bb5O.gif
-rw-r--r--    1 rosas    user         449 May 15 14:18 fig.bb6O.gif
-rw-r--r--    1 rosas    user         249 May 14 20:01 fig.bc0O.gif
-rw-r--r--    1 rosas    user         301 May 14 21:23 fig.bc14O.gif
-rw-r--r--    1 rosas    user         364 May 14 22:15 fig.bc15O.gif
-rw-r--r--    1 rosas    user         439 May 15 14:21 fig.bc16O.gif
-rw-r--r--    1 rosas    user         301 May 14 21:20 fig.bc24O.gif
-rw-r--r--    1 rosas    user         365 May 14 22:37 fig.bc25O.gif
-rw-r--r--    1 rosas    user         441 May 15 14:20 fig.bc26O.gif
-rw-r--r--    1 rosas    user         402 May 14 23:20 fig.bc35O.gif
-rw-r--r--    1 rosas    user         405 May 14 23:24 fig.bc45O.gif
-rw-r--r--    1 rosas    user         434 May 15 10:58 fig.bc55O.gif
-rw-r--r--    1 rosas    user         435 May 15 11:01 fig.bc65O.gif
-rw-r--r--    1 rosas    user         324 May 14 21:54 fig.cc4O.gif
-rw-r--r--    1 rosas    user         334 May 14 22:52 fig.cc5O.gif
-rw-r--r--    1 rosas    user        1640 Mar 12 02:09 fig.chiralBCs.gif
-rw-r--r--    1 rosas    user        1689 Mar 12 02:47 fig.chiralTBCs.gif
-rw-r--r--    1 rosas    user         941 Mar 12 12:16 fig.crowntags.gif
-rw-r--r--    1 rosas    user         823 May 14 16:07 fig.hmx.gif
-rw-r--r--    1 rosas    user         435 May 14 21:32 fig.tb14O.gif
-rw-r--r--    1 rosas    user         435 May 14 22:58 fig.tb15O.gif
-rw-r--r--    1 rosas    user         511 May 15 11:18 fig.tb16O.gif
-rw-r--r--    1 rosas    user         427 May 14 21:34 fig.tb24O.gif
-rw-r--r--    1 rosas    user         459 May 14 23:04 fig.tb25O.gif
-rw-r--r--    1 rosas    user         515 May 15 11:21 fig.tb26O.gif
-rw-r--r--    1 rosas    user         481 May 14 23:07 fig.tb35O.gif
-rw-r--r--    1 rosas    user         489 May 14 23:17 fig.tb45O.gif
-rw-r--r--    1 rosas    user         307 May 14 20:42 fig.tbc-10O.gif
-rw-r--r--    1 rosas    user         311 May 14 20:29 fig.tbc10O.gif
-rw-r--r--    1 rosas    user         377 May 14 21:57 fig.tbc14O.gif
-rw-r--r--    1 rosas    user         394 May 15 10:38 fig.tbc15O.gif
-rw-r--r--    1 rosas    user         379 May 14 21:59 fig.tbc24O.gif
-rw-r--r--    1 rosas    user         389 May 15 10:41 fig.tbc25O.gif
-rw-r--r--    1 rosas    user         396 May 15 10:49 fig.tbc35O.gif
-rw-r--r--    1 rosas    user         392 May 15 10:51 fig.tbc45O.gif
-rw-r--r--    1 rosas    user         280 May 14 20:19 fig.tcc-10O.gif
-rw-r--r--    1 rosas    user         257 May 14 20:03 fig.tcc10O.gif
-rw-r--r--    1 rosas    user         365 May 14 21:27 fig.tcc14O.gif
-rw-r--r--    1 rosas    user         381 May 14 22:44 fig.tcc15O.gif
-rw-r--r--    1 rosas    user         357 May 14 21:28 fig.tcc24O.gif
-rw-r--r--    1 rosas    user         405 May 14 22:48 fig.tcc25O.gif
-rw-r--r--    1 rosas    user       14069 May 15 15:25 tb14O.wrl
-rw-r--r--    1 rosas    user       15190 May 16 15:33 tb15O.wrl
-rw-r--r--    1 rosas    user       16172 May 16 22:26 tb16O.wrl
-rw-r--r--    1 rosas    user       14143 May 15 15:28 tb24O.wrl
-rw-r--r--    1 rosas    user       15177 May 16 15:34 tb25O.wrl
-rw-r--r--    1 rosas    user       16226 May 16 22:27 tb26O.wrl
-rw-r--r--    1 rosas    user       15126 May 16 15:35 tb35O.wrl
-rw-r--r--    1 rosas    user       15168 May 16 15:36 tb45O.wrl
-rw-r--r--    1 rosas    user        9649 May 15 14:02 tbc1.wrl
-rw-r--r--    1 rosas    user       14084 May 15 15:37 tbc14O.wrl
-rw-r--r--    1 rosas    user       15276 May 16 15:40 tbc15O.wrl
-rw-r--r--    1 rosas    user        9654 May 15 14:04 tbc2.wrl
-rw-r--r--    1 rosas    user       14084 May 15 15:38 tbc24O.wrl
-rw-r--r--    1 rosas    user       15220 May 16 15:41 tbc25O.wrl
-rw-r--r--    1 rosas    user        9667 May 15 14:04 tbc3.wrl
-rw-r--r--    1 rosas    user       15116 May 16 15:45 tbc35O.wrl
-rw-r--r--    1 rosas    user        9667 May 15 14:05 tbc4.wrl
-rw-r--r--    1 rosas    user       15141 May 16 15:46 tbc45O.wrl
-rw-r--r--    1 rosas    user        9651 May 15 14:05 tcc1.wrl
-rw-r--r--    1 rosas    user       14027 May 15 15:23 tcc14O.wrl
-rw-r--r--    1 rosas    user       15302 May 16 15:29 tcc15O.wrl
-rw-r--r--    1 rosas    user       14082 May 15 15:24 tcc24O.wrl
-rw-r--r--    1 rosas    user       15238 May 16 15:31 tcc25O.wrl

dissertation/cyclooctane/MOD:
total 1177
```

```
-rw-r--r--    1 rosas    user       56619 Jun 17 11:03 CycloocTotGas.out
-rw-r--r--    1 rosas    user      190512 Jun 17 11:03 HexMeCycloocTotGas.out
-rw-r--r--    1 rosas    user      171493 Jun 17 11:03 PentMeCycloocTotGas.out
-rw-r--r--    1 rosas    user      183139 Jun 17 11:03 TetMeCycloocTotGas.out

dissertation/cyclooctane/MOL:
total 138
-rw-r--r--    1 rosas    user        2697 May 27 13:56 bb5O.mol
-rw-r--r--    1 rosas    user        2901 May 27 13:56 bb6O.mol
-rw-r--r--    1 rosas    user        2698 May 27 13:56 bc15O.mol
-rw-r--r--    1 rosas    user        2902 May 27 13:56 bc16O.mol
-rw-r--r--    1 rosas    user        2698 May 27 13:56 bc25O.mol
-rw-r--r--    1 rosas    user        2902 May 27 13:56 bc26O.mol
-rw-r--r--    1 rosas    user        2698 May 27 13:56 bc35O.mol
-rw-r--r--    1 rosas    user        2698 May 27 13:56 bc45O.mol
-rw-r--r--    1 rosas    user        2698 May 27 13:56 bc55O.mol
-rw-r--r--    1 rosas    user        2698 May 27 13:56 bc65O.mol
-rw-r--r--    1 rosas    user        2697 May 27 13:56 cc5O.mol
-rw-r--r--    1 rosas    user        2698 May 27 13:56 tb15O.mol
-rw-r--r--    1 rosas    user        2902 May 27 13:56 tb16O.mol
-rw-r--r--    1 rosas    user        2698 May 27 13:56 tb25O.mol
-rw-r--r--    1 rosas    user        2902 May 27 13:56 tb26O.mol
-rw-r--r--    1 rosas    user        2698 May 27 13:56 tb35O.mol
-rw-r--r--    1 rosas    user        2698 May 27 13:56 tb45O.mol
-rw-r--r--    1 rosas    user        2699 May 27 13:56 tbc15O.mol
-rw-r--r--    1 rosas    user        2699 May 27 13:56 tbc25O.mol
-rw-r--r--    1 rosas    user        2699 May 27 13:56 tbc35O.mol
-rw-r--r--    1 rosas    user        2699 May 27 13:56 tbc45O.mol
-rw-r--r--    1 rosas    user        2699 May 27 13:56 tcc15O.mol
-rw-r--r--    1 rosas    user        2699 May 27 13:56 tcc25O.mol

dissertation/cyclooctane/PDB:
total 347
-rw-r--r--    1 rosas    user        2899 May 15 11:28 BC.pdb
-rw-r--r--    1 rosas    user        2899 May 15 11:32 TBC1.pdb
-rw-r--r--    1 rosas    user        2899 May 15 11:31 TBC2.pdb
-rw-r--r--    1 rosas    user        2899 May 15 11:34 TBC3.pdb
-rw-r--r--    1 rosas    user        2899 May 15 11:35 TBC4.pdb
-rw-r--r--    1 rosas    user        2899 May 15 11:27 TCC1.pdb
-rw-r--r--    1 rosas    user        4197 May 15 14:56 bb14O.pdb
-rw-r--r--    1 rosas    user        4197 May 15 14:57 bb24O.pdb
-rw-r--r--    1 rosas    user        4550 May 16 15:04 bb5O.pdb
-rw-r--r--    1 rosas    user        4865 May 16 21:49 bb6O.pdb
-rw-r--r--    1 rosas    user        4197 May 15 14:52 bc14O.pdb
-rw-r--r--    1 rosas    user        4550 May 16 14:57 bc15O.pdb
-rw-r--r--    1 rosas    user        4865 May 16 21:49 bc16O.pdb
-rw-r--r--    1 rosas    user        4197 May 15 14:52 bc24O.pdb
-rw-r--r--    1 rosas    user        4550 May 16 14:57 bc25O.pdb
-rw-r--r--    1 rosas    user        4865 May 16 21:50 bc26O.pdb
-rw-r--r--    1 rosas    user        4550 May 16 15:01 bc35O.pdb
-rw-r--r--    1 rosas    user        4550 May 16 15:01 bc45O.pdb
-rw-r--r--    1 rosas    user        4550 May 16 15:04 bc55O.pdb
-rw-r--r--    1 rosas    user        4550 May 16 15:04 bc65O.pdb
-rw-r--r--    1 rosas    user        4197 May 15 14:57 cc4O.pdb
-rw-r--r--    1 rosas    user        4550 May 16 14:58 cc5O.pdb
-rw-r--r--    1 rosas    user        4197 May 15 14:55 tb14O.pdb
-rw-r--r--    1 rosas    user        4550 May 16 14:59 tb15O.pdb
-rw-r--r--    1 rosas    user        4865 May 16 21:47 tb16O.pdb
-rw-r--r--    1 rosas    user        4197 May 15 14:55 tb24O.pdb
-rw-r--r--    1 rosas    user        4550 May 16 14:58 tb25O.pdb
-rw-r--r--    1 rosas    user        4865 May 16 21:48 tb26O.pdb
-rw-r--r--    1 rosas    user        4550 May 16 15:00 tb35O.pdb
-rw-r--r--    1 rosas    user        4550 May 16 14:59 tb45O.pdb
-rw-r--r--    1 rosas    user        4197 May 15 14:57 tbc14O.pdb
-rw-r--r--    1 rosas    user        4550 May 16 15:02 tbc15O.pdb
-rw-r--r--    1 rosas    user        4197 May 15 14:58 tbc24O.pdb
-rw-r--r--    1 rosas    user        4550 May 16 15:02 tbc25O.pdb
-rw-r--r--    1 rosas    user        4550 May 16 15:05 tbc35O.pdb
-rw-r--r--    1 rosas    user        4550 May 16 15:05 tbc45O.pdb
-rw-r--r--    1 rosas    user        4197 May 15 14:53 tcc14O.pdb
-rw-r--r--    1 rosas    user        4550 May 16 14:57 tcc15O.pdb
-rw-r--r--    1 rosas    user        4197 May 15 14:55 tcc24O.pdb
-rw-r--r--    1 rosas    user        4550 May 16 14:58 tcc25O.pdb

dissertation/methylphosp:
total 271
drwxr-xr-x    2 rosas    user         512 Jun 17 11:15 Abinitio
drwxr-xr-x    2 rosas    user         512 Jun 17 11:31 PDB
-rw-r--r--    1 rosas    user       15784 Mar 15 02:53 cegxuh.wrl
-rw-r--r--    1 rosas    user       15993 Mar 15 02:53 duksor.wrl
-rw-r--r--    1 rosas    user       26911 Mar 15 02:54 dumlec.wrl
```

```
-rw-r--r--    1 rosas    user       23386 Mar 15 02:54 felsoe.wrl
-rw-r--r--    1 rosas    user        4000 May 19 10:18 fig.confs.gif
-rw-r--r--    1 rosas    user        4789 May 13 14:31 fig.copo.gif
-rw-r--r--    1 rosas    user        4142 May 13 14:31 fig.cp2o.gif
-rw-r--r--    1 rosas    user        4624 May 13 16:04 fig.crystals.gif
-rw-r--r--    1 rosas    user        4349 May 13 14:31 fig.hcpo.gif
-rw-r--r--    1 rosas    user        3991 May 13 14:31 fig.opo.gif
-rw-r--r--    1 rosas    user        3795 May 13 14:31 fig.pc.gif
-rw-r--r--    1 rosas    user        3817 May 13 14:31 fig.po.gif
-rw-r--r--    1 rosas    user        4658 Jun 12 15:27 fig.profiles.gif
-rw-r--r--    1 rosas    user       13587 Mar 15 02:54 zaysib.wrl

dissertation/methylphosp/Abinitio:
total 303
-rw-r--r--    1 rosas    user       17096 Jun 17 11:14 AngleCP2O.txt
-rw-r--r--    1 rosas    user       19003 Jun 17 11:14 AngleOPO.txt
-rw-r--r--    1 rosas    user       12499 Jun 17 11:14 BondPC.txt
-rw-r--r--    1 rosas    user        9487 Jun 17 11:14 BondPO.txt
-rw-r--r--    1 rosas    user        1958 Jun 17 11:14 CP1O2angle.txt
-rw-r--r--    1 rosas    user       10562 Jun 17 11:14 CP1Oangle.txt
-rw-r--r--    1 rosas    user       59929 Jun 17 11:14 TorCOPO.txt
-rw-r--r--    1 rosas    user       21441 Jun 17 11:14 TorHCPO.txt
-rw-r--r--    1 rosas    user        1014 Jun 17 11:14 diMephopGM.txt

dissertation/methylphosp/PDB:
total 54
-rw-r--r--    1 rosas    user        4491 Mar 15 02:48 cegxuh.pdb
-rw-r--r--    1 rosas    user        4308 Mar 15 02:48 duksor.pdb
-rw-r--r--    1 rosas    user        7539 Mar 15 02:49 dumlec.pdb
-rw-r--r--    1 rosas    user        6677 Mar 15 02:49 felsoe.pdb
-rw-r--r--    1 rosas    user        3508 Mar 15 02:47 zaysib.pdb

dissertation/morpholinium:
total 113
drwxr-xr-x    2 rosas    user         512 Jun 17 11:12 MOD
-rw-r--r--    1 rosas    user        3762 May  1 14:18 TableDiMeMorpholGas.html
-rw-r--r--    1 rosas    user        3635 May  1 14:20 TableDiMeMorpholWat.html
-rw-r--r--    1 rosas    user       13510 May 11 17:36 TableMeOHMorpholGas.html
-rw-r--r--    1 rosas    user       13489 May  1 14:24 TableMeOHMorpholWat.html
-rw-r--r--    1 rosas    user        3031 May  1 13:46 TableMorpholGas.html
-rw-r--r--    1 rosas    user        3655 May  1 14:13 TableMorpholWat.html
-rw-r--r--    1 rosas    user        4232 May  1 14:22 TableSMeMorpholGas.html
-rw-r--r--    1 rosas    user        4452 May  1 14:23 TableSMeMorpholWat.html
-rw-r--r--    1 rosas    user         607 Apr  3 12:04 fig.MeOHtags.gif
-rw-r--r--    1 rosas    user         497 Apr  3 11:42 fig.Morphtags.gif
-rw-r--r--    1 rosas    user         539 Apr  3 11:47 fig.StriMetags.gif
-rw-r--r--    1 rosas    user         440 Mar  4 16:34 fig.morph.gif
-rw-r--r--    1 rosas    user         583 May 19 12:25 fig.savle97.gif
-rw-r--r--    1 rosas    user         527 Apr  3 11:57 fig.tetraMetags.gif

dissertation/morpholinium/MOD:
total 1830
-rw-r--r--    1 rosas    user       58800 Jun 17 11:11 DiMeMorphGas.out
-rw-r--r--    1 rosas    user       76314 Jun 17 11:11 DiMeMorphWat.out
-rw-r--r--    1 rosas    user      384203 Jun 17 11:11 MeOHMorphGas.out
-rw-r--r--    1 rosas    user      224436 Jun 17 11:11 MeOHMorphWat.out
-rw-r--r--    1 rosas    user       34813 Jun 17 11:11 MorphGas.out
-rw-r--r--    1 rosas    user       43515 Jun 17 11:11 MorphWat.out
-rw-r--r--    1 rosas    user       55895 Jun 17 11:11 SMeMorphGas.out
-rw-r--r--    1 rosas    user       57159 Jun 17 11:11 SMeMorphWat.out

dissertation/phosphacinium:
total 1575
drwxr-xr-x    2 rosas    user         512 Jun 17 11:07 MOD
drwxr-xr-x    2 rosas    user         512 Jun 17 10:00 MOL
drwxr-xr-x    2 rosas    user        1024 Jun 17 10:00 PDB
-rw-r--r--    1 rosas    user       21169 May  1 14:35 TableCisMedioxPGas.html
-rw-r--r--    1 rosas    user       22816 May  1 14:35 TableCisMedioxPWat.html
-rw-r--r--    1 rosas    user       28178 May  1 14:36 TableDiMePGas.html
-rw-r--r--    1 rosas    user       41551 Jun 17 10:52 TableDiMePWat.html
-rw-r--r--    1 rosas    user       20393 May 10 11:24 TableDioxPGas.html
-rw-r--r--    1 rosas    user       30599 May  8 20:27 TableDioxPWat.html
-rw-r--r--    1 rosas    user       29038 May  1 14:40 TableTransMedioxPGas.html
-rw-r--r--    1 rosas    user       37001 Jun 17 11:00 TableTransMedioxPWat.html
-rw-r--r--    1 rosas    user       13903 May 16 20:25 bb1PW2.wrl
-rw-r--r--    1 rosas    user       14854 Jun 13 10:44 bb1PW4.wrl
-rw-r--r--    1 rosas    user       13751 May 16 20:27 bb2PW2.wrl
-rw-r--r--    1 rosas    user       14818 May 16 21:40 bb2PW4.wrl
-rw-r--r--    1 rosas    user       14764 May 16 21:38 bbPW3.wrl
-rw-r--r--    1 rosas    user       13665 May 26 11:18 bc1P2.wrl
-rw-r--r--    1 rosas    user       15785 Jun 13 10:45 bc1P5.wrl
```

```
-rw-r--r--    1 rosas    user       13695 May 16 20:28 bc1PW2.wrl
-rw-r--r--    1 rosas    user       14847 May 16 21:36 bc1PW3.wrl
-rw-r--r--    1 rosas    user       14860 May 16 21:37 bc1PW4.wrl
-rw-r--r--    1 rosas    user       13653 May 16 22:40 bc2P2.wrl
-rw-r--r--    1 rosas    user       15785 Jun 16 15:47 bc2P5.wrl
-rw-r--r--    1 rosas    user       13702 May 16 20:32 bc2PW2.wrl
-rw-r--r--    1 rosas    user       14796 May 16 21:36 bc2PW3.wrl
-rw-r--r--    1 rosas    user       14924 May 16 21:37 bc2PW4.wrl
-rw-r--r--    1 rosas    user       14873 May 16 22:55 bcP3.wrl
-rw-r--r--    1 rosas    user       14860 Jun 13 10:47 bcP4.wrl
-rw-r--r--    1 rosas    user         489 May 16 10:42 fig.bb1PW2.gif
-rw-r--r--    1 rosas    user         527 May 16 11:34 fig.bb1PW4.gif
-rw-r--r--    1 rosas    user         457 May 16 10:42 fig.bb2PW2.gif
-rw-r--r--    1 rosas    user         519 May 16 11:29 fig.bb2PW4.gif
-rw-r--r--    1 rosas    user         524 May 16 11:21 fig.bbPW3.gif
-rw-r--r--    1 rosas    user         451 May 15 16:02 fig.bc1P2.gif
-rw-r--r--    1 rosas    user         530 May 16 14:38 fig.bc1P5.gif
-rw-r--r--    1 rosas    user         446 May 16 10:45 fig.bc1PW2.gif
-rw-r--r--    1 rosas    user         477 May 16 11:15 fig.bc1PW3.gif
-rw-r--r--    1 rosas    user         487 May 16 11:39 fig.bc1PW4.gif
-rw-r--r--    1 rosas    user         434 May 15 16:05 fig.bc2P2.gif
-rw-r--r--    1 rosas    user         521 May 16 14:37 fig.bc2P5.gif
-rw-r--r--    1 rosas    user         437 May 16 10:47 fig.bc2PW2.gif
-rw-r--r--    1 rosas    user         482 May 16 11:14 fig.bc2PW3.gif
-rw-r--r--    1 rosas    user         481 May 16 11:44 fig.bc2PW4.gif
-rw-r--r--    1 rosas    user         525 May 16 13:58 fig.bcP3.gif
-rw-r--r--    1 rosas    user         517 May 16 14:06 fig.bcP4.gif
-rw-r--r--    1 rosas    user         695 Mar 25 01:16 fig.cis.gif
-rw-r--r--    1 rosas    user         728 Mar 25 01:25 fig.diMeP.gif
-rw-r--r--    1 rosas    user         827 Apr  3 14:05 fig.example.gif
-rw-r--r--    1 rosas    user         591 Feb  8 23:03 fig.phosp.gif
-rw-r--r--    1 rosas    user         670 Mar 18 22:59 fig.phospTab.gif
-rw-r--r--    1 rosas    user         522 May 16 13:39 fig.tb1P2.gif
-rw-r--r--    1 rosas    user         497 May 16 14:11 fig.tb1P4.gif
-rw-r--r--    1 rosas    user         570 May 16 14:44 fig.tb1P5.gif
-rw-r--r--    1 rosas    user         583 May 16 13:21 fig.tb1PW5.gif
-rw-r--r--    1 rosas    user         516 May 16 13:37 fig.tb2P2.gif
-rw-r--r--    1 rosas    user         536 May 16 14:28 fig.tb2P4.gif
-rw-r--r--    1 rosas    user         552 May 16 14:48 fig.tb2P5.gif
-rw-r--r--    1 rosas    user         601 May 16 13:24 fig.tb2PW5.gif
-rw-r--r--    1 rosas    user         555 May 16 11:07 fig.tbPW3.gif
-rw-r--r--    1 rosas    user         461 May 15 16:13 fig.tbc1P2.gif
-rw-r--r--    1 rosas    user         509 May 16 14:02 fig.tbc1P4.gif
-rw-r--r--    1 rosas    user         460 May 15 16:11 fig.tbc2P2.gif
-rw-r--r--    1 rosas    user         519 May 16 14:17 fig.tbc2P4.gif
-rw-r--r--    1 rosas    user         534 May 16 14:51 fig.tbcP5.gif
-rw-r--r--    1 rosas    user         497 May 16 14:08 fig.tc1P4.gif
-rw-r--r--    1 rosas    user         511 May 16 14:20 fig.tc2P4.gif
-rw-r--r--    1 rosas    user         477 May 16 13:46 fig.tcP2.gif
-rw-r--r--    1 rosas    user         504 May 16 13:51 fig.tcP3.gif
-rw-r--r--    1 rosas    user         529 May 16 14:31 fig.tcP5.gif
-rw-r--r--    1 rosas    user         730 Mar 25 01:12 fig.trans.gif
-rw-r--r--    1 rosas    user       13780 May 16 22:50 tb1P2.wrl
-rw-r--r--    1 rosas    user       14814 Jun 13 10:47 tb1P4.wrl
-rw-r--r--    1 rosas    user       15871 Jun 13 10:49 tb1P5.wrl
-rw-r--r--    1 rosas    user       15969 May 16 21:42 tb1PW5.wrl
-rw-r--r--    1 rosas    user       13732 May 16 22:53 tb2P2.wrl
-rw-r--r--    1 rosas    user       14881 Jun 13 10:50 tb2P4.wrl
-rw-r--r--    1 rosas    user       15844 Jun 13 10:50 tb2P5.wrl
-rw-r--r--    1 rosas    user       15815 May 16 21:43 tb2PW5.wrl
-rw-r--r--    1 rosas    user       14900 May 16 21:36 tbPW3.wrl
-rw-r--r--    1 rosas    user       13678 May 16 22:42 tbc1P2.wrl
-rw-r--r--    1 rosas    user       14853 May 16 23:00 tbc1P4.wrl
-rw-r--r--    1 rosas    user       13697 May 16 22:41 tbc2P2.wrl
-rw-r--r--    1 rosas    user       14857 Jun 13 10:52 tbc2P4.wrl
-rw-r--r--    1 rosas    user       15826 Jun 13 10:53 tbcP5.wrl
-rw-r--r--    1 rosas    user       14841 Jun 13 10:54 tc1P4.wrl
-rw-r--r--    1 rosas    user       14813 Jun 13 10:57 tc2P4.wrl
-rw-r--r--    1 rosas    user       13635 May 16 22:54 tcP2.wrl
-rw-r--r--    1 rosas    user       14910 May 16 22:57 tcP3.wrl
-rw-r--r--    1 rosas    user       15871 Jun 13 10:56 tcP5.wrl

dissertation/phosphacinium/MOD:
total 2564
-rw-r--r--    1 rosas    user      117723 Jun 17 11:05 CisMeDioxTotGas.out
-rw-r--r--    1 rosas    user      127314 Jun 17 11:06 CisMedioxTotWat.out
-rw-r--r--    1 rosas    user      157966 Jun 17 11:05 DiMeTotGas.out
-rw-r--r--    1 rosas    user      234647 Jun 17 11:06 DiMetotalWat.out
-rw-r--r--    1 rosas    user      120205 Jun 17 11:05 DioxTotGas.out
-rw-r--r--    1 rosas    user      208927 Jun 17 11:06 DioxTotWat.out
-rw-r--r--    1 rosas    user      173618 Jun 17 11:05 TransMeDioxTotGas.out
```

```
-rw-r--r--    1 rosas    user      170490 Jun 17 11:06 TransMeDioxTotWat.out

dissertation/phosphacinium/MOL:
total 139
-rw-r--r--    1 rosas    user        2019 May 27 13:56 bb1PW2.mol
-rw-r--r--    1 rosas    user        2223 May 27 13:56 bb1PW4.mol
-rw-r--r--    1 rosas    user        2019 May 27 13:56 bb2PW2.mol
-rw-r--r--    1 rosas    user        2223 May 27 13:56 bb2PW4.mol
-rw-r--r--    1 rosas    user        2222 May 27 13:56 bbPW3.mol
-rw-r--r--    1 rosas    user        2018 May 27 13:56 bc1P2.mol
-rw-r--r--    1 rosas    user        2019 May 27 13:56 bc1PW2.mol
-rw-r--r--    1 rosas    user        2223 May 27 13:56 bc1PW3.mol
-rw-r--r--    1 rosas    user        2223 May 27 13:56 bc1PW4.mol
-rw-r--r--    1 rosas    user        2018 May 27 13:56 bc2P2.mol
-rw-r--r--    1 rosas    user        2019 May 27 13:56 bc2PW2.mol
-rw-r--r--    1 rosas    user        2223 May 27 13:56 bc2PW3.mol
-rw-r--r--    1 rosas    user        2223 May 27 13:56 bc2PW4.mol
-rw-r--r--    1 rosas    user        2221 May 27 13:56 bcP3.mol
-rw-r--r--    1 rosas    user        2221 May 27 13:56 bcP4.mol
-rw-r--r--    1 rosas    user        2018 May 27 13:56 tb1P2.mol
-rw-r--r--    1 rosas    user        2222 May 27 13:56 tb1P4.mol
-rw-r--r--    1 rosas    user        2427 May 27 13:56 tb1PW5.mol
-rw-r--r--    1 rosas    user        2018 May 27 13:56 tb2P2.mol
-rw-r--r--    1 rosas    user        2222 May 27 13:56 tb2P4.mol
-rw-r--r--    1 rosas    user        2427 May 27 13:56 tb2PW5.mol
-rw-r--r--    1 rosas    user        2222 May 27 13:56 tbPW3.mol
-rw-r--r--    1 rosas    user        2019 May 27 13:56 tbc1P2.mol
-rw-r--r--    1 rosas    user        2019 May 27 13:56 tbc2P2.mol
-rw-r--r--    1 rosas    user        2223 May 27 13:56 tbc2P4.mol
-rw-r--r--    1 rosas    user        2222 May 27 13:56 tbcP4.mol
-rw-r--r--    1 rosas    user        2222 May 27 13:56 tc1P4.mol
-rw-r--r--    1 rosas    user        2222 May 27 13:56 tc2P4.mol
-rw-r--r--    1 rosas    user        2017 May 27 13:56 tcP2.mol
-rw-r--r--    1 rosas    user        2221 May 27 13:56 tcP3.mol

dissertation/phosphacinium/PDB:
total 285
-rw-r--r--    1 rosas    user        3508 May 16 15:56 bb1PW2.pdb
-rw-r--r--    1 rosas    user        3823 May 16 21:17 bb1PW4.pdb
-rw-r--r--    1 rosas    user        3508 May 16 15:57 bb2PW2.pdb
-rw-r--r--    1 rosas    user        3823 May 16 21:18 bb2PW4.pdb
-rw-r--r--    1 rosas    user        3823 May 16 21:16 bbPW3.pdb
-rw-r--r--    1 rosas    user        3508 May 16 21:51 bc1P2.pdb
-rw-r--r--    1 rosas    user        4138 Jun 12 15:32 bc1P5.pdb
-rw-r--r--    1 rosas    user        3508 May 16 15:58 bc1PW2.pdb
-rw-r--r--    1 rosas    user        3823 May 16 21:15 bc1PW3.pdb
-rw-r--r--    1 rosas    user        3823 May 16 21:18 bc1PW4.pdb
-rw-r--r--    1 rosas    user        3508 May 16 21:51 bc2P2.pdb
-rw-r--r--    1 rosas    user        4138 Jun 12 15:32 bc2P5.pdb
-rw-r--r--    1 rosas    user        3508 May 16 15:58 bc2PW2.pdb
-rw-r--r--    1 rosas    user        3823 May 16 21:16 bc2PW3.pdb
-rw-r--r--    1 rosas    user        3823 May 16 21:19 bc2PW4.pdb
-rw-r--r--    1 rosas    user        3823 May 16 21:56 bcP3.pdb
-rw-r--r--    1 rosas    user        3823 May 16 21:58 bcP4.pdb
-rw-r--r--    1 rosas    user        3508 May 16 21:54 tb1P2.pdb
-rw-r--r--    1 rosas    user        3823 May 16 22:03 tb1P4.pdb
-rw-r--r--    1 rosas    user        4138 Jun 12 15:32 tb1P5.pdb
-rw-r--r--    1 rosas    user        4138 May 16 21:20 tb1PW5.pdb
-rw-r--r--    1 rosas    user        3508 May 16 21:53 tb2P2.pdb
-rw-r--r--    1 rosas    user        3823 May 16 22:05 tb2P4.pdb
-rw-r--r--    1 rosas    user        4138 Jun 12 15:32 tb2P5.pdb
-rw-r--r--    1 rosas    user        4138 May 16 21:20 tb2PW5.pdb
-rw-r--r--    1 rosas    user        3823 May 16 21:15 tbPW3.pdb
-rw-r--r--    1 rosas    user        3508 May 16 21:52 tbc1P2.pdb
-rw-r--r--    1 rosas    user        3508 May 16 21:52 tbc2P2.pdb
-rw-r--r--    1 rosas    user        3823 May 16 22:03 tbc2P4.pdb
-rw-r--r--    1 rosas    user        3823 May 16 21:57 tbcP4.pdb
-rw-r--r--    1 rosas    user        4138 Jun 12 15:33 tbcP5.pdb
-rw-r--r--    1 rosas    user        3823 May 16 21:59 tc1P4.pdb
-rw-r--r--    1 rosas    user        4138 Jun 12 15:31 tc1P5.pdb
-rw-r--r--    1 rosas    user        3823 May 16 22:04 tc2P4.pdb
-rw-r--r--    1 rosas    user        3508 May 16 21:55 tcP2.pdb
-rw-r--r--    1 rosas    user        3823 May 16 21:56 tcP3.pdb

dissertation/reviews:
total 105
-rw-r--r--    1 rosas    user         573 Feb 21 00:20 fig.2266dioxo.gif
-rw-r--r--    1 rosas    user         516 Feb 21 00:20 fig.22dioxo.gif
-rw-r--r--    1 rosas    user         530 Feb 21 00:20 fig.66dioxo.gif
-rw-r--r--    1 rosas    user         740 Mar 15 01:07 fig.HAC.gif
-rw-r--r--    1 rosas    user         595 Feb 26 01:18 fig.aminocarn.gif
```

```
-rw-r--r--    1 rosas    user          842 Feb 26 01:56 fig.anderson951.gif
-rw-r--r--    1 rosas    user          980 May 14 10:02 fig.anderson952.gif
-rw-r--r--    1 rosas    user         1774 Mar  4 15:45 fig.anomeric.gif
-rw-r--r--    1 rosas    user         2302 Feb 10 16:10 fig.b.gif
-rw-r--r--    1 rosas    user         2486 Feb 10 16:09 fig.bb.gif
-rw-r--r--    1 rosas    user         2304 Feb 10 16:09 fig.bc.gif
-rw-r--r--    1 rosas    user         2416 Feb 10 16:10 fig.c.gif
-rw-r--r--    1 rosas    user         2539 Feb 10 16:10 fig.cc.gif
-rw-r--r--    1 rosas    user         3852 Mar  3 14:56 fig.crown.gif
-rw-r--r--    1 rosas    user          411 May 14 11:36 fig.dioxo.gif
-rw-r--r--    1 rosas    user         2362 Feb 23 00:42 fig.fritz63.gif
-rw-r--r--    1 rosas    user         1231 May 22 14:09 fig.gandour93.gif
-rw-r--r--    1 rosas    user         2714 Apr 15 11:30 fig.hydrolysis2.gif
-rw-r--r--    1 rosas    user          743 May 14 10:00 fig.kumaravel94.gif
-rw-r--r--    1 rosas    user          414 May 14 11:35 fig.oxo.gif
-rw-r--r--    1 rosas    user          581 Feb 26 01:21 fig.saeed93.gif
-rw-r--r--    1 rosas    user          585 Mar  4 16:39 fig.saeed94.gif
-rw-r--r--    1 rosas    user         1157 Apr 15 10:24 fig.sun95.gif
-rw-r--r--    1 rosas    user         2426 Feb 10 16:11 fig.tb.gif
-rw-r--r--    1 rosas    user         2601 Feb 10 16:20 fig.tbc-1.gif
-rw-r--r--    1 rosas    user         2639 Feb 10 16:10 fig.tbc1.gif
-rw-r--r--    1 rosas    user         2500 Feb 10 16:11 fig.tc.gif
-rw-r--r--    1 rosas    user         2446 Feb 10 16:11 fig.tcc.gif
-rw-r--r--    1 rosas    user          432 May 14 11:34 fig.tetraoxo.gif
-rw-r--r--    1 rosas    user          420 May 14 11:36 fig.trioxo.gif
```

(footnotes)

[*FCHIME*] NOTE: The SGI version of Chime will not work reading molfiles in a local filesystem, only through a network.

Vita

Víctor was born in Monterrey, México, on February 24th, 1969. Due to his father's job, the family alternated residence between Monterrey and México City, to finally settle down in Monterrey. There Víctor pursued his B.S. in Industrial Chemistry at UANL and, after graduation, held his first job as a Quality Control chemist. Having decided that his chemical skills required (substantial) polishing, he joined the PhD program at Louisiana State University in Baton Rouge, LA. At LSU he joined Professor Gandour's research group, while thoroughly enjoying the Cajun and Creole heritage of the land (Mardi Gras included). Little he suspected that he would later be transferring to Virginia Tech, following his advisor. While at Virginia Tech, he decided that computers were fun and chemistry was fun so putting them together would be fun^2. Thus he turned his interests to Computational Chemistry, to finally get his Ph.D. as a Computational Bioorganic Chemist.

[Title] [Ded] [Ack] [1] [2] [3] [4] [5] [6] [7] [Bib] [A] [B] [C] [D] [E] [Vita]

Cyclooctane in gas phase										
Conformation	δE	Stat. point	1,2,3,4	2,3,4,5	3,4,5,6	4,5,6,7	5,6,7,8	6,7,8,1	7,8,1,2	8,1,2,3
BC	0.00	min	-43.22	102.45	-69.65	69.65	-102.45	43.22	66.06	-66.06
TCC	0.83	min	64.12	-86.45	113.29	-86.45	64.12	-86.45	113.29	-86.45
TCC'	0.83	min	86.45	-113.29	86.45	-64.12	86.45	-113.29	86.45	-64.12
TBC	1.77	min	47.69	48.72	-119.53	48.72	47.69	-93.34	92.22	-93.34
TBC'	1.77	min	93.34	-47.69	-48.72	119.53	-48.72	-47.69	93.34	-92.22
TBC	2.88	saddle	-77.64	83.09	-75.12	-11.33	98.57	-50.93	-58.68	104.96
TBC'	2.88	saddle	75.12	11.33	-98.57	50.94	58.68	-104.96	77.65	-83.09
TB	3.63	min	-32.20	68.20	32.20	-68.20	-32.20	68.20	32.20	-68.20
BB	4.86	saddle	51.52	51.51	-51.51	-51.52	51.52	51.52	-51.52	-51.51
C	7.76	saddle	-76.95	119.35	-76.87	-0.04	76.95	-119.35	76.87	0.04
TC	8.47	saddle	38.27	-107.79	107.79	-38.27	-38.27	107.79	-107.79	38.27
BC	9.34	mm	65.26	9.38	-96.94	96.94	-9.38	-65.27	104.66	-104.65
TB&#65533;C	10.12	saddle	-56.91	-57.12	74.90	38.61	-84.48	12.25	3.90	70.46
TB&#65533;C	10.12	saddle	57.11	-74.90	-38.61	84.48	-12.25	-3.90	-70.46	56.91
B&#65533;C	10.24	mm	-1.90	76.75	-47.55	-67.56	67.57	47.55	-76.75	1.90
TBC	10.33	saddle	31.62	-115.02	77.05	-36.43	77.05	-115.02	31.62	22.75
TBC'	10.33	saddle	-22.75	-31.62	115.02	-77.05	36.43	-77.05	115.02	-31.62
B	10.55	saddle	-0.04	74.39	-0.05	-74.25	-0.05	74.39	-0.05	-74.25
TB	11.59	saddle	-45.67	108.63	-22.24	-41.51	-22.24	108.63	-45.66	-10.73
TB	12.51	mm	10.87	54.51	-91.94	-7.83	60.38	23.05	-101.86	35.46
TB&#65533;C	22.45	mm	-24.03	102.50	-60.52	-60.53	102.47	-24.01	-10.29	-10.29

Tetramethylcyclooctane in gas phase										
Conformation	δE	Stat. point	1,2,3,4	2,3,4,5	3,4,5,6	4,5,6,7	5,6,7,8	6,7,8,1	7,8,1,2	8,1,2,3
2,2,6,6-tetramethyl-BC	0.00	min	-38.30	108.76	-73.74	58.30	-93.58	55.86	53.60	-63.76
2,2,6,6-tetramethyl-BC'	0.00	min	-93.58	55.86	53.60	-63.76	-38.30	108.76	-73.74	58.30
1,1,5,5-tetramethyl-TCC	0.39	min	52.66	-85.74	118.29	-77.57	52.66	-85.74	118.29	-77.57
1,1,5,5-tetramethyl-TCC'	0.39	min	-52.65	85.73	-118.29	77.57	-52.65	85.74	-118.29	77.57
1,1,5,5-tetramethyl-TB	0.45	min	-40.89	63.11	41.10	-60.81	-40.89	63.11	41.10	-60.81
1,1,5,5-tetramethyl-TB'	0.45	min	40.88	-63.12	-41.10	60.81	40.88	-63.12	-41.10	60.81
2,2,6,6-tetramethyl-BB	0.84	saddle	51.51	-52.29	-52.29	51.51	51.50	-52.29	-52.29	51.50
2,2,6,6-tetramethyl-BB'	0.84	saddle	-51.29	52.53	52.06	-51.74	-51.26	52.49	52.09	-51.75
1,1,5,5-tetramethyl-CC	1.12	saddle	67.83	-101.81	101.81	-67.83	67.83	-101.81	101.81	-67.83
1,1,5,5-tetramethyl-TBC	2.17	min	21.82	67.01	-126.33	50.65	41.70	-96.37	100.00	-78.74
1,1,5,5-tetramethyl-TBC'	2.17	min	-21.82	-67.01	126.33	-50.66	-41.70	96.37	-100.00	78.74
1,1,5,5-tetramethyl-TC	4.42	min	38.29	-109.33	109.30	-38.25	-38.29	109.32	-109.31	38.26
1,1,5,5-tetramethyl-TC'	4.42	min	-38.30	109.33	-109.30	38.24	38.30	-109.33	109.30	-38.24
1,1,5,5-tetramethyl-BC	5.27	min	58.67	-101.88	51.19	50.01	-50.01	-51.20	101.88	-58.67
1,1,5,5-tetramethyl-TBC	6.33	saddle	56.68	-110.67	81.53	-73.00	63.41	11.44	-95.08	49.88
1,1,5,5-tetramethyl-TBC'	6.33	saddle	73.00	-81.54	110.66	-56.68	-49.88	95.08	-11.45	-63.40
1,1,5,5-tetramethyl-TBC	7.87	saddle	65.78	-107.10	71.61	34.35	-83.77	7.86	76.59	-72.53
1,1,5,5-tetramethyl-BC	7.87	saddle	83.77	-7.86	-76.59	72.53	-65.78	107.10	-71.61	-34.35
3,3,7,7-tetramethyl-BC	8.15	saddle	4.86	91.63	-91.62	-4.88	76.17	-91.63	91.63	-76.16
TB-C	8.54	saddle	39.58	-88.94	16.13	3.06	68.61	-58.83	-56.18	72.04
TB-C	8.54	saddle	-68.61	58.83	56.19	-72.04	-39.58	88.94	-16.12	-3.06
1,1,5,5-tetramethyl-TB	9.18	saddle	25.14	21.91	-106.66	71.97	-32.21	77.53	-123.28	36.23
1,1,5,5-tetramethyl-TB	9.18	saddle	32.21	-77.53	123.29	-36.23	-25.14	-21.91	106.66	-71.97
1,1,5,5-tetramethyl-TB	11.50	saddle	-36.57	102.03	-15.70	-35.75	-36.57	102.03	-15.70	-35.75
1,1,5,5-tetramethyl-TB'	11.50	saddle	35.75	15.71	-102.03	36.56	35.77	15.68	-102.02	36.57
TC	14.07	min	93.60	-39.71	-39.66	93.58	-93.60	39.70	39.66	-93.58

3,7-TC	14.29	saddle	100.28	-46.61	-36.80	90.09	-98.13	60.66	12.77	-79.50
2,6-C	16.00	mm	103.98	-85.76	12.67	56.22	-103.98	85.76	-12.67	-56.22
TB&#65533;C	25.05	saddle	-9.88	-92.31	48.98	48.75	-41.63	-13.19	-28.34	78.31
TB&#65533;C	28.27	mm	25.85	-114.42	60.08	50.15	-61.18	-4.91	3.84	26.62
C&#65533;C	29.61	mm	-89.66	93.97	-93.96	89.66	-48.45	-3.80	3.81	48.44
TB&#65533;C	30.06	mm	30.44	86.14	-87.90	-1.37	18.23	12.07	30.44	-86.74

Pentamethylcyclooctane in gas phase										
Conformation	δE	Stat. point	6,7,8,1	7,8,1,2	8,1,2,3	1,2,3,4	2,3,4,5	3,4,5,6	4,5,6,7	5,6,7,8
2,2,4*e*,6,6-pentamethyl-BC	0.00	min	53.37	-62.94	-39.95	109.28	-73.37	58.73	-93.27	55.17
2,2,4*e*,6,6-pentamethyl-BC'	0.00	min	-55.17	93.27	-58.73	73.37	-109.28	39.95	62.94	-53.37
1,1,3*e*,5,5-pentamethyl-TCC	0.43	min	-84.75	52.21	-78.90	119.73	-85.31	52.41	-77.13	117.46
1,1,3*e*,5,5-pentamethyl-TCC'	0.43	min	-117.46	77.13	-52.41	85.31	-119.73	78.90	-52.21	84.75
1,1,3*e*,5,5-pentamethyl-CC	1.49	saddle	-101.30	67.44	-68.28	102.69	-102.69	68.28	-67.44	101.30
2,2,4*e*,6,6-pentamethyl-TB	1.55	min	-40.60	63.70	35.91	-58.58	-43.99	61.64	41.55	-64.96
2,2,4*e*,6,6-pentamethyl-TB'	1.55	min	64.95	-41.55	-61.63	43.99	58.57	-35.91	-63.70	40.61
1,1,3*e*,5,5-pentamethyl-TB	1.59	min	40.60	-63.55	-40.10	68.29	34.12	-58.63	-40.68	63.94
1,1,3*e*,5,5-pentamethyl-TB'	1.59	min	-63.94	40.68	58.64	-34.12	-68.29	40.10	63.55	-40.60
2*e*,4,4,8,8-pentamethyl-BC	1.65	min	75.45	-60.18	91.11	-47.92	-59.50	62.44	42.14	-110.57
2*e*,4,4,8,8-pentamethyl-BC'	1.65	min	110.57	-42.13	-62.44	59.50	47.92	-91.11	60.18	-75.45
1,1,3*e*,5,5-pentamethyl-TBC	1.92	min	96.03	-41.80	-51.29	125.86	-66.14	-22.01	79.12	-99.78
1,1,3*e*,5,5-pentamethyl-TBC'	1.92	min	99.78	-79.12	22.00	66.14	-125.86	51.29	41.80	-96.04
2,2,4*e*,8,8-pentamethyl-BC	2.09	min	-109.94	40.38	59.96	-48.23	-59.47	94.70	-59.02	75.16
2,2,4*e*,8,8-pentamethyl-BC'	2.09	min	-75.16	59.02	-94.70	59.48	48.23	-59.96	-40.37	109.94
2,2,4*e*,6,6-pentamethyl-BB	2.34	saddle	53.52	-54.87	-50.47	56.31	45.50	-46.72	-54.20	52.98
1,1,3*e*,5,5-pentamethyl-TBC	2.61	min	66.83	21.72	-79.56	100.43	-96.79	42.70	50.55	-125.68
1,1,3*e*,5,5-pentamethyl-TBC'	2.61	min	125.67	-50.55	-42.71	96.79	-100.43	79.56	-21.72	-66.82
1,1,3*e*,5,5-pentamethyl-TC	4.35	min	108.72	-37.17	-39.81	109.86	-109.85	39.79	37.19	-108.73
2,2,4*e*,6,6-BC'Me rot	4.58	saddle	-54.91	93.30	-58.15	71.50	-108.13	40.67	63.05	-53.55
2*e*,4,4,8,8-pentamethyl-	4.67	saddle	110.82	-42.03	-61.93	58.81	48.33	-91.47	61.15	-76.35

BC										
1,1,3*e*,5,5-pentamethyl-TCC	4.83	saddle	-117.55	76.83	-52.98	86.46	-119.18	77.04	-51.91	85.84
1,1,3*e*,5,5-pentamethyl-BC	5.42	min	-100.48	58.70	-59.53	102.43	-51.85	-49.50	51.27	49.40
1,1,3*e*,5,5-pentamethyl-BC'	5.42	min	-49.40	-51.27	49.50	51.86	-102.43	59.53	-58.70	100.48
1*e*,3,3,7,7-pentamethyl-TB	5.56	saddle	39.98	-63.26	-39.64	67.03	34.73	-57.23	-43.13	65.58
1*a*,3,3,7,7-pentamethyl-BC	5.92	saddle	-74.34	58.97	-93.59	56.80	49.75	-57.05	-44.81	111.87
1,1,3*e*,5,5-pentamethyl-TC	6.25	saddle	126.36	-52.36	-41.76	96.93	-100.21	79.22	-22.10	-65.92
1,1,3*a*,5,5-pentamethyl-TC	6.35	saddle	95.61	-49.55	-57.75	111.81	-81.96	72.97	-61.65	-13.37
1,1,3*a*,5,5-pentamethyl-TC'	6.35	saddle	13.36	61.65	-72.97	81.96	-111.81	57.75	49.55	-95.61
1,1,3*a*,5,5-pentamethyl-TCC	6.52	min	-49.50	82.60	-82.53	99.54	-64.65	-26.29	100.66	-48.64
1,1,3*a*,5,5-pentamethyl-TCC'	6.52	min	48.64	-100.66	26.28	64.66	-99.53	82.53	-82.60	49.50
2,2,6,6,8*e*-pentamethyl-TBC'	6.72	min	-53.92	64.05	37.47	-96.12	62.75	-57.98	97.55	-56.10
2,2,6,6,8*e*-pentamethyl-TBC	6.72	min	56.10	-97.55	57.98	-62.75	96.12	-37.47	-64.05	53.92
2,2,4*e*,6,6-pentamethyl-TBC	6.81	saddle	79.96	-72.40	66.29	7.23	-93.37	51.37	56.95	-110.58
1,1,3*e*,5,5-pentamethyl-TBC	7.95	saddle	-74.92	72.96	-67.57	107.23	-70.97	-34.09	84.99	-9.90
1,1,3*a*,5,5-pentamethyl-TC'	8.10	min	-129.38	53.39	38.72	-85.23	89.20	-77.66	22.37	66.46
1,1,3*a*,5,5-pentamethyl-TC	8.10	min	-66.45	-22.37	77.66	-89.20	85.23	-38.72	-53.39	129.37
1,1,3*a*,5,5-pentamethyl-TCC'	8.35	min	89.33	-54.56	74.80	-102.24	76.21	-54.16	78.97	-119.39
1,1,3*a*,5,5-pentamethyl-TCC	8.35	min	119.39	-78.97	54.16	-76.21	102.23	-74.80	54.56	-89.33
XXXVIII	8.76	saddle	-106.52	66.44	-73.51	74.73	10.59	-85.86	34.75	70.76
XXXIX	8.80	saddle	91.44	-75.68	3.25	91.83	-91.83	-3.25	75.68	-91.44
XL	8.86		90.98	5.25	-77.50	91.45	-91.45	77.08	-4.42	-91.62
XLI	8.88	saddle	-106.38	71.93	-32.74	77.32	-123.48	37.58	24.15	22.54
XLII	8.88	saddle	-22.54	-24.15	-37.58	123.48	-77.33	32.74	-71.93	106.38
XLIII	8.98	saddle	55.14	-72.11	-40.26	89.53	-16.25	-3.98	-67.68	58.90

XLIV	8.98	saddle	-58.90	67.68	3.98	16.25	-89.53	40.26	72.11	-55.14
XLV	9.27	min	90.92	-81.47	79.15	-80.56	80.67	-79.26	81.37	-90.82
XLVI	9.50	saddle	-121.83	32.63	31.57	15.45	-104.20	73.35	-32.17	77.31
XLVII	9.50	saddle	-77.31	32.17	-73.36	104.19	-15.42	-31.60	-32.62	121.83
XLVIII	9.59	min	-109.82	37.97	38.99	-96.98	96.95	-38.96	-37.99	109.83
XLIX	10.11	saddle	-120.62	46.21	37.24	-92.47	97.22	-55.07	-15.76	94.83
L	10.49		-61.60	-31.41	102.12	-44.19	-52.99	82.34	-80.50	99.30
LI	10.72	min	-101.47	84.19	-29.54	-51.50	108.94	-48.04	-43.66	94.18
LII	10.72	min	-94.18	43.66	48.05	-108.94	51.50	29.54	-84.19	101.47
LIII	10.83	saddle	-95.88	38.41	67.62	-42.56	-68.04	65.40	4.65	24.08
LIV	10.83	saddle	-24.13	-4.65	-65.38	68.08	42.49	-67.61	-38.39	95.92
LV	11.17	saddle	22.02	3.93	63.01	-55.34	-56.35	71.62	40.35	-94.57
LVI	11.25	saddle	-99.64	52.39	45.03	-96.38	26.82	52.39	-84.52	91.64
LVII	11.54	saddle	-99.90	36.70	36.08	14.99	-101.82	37.11	37.69	12.73
LVIII	11.85	saddle	-93.79	47.58	-75.04	111.09	-32.29	-36.88	-1.87	96.39
LIX	11.89	mm	-95.79	48.92	-76.60	102.94	-17.29	-48.52	0.77	98.31
LX	12.15		11.94	-82.68	33.71	69.32	-115.55	75.58	-70.92	68.50
LXI	12.30	saddle	56.45	-79.45	8.28	-12.79	79.54	-39.08	-71.61	61.25
LXII	13.00	saddle	15.25	46.47	-97.18	116.70	-66.79	-10.75	93.82	-93.53
LXIII	13.00	saddle	93.53	-93.82	10.76	66.78	-116.70	97.18	-46.47	-15.25
LXIV	13.17	saddle	-94.42	53.53	51.87	-98.33	73.78	-73.22	64.92	8.74
LXV	13.18	mm	-115.05	73.62	-70.95	69.85	10.03	-82.11	34.46	69.61
LXVI	13.27	min	47.66	-84.18	82.65	-86.14	45.70	36.88	-105.96	51.70
LXVII	13.72	saddle	66.06	12.70	-96.33	92.69	-12.92	-47.81	95.41	-114.75
LXVIII	13.72	saddle	114.74	-95.41	47.83	12.91	-92.69	96.30	-12.66	-66.09
LXIX	14.53	min	40.91	-95.42	90.50	-32.20	-46.08	96.06	-93.60	39.69
LXX	14.53	min	-39.69	93.60	-96.06	46.08	32.20	-90.50	95.43	-40.92
LXXI	14.86	saddle	63.14	-99.25	87.08	-31.30	-51.45	102.61	-78.61	10.95
LXII	14.87	saddle	-37.59	90.36	-98.46	62.43	9.63	-77.84	101.40	-46.84
LXIII	14.88	saddle	10.11	-79.24	98.08	-39.14	-43.76	92.02	-98.47	63.77
LXXIV	15.05	saddle	-16.96	89.71	-39.65	-55.23	92.45	-68.66	76.10	-70.83
LXXV	15.66	mm	-95.52	5.99	27.20	42.78	-73.69	-47.21	92.24	

							116.31			
LXXVI	16.01	mm	-97.18	4.30	68.04	-85.07	85.07	-68.05	-4.30	97.18
LXXVII	17.01	mm	-74.37	89.89	-90.24	73.36	-0.87	-78.32	77.60	2.33
LXXVIII	25.28	saddle	27.14	-77.51	9.61	92.96	-50.39	-47.61	42.45	12.96
LXXIX	25.31	mm	85.50	-58.78	-56.56	115.85	-36.94	-10.81	-5.08	-13.52
LXXX	26.68	mm	-78.36	-5.29	4.28	78.74	-78.74	-4.28	5.29	78.36
LXXXI	27.99	mm	-5.43	-60.69	49.99	59.56	-114.36	26.45	26.88	3.69
LXXXII	30.14	mm	3.80	48.60	-90.78	93.85	-93.81	90.75	-48.63	-3.78
LXXXIII	30.45	mm	25.90	-85.69	32.95	83.94	-88.75	-1.44	20.98	12.89
LXXXIV	32.44	mm	-0.13	-1.31	-9.16	79.99	-102.55	3.18	81.82	-58.99

Hexamethylcyclooctane in gas phase										
Conformation	δE	Stat. point	1,2,3,4	2,3,4,5	3,4,5,6	4,5,6,7	5,6,7,8	6,7,8,1	7,8,1,2	8,1,2,3
2,2,4,4,8,8-hexamethyl-TB'	0.00	min	-36.46	61.22	39.29	-57.59	-44.33	64.48	41.75	-65.41
2,2,4,4,8,8-hexamethyl-TB	0.00	min	36.46	-61.22	-39.29	57.58	44.33	-64.48	-41.76	65.41
2,2,4,4,8,8-hexamethyl-BB	0.82	saddle	44.75	-49.37	-49.37	44.75	58.27	-54.62	-54.61	58.27
2,2,4,4,8,8-hexamethyl-BC'	1.21	min	-91.85	48.12	56.57	-55.99	-47.72	112.64	-77.16	62.38
2,2,4,4,8,8-hexamethyl-BC	1.21	min	91.85	-48.12	-56.57	55.99	47.72	-112.64	77.16	-62.38
2,2,4,4,6,6-hexamethyl-BC'	4.40	min	58.83	-59.94	94.10	-40.12	-62.33	53.23	55.26	-98.43
2,2,4,4,6,6-hexamethyl-BC	4.40	min	-58.83	59.94	-94.10	40.12	62.33	-53.23	-55.26	98.43
2,2,4,4,8,8-hexamethyl-TBC'	5.99	min	79.39	-86.16	82.77	-40.78	-52.27	128.23	-65.70	-23.76
2,2,4,4,8,8-hexamethyl-TBC	5.99	min	-79.39	86.16	-82.77	40.78	52.27	-128.23	65.70	23.76
1,1,3,3,5,5-hexamethyl-TCC'	6.41	min	-77.65	100.41	-73.26	55.30	-80.29	117.61	-87.49	55.30
1,1,3,3,5,5-hexamethyl-TCC	6.41	min	77.65	-100.41	73.26	-55.30	80.28	-117.61	87.49	-55.31
1,1,3,3,5,5-hexamethyl-TC	7.26	min	-41.60	95.11	-95.11	41.60	36.72	-108.97	108.97	-36.72
1,1,3,3,5,5-hexamethyl-CC	7.44	min	80.66	-76.66	76.72	-80.72	82.75	-89.71	89.77	-82.80
XIII (TC)	7.93	saddle	58.97	-94.82	90.14	-40.02	-45.05	120.07	-92.89	12.54
XIV	7.93	saddle	-58.93	94.84	-90.15	40.01	45.02	-120.05	92.95	-12.61
XV (TBC)	8.23	min	-51.42	107.91	-48.50	-29.84	83.76	-101.14	93.50	-42.23
XVI	8.23	min	51.42	-107.91	48.50	29.85	-83.76	101.14	-93.50	42.24
XVII (TBC)	8.91	saddle	-0.10	-69.16	110.92	-54.26	-36.17	98.01	-107.83	66.55
XVIII	8.91	saddle	0.09	69.17	-110.92	54.26	36.17	-98.01	107.83	-66.55
XIX	9.00	saddle	-48.42	93.76	-20.90	-55.26	84.68	-91.76	99.15	-50.75
XX	9.00	saddle	48.42	-93.76	20.89	55.26	-84.67	91.76	-99.16	50.75
XXI	10.26	saddle	10.13	-11.46	77.69	-40.63	-70.78	61.12	55.74	-81.58

XXII	10.26	saddle	40.62	-77.71	11.47	-10.12	81.57	-55.75	-61.11	70.79
XXIII	10.38	saddle	-58.19	71.85	31.25	-61.17	-36.38	108.16	-39.53	-2.12
XXIV	10.38	saddle	61.16	-31.24	-71.85	58.18	2.12	39.54	-108.16	36.38
XXV (C or TBC)	10.59	saddle	-73.74	70.89	-97.04	54.78	52.11	-93.72	9.28	65.48
XXVI	10.59	saddle	73.72	-70.86	97.02	-54.78	-52.11	93.76	-9.31	-65.46
XXVII (TCC)	11.01	saddle	-80.05	73.26	-73.31	80.09	-84.43	91.33	-91.39	84.49
XXVIII (TBC)	11.25	min	83.99	-82.03	39.48	40.52	-106.78	50.89	47.56	-85.15
XXIX (TBC)	11.25	min	-83.99	82.03	-39.47	-40.53	106.78	-50.90	-47.55	85.15
XXX	11.56	saddle	-80.72	81.95	-54.30	-22.57	97.09	-51.92	-49.88	88.59
XXXI (BC)	11.65	min	-61.46	90.16	-49.02	-47.16	72.78	17.50	-88.90	68.58
XXXII	11.65	min	61.47	-90.17	49.02	47.15	-72.78	-17.49	88.89	-68.58
XXXIII	11.85	saddle	76.83	-47.19	-48.29	98.47	-24.81	-67.13	102.81	-78.25
XXXIV (TC)	11.88	saddle	39.19	-95.02	94.69	-41.86	-34.87	106.89	-112.17	41.13
XXXV (TC)	11.88	min	-93.06	38.65	38.65	-93.07	95.46	-41.09	-41.10	95.46
XXXVI (TC)	11.88	min	93.07	-38.65	-38.65	93.06	-95.46	41.10	41.10	-95.46
XXXVII (C or TBC)	11.89		-92.03	26.97	55.76	-66.31	70.09	-112.14	69.55	35.88
XXXVIII	12.07	saddle	89.91	-68.55	70.86	-57.24	-28.61	111.76	-58.45	-44.42
XXXIX (TC)	12.50	saddle	101.19	-44.65	-38.13	88.51	-98.98	66.69	7.84	-77.92
XL	12.55	saddle	77.98	-43.27	-67.79	53.47	59.65	-81.48	7.13	-10.19
XLI	12.55	saddle	-77.98	43.27	67.80	-53.47	-59.65	81.48	-7.13	10.19
XLII (TBC)	12.65	saddle	41.08	50.38	-88.98	71.60	-77.93	67.90	20.70	-91.97
XLIII (TBC)	12.65	saddle	-41.08	-50.38	88.98	-71.59	77.93	-67.90	-20.69	91.97
XLIV	12.66	mm	-72.05	48.22	63.74	-59.71	-54.11	85.52	-9.90	2.55
XLV	12.80	saddle	-78.43	74.01	-74.01	78.44	-11.05	-89.17	89.17	11.05
XLVI (TBC)	13.88		-72.85	5.10	60.17	-91.28	89.36	-42.31	-49.03	106.98
XLVII (C or TBC)	13.88	saddle	72.32	-4.32	-60.63	91.18	-89.17	42.24	49.33	-107.26
XLVIII (C)	14.13	mm	-69.62	81.86	-81.86	69.62	3.29	-96.65	96.65	-3.28
XLIX	14.38	saddle	5.68	22.90	-94.97	72.03	-35.14	79.73	-130.88	55.80
L	14.38	saddle	72.03	-94.97	22.90	5.68	55.80	-130.88	79.73	-35.14
LI (TCC)	15.40	saddle	-47.08	105.01	-40.98	1.98	-57.79	120.73	-47.41	-6.60
LII (TC)	15.95	saddle	97.50	-45.32	-34.01	91.46	-96.39	43.71	37.07	-93.11
LIII	16.26	saddle	18.45	-4.27	67.93	-105.77	72.74	-70.12	106.90	-88.98
LIV (TC)	16.43	saddle	-88.67	24.52	53.19	-98.01	94.29	-46.79	-35.10	96.07
LV	17.38	mm	95.24	-76.72	9.50	-9.43	77.95	-	79.46	-63.54

								119.31		
LVI	17.62	mm	-7.53	-26.67	96.81	-33.50	-49.46	6.68	91.80	-59.84
LVII	17.90	mm	32.33	-105.66	65.68	-36.83	80.94	-100.11	7.46	37.32
LVIII	18.04	mm	79.47	-68.49	2.85	76.16	-80.72	-3.17	78.77	-85.04
LIX	18.49	mm	-46.52	111.67	-71.65	42.51	-80.23	105.08	-27.11	-13.90
LX	19.41	saddle	82.32	-89.13	52.73	-70.81	114.21	-75.00	5.44	-12.66
LXI	19.41	saddle	-82.33	89.13	-52.72	70.81	-114.21	75.00	-5.44	12.67
LXII	19.90	mm	-66.18	60.47	-96.95	75.24	-8.13	13.52	-84.63	106.68
LXIII	32.39	mm	60.74	38.53	-97.60	28.49	24.89	7.82	-9.96	-60.25

Dioxazaphosphacinium in gas phase										
Conformation	δE	Stat. point	1,2,3,4	2,3,4,5	3,4,5,6	4,5,6,7	5,6,7,8	6,7,8,1	7,8,1,2	8,1,2,3
2,2,6*e*-trimethyl-6*a*-oxo-2*N*-5,7-di*O*-6*P*-BC'	0.00	min	72.42	−107.82	49.35	58.41	-56.47	-60.52	109.83	-65.69
2,2,6*e*-trimethyl-6*a*-oxo-2*N*-5,7-di*O*-6*P*-BC	0.00	min	60.53	56.47	-58.42	-49.35	107.83	-72.42	65.69	−109.83
2,2,6*e*-trimethyl-6*a*-oxo-2*N*-5,7-di*O*-6*P*-TBC'	2.37	min	-53.41	100.37	-86.39	82.18	-44.61	-60.90	121.37	-34.73
2,2,6*e*-trimethyl-6*a*-oxo-2*N*-5,7-di*O*-6*P*-TBC	2.37	min	60.91	44.62	-82.19	86.39	−100.37	53.43	34.71	−121.36
2*e*,6,6-trimethyl-2*a*-oxo-6*N*-1,3-di*O*-2*P*-TB'	2.55	min	53.57	62.55	-39.53	-65.89	40.81	66.91	-39.02	-80.15
2*e*,6,6-trimethyl-2*a*-oxo-6*N*-1,3-di*O*-2*P*-TB	2.55	min	-66.92	-40.80	65.90	39.52	-62.56	-53.56	80.15	39.01
3,7,7-trimethyl-3*a*-oxo-7*N*-2,4-di*O*-3*P*-TC	2.75	min	43.67	41.83	-99.40	99.40	-41.84	-43.66	105.29	−105.31
2*e*,6,6-trimethyl-2*a*-oxo-6*N*-1,3-di*O*-2*P*-TBC	4.73	min	54.24	51.19	−114.94	46.51	40.68	-97.62	97.14	-95.42
2*e*,6,6-trimethyl-2*a*-oxo-6*N*-1,3-di*O*-2*P*-TBC'	4.73	min	97.61	-40.67	-46.52	114.94	-51.19	-54.23	95.43	-97.15
3,7,7-trimethyl-3*a*-oxo-7*N*-2,4-di*O*-3*P*-TCC	5.28	min	97.30	-74.14	79.99	-94.55	89.64	-84.31	86.22	−101.42
1*b*,5,5-trimethyl-1*f*-oxo-5*N*-2,8-di*O*-1*P*-TBC'	6.16	min	-48.19	101.59	-17.79	-68.53	80.86	-84.76	104.39	-51.55
1*b*,5,5-trimethyl-1*f*-oxo-5*N*-2,8-di*O*-1*P*-TBC	6.16	min	84.76	-80.85	68.53	17.79	−101.59	48.20	51.55	−104.40
1*b*,5,5-trimethyl-1*f*-oxo-5*N*-2,8-di*O*-1*P*-TBC'	6.70	saddle	94.74	-73.85	-9.13	95.86	-53.44	-61.05	102.63	-83.56
1*b*,5,5-trimethyl-1*f*-oxo-5*N*-2,8-di*O*-1*P*-BC	7.52	min	-38.44	97.28	-58.62	58.62	-97.30	38.48	64.34	-64.37
1*b*,5,5-trimethyl-1*f*-										

oxo-5*N*-2,8-di*O*-1*P*-TBC	7.57	saddle	71.62	-93.00	78.08	22.46	-80.28	6.58	84.02	-92.72
1*b*,5,5-trimethyl-1*f*-oxo-5*N*-2,8-di*O*-1*P*-TBC'	7.57	saddle	-6.58	80.28	-22.46	-78.08	93.00	-71.62	92.73	-84.02
1,1,5*e*-trimethyl-5*a*-oxo-1*N*-4,6-di*O*-5*P*-TBC	9.76	min	-105.98	56.39	48.02	-90.99	74.30	-97.35	83.95	18.78
1,1,5*e*-trimethyl-5*a*-oxo-1*N*-4,6-di*O*-5*P*-TBC'	9.76	min	97.36	-74.28	90.99	-48.05	-56.36	105.96	-18.77	-83.97
2*a*,6,6-trimethyl-2*e*-oxo-6*N*-1,3-di*O*-2*P*-BC'	10.12	min	-63.02	-43.26	108.42	-65.40	54.06	-114.33	78.11	46.34
2*a*,6,6-trimethyl-2*e*-oxo-6*N*-1,3-di*O*-2*P*-BC	10.12	min	114.32	-54.06	65.42	-108.42	43.24	63.01	-46.32	-78.13
B  C	10.70	saddle	0.04	-74.38	64.18	46.26	-60.78	-61.00	103.62	-13.52
3*e*,7,7-trimethyl-3*a*-oxo-7*N*-2,4-di*O*-3*P*-BC	11.18	saddle	-84.25	82.78	21.14	-83.64	77.66	-93.69	97.13	-14.44
3*e*,7,7-trimethyl-3*a*-oxo-7*N*-2,4-di*O*-3*P*-BC'	11.18	saddle	93.71	-77.60	83.74	-21.44	-82.54	84.49	14.15	-97.03
XXIV	11.27	saddle	49.96	43.83	-3.89	-93.84	60.90	4.97	29.57	-114.89
XXIV'	11.27	saddle	-4.98	-60.89	93.84	3.88	-43.83	-49.95	114.88	-29.56
1,1,5*e*-trimethyl-5*a*-oxo-1*N*-4,6-di*O*-5*P*-BC	12.46	min	109.26	-40.93	-60.91	60.90	40.94	-109.26	75.47	-75.48
C  C	12.51	saddle	57.06	-96.31	101.24	-25.54	4.77	-76.88	123.86	-72.62
C  C	12.51	saddle	76.25	-3.66	24.62	-100.95	96.24	-56.89	72.58	-123.86
1,1,5*e*-trimethyl-5*a*-oxo-1*N*-4,6-di*O*-5*P*-TBC	13.02	saddle	-87.30	3.45	88.04	-77.38	53.08	-104.46	88.72	33.98
XXIX	13.03	saddle	82.06	-5.26	40.02	-105.11	29.19	62.97	-21.59	-100.00
XXX	13.03	saddle	-62.97	-29.19	105.10	-40.00	5.24	-82.05	100.00	21.59
1,1,5*a*-trimethyl-5*e*-oxo-1*N*-4,6-di*O*-5*P*-TBC	15.76	min	-83.35	101.49	-95.77	40.86	40.70	-133.52	80.51	28.22
1,1,5*a*-trimethyl-5*e*-oxo-1*N*-4,6-di*O*-5*P*-TBC'	15.76	min	133.52	-40.69	-40.87	95.76	-101.47	83.35	-28.22	-80.50
XXXIII	16.41	saddle	-102.48	29.11	4.75	63.76	-71.30	-49.48	82.40	32.44

TB  C	16.41	saddle	49.48	71.30	-63.76	-4.75	-29.11	102.48	-32.45	-82.40
C  C	16.63	saddle	-3.56	-66.59	115.62	-65.30	45.41	-111.56	109.95	-12.23
XXXVI	16.73	saddle	-72.09	109.87	-101.53	51.14	17.22	-120.22	101.92	8.19
XXXVII	16.73	saddle	120.21	-17.19	-51.17	101.51	-109.84	72.13	-8.24	-101.89
XXXVIII	18.40	mm	-24.41	106.58	-94.06	12.31	52.30	-120.54	114.79	-41.91
XXXIX	20.27	saddle	77.27	-125.81	51.73	10.99	23.39	-120.47	91.01	-38.83
XL	20.27	saddle	120.45	-23.30	-11.10	-51.66	125.80	-77.25	38.80	-91.00
XLI	20.46	saddle	-75.42	67.01	9.17	17.96	-83.82	18.35	74.66	-30.35
XLII	20.68	mm	108.55	-18.00	0.26	-68.41	123.57	-79.36	54.01	-103.51
XLIII (BC)	21.02	min	-78.93	-44.91	61.61	41.01	-112.19	63.63	-38.44	98.47
XLIV (BC)	21.02	min	-63.64	112.20	-41.02	-61.61	44.91	78.93	-98.47	38.45
XLV (BC)	21.60	min	-106.09	46.97	58.21	-58.07	-47.21	106.06	-56.57	56.67
XLVI	22.74	saddle	-32.25	103.40	-39.64	-64.71	42.69	84.32	-84.51	3.72
XLVII	22.74	saddle	-84.30	-42.71	64.71	39.65	-103.39	32.22	-3.71	84.52
XLVIII (TCC)	22.98	min	-68.15	123.60	-78.05	42.86	-74.38	133.62	-74.73	25.44
XLIX	22.98	min	-133.62	74.37	-42.86	78.05	-123.61	68.15	-25.43	74.73
L	23.73	saddle	-39.96	117.98	-73.35	33.58	-70.53	134.68	-57.31	-6.91
LI	24.43	saddle	-110.81	19.83	67.19	-23.72	-85.16	69.39	-5.26	50.37
LII (C)	26.44	saddle	-90.00	86.17	11.37	-88.04	32.42	83.33	-89.60	53.20
LIII	27.05	mm	-37.48	107.04	-40.10	-64.00	43.40	81.12	-81.84	6.54
LIV (TC)	32.80	saddle	-129.70	40.07	42.10	-114.14	82.39	-10.60	-30.00	102.49
LV (C)	34.14	saddle	-70.13	-15.23	93.40	-93.40	15.23	70.13	-95.27	95.27
LVI	35.00	mm	-9.40	-8.73	-16.37	89.59	-59.14	-70.62	112.33	-23.88

cis-Methyldioxazaphosphacinium in gas phase										
Conformation	δE	Stat. point	1,2,3,4	2,3,4,5	3,4,5,6	4,5,6,7	5,6,7,8	6,7,8,1	7,8,1,2	8,1,2,3
2,2,4*e*,6*e*-tetramethyl-6*a*-oxo-2*N*-5,7-di*O*-6*P*-BC'	0.00	min	72.35	-107.92	49.86	58.31	-56.41	-60.41	109.70	-65.91
2,2,6*e*,8*a*-tetramethyl-6*a*-oxo-2*N*-5,7-di*O*-6*P*-BC	2.89	min	60.69	53.07	-52.34	-53.95	108.50	-72.74	67.65	-110.72
(*R*)-1,3*e*,7,7-tetramethyl-3*a*-oxo-7*N*-2,4-di*O*-3*P*-TC	3.50	min	49.53	35.22	-96.77	100.90	-42.03	-44.36	105.24	-107.62
2*e*,4*a*,6,6-tetramethyl-2*a*-oxo-6*N*-1,3-di*O*-2*P*-TB'	4.10	min	54.62	58.54	-33.35	-69.66	39.24	68.43	-38.27	-81.80
2,2,6*e*,8*e*-tetramethyl-6*a*-oxo-2*N*-5,7-di*O*-6*P*-TBC	4.29	min	65.76	38.18	-80.12	88.73	-99.29	48.59	37.96	-124.34
2*e*,4*e*,6,6-tetramethyl-2*a*-oxo-6*N*-1,3-di*O*-2*P*-TBC	4.94	min	97.39	-40.05	-46.83	115.26	-51.21	-54.14	95.36	-97.56
2*e*,4*e*,6,6-tetramethyl-2*a*-oxo-6*N*-1,3-di*O*-2*P*-TCC	5.59	min	99.70	-69.79	76.96	-98.17	92.68	-80.69	82.55	-105.45
1*e*,3*a*,5,5-tetramehtyl-1*a*-oxo-5*N*-2,8-di*O*-1*P*-TB	5.59	min	-59.21	-43.50	67.73	38.37	-63.48	-52.89	84.74	30.10
3*e*,5*e*,7,7-tetramethyl-3*a*-oxo-7*N*-2,4-di*O*-3*P*-TCC	5.70	min	83.07	-90.42	96.25	-79.09	72.75	-97.88	102.50	-85.68
*cis*1*i*,3*e*,7,7-tetramethyl-3*a*-oxo-7*N*-2,4-di*O*-3*P*-TC	5.96	saddle	79.68	-6.67	-71.32	113.48	-49.20	-47.67	98.91	-106.96
1*e*,3*e*,5,5-tetramethyl-1*a*-oxo-5*N*-2,8-di*O*-1*P*-TBC	6.42	min	84.62	-80.32	68.89	17.53	-101.51	48.27	51.45	-105.04
1*e*,3*e*,7,7-tetramethyl-3*a*-oxo-7*N*-2,4-di*O*-3*P*-TBC'	7.12	saddle	94.55	-73.67	-8.55	95.78	-53.45	-60.90	102.66	-84.14
1*e*,3*e*,7,7-tetramethyl-3*a*-oxo-7*N*-2,4-di*O*-3*P*-TBC	7.51	min	55.70	46.36	-114.12	53.55	33.05	-96.74	100.08	-95.27
2*e*,6,6,8*e*-tetramethyl-2*a*-oxo-6*N*-1,3-di*O*-2*P*-TBC	7.82	saddle	71.61	-92.80	78.50	22.38	-80.32	6.81	83.85	-93.24
2,2,4*f*,6*e*-tetramethyl-6*a*-oxo-2*N*-5,7-di*O*-6*P*-TBC'	8.89	min	-36.99	88.91	-86.95	83.71	-43.47	-61.79	125.01	-45.04
XVI (TC) (Me rot.)	9.48	mm	51.93	45.66	-113.48	70.48	9.89	-82.09	105.29	-99.81
2*e*,6,6,8*e*-tetramethyl-2*a*-oxo-6*N*-1,3-di*O*-2*P*-TBC	9.84	saddle	63.92	49.17	-93.10	8.46	74.78	-96.34	83.79	-102.77
1,1,3*e*,5*e*-tetramethyl-5*a*-oxo-1*N*-4,6-di*O*-5*P*-TBC'	10.03	min	97.22	-73.57	91.21	-48.38	-56.26	105.60	-18.56	-84.83
2*a*,4*e*,6,6-tetramethyl-2*a*-oxo-6*N*-1,3-di*O*-2*P*-BC	10.35	min	113.58	-53.13	65.70	-109.02	42.81	63.04	-45.80	-79.04
3*e*,5*e*,7,7-tetramethyl-3*a*-oxo-7*N*-2,4-di*O*-3*P*-BC'	11.45	saddle	93.58	-77.00	84.04	-21.64	-82.47	84.31	14.18	-97.79
XXI	12.40	mm	-3.33	-66.61	83.25	20.92	-52.27	-53.02	111.24	-23.75
1,1,3*e*,5*e*-tetramethyl-5*a*-oxo-1*N*-4,6-di*O*-5*P*-BC	12.80	min	109.49	-43.22	-59.34	63.13	37.82	-108.50	76.18	-75.17

C$\hat{}$C	12.81	saddle	57.12	-96.21	101.33	-24.69	3.67	-75.93	123.75	-73.29
C$\hat{}$C	12.90	saddle	76.72	-4.05	25.27	-101.49	96.19	-56.73	72.34	-124.48
2*e*,6,6,8*e*-tetramethyl-2*a*-oxo-6*N*-1,3-di*O*-2*P*-TBC	13.04	saddle	100.79	-16.20	-76.78	51.49	55.04	-110.81	73.65	-81.60
XXVI	13.22	saddle	104.15	-52.47	77.47	-88.25	-3.64	87.23	-33.79	-89.32
XXVII (TBC)	13.30	min	-54.27	-42.78	112.40	-66.61	47.80	-110.37	89.19	31.73
XXIII	14.40	saddle	-43.02	90.98	-81.93	80.36	-44.93	-60.20	123.94	-41.32
XXIX	14.64	saddle	-31.32	90.02	-65.10	66.61	-83.01	10.90	84.00	-66.93
XXX	14.88	saddle	109.12	-39.97	-62.44	62.75	39.99	-108.74	75.09	-75.67
XXXI	14.97	saddle	-55.34	-34.27	107.62	-41.74	7.60	-83.56	102.14	16.55
XXXII	15.77	saddle	115.89	-57.32	66.28	-105.78	41.63	65.26	-48.56	-76.32
XXXIII (TC)	16.31	min	132.20	-39.17	-41.91	96.43	-101.73	83.41	-28.36	-80.78
XXXIV (TBC)	16.70	min	-93.15	46.94	53.90	-91.20	71.73	-98.28	89.53	12.18
XXXV	16.80	saddle	111.49	-45.31	65.58	-115.92	66.63	3.51	12.17	-110.18
XXXVI	17.07	saddle	120.61	-17.63	-50.79	101.89	-110.06	71.96	-8.43	-101.98
XXXVII	17.80	saddle	130.05	-50.18	-15.57	90.18	-120.15	66.08	2.38	-102.45
XXXVIII	17.81	mm	105.71	-47.64	73.52	-96.27	9.27	72.46	-25.74	-97.02
XXXIX	17.99	saddle	109.11	-41.11	-60.15	61.32	39.77	-108.73	75.34	-75.43
XL	18.20	saddle	92.99	-27.78	59.71	-115.10	48.53	17.54	16.85	-117.64
XLI	18.77	mm	120.29	-52.05	-11.99	93.91	-106.72	24.42	41.98	-115.26
XLII	19.18	saddle	45.22	70.68	-58.98	-0.72	-40.68	108.83	-28.95	-81.21
XLIII	19.86	mm	-65.35	-1.55	92.50	-74.59	42.92	-98.58	106.00	9.32
XLIV	20.18	saddle	77.00	-125.64	52.11	10.90	23.37	-120.33	90.93	-38.89
XLV	20.69	mm	79.04	-122.87	70.23	-1.52	17.74	-107.39	104.43	-55.40
XLVI	22.77	saddle	130.56	-37.77	-44.54	93.72	-98.22	86.77	-32.92	-76.49
XLVII	22.99	saddle	15.31	66.27	-26.29	-1.29	-69.02	81.87	22.11	-93.55
XLVIII (TC)	23.62	min	-72.57	92.73	-95.60	43.70	38.10	-134.98	83.45	23.09
XLIX	24.30	saddle	-74.44	94.01	-95.68	58.45	14.00	-121.25	94.09	18.84
L	25.10	y	132.90	-55.05	-11.86	85.37	-119.07	72.84	-4.69	-97.10
LI (BC)	26.19	min	-68.62	-51.11	59.60	45.41	-114.84	67.55	-43.13	94.87

LII	26.30	saddle	-41.73	110.05	-81.17	18.25	30.57	-105.04	121.64	-36.17
LIII	26.52	mm	-28.69	103.69	-87.37	19.63	35.38	-110.58	122.23	-42.74
LIV (BC)	28.96	min	-45.31	100.16	-42.08	-62.05	47.27	79.78	-100.69	27.94
LV (TBC)	29.38	min	-53.33	-45.51	111.53	-42.79	-53.38	106.90	-80.15	74.74
LVI (TBC)	29.58	min	-80.62	-7.61	90.67	-42.85	-68.87	108.04	-55.03	63.54
LVII	30.65	mm	-0.22	67.12	-17.21	-1.10	-74.72	70.62	37.60	-91.26
LVIII	30.73	mm	52.16	5.89	17.59	-5.83	-80.24	76.23	30.57	-110.96
LIX (TBC)	32.35	min	-89.83	53.56	52.05	-76.70	-19.79	105.28	-68.10	45.85
LX	33.98	mm	-42.82	109.27	-75.78	15.52	29.06	-101.53	122.65	-37.70
LXI (TBC)	34.95	min	-89.30	42.47	49.10	-111.62	38.56	67.77	-85.48	72.32

trans-Methyldioxazaphosphacinium in gas phase										
Conformation	δE	Stat. point	1,2,3,4	2,3,4,5	3,4,5,6	4,5,6,7	5,6,7,8	6,7,8,1	7,8,1,2	8,1,2,3
2,2,4*e*,6*e*-tetramethyl-6*a*-oxo-2*N*-5,7-di*O*-6*P*-TBC	0.00	min	-54.17	100.76	-86.52	82.00	-44.70	-60.68	121.11	-33.96
2,2,6*e*,8*e*-tetramethyl-6*a*-oxo-2*N*-5,7-di*O*-6*P*-BC'	0.20	min	53.18	60.42	-55.64	-53.16	108.08	-73.50	69.00	-107.78
(*R*)-1*i*,3*e*,7,7-tetramethyl-3*a*-oxo-7*N*-2,4-di*O*-3*P*-TC	1.43	min	36.35	47.42	-100.96	98.48	-40.87	-46.08	108.04	-100.85
1*e*,3*e*,5,5-tetramethyl-1*a*-oxo-5*N*-2,8-di*O*-1*P*-TB	1.50	min	-71.13	-33.68	65.29	36.67	-63.16	-51.51	82.80	36.49
1*e*,3*e*,7,7-tetramethyl-3*a*-oxo-7*N*-2,4-di*O*-3*P*-TBC	2.01	min	54.72	48.23	-81.39	84.93	-100.82	51.89	37.98	-119.67
(*R*)-1*i*,3*e*,7,7-tetramethyl-3*a*-oxo-7*N*-2,4-di*O*-3*P*-TC	2.49	saddle	-1.88	72.52	-99.80	92.16	-39.89	-56.21	120.24	-73.55
2*e*,4*e*,6,6-tetramethyl-2*a*-oxo-6*N*-1,3-di*O*-2*P*-TB	2.84	min	46.75	66.31	-37.01	-68.66	39.38	69.24	-39.38	-77.11
(*R*)-1*i*,3*e*,7,7-tetramethyl-3*a*-oxo-7*N*-2,4-di*O*-3*P*-TC	3.65	saddle	51.74	44.30	-91.91	97.84	-75.93	6.58	71.26	-118.86
1*e*,5,5,7-tetramethyl-1*a*-oxo-5*N*-2,8-di*O*-1*P*-TBC'	3.69	min	-49.26	102.28	-18.48	-67.72	80.27	-85.22	104.60	-50.32
2,2,4*a*,6*e*-tetramethyl-6*a*-oxo-2*N*-5,7-di*O*-6*P*-BC'	3.91	min	63.50	-98.88	49.48	57.00	-55.54	-61.17	113.22	-63.66
1*b*,3*e*,5,5-tetramethyl-1*f*-oxo-5*N*-2,8-di*O*-1*P*-BC	5.14	min	-41.98	98.90	-59.04	58.90	-95.11	34.24	67.14	-61.73
1*b*,5,5,7*e*-tetramethyl-1*f*-oxo-5*N*-2,8-di*O*-1*P*-TBC'	5.53	saddle	-3.94	78.87	-23.21	-78.29	93.40	-70.97	91.98	-85.94
1*b*,3*e*,5,5-tetramethyl-1*f*-oxo-5*N*-2,8-di*O*-1*P*-BC	6.13	saddle	-2.91	79.59	-65.02	64.16	-105.13	54.80	50.54	-86.83
1,1,5*b*,7e-tetramethyl-5*f*-oxo-1*N*-4,6-di*O*-5*P*-TBC	7.27	min	-106.21	55.74	48.25	-91.40	74.43	-97.07	83.47	19.68
2*e*,6,6,8*e*-tetramethyl-2*a*-oxo-6*N*-1,3-di*O*-2*P*-TBC	7.62	saddle	53.85	58.67	-95.33	6.55	74.51	-97.05	86.40	-99.21
1*b*,3*e*,7,7-tetramethyl-3*a*-oxo-7*N*-2,4-di*O*-3*P*-BC	8.95	saddle	-84.00	82.60	20.63	-83.73	77.55	-93.34	97.07	-14.15
2*a*,6,6,8*e*-tetramethyl-2*e*-oxo-6*N*-1,3-di*O*-2*P*-BC'	9.06	min	-67.80	-31.11	107.68	-68.60	49.37	-109.69	86.50	39.31
1*b*,3*e*,5,5-tetramethyl-1*f*-oxo-5*N*-2,8-di*O*-1*P*-BC	9.27	mm	-6.54	79.79	-79.23	79.08	-81.23	9.12	81.92	-83.84
1*e*,5,5,7*a*-tetramethyl-1*a*-oxo-5*N*-2,8-di*O*-1*P*-TCC'	9.77	min	70.17	-84.21	97.91	-77.53	68.33	-100.16	108.36	-79.03
XX	10.30	saddle	46.20	46.79	-4.35	-94.07	59.05	7.07	28.77	-113.11
1*b*,3*a*,5,5-tetramethyl-1*f*-oxo-5*N*-2,8-di*O*-1*P*-TBC	10.67	min	74.75	-72.32	68.35	14.53	-100.15	47.58	54.19	-101.94
1,1,5*e*,7*e*-tetramethyl-5*a*-oxo-1*N*-4,6-di*O*-5*P*-TBC	10.69	saddle	-87.45	3.15	88.33	-77.51	52.91	-104.10	88.60	34.53

C C	11.21	mm	50.87	59.91	-30.95	-76.94	69.44	2.44	20.50	-106.42
XXIV	11.30	saddle	-67.12	-22.85	102.68	-41.52	5.53	-81.09	100.99	21.46
BB C	11.45	saddle	2.72	-73.06	58.68	50.74	-60.69	-63.09	105.49	-15.99
XXVI	11.70	saddle	8.45	-66.18	91.25	6.41	-44.46	-48.14	118.45	-41.86
2*e*,4*f*,6,6-tetramethyl-2*a*-oxo-6*N*-1,3-di*O*-2*P*-TBC'	11.99	saddle	85.02	-63.89	-12.56	95.64	-53.49	-61.49	105.72	-82.05
C C	12.02	saddle	61.45	-84.10	78.15	19.60	-78.55	5.48	87.13	-89.42
1,1,3*e*,5*e*-tetramethyl-5*a*-oxo-1*N*-4,6-di*O*-5*P*-TBC	13.55	min	-83.00	102.33	-96.70	40.80	40.11	-133.16	81.57	27.86
C C	13.91	saddle	76.09	-9.60	32.63	-104.44	97.46	-60.46	74.55	-120.72
TB C?	14.16	saddle	-102.65	28.98	4.43	64.11	-71.38	-49.24	82.12	33.13
XXXII	14.25	min	88.01	-65.03	88.87	-50.51	-55.21	108.19	-20.17	-80.79
XXXIII	14.32	saddle	-69.44	111.97	-103.02	48.23	19.74	-121.18	103.41	5.64
XXXIV	14.79	saddle	-67.58	119.81	-90.32	15.75	50.95	-130.88	100.98	-0.29
XXXV	15.30	min	99.34	-36.87	60.89	-112.38	38.66	65.10	-40.90	-83.04
XXXVI	15.65	saddle	84.38	-68.08	82.59	-25.28	-80.91	85.77	14.35	-94.78
XXXVII	15.69	saddle	85.04	-14.36	48.74	-109.89	31.36	64.75	-28.13	-93.54
XXXVIII	16.46		37.69	77.95	-59.60	-4.86	-35.88	108.06	-30.50	-76.68
XXXIX	16.47	mm	-18.60	103.45	-94.65	11.17	54.27	-119.58	114.25	-46.41
XL	16.52	saddle	0.34	-64.51	114.21	-65.74	44.81	-109.08	114.12	-19.88
XLI	16.65	saddle	44.47	-85.37	101.25	-27.49	4.03	-76.36	126.45	-67.00
XLII	17.01	mm	58.79	53.37	-93.44	7.07	75.48	-98.85	85.59	-99.88
XLIII	17.57	mm	11.76	-68.08	108.96	-39.46	10.53	-83.34	123.28	-39.68
XLIV	17.69	saddle	92.41	-38.79	71.38	-89.84	-4.51	88.13	-31.54	-89.10
XLV	17.72	saddle	96.13	-31.37	-66.66	72.91	25.02	-105.68	84.23	-75.51
XLVI	18.30	saddle	-75.05	66.93	8.50	18.23	-83.36	17.76	75.12	-30.23
XLVII	18.44		-19.03	84.34	-18.85	-8.80	-66.84	74.33	30.92	-74.57
XLVIII	18.44	min	-63.87	112.43	-41.83	-61.06	44.55	78.79	-98.52	39.07
XLVIX	18.88	mm	-88.12	97.33	-94.76	61.22	12.16	-116.59	87.74	29.10
L	19.22	min	-105.35	51.41	55.28	-61.89	-41.55	106.17	-58.84	55.16
LI	20.23	saddle	-86.62	98.42	-93.86	43.33	39.20	-131.71	76.67	33.02
LII	20.42	mm	1.54	85.79	-36.97	-1.18	-64.51	96.74	5.07	-74.26
LIII	20.43	min	-68.49	123.64	-78.53	42.93	-74.11	133.19	-74.98	26.19
LIV	20.47	saddle	-30.84	103.09	-40.12	-64.33	41.65	84.78	-83.58	2.10

LV	20.68	saddle	-105.52	46.28	60.26	-61.08	-45.53	104.24	-54.48	55.33
LVI	20.74	saddle	106.46	-55.30	65.02	-109.65	49.38	64.78	-58.81	-62.96
LVII	20.75	min	-132.29	74.82	-43.83	78.59	-123.92	68.91	-25.79	74.10
LVIII	20.89	saddle	106.46	-49.80	61.85	-107.03	43.43	68.82	-54.92	-70.18
LIX	20.95	saddle	-106.62	47.32	57.90	-59.33	-45.56	106.01	-58.01	58.12
LX	21.19	min	-83.78	-37.96	57.56	41.48	-114.31	66.13	-38.37	98.11
LXI	21.35		-37.85	117.60	-72.89	31.94	-69.36	133.65	-55.45	-9.49
LXII	21.36	min	124.11	-31.34	-51.25	96.11	-94.03	89.01	-40.74	-71.91
LXIII	21.44	saddle	-133.45	71.18	-34.86	74.14	-118.71	41.33	6.09	57.01
LXIV	21.60	saddle	115.38	-16.86	-61.31	96.11	-94.27	91.92	-40.09	-75.13
LXV	21.72	saddle	-99.93	-20.63	56.73	30.58	-115.15	58.00	-17.15	84.17
LXVI	22.03	saddle	-110.73	19.08	67.71	-24.04	-84.95	69.69	-5.90	51.36
LXVII	22.29	saddle	-68.73	85.09	23.03	-67.68	-19.15	110.26	-50.24	5.12
LXVIII	23.09	saddle	101.14	-31.96	-15.66	82.44	-123.45	52.55	29.60	-114.13
LXIX	23.35	saddle	-64.08	113.88	-43.96	-58.76	44.03	78.59	-98.34	39.47
LXX	23.81	saddle	-105.33	104.14	-66.60	66.17	-103.89	104.35	-56.33	57.35
LXXI	24.32	saddle	-89.70	87.17	10.45	-86.79	30.50	84.81	-88.99	52.37
LXXII	24.33	mm	-88.27	91.13	9.55	-82.50	23.75	90.78	-86.04	46.19
LXXIII	24.94	saddle	73.00	-117.14	60.20	2.35	25.28	-119.33	100.33	-45.86
LXXIV	25.01		-71.02	122.76	-77.88	45.26	-76.84	132.94	-75.13	28.40
LXXV	25.21	saddle	-131.96	77.00	-45.33	77.29	-123.50	71.81	-27.85	74.09
LXXVI	25.68	mm	69.92	-111.44	75.24	-6.84	17.97	-106.49	112.00	-57.64
LXXVII	26.26	saddle	-80.47	-39.85	52.36	47.73	-116.67	65.98	-40.62	99.05
LXXVIII	26.68	mm	-98.13	-22.53	55.66	35.08	-113.64	48.19	-8.63	80.98
LXXVIX	27.76	saddle	136.59	-60.96	44.19	-88.84	98.04	-13.08	-11.96	-78.10
LXXX	28.01	mm	-76.41	79.95	5.79	-17.58	-7.07	-50.03	109.19	-30.65
LXXXI	28.18	unconv.	-56.37	101.00	-13.10	-25.72	-13.71	-5.33	80.17	-56.11
LXXXII	28.18	unconv.	-56.23	100.92	-12.88	-26.14	-13.49	-5.15	79.97	-56.19
LXXXIII	28.39	mm	130.69	-57.11	54.20	-100.05	92.34	-14.39	0.06	-92.25
LXXXIV (Me rot.)	29.64	mm	71.30	-115.45	51.78	-2.54	43.39	-134.01	89.98	-36.43

LXXXV	30.40	saddle	−129.08	39.23	42.65	−114.50	82.87	−11.20	−29.71	102.63
LXXXVI	31.91	saddle	−69.86	−16.01	94.08	−93.54	15.21	70.11	−95.43	95.90
LXXXVII (Me rot.)	33.72	mm	−130.31	40.83	41.40	−113.73	81.91	−10.63	−29.54	102.50
LXXXVIII	33.79	saddle	−88.95	109.19	−53.18	−53.17	97.59	−12.96	−50.98	70.55

Dimethyldioxazaphosphacinium in gas phase										
Conformation	δE	Stat. point	1,2,3,4	2,3,4,5	3,4,5,6	4,5,6,7	5,6,7,8	6,7,8,1	7,8,1,2	8,1,2,3
1,1,3*e*,7,7-pentamethyl-3*a*-oxo-3*P*-7*N*-TC	0.00	min	42.75	40.35	-98.40	99.92	-40.87	-47.13	108.24	-103.63
2,2,6*e*,8,8-pentamethyl-6*a*-oxo-2*N*-6*P*-BC	0.58	min	50.31	56.51	-44.05	-62.87	106.52	-71.14	72.67	-110.14
2,2,4,4,6*e*-pentamethyl-6*a*-oxo-2*N*-6*P*-BC'	1.71	min	61.98	-97.78	51.12	56.00	-54.99	-60.93	113.77	-64.07
2*e*,4,4,6,6-pentamethyl-2*a*-oxo-2*P*-6*N*-TB	2.58	min	50.72	60.69	-34.34	-70.41	40.10	69.98	-42.78	-76.99
1*e*,3,3,5,5-pentamethyl-1*a*-oxo-1*P*-5*N*-TB	2.61	min	-63.03	-36.55	67.29	35.37	-63.32	-50.99	87.59	27.77
3,3,5,5,7*e*-pentamethyl-7*a*-oxo-3*N*-7*P*-TBC	2.62	min	56.18	44.02	-76.39	82.57	-101.34	50.61	40.33	-121.40
1,1,3,3,7*e*-pentamethyl-7-oxo-3*N*-7*P*-TBC'	4.54	min	-38.77	89.09	-85.98	82.76	-43.85	-61.45	124.86	-43.08
2,2,4,4,6*e*-pentamethyl-6*a*-oxo-3*N*-6*P*-BC'	6.87	saddle	62.04	-98.39	52.31	54.59	-54.83	-60.61	113.66	-64.66
1*e*,5,5,7,7-pentamethyl-1*a*-oxo-1*P*-5*N*-TBC'	7.77	min	-35.38	91.85	-18.33	-66.30	78.28	-84.86	107.15	-58.83
2*e*,4,4,6,6-pentamethyl-2*a*-oxo-2*P*-6*N*-TB	7.77	saddle	48.01	56.54	-19.51	-79.02	33.67	69.55	-31.34	-85.24
1,1,3,3,7*e*-pentamethyl-7*a*-oxo-3*N*-7*P*-TC Me rotation	7.83	saddle	53.11	30.24	-96.26	100.79	-35.88	-51.96	108.31	-107.85
2,2,6*e*,8,8-pentamethyl-6*a*-oxo-2*N*-6*P*-TBC'	8.04	saddle	46.82	46.87	-68.11	75.13	-106.91	57.62	40.25	-115.20
1*e*,5,5,7,7-pentamethyl-1*a*-oxo-1*P*-5*N*-TCC'	8.15	min	68.55	-81.49	98.10	-78.40	68.26	-99.22	108.64	-80.26
1,1,3*e*,7,7-pentamethyl-3*a*-oxo-3*P*-7*N*-TCC'	8.26	min	89.97	-55.46	71.65	-102.70	93.27	-77.34	83.06	-107.55
TB Me rotation	8.33		49.79	61.70	-34.03	-68.96	36.17	72.96	-42.07	-77.81
1*e*,3,3,5,5-pentamethyl-1*a*-oxo-1*P*-5*N*-TBC	8.78	min	72.85	-69.94	68.86	13.39	-99.74	47.95	54.24	-102.59
1*e*,3,3,5,5-pentamethyl-1*a*-oxo-1*P*-5*N*-TB Me rotation	8.81	saddle	-56.83	-40.45	66.11	38.59	-62.97	-53.31	89.73	24.75
2*e*,4,4,6,6-pentamethyl-2*a*-oxo-2*P*-6*N*-TB	8.99	saddle	51.91	42.97	-4.43	-92.74	54.78	13.36	22.54	-114.86
2,2,4,4,6*e*-pentamethyl-6*a*-oxo-2*N*-6*P*-BC'	9.67	saddle	0.15	-71.45	57.49	52.39	-60.59	-63.92	105.00	-13.57
XVIII (BC)	9.79	min	-58.80	-32.47	109.75	-68.31	45.08	-106.53	94.52	27.11
XIX	10.00	saddle	8.56	-65.25	91.25	6.28	-44.26	-47.65	119.20	-43.11
XX (C)	10.01	saddle	56.63	54.62	-90.84	2.71	77.31	-99.04	86.42	-99.42
XXI	10.12	saddle	-26.25	86.92	-65.81	66.88	-83.70	13.04	82.80	-70.40
XXII	10.51	saddle	82.60	-61.90	-11.53	94.32	-53.07	-61.32	106.93	-82.94
XXIII	11.03	mm	-6.61	76.00	-74.74	76.30	-77.79	2.63	88.11	-82.33

XXIV	11.10		5.66	-68.42	77.47	26.16	-52.92	-53.91	115.26	-32.25
XXV	11.19	saddle	-57.55	-28.38	105.32	-43.47	8.23	-82.61	104.62	14.49
XXVI (C)	11.24	saddle	55.58	46.80	-119.85	58.45	30.60	-97.12	97.19	-93.17
XXVII	11.26	saddle	54.18	48.66	-120.84	59.00	29.38	-95.68	97.81	-94.00
XXVIII	11.82	saddle	76.17	-9.52	33.61	-105.35	97.42	-60.55	74.38	-121.55
XXIX (C)	12.07	min	-92.71	43.60	55.70	-91.60	71.37	-98.04	88.68	14.63
XXX (BC)	12.11	saddle	-55.64	-38.65	113.31	-67.01	44.29	-106.13	92.80	28.11
XXXI (C)	12.13	min	-83.48	44.80	57.30	-90.40	63.09	-91.67	97.46	0.03
XXXII	12.21	min	86.50	-61.93	88.46	-51.73	-54.41	107.58	-19.72	-82.28
XXXIII	12.38	saddle	-56.12	-22.24	93.56	-12.39	-37.74	-46.91	105.18	1.42
XXXIV (BC)	13.03	min	97.26	-33.17	60.13	-113.01	37.43	64.76	-38.86	-85.91
XXXV	13.46	saddle	82.90	-10.79	47.08	-109.84	30.73	64.66	-27.47	-94.90
XXXVI	13.67	saddle	82.55	-65.43	82.63	-26.07	-80.50	85.49	14.77	-95.82
XXXVII	14.02	saddle	70.05	47.24	-97.10	71.25	-80.89	109.06	-40.09	-78.75
XXXVIII (C)	14.38	saddle	-89.20	25.83	72.57	-87.46	58.84	-95.96	91.53	19.43
XXXIX	14.53	saddle	-70.28	71.38	24.54	-83.34	75.03	-93.42	100.91	-20.84
XL	14.71	saddle	0.66	-63.61	114.38	-65.79	44.34	-108.07	115.30	-21.61
XLI	14.85	saddle	43.50	-83.78	101.54	-27.76	4.10	-75.74	126.96	-68.00
XLII	15.44	saddle	91.34	-36.84	71.14	-90.04	-5.10	87.96	-30.99	-90.46
XLIII (BC)	15.65	saddle	94.54	-26.57	-69.60	73.02	25.59	-104.99	84.45	-77.85
XLIV	15.91	saddle	-80.36	49.41	52.34	-92.15	66.53	-91.43	98.53	-5.07
XLV	16.24		34.10	76.70	-57.71	4.29	-51.15	113.39	-25.32	-76.27
XLVI	16.87	saddle	63.04	-4.42	52.70	-72.48	-28.42	80.66	2.48	-105.28
XLVII	18.37	saddle	17.94	64.83	-27.36	-0.54	-68.95	81.11	22.07	-95.78
XLVIII	18.59	saddle	-88.77	20.71	-1.79	74.91	-68.37	-56.81	86.57	31.36
XLIX (BC)	18.68	saddle	105.60	-47.63	61.10	-107.41	43.50	68.87	-55.12	-71.33
L	18.77	min	123.59	-28.92	-52.69	96.28	-93.58	88.79	-40.68	-73.62
LI	19.01	saddle	115.19	-14.35	-62.54	96.72	-94.59	91.16	-39.24	-77.65
LII	19.70	saddle	108.99	-50.29	59.65	-106.38	49.35	63.13	-53.93	-70.10
LIII (C)	19.74	min	-71.53	90.90	-96.21	44.82	36.57	-134.51	84.04	23.89
LIV	20.23	saddle	-73.78	92.03	-96.16	58.12	15.14	-122.08	93.15	20.69
LV	20.60	saddle	123.58	-29.03	-52.81	95.88	-93.26	89.73	-41.86	-72.79
LVI (BC)	21.06	saddle	97.17	-52.70	-49.69	78.21	15.05	-105.87	81.44	-63.41

LVII (TC)	21.12		104.04	-30.33	-17.94	85.71	-123.28	51.40	27.95	-116.56
LVIII	21.12	saddle	103.63	-30.99	-16.86	84.83	-123.40	51.51	28.29	-116.31
LIX (C)	21.35	saddle	-70.88	106.55	-86.54	17.37	53.10	-137.10	93.27	12.17
LX	21.35	saddle	-70.86	106.58	-86.52	17.30	53.14	-137.10	93.30	12.13
LXI (TC)	21.67	saddle	-41.30	109.29	-80.70	18.25	29.29	-102.72	121.59	-37.08
LXII	22.39	mm	-20.34	98.88	-89.29	19.35	37.29	-110.77	122.31	-48.29
LXIII	22.39		-20.75	98.93	-89.48	20.15	36.42	-110.55	122.51	-47.98
LXIV	22.47	mm	-53.37	111.89	-94.72	28.71	30.92	-121.90	113.84	-11.78
LXV	22.57	saddle	72.40	-116.63	62.53	1.75	24.40	-117.96	101.38	-47.45
LXVI	22.57	saddle	72.41	-116.63	63.14	0.79	25.15	-118.15	101.40	-47.62
LXVII	23.60	mm	67.65	-109.00	78.96	-9.33	17.58	-104.46	113.86	-59.60
LXVIII	24.34	saddle	72.61	44.46	-93.15	18.00	-1.20	83.53	-71.95	-55.92
LXIX	24.43	saddle	132.00	-39.54	-42.63	94.54	-93.42	86.16	-40.51	-73.63
LXX	24.73	mm	67.02	53.63	-83.43	6.91	-6.78	91.14	-62.29	-65.25
LXXI (BC)	25.04	min	-43.34	98.42	-44.64	-60.15	46.36	79.72	-102.47	28.81
LXXII	25.04	saddle	120.17	-25.20	-56.25	93.97	-90.89	91.11	-43.69	-70.82
LXXIII	25.19	saddle	136.34	-59.96	44.23	-89.09	98.01	-13.17	-11.94	-79.20
LXXIV (BC)	25.37	min	-67.77	-48.95	53.44	50.73	-117.09	70.09	-46.17	95.52
LXXV	25.57	min	-80.60	-6.33	90.51	-44.50	-67.11	108.14	-54.95	63.27
LXXVI	26.30	saddle	-24.50	-79.14	60.77	0.25	36.59	-127.90	58.48	47.23
LXXVII	27.32	saddle	-44.80	104.71	-30.55	-58.66	23.18	100.41	-86.94	11.80
LXXVIII	28.24	min	-89.76	53.14	50.99	-82.53	-10.93	100.15	-70.71	49.28
LXXIX	28.72	saddle	-88.48	35.74	64.45	-68.59	-34.50	108.30	-66.40	53.46
LXXX	29.21	min	-52.24	110.38	-80.53	44.01	-71.70	137.98	-81.58	20.25
LXXXI	29.28	saddle	-42.52	108.59	-79.12	41.03	-70.60	139.51	-76.64	9.40
LXXXII	29.80	saddle	-49.30	99.31	-49.00	8.75	9.04	-72.34	123.42	-46.08
LXXXIII	30.89	mm	125.00	-27.38	-4.57	-60.65	99.76	-5.65	-28.56	-65.38
LXXXIV (C)	31.15	min	-86.66	36.21	52.76	-113.05	39.00	66.50	-86.06	74.97
LXXXV	31.27	saddle	-88.38	42.71	50.81	-106.54	29.08	74.31	-83.80	68.69
LXXXVI (C)	33.80		-68.63	-3.55	81.19	-108.17	33.09	64.50	-93.79	86.89

Dioxazaphosphacinium in water										
Conformation	δE	Stat. point	1,2,3,4	2,3,4,5	3,4,5,6	4,5,6,7	5,6,7,8	6,7,8,1	7,8,1,2	8,1,2,3
2*e*,6,6-trimethyl-2*a*-oxo-6*N*-1,3-di*O*-2*P*-BB	0.00	unconv.	59.61	57.65	-51.63	-56.70	53.04	60.21	-52.82	-65.21
4,4,8*e*-trimethyl-8*a*-oxo-4*N*-1,7-di*O*-8*P*-BB	0.00	min	-60.21	-53.04	56.70	51.63	-57.65	-59.61	65.21	52.82
2,2,6*e*-trimethyl-6*a*-oxo-2*N*-5,7-di*O*-6*P*-BC'	2.52	min	70.07	-108.55	48.23	59.62	-57.80	-60.55	105.62	-60.07
2,2,6*e*-trimethyl-6*a*-oxo-2*N*-5,7-di*O*-6*P*-BC	2.52	min	60.57	57.78	-59.62	-48.22	108.56	-70.07	60.05	-105.62
2*e*,6,6-trimethyl-2*a*-oxo-6*N*-1,3-di*O*-2*P*-BC	3.52	min	63.63	56.71	-99.76	62.15	-73.51	109.45	-38.51	-76.05
2*e*,6,6-trimethyl-2*a*-oxo-6*N*-1,3-di*O*-2*P*-BC'	3.52	min	-109.44	73.54	-62.18	99.76	-56.69	-63.64	76.06	38.50
2*a*,6,6-trimethyl-2*e*-oxo-6*N*-1,3-di*O*-2*P*-BC'	4.75	min	-60.55	-54.69	102.40	-61.96	67.08	-115.62	54.82	61.85
2*a*,6,6-trimethyl-2*e*-oxo-6*N*-1,3-di*O*-2*P*-BC	4.75	min	115.62	-67.08	61.96	-102.40	54.69	60.55	-61.85	-54.83
2,2,6*a*-trimethyl-6*e*-oxo-2*N*-5,7-di*O*-6*P*-BC	7.04	min	-66.70	113.42	-43.76	-58.93	47.90	71.95	-96.94	44.24
2,2,6*a*-trimethyl-6*e*-oxo-2*N*-5,7-di*O*-6*P*-BC'	7.05	min	-71.96	-47.88	58.93	43.75	-113.43	66.70	-44.24	96.94
1,1,5*b*-trimethyl-5*f*-oxo-1*N*-4,6-di*O*-5*P*-TBC'	8.12	min	95.72	-82.78	91.76	-47.05	-51.98	118.73	-38.87	-64.55
1,1,5*b*-trimethyl-5*f*-oxo-1*N*-4,6-di*O*-5*P*-TBC	8.13	min	-118.73	51.98	47.05	-91.76	82.78	-95.72	64.54	38.88
2*e*,6,6-trimethyl-2*a*-oxo-6*N*-1,3-di*O*-2*P*-TBC	8.33	min	55.38	50.09	-112.28	41.56	48.56	-100.29	90.25	-90.55
2*e*,6,6-trimethyl-2*a*-oxo-6*N*-1,3-di*O*-2*P*-TBC'	8.33	min	100.28	-48.55	-41.57	112.28	-50.10	-55.38	90.55	-90.25
1*e*,5,5-trimethyl-1*a*-oxo-5*N*-2,8-di*O*-1*P*-	8.34	min	91.71	-84.48	86.62	-86.26	84.09	-92.08	89.38	-88.98

CC										
1*e*,5,5-trimethyl-1*a*-oxo-5*N*-2,8-di*O*-1*P*-TCC	8.64	min	126.65	-77.31	52.04	-83.15	118.83	-81.78	49.52	-86.87
4*e*,8,8-trimethyl-4*a*-oxo-8*N*-3,5-di*O*-4*P*-TCC'	8.64	min	81.79	-118.83	83.15	-52.05	77.31	-126.65	86.87	-49.52
1*b*,5,5-trimethyl-1*f*-oxo-5*N*-2,8-di*O*-1*P*-TBC'	8.70	min	-59.84	124.95	-51.12	-41.32	90.34	-107.28	91.83	-25.42
1*b*,5,5-trimethyl-1*f*-oxo-5*N*-2,8-di*O*-1*P*-TBC	8.70	min	107.29	-90.34	41.31	51.13	-124.95	59.85	25.41	-91.82
1,1,5*f*-trimethyl-5*b*-oxo-1*N*-4,6-di*O*-5*P*-TBC'	8.82	min	128.63	-48.08	-43.19	93.08	-92.35	89.90	-44.43	-59.60
1,1,5*f*-trimethyl-5*b*-oxo-1*N*-4,6-di*O*-5*P*-TBC	8.82	min	-89.90	92.35	-93.08	43.19	48.08	-128.63	59.60	44.43
1*b*,5,5-trimethyl-1*f*-oxo-5*N*-2,8-di*O*-1*P*-TCC	8.97	saddle	115.58	-77.05	64.15	-89.72	107.65	-83.59	64.03	-94.09
1*b*,5,5-trimethyl-1*f*-oxo-5*N*-2,8-di*O*-1*P*-TCC'	8.97	saddle	83.60	-107.63	89.73	-64.16	77.05	-115.56	94.09	-64.05
2*e*,6,6-trimethyl-2*a*-oxo-6*N*-1,3-di*O*-2*P*-TBC	9.42	saddle	62.35	51.74	-96.09	11.60	74.63	-94.53	77.92	-97.97
1*f*,5,5-trimethyl-1*b*-oxo-5*N*-2,8-di*O*-1*P*-TCC	9.77	min	-77.15	122.22	-80.72	48.66	-78.67	127.65	-77.04	38.02
1*f*,5,5-trimethyl-1*b*-oxo-5*N*-2,8-di*O*-1*P*-TCC'	9.77	min	-127.65	78.67	-48.66	80.72	-122.22	77.15	-38.01	77.03
BC	10.17	saddle	75.11	53.37	-63.13	-46.68	90.65	-13.25	0.14	-87.90
BC	10.17	saddle	13.25	-90.65	46.68	63.13	-53.38	-75.10	87.90	-0.14
3*e*,7,7-trimethyl-3*a*-oxo-7*N*-2,4-di*O*-3*P*-TC	10.43	min	40.57	44.84	-99.47	99.47	-44.86	-40.53	101.90	-101.93
1,1,5*a*-trimethyl-5*e*-oxo-1*N*-4,6-di*O*-5*P*-BC	10.86	min	108.13	-43.35	-59.46	59.44	43.38	-108.13	69.28	-69.29
XXXI (TBC)	11.08	saddle	88.68	-100.32	54.80	48.47	-99.59	13.43	64.85	-87.21
XXXII (crown)	11.20	saddle	-104.32	103.00	-67.67	67.64	-102.97	104.36	-60.22	60.19
XXXIII	11.30	saddle	107.41	-6.91	-70.35	87.87	-86.51	97.79	-43.68	-71.34

XXXIV (TBC)	11.30	saddle	-97.79	86.53	-87.88	70.35	6.91	-107.41	71.36	43.66
XXXV	11.33	saddle	106.16	-67.84	81.75	-80.44	-5.36	94.30	-45.61	-72.11
XXXVI	11.33	saddle	-94.28	5.36	80.46	-81.74	67.81	-106.16	72.15	45.57
XXXVII	11.51	min	-111.79	96.21	-38.58	-50.93	125.14	-78.96	-0.67	74.87
XXXVIII (C)	11.52	min	78.96	-125.13	50.91	38.60	-96.20	111.78	-74.88	0.69
XXXIX	11.56	saddle	108.92	-62.77	-45.55	82.97	4.77	-94.62	78.64	-67.26
XL	11.71	saddle	40.82	52.30	-111.78	79.27	-7.44	-70.80	106.32	-94.90
XLI	11.86	saddle	97.19	-118.77	47.24	38.01	-102.60	113.33	-57.86	-23.34
XLII	11.87	saddle	-113.33	102.59	-38.01	-47.25	118.78	-97.17	23.32	57.88
XLIII	11.90	saddle	-75.79	-50.58	63.98	44.45	-95.14	15.89	4.07	80.99
XLIV (BC)	12.00	min	-41.12	100.64	-62.71	62.71	-100.64	41.12	58.81	-58.81
XLV (BC)	12.20	min	-105.89	46.61	57.78	-57.90	-46.42	105.91	-59.14	59.06
XLVI	12.41	saddle	-10.49	86.96	-67.58	64.89	-107.17	58.66	45.51	-77.69
XLVII	12.44	min	-65.32	-38.52	104.99	-37.84	-59.62	101.11	-74.27	82.98
XLVIII (TBC)	12.44	min	-101.10	59.65	37.80	-104.98	38.55	65.31	-83.00	74.27
XLIX	12.58	saddle	-89.55	115.70	-73.60	0.35	73.29	-131.12	74.32	22.37
L	12.58	saddle	131.10	-73.41	-0.26	73.50	-115.66	89.67	-22.50	-74.17
LI	13.01	saddle	-72.22	-40.77	92.70	-14.39	-79.80	92.80	-62.68	89.61
LII	13.01	saddle	-92.80	79.80	14.39	-92.70	40.77	72.22	-89.61	62.68
LIII	13.05	saddle	91.54	-80.40	79.06	-9.35	-91.95	78.53	20.81	-95.16
LIV	13.52	saddle	-88.45	-5.32	87.90	-40.33	-69.00	104.55	-58.06	73.47
LV	13.62	saddle	-124.10	85.20	-4.22	-66.34	107.52	-103.72	44.63	49.91
LVI	14.10	saddle	80.61	2.59	23.57	-98.56	40.87	66.48	-38.40	-83.49
LVII	14.10	saddle	-66.48	-40.88	98.55	-23.56	-2.58	-80.63	83.47	38.43
LVIII	14.89	saddle	49.03	71.68	-66.69	-5.48	-23.09	102.15	-39.44	-74.57
LIX	14.89	saddle	-102.17	23.12	5.48	66.67	-71.70	-49.00	74.56	39.43
LX	15.34		69.68	51.70	-91.24	14.03	-3.15	83.75	-62.32	-60.99
LXI	15.34	saddle	-83.80	3.19	-13.89	91.13	-51.81	-69.64	61.14	62.17
LXII	15.41	saddle	-16.90	106.58	-79.45	38.45	-74.10	133.72	-51.15	-22.40

LXIII	15.41	saddle	−133.71	74.10	−38.43	79.44	−106.59	16.91	22.42	51.13
LXIV	15.46	saddle	15.85	−102.96	83.12	−41.91	72.26	−136.86	61.24	16.63
LXV	15.46	saddle	136.86	−72.27	41.90	−83.11	102.96	−15.85	−16.64	−61.22
LXVI	15.78	saddle	66.86	−124.91	47.67	12.85	27.66	−123.55	78.60	−22.81
LXVII	15.78		123.57	−27.64	−12.93	−47.60	124.89	−66.80	22.73	−78.54
LXVIII	16.24	mm	−8.50	82.21	−81.81	81.81	−82.22	8.50	79.92	−79.91
LXIX	16.51	saddle	−122.85	30.06	14.23	45.33	−124.37	60.67	−12.40	68.78
LXX	16.58	saddle	8.63	−79.52	111.40	−66.14	57.13	−121.73	101.38	−10.86
LXXI	16.58	saddle	121.73	−57.13	66.14	−111.40	79.52	−8.63	10.86	−101.38
LXXII	17.20	mm	84.20	−3.92	−83.78	83.78	3.92	−84.20	92.68	−92.68
LXXIII	18.46	saddle	13.09	−98.77	50.61	54.23	−106.07	84.94	−71.93	55.47
LXXIV	18.53		120.28	−62.24	−6.71	93.24	−100.93	15.13	46.64	−107.17
LXXV	18.53	mm	−15.65	101.08	−93.61	7.41	61.62	−120.52	107.33	−46.07
LXXVI	18.64	saddle	74.57	2.02	19.98	−99.44	96.56	−54.04	67.23	−121.19
LXXVII	18.64	saddle	54.04	−96.56	99.44	−19.99	−2.01	−74.58	121.19	−67.23
LXXVIII (BC)	19.18	min	48.59	−104.72	63.20	−58.83	104.43	−64.06	−29.98	39.62
LXXIX	19.72	mm	0.47	−97.91	53.92	9.18	33.12	−124.35	51.83	36.02
LXXX	19.83	saddle	−63.09	−21.48	94.22	−94.21	21.46	63.10	−94.64	94.63
LXXXI	20.21	saddle	15.98	−87.85	112.04	−40.86	−40.20	125.32	−100.94	30.25
LXXXII	20.21	saddle	−125.32	40.20	40.86	−112.04	87.85	−15.98	−30.25	100.94
LXXXIII	20.43	mm	94.29	−8.37	7.90	−82.79	114.21	−69.65	60.17	−112.04
LXXXIV	20.43	mm	69.65	−114.21	82.79	−7.89	8.37	−94.30	112.04	−60.17
LXXXV	21.32	saddle	−79.18	−15.78	83.39	−106.62	65.62	8.21	−63.48	110.98
LXXXVI	23.53	mm	8.64	−91.70	86.26	3.10	−78.30	119.22	−90.75	43.66
LXXXVII	27.79	mm	−11.68	82.45	−101.11	22.87	−3.54	90.72	−110.07	21.27
LXXXVIII	27.79	mm	−90.72	3.54	−22.88	101.12	−82.44	11.68	−21.27	110.07
LXXXIX	33.56	saddle	168.62	31.47	−67.32	95.63	−97.02	61.04	−22.56	−

										176.78
XC	33.90	mm	0.69	3.54	57.84	-95.73	81.28	-92.39	102.95	-56.80
XCI	34.39		59.89	-97.29	95.61	-67.21	31.04	166.31	-176.13	-20.27
XCII	34.39	saddle	-166.34	-31.01	67.21	-95.64	97.26	-59.88	20.29	176.10
XCIII	35.08		-5.61	-9.49	-27.86	99.35	-56.17	-74.62	103.12	-17.84

cis-Methyldioxazaphosphacinium										
Conformation	δE	Stat. point	1,2,3,4	2,3,4,5	3,4,5,6	4,5,6,7	5,6,7,8	6,7,8,1	7,8,1,2	8,1,2,3
2*e*,4*a*,6,6-tetramethyl-2*a*-oxo-6*N*-1,3-di*O*-2*P*-TB'	0.00	unconv.	56.50	57.22	-41.00	-64.80	48.14	65.74	-49.27	-69.28
2,2,4*e*,6*e*-tetramethyl-6*a*-oxo-2*N*-5,7-di*O*-6*P*-BC'	0.19	min	70.00	-108.52	48.90	59.40	-57.68	-60.34	105.52	-60.51
4,4,6*e*,8*e*-tetramethyl-8*a*-oxo-4*N*-1,7-di*O*-8*P*-BB	1.71	min	-48.47	-60.34	52.76	57.37	-55.92	-64.28	66.70	48.22
2*a*,4*e*,6,6-tetramethyl-2*a*-oxo-6*N*-1,3-di*O*-2*P*-BC	2.84	min	114.92	-66.18	62.50	-103.12	54.48	60.60	-61.78	-55.62
2,2,6*e*,8*a*-tetramethyl-6*a*-oxo-2*N*-5,7-di*O*-6*P*-BC	3.25	min	61.95	53.89	-54.57	-51.62	109.78	-71.23	61.57	-106.37
2*e*,6,6,8*e*-tetramethyl-2*a*-oxo-6*N*-1,3-di*O*-2*P*-BC	3.98	min	68.87	49.04	-97.62	65.50	-75.24	110.00	-41.50	-74.94
2*e*,4*b*,6,6-tetramethyl-2*a*-oxo-6*N*-1,3-di*O*-2*P*-TBC'	6.16	min	99.80	-46.75	-42.62	113.12	-50.41	-54.78	90.44	-91.40
1,1,3*e*,5*e*-tetramethyl-5*a*-oxo-1*N*-4,6-di*O*-5*P*-TBC'	6.23	min	95.63	-81.20	92.28	-47.93	-51.90	117.46	-37.38	-66.86
4,4,6*e*,8*e*-tetramethyl-8*a*-oxo-4*N*-1,7-di*O*-8*P*-CC	6.32	min	100.55	-73.22	77.70	-96.22	93.27	-81.28	78.51	-100.14
4*e*,6*e*,8,8-tetramethyl-4*a*-oxo-8*N*-3,5-di*O*-4*P*-TCC'	6.56	min	81.14	-119.26	83.80	-51.56	76.82	-126.80	86.70	-49.22
1*b*,3*e*,5,5-tetramethyl-1*f*-oxo-5*N*-2,8-di*O*-1*P*-TBC	6.64	min	106.99	-89.91	42.09	50.96	-124.64	59.20	25.90	-92.82
1*e*,3*e*,5,5-tetramethyl-1*a*-oxo-5*N*-2,8-di*O*-1*P*-TCC	6.88	min	125.23	-76.95	53.66	-84.10	118.08	-82.39	50.97	-88.05
2*a*,6,6,8*a*-tetramethyl-2*a*-oxo-6*N*-1,3-di*O*-2*P*-BC'	7.03	min	-51.60	-58.53	104.10	-62.81	66.56	-118.53	61.51	52.61
1,1,5*f*,7*e*-tetramethyl-5*b*-oxo-1*N*-4,6-di*O*-5*P*-TBC'	7.17	min	127.02	-46.93	-44.29	93.78	-91.88	90.06	-45.68	-58.80
BC	8.35	saddle	12.10	-90.50	46.35	63.72	-52.32	-75.89	86.59	2.05
2*e*,6,6,8*e*-tetramethyl-2*a*-oxo-6*N*-1,3-di*O*-2*P*-TBC	8.49	min	65.01	36.80	-107.01	44.79	50.27	-103.82	86.33	-88.87
(*R*)-1*i*,3*e*,7,7-tetramethyl-3*a*-oxo-7*N*-2,4-di*O*-3*P*-TC	8.90	min	51.07	33.74	-94.72	102.69	-46.79	-39.68	99.92	-106.38
1,1,3*e*,5*b*-tetramethyl-5*f*-oxo-1*N*-4,6-di*O*-5*P*-BC	8.95	min	107.76	-43.36	-59.32	60.53	42.17	-107.84	69.63	-69.63
2*e*,4*a*,6,6-tetramethyl-2*a*-oxo-6*N*-1,3-di*O*-2*P*-BC'	9.05	min	-94.60	71.60	-62.64	98.98	-57.32	-65.36	86.75	24.59
XX	9.31	min	78.27	-124.76	51.49	38.60	-95.94	111.63	-75.17	0.71
1,1,3*e*,5*e*-tetramethyl-5*a*-oxo-1*N*-4,6-di*O*-5*P*-TBC'	9.33	saddle	105.66	-65.81	81.74	-81.40	-5.43	93.60	-44.44	-74.18
2,2,6*a*,8*e*-tetramethyl-6*e*-oxo-2*N*-5,7-di*O*-6*P*-BC'	9.40	min	-61.60	-53.98	57.12	47.59	-115.73	70.06	-47.82	92.50
TBC	11.01	saddle	89.01	36.00	-60.36	-40.57	99.16	-21.98	-4.95	-81.25

TB•C	11.46	saddle	62.82	57.41	-43.83	-65.58	80.15	-5.95	14.72	-101.13
B•C	11.63	mm	72.07	53.32	-53.86	-55.61	87.26	-9.72	4.91	-93.31
XXVI	12.10	saddle	80.01	3.08	25.04	-99.75	39.40	66.12	-36.44	-85.98
XXVII	13.48	saddle	66.72	-124.55	48.35	12.46	27.85	-123.47	78.86	-23.31
2,2,4*a*,6*a*-tetramethyl-6*e*-oxo-2*N*-5,7-di*O*-6*P*-BC	13.59	min	-52.29	102.10	-43.92	-59.24	48.97	73.35	-100.06	37.46
XXIX	13.93	saddle	135.48	-72.43	42.57	-83.51	103.61	-16.33	-17.23	-60.23
XXX	14.03	saddle	11.54	-101.31	83.46	-41.42	72.31	-136.04	58.70	20.79
XXXI	14.10	saddle	107.58	-42.51	-59.39	59.86	42.51	-107.70	69.18	-69.60
XXXII	14.17		122.75	-27.32	-11.84	-48.96	125.51	-67.57	23.69	-79.52
XXXIII (C)	14.21	min	-100.62	42.82	55.02	-92.72	77.54	-98.07	76.85	25.70
XXXIV (TBC)	14.22	min	-49.41	-49.66	110.73	-41.38	-52.98	104.77	-81.52	75.71
XXXV	14.42	saddle	119.22	-54.81	66.90	-113.16	77.40	-6.97	11.59	-103.26
XXXVI	14.83	saddle	-90.36	14.97	75.59	-87.05	69.04	-104.03	79.50	32.89
XXXVII	15.10	saddle	5.80	-76.71	113.33	-67.17	55.66	-119.70	102.62	-10.80
XXXVIII (C)	15.32	min	-78.29	84.41	-93.29	45.05	46.70	-130.94	62.98	38.46
XXXIX	15.34	mm	12.17	-87.43	104.29	-60.78	63.32	-129.68	92.44	-4.20
XL	15.86	saddle	-65.44	-57.71	61.64	49.73	-95.46	14.11	3.84	77.19
XLI	16.05	saddle	74.30	39.97	-94.31	22.18	-1.21	80.92	-72.71	-51.12
XLII	16.54	saddle	75.30	1.52	20.77	-100.07	96.30	-53.66	66.81	-122.13
XLIII	16.55	mm	120.17	-60.72	-7.30	93.65	-101.45	15.93	45.95	-108.28
XLIV	17.17	mm	64.16	57.56	-76.49	1.65	-11.45	93.76	-52.64	-69.96
XLV	17.45	min	68.18	-104.70	59.14	-64.68	102.61	-41.37	-44.23	27.13
XLVI	17.52	saddle	-82.52	86.45	-90.57	66.66	7.88	-112.98	82.90	29.27
XLVII	17.84	saddle	-31.99	-79.49	65.28	5.52	24.44	-113.20	52.82	54.58
XLVIII	18.20	mm	123.95	-33.75	-7.73	-55.11	98.64	-1.14	-35.82	-51.88
XLIX (TCC)	18.20	min	-64.19	111.09	-79.33	48.76	-79.02	132.04	-79.12	31.69
L	18.34	mm	69.49	-113.73	83.83	-8.40	8.17	-93.43	112.18	-61.18
LI	18.64	mm	-13.33	81.29	-76.01	78.14	-80.81	4.10	84.67	-75.64
LII	19.31	min	-99.38	89.00	-37.62	-52.60	128.77	-78.10	-1.40	69.90
LIII	19.32	saddle	-54.44	-39.24	104.49	-40.12	-61.44	109.31	-72.38	68.06

LIV	19.41	saddle	-87.41	15.29	-3.17	79.02	-67.00	-58.79	78.84	37.79
LV (TCC)	19.99	min	-60.88	99.08	-93.94	64.88	-73.56	120.60	-95.30	46.38
LVI (C)	20.19	min	-87.39	41.02	48.16	-111.20	42.59	63.15	-85.55	74.39
LVII	20.25	saddle	-27.74	104.39	-77.11	39.29	-74.04	138.63	-64.50	-5.98
LVIII	20.44	mm	135.01	-73.93	38.19	-77.57	99.51	-7.64	-27.97	-51.33
LIX	20.50	saddle	-102.74	84.14	-0.07	-67.16	96.03	-109.37	69.34	23.17
LX (C)	20.98	min	-91.57	57.01	47.91	-81.58	-8.97	98.46	-71.30	50.17
LXI	20.99	mm	-35.41	94.63	-109.01	55.74	15.20	-117.92	110.75	-19.44
LXII	22.50	saddle	-76.42	86.17	13.57	-75.11	9.46	100.71	-79.03	32.55
LXIII	25.79	mm	-79.43	12.26	77.99	-84.97	-6.63	90.99	-83.97	73.03
LXIV	26.37	saddle	-82.16	101.13	-48.39	-54.47	96.23	-10.24	-52.91	67.98
LXV	30.35	saddle	-49.64	98.83	-88.10	14.55	-8.22	95.54	-116.32	49.72
LXVI	30.76	mm	-55.40	106.36	-80.41	9.76	-14.47	104.52	-109.21	44.73
LXVII	32.56	saddle	60.09	-97.67	96.20	-67.08	31.02	166.41	-176.31	-20.79
LXVIII	34.76		131.08	-41.84	-58.38	64.77	2.66	-0.94	-15.43	-55.92

trans-Methyldioxazaphosphacinium in water											
Conformation	Energy	δE	Stat.point	1,2,3,4	2,3,4,5	3,4,5,6	4,5,6,7	5,6,7,8	6,7,8,1	7,8,1,2	8,1,2,3
4,4,6*a*,8*e*-tetramethyl-8*a*-oxo-4*N*-1,7-di*O*-8*P*-BB	−469.13	0.00	unconv.	-61.868	-48.662	52.191	54.573	-57.97	-61.02	67.324	52.048
2,2,6*a*,8*e*-tetramethyl-6*e*-oxo-2*N*-5,7-di*O*-6*P*-BB	−467.09	0.49	min	51.477	62.707	-48.406	-60.949	51.354	63.698	-53.323	-62.536
2*e*,4*e*,6,6-tetramethyl-2*a*-oxo-6*N*-1,3-di*O*-2*P*-BC'	−465.42	0.89	min	−109.356	72.94	-62.434	100.139	-56.85	-63.336	75.993	39.151
2,2,6*e*,8*e*-tetramethyl-6*a*-oxo-2*N*-5,7-di*O*-6*P*-BC	−456.66	2.98	min	52.35	62.702	-57.592	-51.635	109.061	-71.982	63.843	-103.17
2,2,4*e*,6*a*-tetramethyl-6*e*-oxo-2*N*-4,6-di*O*-5*P*-BC	−450.89	4.36	min	-66.556	113.386	-44.535	-58.563	47.604	71.836	-96.878	44.594
2*a*,6,6,8*e*-tetramethyl-2*e*-oxo-6*N*-1,3-di*O*-2*P*-BC'	−449.52	4.69	min	-64.534	-47.268	100.971	-65.109	67.75	−116.391	59.513	59.025
2*e*,6,6,8*a*-tetramethyl-2*a*-oxo-6*N*-1,3-di*O*-2*P*-BC	−449.02	4.81	min	57.806	59.934	−100.555	62.157	-73.701	112.552	-42.755	-70.064
1,1,5*e*,7*e*-tetramethyl-5*a*-oxo-1*N*-4,6-di*O*-5*P*-TBC	−446.22	5.48	min	−117.517	51.329	47.671	-92.254	82.233	-95.568	65.641	38.116
1*b*,5,5,7*e*-tetramethyl-1*a*-oxo-5*N*-2,8-di*O*-1*P*-TBC'	−445.06	5.75	min	-59.389	124.42	-51.344	-41.416	90.164	−107.148	91.979	-25.486
2,2,6*e*,8*e*-tetramethyl-6*a*-oxo-2*N*-5,7-di*O*-6*P*-TBC	−442.85	6.28	min	54.296	55.394	-85.917	78.151	-99.534	68.943	20.303	−109.444
2,2,6*e*,8*e*-tetramethyl-6*a*-oxo-2*N*-5,7-di*O*-6*P*-TBC	−442.59	6.34	saddle	55.158	59.757	-90.037	71.432	-94.067	83.039	4.288	−100.729
1,1,3*e*,5*a*-tetramethyl-5*e*-oxo-1*N*-4,6-di*O*-5*P*-TBC	−441.52	6.60	min	-89.927	91.88	-93.804	43.687	47.689	−128.237	59.628	45.346
XIII	−439.03	7.19	min	-76.696	122.245	-81.34	48.521	-78.308	127.477	-76.971	38.067
2,2,6*a*,8*a*-tetramethyl-6*e*-oxo-2*N*-5,7-di*O*-6*P*-BC'	−438.97	7.21	min	-75.4	-42.33	54.604	45.688	−115.181	68.702	-45.008	97.51
2,2,4*a*,6*e*-tetramethyl-6*a*-oxo-2*N*-5,7-di*O*-6*P*-BC'	−438.35	7.36	min	60.341	-98.708	48.467	58.517	-57.625	-60.696	109.254	-58.174
XIV	−438.12	7.41	min	−126.706	78.614	-49.61	81.125	-122.19	77.643	-38.299	77.156
XV	−437.77	7.50	saddle	51.061	63.169	-55.567	-53.542	109.845	-71.667	64.337	−102.838
XVI	−435.70	7.99	saddle	-59.45	124.45	-51.353	-41.389	90.154	−107.203	91.983	-25.419
XVII	−433.29	8.57	min	46.51	56.134	−115.232	44.149	44.547	−102.249	94.144	-85.624
XVIII	−432.33	8.80	saddle	-8.714	96.945	-49.213	-55.4	101.146	-87.118	85.884	-68.06
XIX	−432.05	8.86	saddle	−104.757	102.765	-68.171	67.836	−102.924	103.659	-59.661	61.021
XX	−431.65	8.96	saddle	-97.949	85.934	-88.39	70.407	7.39	−107.291	70.865	44.878
XXI	−431.39	9.02	min	28.21	53.61	−101.576	97.688	-42.481	-45.851	107.281	-93.883
XXII	−431.16	9.08	min	−111.931	96.057	-39.294	-50.773	124.815	-79.099	-0.141	75.41
XXIII	−430.08	9.33	saddle	−113.246	101.86	-38.9	-47.462	119.364	-95.29	21.069	60.226
XXIV	−429.90	9.38	min	-45.948	102.536	-63.095	63.295	-97.885	35.146	62.637	-55.325
XXV	−	9.71	min	−	47.827	56.852	-59.725	-44.007	105.152	-59.634	59.331

	428.51			106.059							
XXVI	−428.33	9.75	saddle	−13.936	94.402	−44.662	−64.211	49.834	76.072	−79.859	−6.335
XXVII	−427.34	9.99	min	−101.32	57.827	39.079	−105.786	38.358	64.714	−82.513	75.654
XXVIII	−427.21	10.02	min	106.86	−60.198	59.164	−103.189	55.575	62.28	−65.725	−51.17
XXIX	−427.09	10.05	saddle	−88.756	115.79	−75.614	2.238	71.451	−131.029	75.311	22.253
XXX	−426.62	10.16	saddle	47.674	46.22	−94.373	99.571	−71.004	−2.083	76.207	−113.3
XXXI	−425.47	10.43	saddle	54.139	57.999	−95.528	7.968	75.944	−96.896	80.887	−94.581
XXXII	−425.39	10.45	saddle	−63.533	−52.377	54.163	50.709	−114.067	70.042	−51.727	97.819
XXXIII	−424.68	10.62	saddle	−79.317	91.084	9.773	−79.461	80.106	−91.461	94.768	−19.295
XXXIV	−424.45	10.68		−64.18	−48.18	98.507	−63.582	69.316	−117.227	57.642	59.943
XXXV	−424.35	10.70	saddle	34.559	57.965	−114.319	75.695	−2.283	−76.547	108.098	−89.76
XXXVI	−423.72	10.85	saddle	−92.321	80.099	12.935	−92.189	40.662	72.289	−89.793	63.133
XXXVII	−422.91	11.05	mm	−8.7	96.92	−49.186	−55.412	101.158	−87.143	85.886	−68.06
XXXVIII	−421.92	11.28	saddle	−123.386	84.617	−3.89	−67.003	106.715	−103.68	46.171	49.278
XXXIX	−421.14	11.47	saddle	−116.337	48.934	49.53	−90.028	80.129	−96.252	66.743	37.598
XL	−420.99	11.51	saddle	12.966	−83.016	49.209	60.731	−58.264	−69.74	97.808	−11.814
XLI	−419.80	11.79	saddle	−125.219	83.846	−52.701	78.136	−119.843	81.996	−40.866	74.858
XLII	−418.85	12.02	saddle	54.856	65.625	−47.983	−64.395	79.374	−4.511	13.658	−96.888
XLIII	−417.60	12.32	saddle	−89.123	−32.507	59.766	38.877	−102.974	25	7.505	75.009
XLIV	−417.42	12.36	saddle	69.138	57.317	−61.68	−49.822	92.205	−13.835	0.639	−85.269
XLV	−417.06	12.45	saddle	−102.543	23.281	5.344	66.657	−72.037	−48.333	74.386	39.835
XLVI	−416.35	12.61	saddle	−81.027	−30.245	86.633	−13.674	−84.105	93.533	−57.347	88.199
XLVII	−415.89	12.72		−78.81	121.506	−79.285	49.184	−80.759	126.915	−75.686	39.136
XLVIII	−414.83	12.98	saddle	−131.797	74.442	−39.038	79.594	−107.604	17.9	23.163	49.382
XLIX	−414.57	13.04	min	84.307	−22.551	−57.955	117.875	−53.517	−51.069	93.529	−94.626
L	−414.01	13.17	min	86.431	−74.521	90.99	−48.713	−51.725	120.305	−39.275	−62.018
LI	−413.91	13.20	saddle	−84.366	3.255	−12.96	90.712	−52.679	−69.023	62.234	61.885
LII	−413.54	13.29	saddle	−69.584	−26.967	98.858	−30.38	−4.754	−75.237	92.975	27.669
LIII	−412.89	13.44	saddle	−12.553	105.167	−79.374	37.444	−73.938	132.092	−47.474	−27.507
	−								−		

LIV	412.31	13.58	min	70.308	-84.106	96.484	-78.991	71.803	100.512	102.971	-75.647
LV	-411.74	13.72	saddle	-60.857	124.195	-46.186	-13.683	-30.212	122.657	-69.226	13.191
LVI	-409.81	14.18	min	98.37	-82.583	39.255	52.042	-126.601	58.706	27.48	-90.394
LVII	-409.69	14.21	saddle	-122.502	30.95	12.417	46.904	-124.771	60.056	-11.542	68.328
LVIII	-409.25	14.31	min	117.571	-35.478	-52.984	93.914	-88.166	92.465	-50.608	-56.826
LIX	-406.68	14.93	saddle	105.372	-13.744	-68.838	91.266	-84.228	98.045	-52.95	-59.597
LX	-406.43	14.99	saddle	33.939	80.543	-60.979	-6.441	-31.768	110.185	-37.142	-67.848
LXI	-405.43	15.22	min	78.199	-103.911	81.696	-58.811	81.192	-123.564	90.288	-55.814
LXII	-404.25	15.51	saddle	84.839	-63.871	-15.727	97.417	-52.658	-62.425	100.712	-76.863
LXIII	-404.16	15.53	saddle	44.661	58.469	-116.222	45.986	41.203	-101.179	94.916	-84.733
LXIV	-401.97	16.05	min	114.977	-71.517	53.711	-85.066	117.557	-85.705	54.646	-86.052
LXV	-401.8	16.09	saddle	77.795	-1.53	33.197	-104.696	38.554	66.937	-37.156	-82.686
LXVI	-401.58	16.14	saddle	-105.22	54.718	42.436	-104.47	35.826	62.931	-78.922	78.752
LXVII	-400.57	16.39	saddle	65.559	46.289	-99.208	22.941	0.67	80.146	-76.549	-44.27
LXVIII	-398.92	16.78	mm	43.843	47.61	-92.626	96.914	-67.186	-8.587	81.931	-110.715
LXIX	-398.11	16.97	saddle	96.894	-57.903	78.823	-83.316	-3.553	94.536	-46.093	-70.808
LXX	-397.43	17.14	mm	58.789	62.067	-84.225	5.918	-8.29	91.568	-58.19	-62.488
LXXI	-395.57	17.58	saddle	95.877	-36.817	-62.864	73.267	24.266	-104.252	79.376	-69.495
LXXII	-395.32	17.64	saddle	10.731	-73.758	112.671	-68.625	54.404	-116.142	108.666	-21.038
LXXIII	-395.16	17.68	saddle	-124.719	38.954	41.643	-112.53	88.154	-16.462	-29.871	101.356
LXXIV	-393.26	18.13	saddle	80.758	-70.776	78.623	-12.416	-91.078	77.281	24.008	-93.651
LXXV	-392.69	18.27	mm	53.767	57.523	-95.059	9.365	75.331	-99.045	81.811	-92.898
LXXVI	-390.39	18.82	mm	-83.353	3.235	84.538	-84.35	-3.94	82.958	-87.1	88.304
LXXVII	-389.63	19.00	saddle	-81.95	-13.442	81.861	-107.351	66.688	7.352	-62.374	112.47
LXXVIII	-389.23	19.10	saddle	95.412	-99.307	67.169	0.606	-81.677	128.697	-54.264	-42.288
LXXIX	-388.14	19.36	mm	64.01	48.108	-90.184	6.491	81.415	-98.081	75.063	-94.76
LXXX	-387.44	19.52	saddle	122.725	-69.458	-2.449	69.55	-109.924	98.595	-34.382	-64.451
LXXXI	-386.96	19.64	saddle	25.417	-101.383	78.687	-40.563	72.085	-140.769	70.514	4.109
LXXXII	-386.73	19.69	saddle	73.582	-3.345	28.33	-103.791	97.112	-56.601	69.001	-118.412

LXXXIII	−385.88	19.90	mm	82.301	-9.082	-79.778	85.295	4.858	-89.561	91.213	-84.214
LXXXIV	−383.71	20.42	saddle	115.131	-32.437	-55.418	91.609	-86.024	93.98	-52.578	-55.114
LXXXV	−383.05	20.57	saddle	70.814	-67.566	89.483	-87.51	71.118	-85.459	102.258	-91.48
LXXXVI	−380.18	21.26	saddle	23.055	-96.65	48.939	49.58	−104.616	98.505	-77.73	43.517
LXXXVII	−379.84	21.34	saddle	132.473	-63.231	41.223	-85.708	105.317	-21.691	-10.112	-69.895
LXXXVIII	−379.54	21.41	mm	34.424	80.543	-61.916	-4.821	-33.391	111.093	-37.229	-67.638
LXXXIX	−379.38	21.45	mm	95.978	-84.175	66.94	3.939	-98.615	100.291	-8.169	-76.221
XC	−374.51	22.61	saddle	114.972	-26.728	-0.989	-61.403	129.885	-72.073	30.399	-82.574
XCI	−374.07	22.72	saddle	104.864	-40.426	62.835	−117.462	72.725	-2.86	14.76	−106.108
XCII	−373.60	22.83	saddle	26.007	-84.748	108.527	-42.463	-40.77	130.947	-94.896	15.626
XCIII	−366.79	24.46	mm	64.876	49.922	-95.041	18.087	-0.318	83.104	-73.137	-47.596
XCIV	−366.53	24.52	mm	−123.228	36.967	43.147	−112.531	89.195	-17.518	-29.232	100.553
XCV	−364.83	24.93	mm	107.388	-95.418	34.747	52.1	−123.334	95.661	-22.174	-58.092
XCVI	−359.74	26.14	mm	-9.936	80.828	−102.173	23.672	-3.488	90.139	−110.386	20.867
XCVII	−356.60	26.90	mm	61.136	−104.233	82.753	-10.748	11.097	-97.049	115.857	-58.429
XCVIII	−351.54	28.10	mm	−104.593	7.52	-7.778	86.091	-93.697	11.067	-2.246	95.314
XCIX	−338.33	31.26	saddle	-61.08	97.429	-96.185	67.186	-31.584	−168.753	177.311	22.883
C	−337.95	31.35	mm	-64.976	70.446	20.385	-21.418	-69.679	64.565	28.195	-27.778
CI	−335.22	32.01	mm	−127.087	50.461	56.086	-71.934	1.814	3.839	17.476	45.758
CII	−325.36	34.36	mm	-58.968	104.334	-17.398	-21.798	-13.531	-7.326	78.716	-51.856
CIII	−325.00	34.45	mm	-79.065	84.387	0.059	-12.749	-10.636	-46.926	103.871	-27.947

DiMephosphacinium in water										
Conformation	δE	Stat. point	1,2,3,4	2,3,4,5	3,4,5,6	4,5,6,7	5,6,7,8	6,7,8,1	7,8,1,2	8,1,2,3
4,4,6,6,8-pentamethyl-8*e*-oxo-4*N*-1,7-di*O*-8*P*-TB'	0.00	unconv.	51.17	59.78	-40.35	-66.69	48.39	67.46	-52.54	-64.79
4,4,6,6,8-pentamethyl-8*e*-oxo-4*N*-1,7-di*O*-8*P*-TB	1.47	min	-45.46	-59.84	43.20	65.00	-51.91	-70.07	65.42	50.49
2,2,6*e*,8,8-pentamethyl-6*a*-oxo-2*N*-5,7-di*O*-6*P*-BC	3.57	min	51.41	59.65	-50.23	-57.57	109.28	-72.35	66.69	-104.37
TB (Me rot.)	3.73	saddle	-58.82	-43.41	60.78	45.32	-64.89	-53.88	80.82	33.03
2,2,6*e*,8,8-pentamethyl-6*a*-oxo-2*N*-5,7-di*O*-6*P*-BC'	4.89	min	58.97	-97.45	50.44	57.23	-57.05	-60.14	110.02	-59.19
2*e*,6,6,8,8-pentamethyl-2*a*-oxo-6*N*-1,3-di*O*-2*P*-BC	5.68	min	64.12	50.45	-100.05	66.50	-73.61	113.12	-49.61	-66.48
TB (Me rot.)	5.81	saddle	52.42	60.15	-42.91	-63.42	47.35	68.11	-53.09	-64.40
2*e*,4,4,6,6-pentamethyl-2*a*-oxo-6*N*-1,3-di*O*-2*P*-BC'	6.35	min	-94.49	68.50	-62.39	100.07	-57.32	-65.10	85.30	27.75
2,2,6*e*,8,8-pentamethyl-6*a*-oxo-2*N*-5,7-di*O*-6*P*-TBC	7.09	min	54.98	48.54	-78.14	79.64	-103.66	61.17	29.92	-114.38
2*a*,6,6,8,8-pentamethyl-2*e*-oxo-6*N*-1,3-di*O*-2*P*-BC'	7.40	min	-55.60	-47.74	105.34	-67.60	63.35	-117.45	73.09	43.92
2*a*,4,4,6,6-pentamethyl-2*e*-oxo-6*N*-1,3-di*O*-2*P*-BC	7.49	min	106.47	-57.49	58.94	-103.93	55.28	61.96	-64.62	-54.03
1,1,3*e*,7,7-pentamethyl-3*a*-oxo-7*N*-2,4-di*O*-3*P*-TC	7.51	min	41.52	40.91	-97.29	100.96	-44.25	-44.39	104.68	-100.83
										-

XIII Me rot.	7.53	saddle	51.24	58.63	-47.17	-59.83	109.29	-71.33	67.22	105.60
XIV Me rot.	8.03	saddle	-96.50	67.69	-62.11	100.55	-57.00	-65.38	83.38	30.91
2,2,6*e*,8,8-pentamethyl-6*a*-oxo-2*N*-5,7-di*O*-6*P*-TBC	8.13	saddle	60.63	53.90	-87.24	70.69	-94.70	88.86	-3.67	-97.56
XV Me rot.	8.85	saddle	56.96	54.19	-49.25	-57.23	110.03	-73.33	66.17	-107.24
XVI Me rot.	9.08	saddle	67.45	45.62	-100.61	70.61	-74.16	111.98	-51.94	-65.31
XVII (BB?)	9.11	saddle	55.74	39.20	-89.50	99.87	-76.21	4.06	71.05	-118.03
2*e*,6,6,8,8-pentamethyl-2*a*-oxo-6*N*-1,3-di*O*-2*P*-TBC	9.19	min	49.48	49.47	-113.26	48.22	42.13	-105.60	94.42	-82.94
B  C	9.33	saddle	10.25	-80.72	50.23	60.27	-58.28	-69.22	98.62	-11.27
2,2,4,4,6*e*-pentamethyl-6*a*-oxo-2*N*-5,7-di*O*-6*P*-TBC'	10.11	saddle	-15.20	76.26	-93.71	90.08	-42.74	-60.49	122.17	-58.87
2,2,6*a*,8,8-pentamethyl-6*e*-oxo-2*N*-5,7-di*O*-6*P*-BC'	10.22	min	-60.56	-51.77	51.05	52.83	-117.43	72.07	-50.53	93.03
1,1,3,3,5*e*-pentamethyl-5*a*-oxo-1*N*-4,6-di*O*-5*P*-TBC'	11.01	min	85.14	-70.35	90.79	-50.33	-51.24	118.58	-36.90	-65.48
1,1,3,3,5*e*-pentamethyl-5*a*-oxo-1*N*-4,6-di*O*-5*P*-TBC	11.24	min	-100.55	39.31	56.75	-93.25	77.43	-97.49	75.45	28.90
1,1,5*a*,7,7-pentamethyl-5*e*-oxo-1*N*-4,6-di*O*-5*P*-TBC'	11.47	min	117.21	-32.26	-54.61	94.30	-87.99	91.92	-49.77	-59.67
XXV (BC)	11.52	min	-49.27	100.12	-46.54	-57.56	48.04	73.38	-101.18	37.31
XXVI (TCC or CR)	11.69	min	69.53	-80.29	95.92	-80.79	72.43	-98.58	102.53	-78.29
XXVII	11.70		64.14	50.53	-97.38	65.15	-74.94	113.67	-48.26	-67.17
XXVIII (C)	11.77	min	97.98	-80.70	39.89	51.64	-126.05	58.71	27.47	-92.46
XXIX (CC or C)	11.83	min	88.91	-58.49	74.22	-101.13	92.30	-77.95	80.63	-102.22
								-		

XXX	11.83	saddle	-90.67	14.11	75.77	-88.24	69.94	103.14	78.36	34.68
XXXI	12.05	saddle	105.52	-11.49	-69.81	92.06	-84.80	97.08	-51.68	-62.41
XXXII	12.09	saddle	61.07	50.32	-88.67	2.81	82.14	-98.16	76.75	-94.80
XXXIII	12.15	saddle	54.34	58.73	-34.47	-74.35	74.50	-2.08	18.65	103.43
XXXIV	12.39	saddle	53.54	48.91	-75.64	76.97	104.06	62.32	29.99	113.73
XXXV	12.56	saddle	-21.04	90.08	-46.80	-61.02	52.03	74.12	-93.19	11.06
XXXVI (TBC)	12.62	min	-45.42	112.11	-52.06	-39.55	84.35	109.52	99.99	-33.35
XXXVII	12.86	saddle	-50.70	-49.00	106.87	-68.62	62.87	118.81	77.54	38.76
XXXVIII	13.26	saddle	106.49	-58.21	60.15	102.67	50.56	66.24	-65.13	-55.20
XXXIX (TCC or CR)	13.35	min	76.38	103.44	83.46	-58.17	79.68	123.78	91.41	-56.24
XL	13.41		89.42	32.48	-58.67	-39.59	105.21	-28.99	-4.87	-76.64
XLI (C)	13.43	min	-76.74	81.11	-93.60	46.29	45.90	130.63	62.52	40.09
XLII	13.50	saddle	76.91	0.75	31.88	104.64	38.41	66.75	-37.35	-83.77
XLIII	13.56	saddle	77.77	-94.68	85.93	-67.55	81.17	114.93	93.71	-65.99
XLIV	13.65	saddle	-59.71	-30.36	101.95	-33.31	-3.08	-75.52	99.11	17.92
XLV (TCC or CR)	13.68	min	116.91	-67.28	52.51	-86.74	118.04	-82.15	52.16	-90.36
XLVI	13.76	saddle	81.86	-61.90	-13.78	95.67	-52.77	-61.90	102.52	-78.15
XLVII	13.88	saddle	80.50	-90.10	52.89	49.32	101.78	15.45	64.30	-86.91
XLVIII	13.96	mm	71.72	52.67	-55.14	-54.58	93.53	-14.22	1.33	-86.83
XLIX	14.48	saddle	95.50	-52.99	77.72	-84.73	-4.01	93.27	-43.31	-75.02
L	14.70	saddle	30.46	79.44	-58.60	0.54	-44.96	117.82	-35.07	-65.95
LI (TBC)	15.07	min	-48.68	-46.06	110.54	-45.96	-48.42	107.68	-83.48	72.15
LII	15.08	min	-70.98	-18.24	95.32	-43.27	-64.76	109.63	-62.89	66.66
LIII	15.13	saddle	75.46	1.16	-75.33	116.27	-51.32	-45.75	93.48	104.43
LIV	15.16		94.26	-30.24	-66.99	72.74	26.03	103.64	79.56	-72.90
LV	15.19	saddle	-28.52	88.97	-68.24	69.89	-86.98	14.96	78.55	-66.11
LVI	15.27	saddle	-81.57	83.91	-90.85	66.28	9.38	113.82	81.90	31.28
LVII	15.36	saddle	-65.38	-47.07	50.34	52.00	118.04	73.42	-50.13	94.97
LVIII	15.54	saddle	84.70	-68.66	90.59	-50.99	-50.82	117.94	-36.18	-66.82

LIX	15.82	saddle	8.83	-70.98	113.48	-69.20	53.42	-114.55	110.21	-22.03
LX	16.18	saddle	48.37	51.38	-113.79	49.29	39.67	-104.42	94.72	-82.61
LXI	16.24	mm	-7.05	77.05	-77.24	79.30	-79.73	2.99	85.35	-79.59
LXII	16.30	saddle	-78.83	103.28	-80.35	12.79	62.67	-135.48	79.39	21.67
LXIII	16.39	saddle	-68.63	78.99	14.90	-80.31	78.31	-92.44	97.16	-22.76
LXIV (TCC or CR)	16.59	min	-60.95	109.69	-81.95	48.54	-76.67	131.81	-81.10	31.62
LXV	16.59	saddle	68.28	37.21	-99.08	27.75	0.68	78.68	-83.42	-37.86
LXVI	16.69	saddle	-87.04	14.31	-3.45	79.79	-66.98	-58.47	78.75	38.95
LXVII	16.99	saddle	95.08	-97.12	69.32	-1.87	-80.15	128.42	-53.40	-45.13
LXVIII	17.01	saddle	74.12	-3.64	29.55	-104.78	96.88	-56.56	68.71	-119.58
LXIX	17.21	saddle	-93.08	-17.95	53.76	30.97	-119.91	57.75	-9.61	69.45
LXX	17.25	mm	81.67	-7.13	-80.96	85.89	4.74	-89.12	90.91	-85.37
LXXI	17.31	saddle	123.25	-66.73	-1.74	68.67	-109.41	97.61	-32.87	-69.04
LXXII	17.38	saddle	-65.05	-44.51	86.47	-3.52	-87.38	95.60	-62.28	85.01
LXXIII	17.39	min	-98.50	86.76	-38.99	-51.62	127.82	-79.03	-0.41	71.61
LXXIV	17.42	saddle	-100.00	88.45	-38.96	-50.35	126.05	-85.50	7.50	67.33
LXXV	17.62	saddle	74.72	-67.67	64.66	15.10	-104.36	54.84	46.67	-100.77
LLXVI	17.65	saddle	78.06	-48.77	84.15	-59.59	-48.21	104.00	-16.46	-83.32
LXXVII	17.68	saddle	-22.03	-81.88	58.18	2.12	38.93	-124.76	50.25	49.51
LXXVIII (TC)	17.87	min	-44.58	-33.94	97.71	-95.58	25.00	66.33	-101.02	84.84
LXXIX (TCC or CR)	18.02	min	-114.62	70.74	-50.20	83.81	-122.99	78.79	-38.30	74.58
LXXX	18.03	saddle	-61.61	-58.01	49.82	61.18	-91.98	11.24	-3.06	84.19
LXXXI	18.09	saddle	-42.23	-40.28	104.89	-83.95	6.01	80.66	-101.59	80.59
LXXXII	18.21	mm	-67.36	-52.93	56.03	53.76	-98.30	15.39	4.67	76.03
LXXXIII (C)	18.23	min	-84.26	33.87	52.55	-112.83	42.78	61.92	-85.88	76.90
LXXXIV	18.28	saddle	-71.82	73.83	-94.31	51.01	45.27	-129.66	58.72	41.62
LXXXV	18.33	saddle	-105.34	80.08	-0.32	-66.61	96.82	-108.81	65.15	30.72
LXXXVI	18.37	saddle	22.21	-99.44	79.58	-39.59	70.27	-	71.52	5.42

								140.53		
LXXXVII	18.40	saddle	-98.30	86.90	-64.47	74.12	-108.61	98.54	-55.96	63.51
LXXXVIII (C)	18.55	min	-90.76	53.29	49.59	-83.87	-6.53	96.02	-72.21	53.25
LXXXIX	18.56	saddle	132.42	-61.67	41.88	-86.53	104.94	-21.99	-9.26	-72.63
XC	18.64	saddle	79.21	-46.96	72.52	-103.86	82.92	-68.72	86.48	-110.17
XCI	18.80	saddle	-24.53	102.22	-78.93	39.22	-72.34	138.32	-66.34	-6.62
XCII (TCC or CR)	18.93	min	-56.04	95.18	-97.17	66.22	-71.43	119.55	-98.21	46.77
XCIII	18.94	saddle	-24.51	85.49	-109.81	45.26	34.97	-130.15	101.97	-19.70
XCIV	19.03	saddle	-89.45	36.86	62.65	-70.21	-30.93	105.11	-67.67	56.37
XCV	19.08	mm	20.24	-90.39	92.48	-54.42	69.76	-137.16	88.52	-6.82
XCVI	19.08	saddle	88.49	-92.43	74.24	-67.38	92.04	-112.78	82.34	-68.39
XCVII	19.32	saddle	72.63	-116.87	54.11	35.65	-92.59	116.28	-78.11	-1.09
XCVIII	19.36	mm	-52.46	-33.12	104.06	-35.59	-0.74	-76.79	103.37	10.88
XCIX	19.39	saddle	-88.91	49.03	48.07	-97.73	18.30	80.83	-80.08	62.68
C (?)	19.51	mm	59.57	58.76	-78.64	3.57	-11.26	96.02	-59.72	-62.14
CI	19.71	saddle	-70.21	1.11	76.42	-109.70	37.97	59.34	-90.36	86.36
CII	19.71		19.88	-94.84	51.73	47.34	-103.02	99.99	-78.90	44.41
CIII	19.76	saddle	104.40	-38.49	62.71	-117.87	72.22	-2.78	14.87	-108.05
CIV	19.90	mm	62.36	47.41	-88.68	6.81	81.11	-101.28	76.66	-92.23
CV	19.97	saddle	-77.99	65.98	16.80	-93.63	42.66	72.29	-93.76	60.66
CVI	20.13	saddle	61.51	-115.42	58.60	2.29	30.68	-124.49	90.15	-30.64
CVII	20.48	saddle	114.68	-24.56	0.25	-63.67	128.89	-71.79	31.93	-87.08
CVIII	20.71	saddle	-73.91	84.52	12.17	-73.95	8.32	101.61	-79.87	32.70
CIX	20.71	saddle	-18.01	83.05	-105.87	66.01	-63.35	125.58	-99.91	15.97
CX	20.87	mm	-48.01	-62.52	77.25	-3.10	12.87	-104.20	70.36	48.72
CXI	21.07	saddle	-37.38	-41.34	102.05	-92.20	20.05	71.19	-103.07	80.51
CXII	21.16		84.11	-9.37	41.92	-113.83	68.42	-1.73	23.56	-114.31
CXIII	21.64	saddle	22.81	-80.56	109.18	-43.77	-40.67	131.50	-93.58	15.26

CXIV	21.72	mm	-80.67	69.25	-86.08	70.52	11.98	-116.13	72.49	41.87
CXV	22.08	mm	97.70	-12.48	9.30	-81.05	121.41	-75.12	55.38	-105.78
CXVI	22.10	mm	-20.59	96.41	-93.52	12.40	56.00	-128.74	109.65	-35.19
CXVII	23.66	saddle	-84.86	78.18	-71.28	0.00	99.03	-95.85	2.19	75.06
CXVIII	23.67		94.35	-88.88	71.53	-12.64	-73.48	130.44	-51.28	-50.27
CXIX	23.85	mm	-87.67	82.04	-68.13	-5.10	100.57	-101.82	11.60	69.09
CXX	24.10	saddle	-114.10	30.98	-0.53	61.26	-129.52	59.78	-11.31	67.84
CXXI	24.82	mm	59.23	-101.94	85.24	-12.33	10.89	-95.49	117.04	-60.05
CXXII	24.96	mm	-64.22	98.79	-82.88	59.52	-82.58	126.34	-85.29	42.66
CXXIII	25.99	saddle	-89.91	11.29	-22.36	94.99	-111.63	65.20	-56.61	110.11
CXXIV	27.82	saddle	-111.10	49.49	-64.31	114.78	-85.98	12.59	-8.53	94.98
CXXV	28.10	mm	-117.02	54.95	-61.33	108.85	-93.03	18.12	-5.57	89.59
CXXVI	28.72	saddle	-46.86	96.33	-89.70	15.56	-8.61	95.42	-117.08	49.63
CXXVII	29.08	mm	-52.41	103.56	-83.36	11.73	-14.66	103.76	-110.66	45.37
CXXVIII	29.69	mm	-20.76	82.76	-96.29	20.58	-5.39	93.40	-116.04	31.46
CXXIX	33.85	mm	45.59	7.71	17.75	-1.43	-86.55	77.11	30.25	-103.68
CXXX	35.43	mm	103.60	-59.07	-2.72	-4.33	76.67	-114.38	72.14	-72.92
CXXXI	35.74	saddle	-46.24	85.00	-96.20	69.53	-32.83	-170.38	179.03	16.84

1,1-dimethylcyclohexane in gas phase								
Conformation	δE	Stat. point	1,2,3,4	2,3,4,5	3,4,5,6	4,5,6,1	5,6,1,2	6,1,2,3
C	0.00	min	56.6	-58.0	58.0	-56.6	53.7	-53.7
TB	5.09	min	-65.7	31.3	31.3	-65.7	31.5	31.5
TB	5.09	min	67.5	-31.3	-31.3	65.7	-31.5	-31.5
TB	6.12	min	44.1	-63.3	20.0	39.4	-58.4	14.8
TB	6.12	min	-44.1	63.3	-20.0	-39.7	58.4	-14.8
B	6.51	saddle	56.3	-56.6	3.9	49.9	-50.0	-3.2
B	9.99	saddle	-2.0	48.7	-48.7	2.0	44.0	-44.0
half-C	10.98	saddle	13.9	14.8	-40.0	-1.5	67.5	-53.4
half-C	10.98	saddle	-13.9	-14.8	40.0	1.5	-67.5	53.4
half-C	11.19	saddle	-5.6	-30.7	66.5	-66.9	30.2	5.9
half-C	11.19	saddle	5.6	30.7	-66.5	66.9	-30.2	-5.9
half-C	12.12	saddle	-65.8	33.6	3.1	-10.1	-20.1	58.3
half-C	12.12	saddle	65.8	-33.6	-3.1	10.1	20.1	-58.3

(R)-1,1,3-trimethylcyclohexane								
Conformation	δE	Stat. point	1,2,3,4	2,3,4,5	3,4,5,6	4,5,6,1	5,6,1,2	6,1,2,3
C	0.00	min	56.6	-58.0	58.2	-56.7	53.7	-53.8
C	3.61	min	-47.6	52.3	-58.6	58.6	-51.8	47.1
TB	5.10	min	65.9	-31.7	-30.9	65.6	-31.7	-31.5
TB	6.14	min	44.1	-63.4	20.3	39.6	-58.3	14.8
TB	6.28	min	40.1	19.9	-63.4	44.2	14.8	-58.8
B	6.68	saddle	50.3	3.3	-56.4	56.6	-3.6	-50.0
TB	7.44	min	-28.4	-30.8	67.4	-40.9	-17.6	54.2
TB	7.63	min	-55.4	18.9	39.5	-67.3	30.9	28.5
TB	8.53	min	-29.1	57.1	-26.7	-30.0	57.1	-26.0
B	8.76	saddle	-39.3	-11.1	61.3	-62.3	12.7	38.3
B	10.09	saddle	1.7	-48.9	49.9	-3.2	-43.3	44.1
B	10.52	saddle	1.9	44.4	-44.1	-2.9	47.9	-47.4
half-C	11.22	saddle	41.5	0.2	-14.6	-13.1	52.8	-68.3
half-C	11.57	saddle	-14.6	-10.0	-5.3	44.9	-68.4	52.2
half-C	11.83	saddle	5.8	28.7	-65.3	68.0	-33.1	-3.6
half-C	17.05	mm	-56.5	24.7	5.8	-7.7	-21.0	54.3

1,1,3,3-tetramethylcyclohexane								
Conformation	δE	Stat. point	1,2,3,4	2,3,4,5	3,4,5,6	4,5,6,1	5,6,1,2	6,1,2,3
C	0.00	min	46.8	-51.7	58.7	-58.7	51.7	-46.8
TB	3.93	min	54.6	-17.7	-40.2	67.1	-30.4	-28.8
TB	3.93	min	-54.6	17.7	40.2	-67.1	30.4	28.8
TB	4.75	min	27.3	-56.5	28.2	28.2	-56.5	27.3
TB	4.75	min	-27.3	56.5	-28.2	-28.2	56.5	-27.3
B	5.23	saddle	38.0	12.6	-62.4	62.4	-12.6	-38.0
B	6.57	saddle	-47.7	47.8	-2.6	-44.6	44.4	2.3
half-C	8.09	saddle	4.5	31.3	-67.1	67.1	-31.3	-4.5
half-C	8.25	saddle	54.3	-68.0	43.6	-4.6	-8.8	-17.1
half-C	8.25	saddle	-54.3	68.0	-43.6	4.6	8.8	17.1
half-C	9.60	saddle	21.7	9.8	-4.7	-31.7	65.1	-59.5
half-C	13.12	saddle	6.2	27.8	-64.9	69.3	-34.9	-2.6
half-C	14.07	saddle	-57.5	66.6	-40.5	2.8	6.9	21.4
half-C	14.07	saddle	57.4	-66.7	40.7	-2.9	-6.9	-21.3

(R)-1-ethyl-1,3,3-trimethylcyclohexane									
Conformation	δE	Stat. point	1,2,3,4	2,3,4,5	3,4,5,6	4,5,6,1	5,6,1,2	6,1,2,3	1,6,7,8
C	0.00	min	46.2	-50.8	58.2	-58.6	52.3	-47.4	-178.9
C	0.35	min	-48.0	52.4	-59.0	58.3	-51.8	48.0	173.1
C	0.74	min	-48.1	52.2	-58.7	57.9	-51.6	48.1	-74.6
C	0.74	min	44.9	-50.6	59.5	-59.5	51.3	-45.5	-62.3
C	1.64	min	47.7	-51.7	58.1	-58.0	51.6	-47.8	66.7
C + Et	3.72	saddle	-46.4	52.3	-60.3	59.7	-52.2	46.8	-127.4
TB	4.10	min	28.9	30.6	-67.5	40.3	17.6	-54.9	179.3
TB	4.10	min	-28.4	-31.0	67.6	-40.0	-17.8	54.7	-55.7
TB	4.21	min	53.4	-15.7	-41.9	67.2	-29.8	-29.3	-176.7
TB	4.46	min	-54.2	15.5	42.4	-67.6	29.4	30.2	-73.6
TB	4.49	min	-54.4	16.2	41.7	-67.4	29.8	29.9	179.8
TB	4.51	min	54.0	-18.4	-38.9	66.6	-31.4	-27.6	-62.7
TB	4.60	min	-29.2	-30.3	67.4	-40.3	-17.4	55.0	-167.7
TB	4.79	min	27.6	-56.3	27.5	29.2	-56.8	26.9	-178.1
TB	4.83	min	28.3	31.1	-67.8	40.1	17.6	-54.7	-72.1
TB	4.92	min	54.3	-15.9	-41.8	67.0	-28.9	-30.2	71.8
C + Et	5.04	saddle	46.9	-51.9	59.4	-58.2	51.0	-47.1	-0.2
TB	5.23	min	25.2	-55.3	28.7	27.3	-56.3	28.7	-63.4
B	5.33	saddle	37.8	13.2	-63.0	62.3	-12.4	-38.4	178.6
TB	5.39	min	-30.0	59.6	-31.5	-25.3	53.7	-24.4	-51.9
TB	5.49	min	29.9	28.4	-65.8	40.5	16.3	-54.1	52.1
C + Et	5.55	saddle	47.2	-52.0	59.2	-57.9	50.9	-47.4	-121.6
B	5.55	saddle	-38.1	-12.6	62.7	-62.9	13.3	37.8	-64.9
TB	5.56	min	-28.1	58.3	-31.0	-26.0	55.1	-26.4	-165.3
TB	5.74	min	24.3	-56.3	31.4	24.3	-55.3	29.5	50.5
TB	6.17	saddle	36.5	14.3	-63.5	62.1	-12.5	-37.6	-72.3
TB	6.36	saddle	36.1	14.7	-63.6	62.2	-12.3	-37.4	58.1
TB	6.39	min	-30.2	38.2	-54.9	63.0	-53.8	38.0	72.1
B	6.77	saddle	-2.7	-43.9	43.9	3.6	-48.5	48.3	-56.2
TB	7.00	min	-15.7	-39.5	65.8	-32.6	-21.4	47.5	66.7
B	7.06	saddle	0.7	45.7	-43.9	-4.9	49.4	-47.3	-169.5
B	7.10	saddle	-53.7	46.2	3.5	-48.9	41.4	10.4	-43.5
TB	7.44	min	-4.0	36.8	-19.1	-30.8	62.5	-43.9	62.2
TB	7.63	saddle	11.5	32.9	-33.2	-11.5	53.9	-54.2	53.7
half-C	8.29	saddle	-4.2	-32.5	68.2	-66.3	29.8	5.6	-56.0

TB	8.42	saddle	50.7	-51.5	8.3	38.1	-38.8	-6.4	63.6
c2	8.52	saddle	7.3	24.1	-61.8	69.4	-37.9	-0.3	57.7
half-C	8.67	saddle	-4.8	-32.6	68.4	-65.8	28.8	6.7	-165.6
half-C	8.78	saddle	19.5	9.5	0.9	-39.8	66.8	-56.8	-175.9
half-C	8.86	saddle	1.7	33.7	-68.4	66.6	-31.4	-2.9	-169.0
half-C	9.20	saddle	18.3	11.3	-0.6	-39.4	66.9	-56.5	-70.0
half-C	9.39	saddle	2.4	32.8	-68.0	67.0	-32.0	-2.7	-67.2
half-C	9.58	saddle	-8.3	-6.6	-15.9	53.7	-67.5	44.1	69.3
C + Et	9.69	saddle	-39.8	51.6	-64.3	62.3	-48.6	38.8	117.8
TB	10.03	saddle	53.9	-16.8	-40.2	65.8	-29.3	-29.5	-119.9
TB	10.07	min	-25.7	-33.1	67.6	-38.5	-18.6	53.4	19.0
TB	10.13	min	-50.5	6.4	49.8	-66.6	23.2	34.6	20.9
TB	10.30	saddle	29.1	31.1	-68.9	41.4	16.5	-55.0	1.4
TB	10.33	saddle	54.7	-19.2	-37.8	64.9	-29.8	-28.8	3.8
TB	10.81	saddle	29.4	-57.9	30.2	25.7	-53.1	24.1	119.3
B + Et r	12.22	saddle							
half-C	14.16	saddle							
half-C	14.51	saddle							
half-C	15.04	saddle	-8.2	51.8	-75.7	51.5	-8.9	-13.5	126.6
half-C	15.09	saddle							

N,N-dimethylmorpholinium								
Conformation	δE	Stat. point	1,2,3,4	2,3,4,5	3,4,5,6	4,5,6,1	5,6,1,2	6,1,2,3
C	0.00	min	55.9	-61.7	61.7	-55.9	50.2	-50.2
TB	4.51	min	24.2	39.7	-68.9	30.9	29.5	-58.2
TB	4.51	min	-24.2	-39.7	68.9	-30.9	-29.5	58.2
B	5.38	saddle	-3.0	57.8	-57.8	3.0	47.8	-47.8
TB	7.12	min	63.1	-29.6	-29.6	63.1	-29.1	-29.1
TB	7.12	min	-63.1	29.6	29.6	-63.1	29.1	29.1
B	7.55	saddle	-61.8	52.4	1.8	-51.2	40.2	13.1
B	7.55	saddle	61.8	-52.4	-1.8	51.2	-40.2	-13.1
half-C	10.80	saddle	28.3	6.3	-6.3	-28.3	60.1	-60.1
half-C	11.11	saddle	-61.7	75.3	-45.6	1.9	9.2	20.3
half-C	11.11	saddle	61.7	-75.3	45.6	-1.9	-9.2	-20.3

Morpholinium in GB/SA water									
Conformation	δE	Stat. point	4,5,6,1	5,6,1,2	6,1,2,3	1,2,3,4	2,3,4,5	3,4,5,6	Solvation
C	0.00	min	55.9	-50.2	50.2	-55.9	60.3	-60.3	-56.66
TB	4.92	min	25.8	37.0	-67.6	32.1	28.4	-58.2	-55.35
TB	4.92	min	-25.8	-37.0	67.6	-32.1	-28.5	58.2	-55.35
B	5.93	saddle	-2.9	56.5	-56.5	2.9	47.7	-47.7	-54.91
TB	6.66	min	63.1	-29.5	-29.5	63.1	-28.8	-28.8	-57.52
TB	6.66	min	-63.1	29.5	29.5	-63.1	28.8	28.8	-57.52
B	7.23	saddle	-60.3	53.2	0.0	-50.4	41.7	10.2	-57.06
B	7.23	saddle	60.3	-53.2	0.0	50.4	-41.7	-10.3	-57.05
half-C	10.66	saddle	27.5	7.5	-7.5	-27.5	59.8	-59.8	-56.22
half-C	11.07	saddle	63.5	-72.8	41.4	0.5	-22.3	-8.7	-56.47
half-C	12.83	saddle	64.8	-33.6	-2.4	10.9	18.2	-54.6	-57.15
half-C	12.83	saddle	-65.1	34.1	2.0	-11.1	-17.8	54.3	-57.16

(*S*)-3-methyl-N,N-dimethylmorpholinium								
Conformation	δE	Stat. point	4,5,6,1	5,6,1,2	6,1,2,3	1,2,3,4	2,3,4,5	3,4,5,6
C	0.00	min	55.9	-61.6	61.7	-55.9	50.3	-50.3
TB	4.49	min	30.8	-68.9	39.8	24.1	-58.2	29.6
C	4.73	min	-46.2	54.3	-60.2	58.2	-50.2	44.5
TB	4.89	min	-16.3	-46.1	68.5	-25.0	-33.7	55.5
B	5.35	saddle	3.1	-57.9	57.7	-2.6	-48.0	47.7
TB	5.37	min	29.8	33.5	-66.5	32.8	27.4	-59.8
TB	6.84	min	-16.6	60.5	-42.2	-17.9	57.7	-39.4
TB	7.04	min	63.0	-29.0	-30.2	63.3	-28.8	-29.5
B	7.55	saddle	61.6	-52.9	-0.9	50.8	-40.4	-12.7
TB	9.06	min	-48.6	7.4	47.4	-67.5	26.2	27.9
B	9.41	saddle	16.7	44.9	-61.3	13.5	43.9	-60.1
half-C	10.91	saddle	30.5	6.0	-8.7	-25.1	58.7	-61.6
half-C	11.11	saddle	62.5	-75.0	44.7	-1.0	-8.9	-21.3
half-C	11.61	saddle	-19.3	-4.4	-6.9	42.4	-63.8	52.0
B	11.68	saddle	-48.8	46.5	0.1	-47.0	42.6	3.1
half-C	12.22	saddle	4.4	32.8	-67.9	68.5	-32.6	-2.7

[(*S*)-methylmorpholinium in GB/SA water]									
Conformation	δE	Stat. point	4,5,6,1	5,6,1,2	6,1,2,3	1,2,3,4	2,3,4,5	3,4,5,6	Solvation
C	0.00	min	55.9	-60.4	60.5	-55.8	50.2	-50.3	-55.27
TB	4.87	min	31.8	-67.6	37.4	25.6	-58.3	28.7	-53.97
C	4.88	min	-46.0	52.3	-58.9	58.2	-50.1	44.4	-54.98
TB	5.36	min	-16.8	-44.6	67.6	-25.7	-33.1	55.4	-53.66
TB	5.76	min	31.4	30.9	-65.1	33.9	26.2	-59.6	-54.12
B	5.86	saddle	2.9	-56.6	56.6	-2.7	-47.9	47.8	-53.52
TB	6.63	min	63.2	-29.5	-29.6	63.1	-28.7	-29.1	-56.08
B	7.33	saddle	49.7	1.9	-54.3	58.8	-7.6	-43.5	-55.54
TB	7.54	min	-16.4	58.8	-40.3	-18.7	57.8	-39.4	-53.50
TB	8.87	min	-48.7	7.4	47.4	-67.5	26.2	27.9	-55.59
half-C	10.84	saddle	31.4	6.3	-10.7	-22.6	57.4	-62.0	-54.76
half-C	11.15	mm	0.1	-41.8	73.1	-63.6	22.8	8.0	-55.02
half-C	12.57	mm	58.5	-54.4	1.5	51.4	-45.4	-6.5	-55.59
half-C	14.93	mm	30.1	7.3	-10.4	-23.9	58.1	-61.3	-54.75
half-C	18.28	mm	66.7	-37.6	0.3	13.1	13.7	-51.8	-55.73

3,3-dimethyl-N,N-dimethylmorpholinium								
Conformation	δE	Stat. point	4,5,6,1	5,6,1,2	6,1,2,3	1,2,3,4	2,3,4,5	3,4,5,6
C	0.00	min	44.9	-53.2	60.3	-58.5	50.1	-43.9
C	0.00	min	-44.9	53.2	-60.3	58.5	-50.1	43.9
TB	1.25	min	19.3	41.8	-64.4	22.2	35.0	-57.2
TB	1.25	min	-19.4	-41.8	64.4	-22.2	-35.0	57.2
TB	1.56	min	-14.4	59.4	-43.0	-16.7	57.5	-40.9
TB	1.56	min	14.4	-59.4	43.0	16.7	-57.5	40.9
TB	3.93	min	26.4	27.6	-48.3	7.5	47.1	-67.5
TB	3.93	min	-26.4	-27.6	48.3	-7.5	-47.1	67.5
half-C	6.69	saddle	18.8	4.8	7.0	-42.8	63.9	-51.7
B	6.86	saddle	-47.0	45.3	-0.0	-46.3	42.5	2.2
B	6.86	saddle	47.0	-45.3	0.0	46.3	-42.5	-2.2
half-C	6.98	saddle	-3.8	-32.6	67.5	-68.9	34.0	1.2
half-C	8.73	saddle	55.9	-70.3	46.1	-5.8	-5.8	-19.2
half-C	13.32	mm	56.9	-26.9	-3.1	7.8	19.0	-50.6

3,3-dimethylmorpholinium in GB/SA water									
Conformation	δE	Stat. point	4,5,6,1	5,6,1,2	6,1,2,3	1,2,3,4	2,3,4,5	3,4,5,6	Solvation
C	0.00	min	-44.6	51.8	-59.0	58.4	-50.1	43.8	-53.71
C	0.00	min	44.6	-51.8	59.0	-58.4	50.1	-43.8	-53.71
TB	1.63	min	20.2	40.1	-63.7	23.3	34.1	-57.1	-52.40
TB	1.63	min	-20.3	-40.1	63.7	-23.3	-34.1	57.1	-52.40
TB	2.07	min	14.1	-57.8	41.4	17.4	-57.6	41.0	-52.23
TB	2.07	min	-14.1	57.8	-41.4	-17.4	57.5	-41.0	-52.23
TB	3.67	min	48.6	-8.4	-46.1	67.1	-26.3	-27.3	-54.27
TB	3.67	min	-48.6	8.4	-46.1	-67.1	26.3	27.3	-54.27
B	4.18	saddle	-34.7	-16.6	63.7	-61.5	10.8	35.3	-53.82
half-C	6.47	saddle	-17.7	-6.1	-6.1	42.5	-63.8	51.3	-53.57
B	6.67	saddle	45.2	-44.0	-0.6	46.8	-43.7	-0.2	-53.85
half-C	9.95	mm	27.0	-62.8	63.8	-28.3	-4.7	5.3	-53.13

(*R*)-3-(hydroxymethyl)-3-methyl-N,N-dimethylmorpholinium

Conformation	δE	Stat. point	4,5,6,1	5,6,1,2	6,1,2,3	1,2,3,4	2,3,4,5	3,4,5,6	O-C-C-O	C-C-O-H
C	0.00	min	43.8	-52.8	60.6	-59.2	50.1	-43.0	45.6	-45.3
C	0.81	min	44.6	-52.8	59.9	-58.6	50.2	-43.8	-47.1	35.0
TB	1.14	min	14.0	-59.2	43.4	16.1	-57.2	41.1	49.1	-51.9
TB	1.20	min	-10.1	56.9	-44.7	-13.2	55.7	-43.2	75.1	-175.2
C	1.60	min	-41.6	51.8	-61.0	60.2	-49.9	41.1	-39.6	21.2
C	1.77	min	-49.7	53.9	-57.8	56.0	-51.3	49.0	155.0	164.8
C	2.01	min	-38.5	50.2	-61.2	60.8	-49.3	38.8	76.3	-171.2
TB	2.13	min	19.3	41.6	-64.2	22.4	34.9	-57.1	-42.8	26.2
TB	2.18	min	-6.7	-48.9	54.9	-3.7	-47.6	53.3	68.4	-166.4
C	2.19	min	44.7	-52.9	60.1	-58.4	50.2	-44.0	174.1	172.8
TB	2.20	min	-17.5	-42.8	63.4	-20.2	-36.4	56.5	-43.9	30.5
TB	2.35	min	13.7	-58.7	42.8	16.5	-57.4	41.3	-48.6	35.6
C	2.56	min	43.0	-51.2	59.4	-59.3	51.0	-43.3	61.5	-161.6
C + rot	2.63	saddle	43.0	-51.2	59.4	-59.3	50.9	-43.3	60.7	-137.1
TB	2.71	min	-9.2	55.9	-43.7	-14.1	56.8	-44.4	-43.1	22.2
C	2.73	min	-45.1	45.9	-51.8	56.7	-55.3	50.0	9.9	-35.3
TB	3.66	min	-42.2	-3.6	55.3	-66.0	20.4	30.5	36.2	-47.3
TB	3.90	min	21.2	40.1	-64.4	23.6	33.8	-57.7	176.6	170.8
TB	4.06	min	48.6	-8.7	-46.1	67.6	-27.3	-26.8	48.7	-51.1
TB	4.11	min	17.0	-60.5	42.1	18.2	-57.4	38.8	174.6	172.2
TB	4.32	min	-20.5	-40.8	64.7	-23.4	-34.0	57.5	176.9	168.4
B?	4.45	saddle	-29.6	-26.1	68.6	-54.7	0.9	40.6	31.4	-39.5
C	4.51	min	44.3	-54.0	61.6	-58.8	49.4	-43.0	-64.6	170.2
TB	4.58	min	48.7	-8.3	-46.3	67.4	-26.6	-27.4	-44.6	32.2
C	5.08	min	-43.8	54.0	-62.0	59.2	-49.4	42.4	-56.6	-178.2
TB	5.36	min	-11.1	57.4	-43.5	-15.5	57.4	-43.2	-174.4	90.3
TB	5.39	min	-38.8	0.3	50.9	-69.1	30.0	20.4	60.7	-159.3
TB	5.55	min	18.4	42.9	-64.8	21.4	35.7	-57.1	-56.1	179.0
TB	5.63	saddle	39.5	7.1	-58.3	67.9	-21.7	-29.0	64.0	-164.6
TB	5.64	min	-42.4	2.4	50.3	-69.1	28.6	23.4	-46.4	30.7
TB	5.81	min	16.4	-61.2	44.0	16.6	-56.9	39.3	-64.7	171.9
TB	5.84	min	-50.3	8.2	46.8	-66.5	24.3	30.2	167.6	163.5
TB	5.88	min	-14.3	60.7	-45.4	-14.9	56.6	-41.0	-50.9	-175.6
TB	6.08	min	47.9	-6.8	-47.6	67.5	-26.2	-27.6	178.4	172.3
TB	6.10	min	-17.3	-43.6	64.2	-19.9	-36.7	56.8	-60.8	175.5

C + anti OH	7.79	saddle	-44.8	54.1	-61.5	58.6	-49.4	43.5	-170.7	-28.4
TB	8.53	min	47.9	-7.4	-47.0	67.6	-27.0	-27.0	-60.7	171.3
TB	9.32	min	-46.4	6.9	47.1	-68.1	23.3	25.2	-57.7	-59.1
TB + g- OH	9.36	min	-46.3	4.7	49.2	-67.9	26.2	27.3	-65.9	174.7
TB OH e Me	9.55	saddle	19.8	42.6	-67.4	25.1	33.1	-57.4	-115.6	170.4
TB + g- OH	9.72	saddle	2.4	31.9	-66.3	69.4	-36.4	1.6	-176.1	169.4
half-C + OH e OC	11.07	mm	19.6	4.6	6.4	-42.1	63.7	-52.5	0.4	-14.4
half-C + g- OH	11.38	saddle	20.1	4.3	6.4	-41.7	63.6	-52.7	-60.4	172.8
half-C + OH e Me	15.37	mm	19.7	44.1	-69.8	26.4	32.8	-57.9	122.3	-5.9
half-C + OH e OC	16.71	mm	20.1	2.6	8.8	-43.4	63.6	-52.0	-1.4	-169.4

[(*R*)-(methylenehydroxy)methyl morpholinium in GB/SA water]											
Conformation	δE	Stat. point	4,5,6,1	5,6,1,2	6,1,2,3	1,2,3,4	2,3,4,5	3,4,5,6	O-C-C-O	C-C-O-H	Solvation
C	0.00	min	44.1	-51.4	58.8	-58.6	50.1	-43.5	-48.2	35.5	-59.59
C	0.81	min	43.7	-51.7	59.5	-59.0	49.9	-43.0	44.4	-42.5	-56.84
C	0.86	min	-41.1	50.4	-59.9	60.1	-49.8	40.9	-42.8	27.0	-59.57
TB	1.45	min	19.8	40.3	-63.5	23.0	34.4	-57.0	-44.7	29.4	-58.46
TB	1.79	min	-17.6	-41.8	62.4	-20.2	-36.3	56.3	-45.6	32.9	-58.51
TB	1.90	min	13.6	-57.4	41.3	17.1	-57.5	41.3	-49.5	36.0	-58.34
TB	2.62	min	15.8	-58.9	41.4	17.7	-57.3	39.7	46.9	-46.5	-54.83
C	2.87	min	43.2	-51.7	59.9	-59.0	49.6	-42.5	-56.8	-65.8	-60.77
C	3.20	min	43.1	-50.5	58.7	-59.1	50.5	-43.2	55.2	-172.7	-55.44
C	3.31	min	-42.8	52.2	-60.8	59.5	-49.3	41.8	-52.5	-179.0	-60.22
TB	3.48	min	48.4	-8.4	-46.0	67.2	-26.4	-27.1	-45.7	33.2	-60.20
TB	4.06	min	-7.7	53.3	-41.7	-14.7	56.8	-44.9	70.0	-177.4	-50.52
TB	4.14	min	19.2	41.2	-64.0	22.6	34.6	-56.9	-53.2	179.6	-58.31
C	4.42	min	-38.1	47.0	-57.9	60.0	-50.2	39.9	63.3	-173.9	-52.24
TB	4.52	min	5.2	-53.4	45.1	10.9	-55.5	47.0	60.2	-172.4	-52.11
TB	4.56	min	14.1	-58.1	42.1	16.6	-57.1	40.9	-55.1	-53.1	-59.27
TB	4.57	min	48.7	-9.4	-45.1	67.2	-27.1	-26.5	46.6	-46.8	-57.10
TB	4.66	min	-12.6	58.0	-43.7	-14.9	56.6	-42.1	-49.8	-178.7	-58.12
TB	4.68	min	-42.8	3.4	49.3	-68.7	28.2	23.4	-47.9	33.4	-60.28
TB	4.84	min	-18.4	-41.6	63.2	-21.2	-35.3	56.6	-56.2	178.2	-58.63
C	4.95	min	44.7	-51.6	58.7	-58.2	50.2	-44.2	178.9	176.4	-53.66
TB	4.98	min	23.9	34.6	-59.0	21.3	34.3	-58.3	57.7	-79.4	-53.81
TB	5.11	min	42.8	-2.5	54.3	-65.8	20.2	30.7	34.6	-45.2	-54.89
B	5.18	saddle	10.2	42.1	-46.7	-2.2	50.8	-55.3	62.5	-92.5	-52.60
C	5.20	min	-47.9	52.9	-58.1	56.8	-50.4	46.8	168.4	172.5	-53.03
TB	6.34	min	45.4	-3.4	-50.2	68.0	-25.3	-27.3	58.3	-173.4	-55.40
TB	6.45	min	47.8	-7.6	-46.7	67.3	-26.4	-27.0	-55.6	177.0	-60.40
TB	6.63	min	20.8	39.6	-63.9	23.7	33.6	-57.4	-177.6	175.9	-53.15
TB	6.91	min	-42.7	2.3	50.0	-67.6	26.3	24.9	50.2	-169.3	-53.55
TB	7.22	min	-45.7	6.4	47.2	-68.0	27.9	24.8	-56.6	-64.4	-60.93
TB	7.24	min	16.0	-58.6	40.7	18.5	-57.5	39.4	178.9	176.5	-52.68
TB	7.30	min	-20.3	-39.9	63.5	-22.9	-34.1	57.2	-	174.9	-53.21

									177.2		
B	7.44	saddle	-6.1	54.3	-45.5	-11.1	55.5	-46.4	171.5	175.5	-53.61
B	7.65	saddle	-33.9	-15.6	63.2	-63.8	14.7	31.9	-58.7	177.6	-60.59
TB	7.88	saddle	-20.3	-39.9	63.4	-22.9	-34.2	57.2	176.7	118.5	-52.85
TB	8.53	min	48.1	-7.2	-47.1	67.1	-25.6	-27.8	176.6	176.3	-54.25
T$\diamond$C	8.54	saddle	6.1	19.4	-55.4	69.7	-43.7	7.5	56.6	-65.5	-55.07
TB	8.84	min	48.1	-7.0	-47.3	67.0	-25.4	-28.1	174.8	76.9	-55.81
TB	8.95	min	-50.2	9.7	45.2	-66.4	25.4	28.7	173.8	172.2	-53.65
half-C	9.67	mm	-16.3	-6.0	-7.7	44.2	-64.1	50.1	-51.1	178.0	-60.15
half-C	17.68	saddle	55.8	-26.7	-3.0	7.5	19.1	-50.3	174.7	176.2	-54.17

Minima for acetylcarnitine in gas phase by AM1										
A	B	C	D	E	δH_f	μ	F	%	Cont. δH_f	Cont. μ
a	g-	g+	g-	s	-126.9	12.15	0.51	51.37	-65.18	6.13
g-	g-	g+	a	s	-126.7	12.66	0.35	34.83	-44.12	4.56
g-	g-	g+	g+	s	-126.1	14.29	0.13	13.30	-16.77	1.87
a	g-	g+	a	s	-124.1	14.92	0.00	0.49	-0.61	0.07
									-126.68	12.63

Torsion A= N-C-C-O, torsion B= C-C-C-COO^-, torsion C= C-C-C(O)-O-, torsion D= C-C-O-(Ac or H), torsion, E= C-O-C(O)-CH_3

Minima for carnitine in gas phase by AM1									
A	B	C	D	δH_f	μ	F	%	Cont. δH_f	Cont. μ
g+	g+	a	g-	-91.21	12.74	0.80	80.31	-73.25	10.23
g+	g+	a	a	-90.27	13.42	0.16	16.42	-14.82	2.20
g-	g+	a	a	-88.9	15.25	0.02	1.62	-1.44	0.25
a	g+	s	g-	-88.62	12.91	0.01	1.01	-0.90	0.13
g-	g-	a	g-	-88.35	12.91	0.01	0.64	-0.57	0.08
								-90.97	12.90

Minima for acetylcholine in gas phase by AM1								
A	D	E	δH_f	μ	F	%	Cont. δH_f	Cont. μ
g+	g−	s	64.7	5.92	0.32	32.01	20.71	1.89
g−	g+	s	64.7	5.92	0.32	32.01	20.71	1.89
a	g+	s	65.15	6.2	0.15	14.98	9.75	0.93
g+	g+	s	65.36	6.83	0.11	10.51	6.86	0.72
g−	g−	s	65.36	6.84	0.11	10.51	6.86	0.72
							64.91	6.15

Minima for choline in gas phase by AM1.							
A	C	δH_f	μ	F	%	Cont. δH_f	Cont. μ
g+	a	102.97	2.34	0.50	49.99	51.48	1.17
g-	a	102.97	2.34	0.50	49.99	51.48	1.17
a	a	107.86	4.1	0.00	0.01	0.01	0.00
						102.97	2.34

Minima for 3-acetoxypropanoate in gas phase by AM1										
A	B	C	D	E	δH_f	μ	F	%	Cont. δH_f	Cont. μ
	g-	g+	g-	g+	-214.50	6.68	0.59	59.08	-126.72	3.95
	g-	g-	g-	g+	-214.26	6.64	0.39	39.27	-84.13	2.61
	g-	g-	g+	a	-211.71	13.37	0.01	0.53	-1.11	0.07
	g-	g-	g-	a	-211.40	13.22	0.00	0.31	-0.66	0.04
	g-	a	g-	g+	-211.31	9.43	0.00	0.27	-0.57	0.03
	g-	g+	a	a	-211.22	13.20	0.00	0.23	-0.49	0.03
	g-	g-	a	a	-210.38	13.28	0.00	0.06	-0.12	0.01
	a	a	g+	a	-210.30	11.20	0.00	0.05	-0.10	0.01
	g+	a	g+	a	-210.27	11.30	0.00	0.05	-0.10	0.01
	a	g+	g+	a	-210.26	11.16	0.00	0.05	-0.10	0.01
	a	a	g-	a	-210.17	11.22	0.00	0.04	-0.08	0.00
	g+	g-	a	a	-210.14	11.31	0.00	0.04	-0.08	0.00
	g+	g-	g+	a	-210.13	10.99	0.00	0.04	-0.08	0.00
	a	g-	g+	a	-208.60	9.51	0.00	0.00	-0.01	0.00
									-214.35	6.76

A= N-C-C-O, torsion B= H-C-C-COO^-, torsion C= C-C-C(O)-O-, torsion D= H-C-O-(Ac or H), torsion E= C-O-C(O)-CH_3

Minima for 3-hydroxypropanoate in gas phase by AM1								
B	C	D	δH_f	μ	F	%	Cont. δH_f	Cont. μ
g+	g+	g-	-177.41	5.37	0.26	25.83	-45.83	1.39
g+	a	g-	-177.41	5.37	0.26	25.62	-45.44	1.38
a	g-	a	-177.38	5.35	0.24	24.39	-43.27	1.30
a	a	a	-177.37	5.34	0.24	24.07	-42.68	1.29
g-	g-	g-	-173.34	6.57	0.00	0.03	-0.05	0.00
g-	g+	g-	-173.25	6.63	0.00	0.02	-0.04	0.00
g-	g-	a	-173.25	6.63	0.00	0.02	-0.04	0.00
g-	g-	a	-173.18	6.57	0.00	0.02	-0.04	0.00
g-	a	g+	-170.37	7.27	0.00	0.00	0.00	0.00
g-	g-	g+	-170.40	7.22	0.00	0.00	0.00	0.00
g-	g-	g+	-170.04	7.29	0.00	0.00	0.00	0.00
							-177.39	5.36

A= N-C-C-O, torsion B= H-C-C-COO^-, torsion C= C-C-C(O)-O-, torsion D= H-C-O-(Ac or H), torsion E= C-O-C(O)-CH_3

Minima for acetylcarnitine in water by AM1/COSMO										
A	B	C	D	E	δH_f	μ	F	%	Cont. δH_f	Cont. μ
g-	g-	a	g-	s	-191.8	26.67	0.41	40.73	-78.11	11.22
g-	a	a	a	s	-191.7	29.90	0.37	37.43	-71.77	10.62
g+	a	g+	a	s	-190.8	28.67	0.07	7.40	-14.11	2.23
a	a	g+	s	s	-190.6	26.35	0.06	5.74	-10.95	1.46
g-	g+	a	g-	s	-190	24.93	0.02	1.88	-3.58	0.50
g-	a	g-	a	s	-190	28.34	0.02	1.88	-3.58	0.57
g-	g-	g-	g-	s	-189.9	25.42	0.02	1.62	-3.07	0.43
a	a	g-	a	s	-189.7	26.52	0.01	1.14	-2.15	0.32
g-	g-	g-	a	s	-189.2	25.65	0.01	0.54	-1.02	0.13
a	g-	g+	g-	s	-189.2	22.03	0.01	0.50	-0.95	0.12
g+	g-	a	g-	s	-188.9	23.99	0.00	0.34	0.64	0.08
a	g-	g+	a	s	-188.9	21.55	0.00	0.31	-0.59	0.07
g-	g-	g-	a	s	-188.7	24.92	0.00	0.24	-0.45	0.06
a	g+	a	g-	s	-188.4	24.57	0.00	0.13	-0.24	0.03
g-	g-	a	a	a	-188.3	21.55	0.00	0.12	-0.22	0.02
									-191.44	27.86

Minima for carnitine in water by AM1/COSMO									
A	B	C	D	δH_f	μ	F	%	Cont. δH_f	Cont. μ
g-	a	g-	a	-153.8	29.17	0.57	57.2	-87.93	16.04
g-	g-	g-	s	-153.2	23.89	0.18	18.1	-27.76	4.77
g-	g+	g-	a	-152.7	23.69	0.09	8.77	-13.39	2.03
g-	g-	g-	a	-152.3	23.15	0.04	3.97	-6.04	1.01
g-	a	a	s	-152.2	27.87	0.04	3.77	-5.74	1.03
a	a	g-	a	-152	27.88	0.03	2.51	-3.82	0.73
g-	g-	g-	a	-151.9	24.04	0.02	2.27	-3.45	0.54
g-	g-	a	s	-151.8	23.57	0.02	1.82	-2.77	0.44
a	g+	g-	a	-151.4	23.49	0.01	0.99	-1.5	0.22
g-	g-	a	a	-151.2	23.15	0.01	0.61	-0.92	0.16
								-153.32	26.98

Minima for acetylcholine in water by AM1/COSMO								
A	D	E	δH_f	μ	F	%	Cont. δH_f	Cont. μ
g−	a	s	5.35	10.85	0.37	36.80	1.97	3.99
g−	g−	s	5.5	9.38	0.29	28.57	1.57	2.68
g+	g+	s	5.72	9.44	0.20	19.70	1.13	1.86
g+	a	s	6.44	8.66	0.06	5.84	0.38	0.51
a	g+	s	6.62	9.24	0.04	4.31	0.29	0.40
g+	a	a	7.3	12.6	0.01	1.37	0.10	0.17
g−	a	a	7.32	12.63	0.01	1.32	0.10	0.17
g−	a	a	7.36	12.58	0.01	1.23	0.09	0.16
g+	g+	a	7.95	12.72	0.00	0.46	0.04	0.06
g−	g−	a	8.02	12.72	0.00	0.41	0.03	0.05
							5.68	10.04

Minima for choline in water by AM1/COSMO							
A	C	δH_f	μ	F	%	Cont. δH_f	Cont. μ
g+	g−	48.07	5.25	0.45	45.36	21.81	2.40
g−	a	48.08	4.38	0.45	45.36	21.81	1.97
a	a	49.01	5.07	0.09	9.27	4.55	0.47
						48.16	4.48

Minima for 3-acetoxypropanoate in water by AM1/COSMO										
A	B	C	D	E	δH_f	μ	F	%	Cont. δH_f	Cont. μ
	g-	g-	a	a	-309.35	17.43	0.24	23.81	-73.66	4.15
	g-	g-	g+	a	-309.15	17.37	0.17	17.05	-52.70	2.96
	a	a	g+	a	-308.97	14.56	0.13	12.62	-39.00	1.84
	g+	g-	g+	a	-308.95	14.41	0.12	12.10	-37.39	1.74
	a	a	g-	a	-308.81	14.63	0.10	9.57	-29.55	1.40
	g+	g-	a	a	-308.71	14.53	0.08	8.03	-24.79	1.17
	g-	g-	g-	a	-308.70	17.28	0.08	7.91	-24.41	1.37
	g-	g+	a	a	-308.62	17.18	0.07	6.97	-21.50	1.20
	g-	a	g-	g+	-307.62	11.96	0.01	1.28	-3.92	0.15
	a	g-	a	a	-306.91	14.26	0.00	0.38	-1.18	0.05
	g-	g+	g-	g+	-306.73	13.95	0.00	0.28	-0.87	0.04
									-308.98	16.07

A= N-C-C-O, torsion B= H-C-C-COO^-, torsion C= C-C-C(O)-O-, torsion D= H-C-O-(Ac or H), torsion E= C-O-C(O)-CH_3

Minima for 3-hydroxypropanoate in water by AM1/COSMO								
B	C	D	δH_f	μ	F	%	Cont. δH_f	Cont. μ
g-	g-	g-	-267.81	9.24	0.30	30.39	-81.39	2.81
g-	g-	a	-267.70	9.09	0.25	25.45	-68.14	2.31
g+	a	g-	-267.19	7.91	0.11	10.74	-28.71	0.85
g-	g-	a	-267.19	9.19	0.11	10.83	-28.95	1.00
a	g-	a	-267.16	7.88	0.10	10.30	-27.52	0.81
g-	g+	g-	-267.08	9.13	0.09	8.89	-23.75	0.81
g-	g-	g+	-266.22	9.97	0.02	2.08	-5.53	0.21
g-	g+	g+	-265.60	10.09	0.01	0.73	-1.94	0.07
g-	a	g+	-265.46	10.01	0.01	0.58	-1.53	0.06
							-267.45	8.93

A= N-C-C-O, torsion B= H-C-C-COO^-, torsion C= C-C-C(O)-O-, torsion D= H-C-O-(Ac or H), torsion E= C-O-C(O)-CH_3

/***
The following are 6 archive entries generated by Gaussian94, and one
archive entry generated by Gaussian92, for the stretch of the P-C
bond in phosphonates.
At the end you will find the CHelpG output.
***/

1\1\GINC-SPIDER08\POpt\RHF\6-31+G(d)\C3H9O3P1\ROSAS\02-Jul-1996\1\\#RH
F 6-31+G* POPT SCF=DIRECT MAXDISK=10000000 GEOM=(CHECK, NOANGLE, NODIS
)\\global minimum for methylphosphonate\\0,1\P\O,1,r2\C,1,1.49751094,2
,a3\O,1,r4,2,a4,3,d4,0\C,4,r5,1,a5,2,d5,0\O,1,r6,2,a6,3,d6,0\C,6,r7,1,
a7,2,d7,0\H,3,r8,1,a8,2,d8,0\H,3,r9,1,a9,2,d9,0\H,3,r10,1,a10,2,d10,0\
H,5,r11,4,a11,1,d11,0\H,5,r12,4,a12,1,d12,0\H,5,r13,4,a13,1,d13,0\H,7,
r14,6,a14,1,d14,0\H,7,r15,6,a15,1,d15,0\H,7,r16,6,a16,1,d16,0\\r2=1.45
918885\a3=116.62263234\r4=1.59995561\a4=113.65066774\d4=-120.71597819\
r5=1.41871573\a5=121.25773067\d5=-34.23579237\r6=1.60109725\a6=110.168
21307\d6=123.38268836\r7=1.40925615\a7=125.29378933\d7=169.06112967\r8
=1.08261368\a8=114.65802958\d8=-177.58760781\r9=1.08292458\a9=110.5394
4808\d9=-56.57809938\r10=1.08372402\a10=110.00106926\d10=60.88328382\r
11=1.07958478\a11=106.60573556\d11=172.68763953\r12=1.08307464\a12=110
.43795199\d12=-68.29843227\r13=1.08001616\a13=110.29519769\d13=52.8795
328\r14=1.07966287\a14=106.86300885\d14=-170.5225183\r15=1.08253361\a1
5=111.11184789\d15=-51.0557592\r16=1.08494465\a16=110.96958777\d16=70.
96371703\\Version=IBM-RS6000-G94RevC.2\HF=-684.1613798\RMSD=2.339e-09\
RMSF=6.015e-02\Dipole=0.076348,0.234187,-1.9593291\PG=C01 [X(C3H9O3P1)
]\\@

1\1\GINC-SPIDER09\POpt\RHF\6-31+G(d)\C3H9O3P1\ROSAS\03-Jul-1996\1\\#RH
F 6-31+G* POPT SCF=DIRECT MAXDISK=10000000 GEOM=(NOANGLE, NODIS)\\glob
al minimum for methylphosphonate\\0,1\P\O,1,r2\C,1,1.59751094,2,a3\O,1
,r4,2,a4,3,d4,0\C,4,r5,1,a5,2,d5,0\O,1,r6,2,a6,3,d6,0\C,6,r7,1,a7,2,d7
,0\H,3,r8,1,a8,2,d8,0\H,3,r9,1,a9,2,d9,0\H,3,r10,1,a10,2,d10,0\H,5,r11
,4,a11,1,d11,0\H,5,r12,4,a12,1,d12,0\H,5,r13,4,a13,1,d13,0\H,7,r14,6,a
14,1,d14,0\H,7,r15,6,a15,1,d15,0\H,7,r16,6,a16,1,d16,0\\r2=1.45733246\
a3=116.24882103\r4=1.59584072\a4=114.19018359\d4=-119.87970402\r5=1.41
994352\a5=121.35850644\d5=-33.94107944\r6=1.59609034\a6=110.7614721\d6
=122.87564347\r7=1.41088501\a7=125.33225768\d7=170.34924623\r8=1.08343
783\a8=113.74982037\d8=-177.3980624\r9=1.0835696\a9=110.12525765\d9=-5
6.68437801\r10=1.08439628\a10=109.82893837\d10=61.20427921\r11=1.07936
228\a11=106.52253023\d11=171.55891981\r12=1.0829064\a12=110.35303436\d
12=-69.45639692\r13=1.07991698\a13=110.26053585\d13=51.77690809\r14=1.
07949114\a14=106.79143548\d14=-168.43607531\r15=1.0823602\a15=111.0790
4247\d15=-48.99414921\r16=1.08423817\a16=110.7906472\d16=73.03545695\\
Version=IBM-RS6000-G94RevC.2\HF=-684.2026712\RMSD=5.890e-09\RMSF=3.110
e-02\Dipole=-0.0439796,0.2504213,-1.9253029\PG=C01 [X(C3H9O3P1)]\\@

1\1\GINC-IRISDAV\POPT\RHF\6-31+G(D)\C3H9O3P1\ROSAS\5-Aug-1996\1\\#RHF
6-31+G* POPT SCF=DIRECT MAXDISK=10000000 GEOM=(NOANGLE, NODIS)\\global
 minimum for methylphosphonate\\0,1\P\O,1,r2\C,1,1.69751094,2,a3\O,1,r
4,2,a4,3,d4,0\C,4,r5,1,a5,2,d5,0\O,1,r6,2,a6,3,d6,0\C,6,r7,1,a7,2,d7,0
\H,3,r8,1,a8,2,d8,0\H,3,r9,1,a9,2,d9,0\H,3,r10,1,a10,2,d10,0\H,5,r11,4
,a11,1,d11,0\H,5,r12,4,a12,1,d12,0\H,5,r13,4,a13,1,d13,0\H,7,r14,6,a14
,1,d14,0\H,7,r15,6,a15,1,d15,0\H,7,r16,6,a16,1,d16,0\\r2=1.45593955\a3

=116.02270262\r4=1.59290662\a4=114.57568362\d4=-119.14066218\r5=1.4212
2444\a5=121.40471063\d5=-33.31939658\r6=1.59203079\a6=111.23454166\d6=
122.55856705\r7=1.41217066\a7=125.31731655\d7=171.80580784\r8=1.083662
19\a8=112.83391211\d8=-177.09532616\r9=1.08365283\a9=109.53919923\d9=-
56.73799168\r10=1.08438986\a10=109.61146189\d10=61.5406998\r11=1.07917
525\a11=106.44486772\d11=172.71677369\r12=1.0827243\a12=110.37831879\d
12=-68.2923733\r13=1.07982356\a13=110.23230051\d13=52.97864899\r14=1.0
7931427\a14=106.70392885\d14=-168.43295712\r15=1.08220938\a15=111.0273
1067\d15=-49.01685812\r16=1.08366525\a16=110.68879163\d16=73.01995132\
\Version=SGI-G92RevE.2\HF=-684.2220776\RMSD=7.282e-09\RMSF=1.218e-02\D
ipole=-0.1350396,0.2621133,-1.8966862\PG=C01 [X(C3H9O3P1)]\\@

1\1\GINC-SPIDER05\POpt\RHF\6-31+G(d)\C3H9O3P1\ROSAS\03-Jul-1996\1\\#RH
F 6-31+G* POPT SCF=DIRECT MAXDISK=10000000 GEOM=(NOANGLE, NODIS)\\glob
al minimum for methylphosphonate\\0,1\P\O,1,r2\C,1,1.79751094,2,a3\O,1
,r4,2,a4,3,d4,0\C,4,r5,1,a5,2,d5,0\O,1,r6,2,a6,3,d6,0\C,6,r7,1,a7,2,d7
,0\H,3,r8,1,a8,2,d8,0\H,3,r9,1,a9,2,d9,0\H,3,r10,1,a10,2,d10,0\H,5,r11
,4,a11,1,d11,0\H,5,r12,4,a12,1,d12,0\H,5,r13,4,a13,1,d13,0\H,7,r14,6,a
14,1,d14,0\H,7,r15,6,a15,1,d15,0\H,7,r16,6,a16,1,d16,0\\r2=1.45487976\
a3=115.88491861\r4=1.59078338\a4=114.85769197\d4=-118.58171934\r5=1.42
240708\a5=121.48478314\d5=-32.39677871\r6=1.58920376\a6=111.62169831\d
6=122.27787786\r7=1.41318941\a7=125.15881935\d7=173.12823077\r8=1.0833
4324\a8=111.94607674\d8=-175.78977748\r9=1.08327933\a9=108.81490901\d9
=-55.64258237\r10=1.08398142\a10=109.21933827\d10=62.86106788\r11=1.07
90397\a11=106.39234838\d11=172.10690727\r12=1.08257547\a12=110.3505863
9\d12=-68.92103001\r13=1.0797181\a13=110.23257004\d13=52.38902098\r14=
1.07919108\a14=106.63926727\d14=-168.52883941\r15=1.08207207\a15=110.9
9796385\d15=-49.12573429\r16=1.08326249\a16=110.59582411\d16=72.914628
64\\Version=IBM-RS6000-G94RevC.2\HF=-684.2272975\RMSD=3.554e-09\RMSF=5
.746e-06\Dipole=-0.2006816,0.2755983,-1.8693719\PG=C01 [X(C3H9O3P1)]\\
@

1\1\GINC-SPIDER11\POpt\RHF\6-31+G(d)\C3H9O3P1\ROSAS\04-Jul-1996\1\\#RH
F 6-31+G* POPT SCF=DIRECT MAXDISK=10000000 GEOM=(NOANGLE, NODIS)\\glob
al minimum for methylphosphonate\\0,1\P\O,1,r2\C,1,1.89751094,2,a3\O,1
,r4,2,a4,3,d4,0\C,4,r5,1,a5,2,d5,0\O,1,r6,2,a6,3,d6,0\C,6,r7,1,a7,2,d7
,0\H,3,r8,1,a8,2,d8,0\H,3,r9,1,a9,2,d9,0\H,3,r10,1,a10,2,d10,0\H,5,r11
,4,a11,1,d11,0\H,5,r12,4,a12,1,d12,0\H,5,r13,4,a13,1,d13,0\H,7,r14,6,a
14,1,d14,0\H,7,r15,6,a15,1,d15,0\H,7,r16,6,a16,1,d16,0\\r2=1.45411302\
a3=115.88014097\r4=1.58924636\a4=115.054377\d4=-118.11118209\r5=1.4233
4074\a5=121.49966598\d5=-31.79148713\r6=1.58718663\a6=111.90962481\d6=
122.12372708\r7=1.41397909\a7=124.93338366\d7=174.50791459\r8=1.082653
3\a8=111.00507304\d8=-173.92803724\r9=1.08255318\a9=107.96198332\d9=-5
3.98518862\r10=1.08316779\a10=108.75002344\d10=64.69905851\r11=1.07893
663\a11=106.32578866\d11=172.25166222\r12=1.08244806\a12=110.32368542\
d12=-68.78260838\r13=1.07963862\a13=110.21265167\d13=52.55436417\r14=1
.07907231\a14=106.57250047\d14=-169.55741654\r15=1.08195822\a15=110.93
516823\d15=-50.18202473\r16=1.0829712\a16=110.57012823\d16=71.85762115
\\Version=IBM-RS6000-G94RevC.2\HF=-684.2234566\RMSD=7.572e-09\RMSF=7.6
93e-03\Dipole=-0.2459652,0.2834066,-1.848513\PG=C01 [X(C3H9O3P1)]\\@

1\1\GINC-SPIDER11\POpt\RHF\6-31+G(d)\C3H9O3P1\ROSAS\05-Jul-1996\1\\#RH
F 6-31+G* POPT SCF=DIRECT MAXDISK=10000000 GEOM=(CHECK, NOANGLE, NODIS
)\\global minimum for methylphosphonate\\0,1\P\O,1,r2\C,1,1.99751094,2

,a3\O,1,r4,2,a4,3,d4,0\C,4,r5,1,a5,2,d5,0\O,1,r6,2,a6,3,d6,0\C,6,r7,1,
a7,2,d7,0\H,3,r8,1,a8,2,d8,0\H,3,r9,1,a9,2,d9,0\H,3,r10,1,a10,2,d10,0\
H,5,r11,4,a11,1,d11,0\H,5,r12,4,a12,1,d12,0\H,5,r13,4,a13,1,d13,0\H,7,
r14,6,a14,1,d14,0\H,7,r15,6,a15,1,d15,0\H,7,r16,6,a16,1,d16,0\\r2=1.45
355416\a3=115.94996778\r4=1.58824145\a4=115.16419059\d4=-117.80046945\
r5=1.42450516\a5=121.52063981\d5=-31.10963039\r6=1.58577872\a6=112.136
54699\d6=122.02788163\r7=1.41459552\a7=124.67519726\d7=175.69195874\r8
=1.08170823\a8=110.02909991\d8=-172.04278797\r9=1.0816024\a9=107.04407
492\d9=-52.23259027\r10=1.08211779\a10=108.15437394\d10=66.58160012\r1
1=1.07885185\a11=106.3147156\d11=172.31357431\r12=1.08235229\a12=110.3
5189589\d12=-68.71981067\r13=1.07955994\a13=110.21985526\d13=52.642222
74\r14=1.07898419\a14=106.53592138\d14=-170.37234006\r15=1.08188174\a1
5=110.95178509\d15=-50.97929288\r16=1.08274876\a16=110.48947187\d16=71
.04672139\\Version=IBM-RS6000-G94RevC.2\HF=-684.2139837\RMSD=4.845e-09
\RMSF=1.235e-02\Dipole=-0.2730956,0.2908895,-1.8309469\PG=C01 [X(C3H9O
3P1)]\\@

1\1\GINC-SPIDER03\POpt\RHF\6-31+G(d)\C3H9O3P1\ROSAS\08-Jul-1996\1\\#RH
F 6-31+G* POPT SCF=DIRECT MAXDISK=10000000 GEOM=(CHECK, NOANGLE, NODIS
)\\global minimum for methylphosphonate\\0,1\P\O,1,r2\C,1,2.09751094,2
,a3\O,1,r4,2,a4,3,d4,0\C,4,r5,1,a5,2,d5,0\O,1,r6,2,a6,3,d6,0\C,6,r7,1,
a7,2,d7,0\H,3,r8,1,a8,2,d8,0\H,3,r9,1,a9,2,d9,0\H,3,r10,1,a10,2,d10,0\
H,5,r11,4,a11,1,d11,0\H,5,r12,4,a12,1,d12,0\H,5,r13,4,a13,1,d13,0\H,7,
r14,6,a14,1,d14,0\H,7,r15,6,a15,1,d15,0\H,7,r16,6,a16,1,d16,0\\r2=1.45
326909\a3=116.01906879\r4=1.58767884\a4=115.2433084\d4=-117.54567746\r
5=1.42497121\a5=121.52869004\d5=-30.13908837\r6=1.58475594\a6=112.3374
9948\d6=121.93004385\r7=1.41489931\a7=124.40366304\d7=176.88939681\r8=
1.08057107\a8=109.01393503\d8=-168.91674636\r9=1.08042739\a9=106.00349
145\d9=-49.21783805\r10=1.08091722\a10=107.49260205\d10=69.68749364\r1
1=1.07880712\a11=106.23382876\d11=172.29976037\r12=1.08225003\a12=110.
29576259\d12=-68.74838529\r13=1.07950034\a13=110.21560915\d13=52.63013
73\r14=1.07890437\a14=106.48704916\d14=-171.71260863\r15=1.08178658\a1
5=110.86509996\d15=-52.34901813\r16=1.08264299\a16=110.50318511\d16=69
.65870195\\Version=IBM-RS6000-G94RevC.2\HF=-684.201192\RMSD=4.140e-09\
RMSF=1.501e-02\Dipole=-0.2806338,0.2984538,-1.8161212\PG=C01 [X(C3H9O3
P1)]\\@

/***
CHelpG results
***/

Breneman (CHELPG) radii used.
Generate Potential Derived Charges using the Breneman model, NDens= 1.
Grid spacing= .300 Box extension= 2.800
NStep X,Y,Z= 38 35 30 Total possible points= 39900
Number of Points to Fit= 11536

****

Electrostatic Properties Using The SCF Density

****

Atomic Center 1 is at .012844 .485266 -.176525

```
     Atomic Center    2 is at    .702230  1.193383 -1.244229
     Atomic Center    3 is at   -.839721  1.514896  1.025157
     Atomic Center    4 is at    .951911  -.398857   .754643
     Atomic Center    5 is at   2.117342 -1.035015   .244431
     Atomic Center    6 is at  -1.065488  -.531867  -.749420
     Atomic Center    7 is at  -1.797899 -1.461716   .022630
     Atomic Center    8 is at  -1.267768   .928689  1.829378
     Atomic Center    9 is at   -.132153  2.218386  1.446991
     Atomic Center   10 is at  -1.625558  2.069965   .525785
     Atomic Center   11 is at   2.638986 -1.443369  1.096172
     Atomic Center   12 is at   1.844141 -1.833268  -.433893
     Atomic Center   13 is at   2.739523  -.317792  -.269644
     Atomic Center   14 is at  -2.281565 -2.128946  -.674166
     Atomic Center   15 is at  -1.143190 -2.026605   .673120
     Atomic Center   16 is at  -2.552642  -.956303   .612865
  11536 points will be used for fitting atomic charges
Fitting point charges to eletrostatic potential
Charges from ESP fit, RMS=    .00240 RRMS=    .10857:
Charge=    .00000 Dipole=    -1.5375    -2.7574     3.6366 Tot=     4.8158
            1
 1  P    1.368600
 2  O    -.784336
 3  C    -.579133
 4  O    -.503634
 5  C     .145347
 6  O    -.530850
 7  C     .216839
 8  H     .138268
 9  H     .157603
10  H     .173251
11  H     .039414
12  H     .045974
13  H     .052397
14  H     .046796
15  H     .006564
16  H     .006900
-------------------------------------------------------------------

          Electrostatic Properties (Atomic Units)

-------------------------------------------------------------------
  Center     Electric        -------- Electric Field --------
             Potential         X           Y           Z
-------------------------------------------------------------------
   1 Atom    -53.999948
   2 Atom    -22.370070
   3 Atom    -14.717712
   4 Atom    -22.271626
   5 Atom    -14.662224
   6 Atom    -22.272658
   7 Atom    -14.653863
   8 Atom     -1.079319
   9 Atom     -1.081316
  10 Atom     -1.080620
```

11	Atom	-1.099444
12	Atom	-1.101122
13	Atom	-1.104207
14	Atom	-1.093588
15	Atom	-1.092637
16	Atom	-1.092799

]> *R*)-Carnitine, (*R*)-Acetylcarnitine, Morpholinium rings, and 2-Oxo-1,3,6-dioxazaphosphacinium rings. Víctor Manuel Rosas-García Dissertation Virginia Polytechnic Institute and State University Doctor of Philosophy Chemistry Richard D. Gandour Mark Anderson David Bevan Harry Gibson Thomas Hudliçky James Tanko Blacksburg Virginia carnitine acylcarnitine modeling of morpholinium rings phosphonate modeling of medium-sized rings conformational analysis Copyright 1997, Víctor M. Rosas-García

Full grid-search semiempirical calculations (AM1 and AM1/COSMO) on zwitterionic acetylcarnitine and carnitine, cationic acetylcholine and choline, and 3-acetoxypropanoate and 3-hydroxypropanoate in the gas phase and solution were performed. The calculated δH°_{hydr} for hydrolyses of acetylcarnitine to carnitine and of acetylcholine to choline show reasonable agreement with the experimental values in unbuffered solution (acetylcarnitine: -4.63 kcal/mol calc. vs. -7.43 kcal/mol exp.; acetylcholine: -3.20 kcal/mol calc. vs. -3.06 kcal/mol exp.) The results suggest that a change in the conformational populations of acetylcarnitine-carnitine upon hydrolysis maintains a nearly constant polarity, which keeps the work of desolvation of the products to a minimum. Acetylcholine-choline and acetoxypropanoate-hydroxypropanoate present a much higher work of desolvation, therefore yielding a lower free enthalpy of hydrolysis. Ab initio calculations at the RHF/6-31G* level for the carnitines and the cholines, and RHF/6-31+G for the propanoates, were done to calibrate the quality of the AM1 results for both the gas phase and in solution. The calculations in the gas phase involved full optimization of the AM1-optimized structures at the RHF/6-31G* level and RHF/6-31+G level, and single points at the MP2//RHF/6-31G* and MP2//RHF/6-31+G level to estimate correlation effects. The ab initio calculations in solution were single points on the AM1-optimized geometries and used the Tomasi solvent model. The ab initio results confirmed the qualitative reliability of the semiempirical results.

The conformational behavior of several 4,4-dimethylmorpholinium rings and 4,4-dimethyl-2-oxo-1,3,6-dioxazaphosphacinium rings was examined by molecular mechanics (AMBER* and AMBER*-GB/SA). The contrast between the behavior of these heterocycles and that of the parent saturated hydrocarbon systems formed a picture of the conformational behavior of these six- and eight-membered heterocycles. Influences of factors such as shortened bond lengths, varied bond angles, presence or absence of lone pairs and substituents, and dipolar alignment are described. Morpholinium rings show increased stabilization of the twist-boat with 1,1,3,3-di*gem* substitution, as compared to the parent cyclohexane systems. In the gas phase, the lowest chair/twist-boat energy gap is found in 2-(hydroxymethyl)-2,4,4-trimethylmorpholinium at 1.14 kcal/mol. The gap in the congruent hydrocarbon system is 5.23 kcal/mol. Differential solvation destabilizes the lowest energy twist-boat found in the gas phase, increasing the energy gap to 2.62 kcal/mol. The lowest chair/twist-boat energy gap in GB/SA water amounts to 1.45 kcal/mol, stabilized by solvation from an initial 2.13 kcal/mol in the gas phase.

In the dioxazaphosphacinium rings, the preferred conformation in the gas phase is the boat-chair (BC) and the populations are conformationally heterogeneous. As substituents approach a 1,1,3,3-di*gem* pattern, the twist-chair (TC) and twist-boat (TB) conformers are stabilized. Solvation favors boat-boat (BB) conformers, with the substituents exerting influence on the conformational preference only to stabilize the TB in two instances (*cis*-substituted ring and disubstituted ring). Solvation reduces the heterogeneity of the conformational populations.

Modeling of phosphonate moieties required development of molecular mechanics parameters for dimethyl methylphosphonate. Dimethyl methylphosphonate conformations were calculated at the RHF/6-31+G* level. Charges were calculated by the CHelpG scheme. The results were used to generate AMBER* parameters for modeling of alkylphosphonates in the gas phase and in solution. Comparison of the results of our AMBER* parameters against three other common force fields (MM2*, MMX and UFF) showed that AMBER* reproduced better the ab initio results when comparing absolute deviations in bond lengths, bond angles and torsion angles. The modified AMBER* reproduced better than the other three force fields several X-ray geometries of alkylphosphonates. Part of this work was supported by NIH Grant GM 42016

A mis padres, que me enseñaron el buen camino.

> "(. . .)I had an extreme desire to acquire instruction. But so soon as I had achieved the entire course of study at the close of which one is usually received into the ranks of the learned, I entirely changed my opinion. For I found myself embarrassed with so many doubts and errors that it seemed to me that the effort to instruct myself had no effect other than the increasing discovery of my own ignorance."

Rene Descartes, Discourse on the Method, ed. James Fieser (Internet Release, 1996)

I want to thank many people: first comes Rich, who provided guidance and taught me the intellectual habits that make a good scientist. Also my friends from Baton Rouge, especially Guillermo (G-man) and Renee Morales, for all the fun we had together and for their support. Here at Virginia Tech I cannot forget Brett Kite, for providing an always challenging environment; Alex Lostetter, Dan Lough and the people in the Newman Communities (LSU and Va Tech) for helping me keep my sanity. I thank Ms. Paige Phillips for her friendship and support, and for all those discussions about chemistry.

I extend my appreciation also to my professors back in UANL (Monterrey), especially Alejandro García, Celso Rodríguez and Ricardo Flores for their exhaustive teaching and for encouraging me to pursue advanced studies.

Quentin MacDonald (Columbia Univ.) provided invaluable help by teaching me the how-to of parameter development for molecular mechanics force fields. The Computing Center at Virginia Tech gave me a generous allocation of CPU time in the IBM SP2 and SMP machines. Without these contributions, many of my calculations would have been impossible.

I thank Jan Labanowski (Ohio Supercomputer Center) for his excellent job running the Computational Chemistry List (CCL) and the members of the CCL for the high quality of their discussions about computational chemistry. Interacting with them has been (and still is) a great educational experience.

Steve Young from MDL Information Systems, Inc. provided a free copy of the software used for the chemical drawings in this dissertation (ISIS/Draw v.1.2).

This has been a time of growth and change, and many people, too numerous to list here, have influenced my life. To those that go unmentioned, I express my deepest thanks. Rest assured that the seed you planted in me will not be lost.
Introduction.

This research attempted to determine the conformational behavior of several building blocks employed in our group for the design of enzymatic inhibitors. To this effect, this dissertation covers three main projects:

1. A computational study of the energetics of the hydrolysis of acetylcarnitine, accounting for the effects of changes in the predominant conformation due to solvation.
2. Effect of substitution on the conformational behavior of 4,4-dimethylmorpholinium rings, studied by computational techniques. fig.morph.gif, 0.44k 4,4-dimethylmorpholinium ring.
3. Development of parameters for AMBER* force field, and modeling of the conformational behavior of 4,4-dimethyl-2-oxo-1,3,6-dioxazaphosphacinium rings. fig.phosp.gif, 0.591KB 2,4,4,-trimethyl-2-oxo-1,3,6-dioxazaphosphacinium ring.

Purpose of study.

Our group designs and synthesizes transition-structure analogs (TSA) as inhibitors for carnitine acetyl-, octanoyl- and palmitoyltransferases (CAT, COT and, CPT-I and CPT-II). Normally the designer of an inhibitor tries to imitate the geometry of the transition structure Wolfenden, 1969 for the reaction catalyzed by the enzyme. Ideally, knowing the shape of the active site in an enzyme would enable us to design strong inhibitors. Presently, we only know the aminoacid sequences for CAT, COT, CPT-I and CPT-II, but their tertiary structures remain unknown. Until the resolution of the tertiary structures, only indirect methods can yield information about the shape of the active site. Knowledge of the preferred conformations adopted by TSAs, together with their measured inhibitory potency, can shed some light on the shape of the active site of these enzymes.

Inhibitors for CAT, COT and CPT can help us understand the role of each carnitine acyltransferase in the cell. Such understanding will help us in the design of potentially therapeutic compounds for diseases like diabetes and myocardial ischemia.

As the costs of experimentation and waste disposal continue to increase, it is imperative to find more efficient ways to choose targets for synthesis, especially those compounds with a greater chance of success as inhibitors. Computer modeling allows us to examine many compounds before choosing a target. The question then becomes: are there any modeling methods refined to the point they can yield reliable results for charged species? In particular, modeling of species with charges such as morpholinium, and zwitterions as that of carnitine in solution is difficult. Note. Cramer and Truhlar Cramer, 1995 have reviewed the performance of several solvation models and critically analyzed their implementations. One of their conclusions is that few software packages take into account both the contributions of charge and of multipolar moments, such as dipole, quadrupole, octapole and hexadecapole moments. We need, however, such modeling to understand the conformational preferences of the reactants --acetylcarnitine, carnitine-- and the enzymic reaction intermediate to achieve a more rational design of inhibitors. As several of our inhibitors include phosphonate substructures, we require methods able to deal with them. Such methods are not widely available; modeling of phosphonates has certainly lagged behind that of more popular phosphorus species, such as phosphates.

For these purposes we want to assess the ability of current state-of-the-art computational methods to model the compounds of our concern. We put particular emphasis on the inclusion of solvent effects, so we want to see the abilities of methods such as COSMO to reproduce properties such as dipole moments and heats of formation in solution. As we need to consider hundreds of conformations and configurations in crowded, charged species, optimization of computer resources is essential. We therefore need to evaluate the applicability of ab initio, semiempirical and molecular mechanics methods so that we spend a minimum of resources without undermining the quality of the predictions.

Among the problems we face are: the high free energy of hydrolysis of acetylcarnitine, which qualifies it as a high-energy molecule. This high energy has remained unexplained for about three decades. Friedman, 1955 The conformational dynamics of six- and eight-membered heterocycles are still imperfectly understood. Eliel, 1994 All these pieces of information can help us understand the mode of action of the inhibitors already available to us.

We can take two approaches to deal with modeling:

1. As a tool oriented to engineering of results, meaning that achieving experimental accuracy is the most important matter, even though the methods may not have full theoretical justification.
2. As a research tool, where the theoretical basis of the method can provide insight on the mechanisms underlying the phenomenon of interest, even if the approximation to experiment is only qualitative.

In general, molecular modelers use a combination of the two approaches, and it would be difficult to find examples of "pure" techniques, (techniques that adhere strictly to only one approach). Regardless of the "purity" of the technique employed, if we can model experimental results, we can gain confidence on the predictions generated for systems that have not been tested yet. How closely should the modeling results approach the experimental results to render the modeling as reliable? This is a somewhat subjective matter, as there are no hard guidelines to make such a decision. Historical. Introduction.

This review reproduces the latest advances in the design of carnitine acyltransferase inhibitors, and provides only the background necessary for a fruitful discussion of the conformational behavior of the inhibitors mentioned below. Acyltransferase inhibitors.

One common strategy to design enzymatic inhibitors is to use transition-structure-analog theory Wolfenden, 1969 to design a compound that the enzyme can recognize. Binding of the following tetrahedral intermediate is commonly considered important in the transfer of acyl groups to CoA: fig.gandour93.gif, 1.231KB Tetrahedral intermediate for Carnitine-CoA acyl transfer.

We can classify enzymatic inhibitors according to their observed effects on enzymatic activity (reversible or irreversible) or by their mechanism of action (competitive or noncompetitive). Irreversible inhibitors eliminate enzymatic activity in such a way that the enzyme does not recover its original activity. Reversible inhibitors allow the recovery of catalytic activity after elimination of the inhibitor. Competitive inhibitors bind to the active site instead of the substrate, while noncompetitive inhibitors do not attach themselves to the active site, so the substrate can still bind to the enzyme. Thus we have four main types of enzymatic inhibitors:

1. Competitive reversible
2. Competitive irreversible
3. Noncompetitive reversible
4. Noncompetitive irreversible

Competitive carnitine analogs constitute our primary concern, but we include summaries of the other types for the sake of completeness. We offer only a brief description of each, as Colucci and Gandour Colucci, 1988 have reviewed extensively CAT inhibitors. Competitive reversible inhibitors.

(*S*)-Carnitine and (*S*)-acetylcarnitine inhibit competitively pigeon CAT. Tipton, 1969 Tipton and Chase justified the recognition of the *S* isomers by postulating a two-point recognition site that binds only to carboxylate and ammonium. CATs extracted from bovine heart, pig heart and mouse-liver peroxisomes discriminated substantially between the (*R*) and the (*S*) isomers. The authors postulated a more restricted two-point recognition site, or a three-point recognition site for these CATs.

Aminocarnitine fig.aminocarn.gif, 0.595KB. Aminocarnitine. is a weak reversible competitive inhibitor for CAT, although it inhibits strongly both CPT-I and CPT-II. Kanamaru, 1985 Jenkins, 1985 Jenkins, 1986 Due to the isosteric relationship to carnitine, *N*-Acylated derivatives of racemic aminocarnitine can also inhibit reversibly carnitine acyltransferases, as shown by the great inhibitory potency of D,L-acetylaminocarnitine. Jenkins, 1985 (*R*)-acetylaminocarnitine --named "emeriamine" because it was isolated from a culture filtrate of *Emericella quadrilineata*-- showed even stronger inhibitory action than the racemic compound. Shinagawa, 1987

Gandour *et al.* Gandour, 1986 Gandour, 1992 showed good inhibition of CAT by hemiacylcarnitinium (HAC). Later, the same authors Gandour, 1988 Gandour, 1993 demonstrated the strong activity of hemipalmitoylcarnitinium (HPC) as a competitive inhibitor of CPT-I. HAC inhibits CAT, but not CPT. HPC inhibits CPT, but not CAT. It seemed that CPT requires a long chain for proper recognition of the substrate. These differences in the specificity of the inhibitors allowed for a partial mapping of the topographies of the active sites in both enzymes. The design of all these inhibitors relied on making them analogs of the tetrahedral intermediate mentioned previously by means of restricting the conformations with a morpholinium moiety: fig.HAC.gif, 0.740KB Hemiacylcarnitinium moiety.

The morpholinium ring locks the N-CH_2-CH-OH(Ac) torsion of the carnitine backbone in the *gauche* conformation. The authors stated the difficulty of excluding selective binding of the open form of the hemiacetal, but "presumably" hemiacylcarnitiniums bind as cyclic structures. NMR did not detect any open form of the compound in solution.

Saeed *et al.* Saeed, 1993 showed that 3-hydroxy-5,5-dimethylhexanoic acid fig.saeed93.gif, 0.581KB 3-hydroxy-5,5-dimethylhexanoic acid. competitively inhibited CAT, CPT-I and CPT-II, indicating that these enzymes require a positively charged center to show catalysis. Saeed *et al.* Saeed, 1994 later reported the inhibitory properties of 3-amino-5,5-dimethylhexanoic acid. fig.saeed94.gif, 0.585KB 3-amino-5,5-dimethylhexanoic acid. Both 3-hydroxy- and 3-amino-5,5-dimethylhexanoic acid are alternative substrates for CAT.

Gandour's group evaluated Protein Kinase C, COT and CPT inhibitors based on a 2-oxo-1,3,6-dioxazaphosphacinium moiety. Kumaravel, 1994 fig.kumaravel94.gif, 0.743KB 4-hexadecyl-2,4,4-trimethyl-2-oxo-1,3,6-dioxazaphosphacinium bromide. The authors tested racemic mixtures (2*S*, 4*S*)/(2*R*, 4*R*) and (2*S*, 4*R*)/(2*R*, 4*S*) and found they inhibited COT and CPT-II moderately.

Gandour's group also reported several CAT inhibitors incorporating a methylenecarboxylate substructure on a morpholinium ring. Sun, 1995 fig.sun95.gif, 1.157KB 6-(Carboxylatomethyl)-2-(hydroxymethyl)-2,4,4-trimethylmorpholinium. All four stereoisomers were evaluated for inhibitory activity and the authors concluded that "CAT recognizes both configurations at C2 and C6 in the analogues."

Anderson *et al.* Anderson, 1995 reported on the potency of a series of CPT-I inhibitors based on a phosphonate moiety designed by transition-structure-analog theory. fig.anderson951.gif, 0.842KB Anderson's phosphonate. This compound showed appreciable inhibitory activity. After trying systematic structural variations, they found that the following

phosphate: fig.anderson952.gif, 0.980KB Anderson's phosphate. inhibited to a level comparable to the phosphonate. Both the phosphonate and the phosphate could show similar detergency, thus explaining the similar inhibition. The authors discarded such an explanation due to the stronger inhibition shown by the *R* enantiomers when compared to the *S* enantiomers. Competitive irreversible inhibitors.

We can visualize the enzyme and the substrates as part of a ternary complex. Bisubstrate inhibitors resemble the spatial disposition of the substrates, leaving the enzyme as the "third" component. One of the earliest examples of a bisubstrate inhibitor is *S*-carboxymethyl-CoA-(*R*)-carnitine ester, reported by Chase and Tubbs. Bromoacetyl-CoA and bromoacetyl-(*R*)-carnitine are also bisubstrate inhibitors for CAT. Chase, 1969

Fritz and Schultz Fritz, 1965 reported inhibition of CAT by *p*-hydroxymercuribenzoate (HMB) at a concentration of 2.6 µM. Such inhibition was prevented or *partially* reversed by addition of acetyl-CoA, which suggested to these authors that HMB may bind to the active site.

Several groups have reported compounds possessing inhibitory activity towards carnitine acyltransferases. Etomoxir (2-[6-(4-chlorophenoxy)hexyl]oxirane-2-carboxylate) is an irreversible inhibitor of CPT-I. Eistetter, 1982 Tetradecylglycidate (TDGA) is also an oxirane-based irreversible competitive inhibitor of CPT-I. Tutwiler, 1985

Another competitive inhibitor is methoxycarbonylCoA disulfide, Venkatraghavan, 1983 which modifies selectively a sulfhydryl group in the active site. Dithioerythritol or thiocholine can partially reverse its action. Noncompetitive reversible inhibitors.

5,5'-Dithiobis(2-nitrobenzoic acid) (DTNB), reacts with sulfhydryl groups in a non-specific way. It inhibits pig heart CAT Fritz, 1963 and pigeon breast CAT. Venkatraghavan, 1983 Because this reagent forms disulfide linkages, adding a disulfide exchange reagent such as dithiothreitol, dithioerythritol or thiocholine can restore enzymatic activity.

Derrick and Ramsay Derrick, 1989 showed that malonylCoA is a reversible inhibitor of peroxisomal CPT-I, but does not show competitive behavior. These authors estimated that peroxisomal palmitoyltransferase activity constituted up to 20% of the peroxisomal + overt-mitochondrial pool in fed-rat liver. A concentration lower than 10µM of malonyl-CoA was enough to show 90% inhibition of the peroxisomal palmitoyltranferase. Noncompetitive irreversible inhibitors.

Fritz and Schultz Fritz, 1969 reported the inhibitory activity of $ZnCl_2$, $HgCl_2$, *N*-ethylmaleimide and iodoacetamide. Addition of ethanethiol prevented or partially reversed $HgCl_2$ inhibition. The authors did not cite the values of K_i for these compounds. Acetylcarnitine hydrolysis. Review of literature. Acylcarnitines in cellular metabolism.

Carnitine transports long-chain fatty acids across the mitochondrial membrane; thus, it is essential for lipid metabolism. Bieber reviewed the metabolic roles of acylcarnitine. Bieber, 1992 In microsomes and peroxisomes, carnitine transports medium-chain fatty acids into the cytosol. Non-Insulin-Dependent Diabetes (NIDD) and myocardial ischemia are among the diseases thought to bear a relationship to carnitine. Carnitine abounds in semen, although the reason for its presence remains a matter of speculation.

CAT catalyzes the acetylation of carnitine. Colucci, 1988 Acetylated carnitine has a large group-transfer potential, which makes it an active form of acetate that the mitochondria can use efficiently for oxidation. A carrier of acetyl groups is necessary, because the inner mitochondrial membrane is impermeable to Coenzyme A (CoA) and AcetylCoenzyme A (AcCoA).

There are (at least) two kinds of CPT, usually designated as CPT-I and CPT-II. CPT-I resides inside the inner mitochondrial membrane, while CPT-II is attached to the outside of the outer mitochondrial membrane. MalonylCoA, CPT-I and fatty acylCoA form part of a mechanism that regulates glucose levels. Inhibition of CPT-I by high malonylCoA levels suppresses fatty acid synthesis and oxidation in the liver, while a high level of fatty acylCoA lowers malonylCoA levels. Thus, CPT inhibitors are potential therapeutic agents for diabetes.

COT is the long-chain carnitine acyltransferase on peroxisomes. Peroxisomes have the ability to oxidize fatty acids.

COT is likely the enzyme responsible for forming carnitine esters of aromatic and branched alkyl acids, which form in the metabolism of drugs. Thermodynamics of acetylcarnitine hydrolysis. High-energy compounds.

The high energy of hydrolysis of acetylcarnitine places it in the "energy-rich" category, like ATP, but the body does not use acetylcarnitine for energy storage. Two basic questions are:

1. How does acetylcarnitine store chemical energy?
2. Why the need for such a high energy?

In this work we shall address mostly the first question, but first a note on terminology: we use the definition of energy-rich compound (also called "high-energy" compound) suggested by Jencks: Jencks, 1960

> "(. . .)an "energy-rich" compound is one which will react, *under physiological conditions*, with a substance that is commonly present in the environment, to liberate a large amount of free energy."

A free energy of hydrolysis is "high-energy" if it releases more than -7.0 kcal/mol, according to Jencks. In addition to ATP, other biomolecules qualify as energy-rich compounds.

Burton Burton, 1954 measured the free energy of hydrolysis of the thioester bond in AcCoA, reaching a value close to -8 kcal/mol. Burton noticed that this high free energy of hydrolysis puts AcCoA in the same category of "high-energy molecule" as ATP. Later, after determining the free energy of hydrolysis of thiol esters and aminoacid esters, Jencks *et al.* Jencks, 1960 concluded that both qualified as energy-rich compounds. Thiol esters had a free energy of hydrolysis of approx. -7.7 kcal/mol. They reported that, in general, the difference in free energies of hydrolyses between oxygen esters and thiol esters, was approx. 2.5 kcal/mol. This lower value of free energy of hydrolysis placed the oxygen esters outside the energy-rich range. Aminoacids seemed a special case, given that hydrolysis of glycine ethyl ester to the dissociated acid (zwitterionic form) had a free energy change of -8.4 kcal/mol *at pH=7.0*. As a comparison, hydrolysis of glycine ethyl ester to the undissociated acid yielded a free energy change of -1.97 kcal/mol, very similar to that of ethyl acetate. Jencks ascribed the high free energy of hydrolysis of glycine ethyl ester to a destabilizing effect of the positively charged ammonium group, rather than to the high acidity of glycine.

The first indication of the high-energy status of acetylcarnitine came from Friedman and Fraenkel Friedman, 1955 who reported on the ability of acetylcarnitine to transfer an acetyl group to CoA. They studied the effects of added carnitine on the enzymatic acetylation of *p*-aminobenzoic acid. Carnitine inhibited the acetylation reaction, while neither the zwitterion of glycine, choline or β-hydroxybutyrate showed any inhibitory activity. Acetylcarnitine reversed the inhibition produced by carnitine, while an equivalent amount of acetate added to a carnitine-inhibited system failed to restore enzymatic activity. A few years later, Fritz *et al.* Fritz, 1963 were the first to measure the high free energy change in the hydrolysis of acetylcarnitine. They reported a value of -7.9 kcal/mol at pH=7.0. This value changed little when using chains longer than acetyl. Acetylcarnitine participated in an acetyl group exchange equilibrium with AcCoA, with an equilibrium constant approximately equal 0.6. Their results indicated that acetylcarnitine required a free carboxylate group to show activity and they postulated anchimeric assistance of the carboxylate (fig.fritz63.gif, 2.362KB) as a step in the acetyl hydrolysis.

Müller and Strack Müller, 1973 determined the enthalpies of hydrolysis of a series of acylcarnitines, acetylcholine see figure, glycine methyl ester and acetyl-β-methylcholine by microcalorimetry. Their results show that the enthalpic term contributes the most to the free energy of hydrolysis. For the acylcarnitines, the entropic term is relatively small and invariant with chain length. Glycine methyl ester, acetyl-β-methylcholine, and acetylcarnitine methyl ester had less negative enthalpies of hydrolysis than acetylcarnitine, at pH=7.0, by about 2 kcal/mol. fig.hydrolysis2.gif, 2.714KB Comparison of free energies of hydrolysis between acetylcarnitine and acetylcholine. The previous values were determined at buffered pH=7.0. For the process at pH=4.0 (producing HOAc instead of $^-$OAc), the values are -4.63 kcal/mol for acetylcarnitine, and -3.20 kcal/mol for acetylcholine. The difference (1.43 kcal/mol) does not depend on pH.

Pierlik and Guynn Pierlik, 1975 compared the group-transfer potential of acetylcarnitine and acetylcholine under physiological conditions. They found the free energy of hydrolysis of acetylcarnitine only 1.21 kcal/mol more negative

than that for the hydrolysis of acetylcholine: -8.20 kcal/mol for acetylcarnitine vs. -6.99 kcal/mol for acetylcholine. Effects of solvation on thermodynamic quantities.

George *et al.* George, 1970 called attention to solvation effects in the hydrolysis of ATP. Their work remarked the influence of differential solvation between reactants and products as a "(. . .) major factor contributing to the thermodynamic reactivity (. . .)". They found that, as the charge increased, water solvation could stabilize multiply charged species such as phosphates, compensating for the increased electrostatic repulsion of the multiple negative charges present in such anions as pyrophosphate, tripolyphosphate, and glucose-6-phosphate.

Wolfenden discussed a similar question about the contributions of solvent effects in group-transfer potentials of uncharged species, mostly of mixed anhydrides of phosphoric and carboxylic acids, Wolfenden, 1989 as well as carbohydrates. Wolfenden, 1988 He pointed to the role of solvation energy of the products as a driving force for the reaction when he inquired "(. . .)whether the large negative change in free energy, that normally accompanies conversion of mixed phosphoric-carboxylic anhydrides to the products of their hydrolysis in dilute aqueous solution, may depend on differences in free energy of solvation between the reactants and the products." One of his findings was that "(. . .)the uncharged products of hydrolysis of acetyl dimethyl phosphate are solvated much more strongly by water than are the reactants."

Hayes *et al.* Hayes, 1978 did ab initio calculations on hydrolytic reactions of several high-energy molecules. Their results, which included "a crude reaction field solvent model", pointed out that the greatest contributions to the energies of hydrolysis came from the relative solvation energies of reactants and products. The relative solvation energies were "by far the most important factors in determining the energies", especially in those cases of greatest importance in energy storage and transduction, namely,

```
ATP --> ADP + orthophosphate
```

and

```
phosphocreatine + ADP --> creatine + ATP
```

Marsh *et al.* Marsh, 1980 applied ab initio methods together with molecular mechanics to the study of AMP derivatives. The greater exothermicity of 3',5'-cyclic AMP vs. trimethylene phosphate was attributed to: strain due to *trans* fusion in 3',5'-cyclic AMP (4-5 kcal/mol), an unfavorable O-C-C-O interaction relieved by ring opening (1-2 kcal/mol, because the interaction depends on the solvent), and 1-2 kcal/mol ascribable to differential solvation between reactants and products. Relationship between conformational preference and thermodynamics.

Colucci *et al.* Colucci, 1986 conducted NMR measurements in D_2O and MM2 calculations that showed that, upon hydrolysis, the predominant conformation of the carnitine skeleton changes from "folded" to "extended". The N-CH_2-CH-OH(Ac) torsion angle remained *g*- throughout. Results and Discussion.

The carnitine backbone can present two major conformations: fig.folded.gif, 0.510KB "Folded" conformer of carnitine. fig.extended.gif, 0.608KB "Extended" conformer of carnitine.

We can break down the process of hydrolysis to that of individual conformers: fig.hydrolysis1.gif, 2.491KB Hydrolyses of extended and folded conformers. In general, the ratios extended:folded before and after hydrolysis are not the same.

We studied the thermodynamics of acetylcarnitine hydrolysis by semiempirical and ab initio methods both in the gas phase and solvent. Conformational analyses in gas phase.

We calculated the enthalpies of formation and dipole moments of acetylcarnitine, carnitine, acetylcholine, choline, 3-acetoxypropanoate and 3-hydroxypropanoate in gas phase (see tables). We justified our use of enthalpies instead of free energies on the results reported by Müller and Strack. See review of literature.

- Acetylcarnitine in gas phase.
- Carnitine in gas phase.

- Acetylcholine in gas phase.
- Choline in gas phase.
- 3-Acetoxypropanoate in gas phase.
- 3-Hydroxypropanoate in gas phase.

The labels for torsion angles in the tables are as follows: fig.torsions.gif, 0.731KB Labels for torsion angles used in acetylcarnitine.

A
N-CH_2-CH-OH(Ac)

B
CH_2-CH-$CH_2$$COO^-$

C
C-C-C(O)-O^-

D
CH_2-CH-O-H(Ac)

E
C-O-C(O)-CH_3

The hydrolyses of acetylcholine to choline and of 3-acetoxypropanoate to 3-hydroxypropanoate constituted our reference points.

Acetylcholine and choline cannot show an extended or a folded conformation because they lack the methylenecarboxylate group, so they helped us assess the importance of the gauche effect (see section below) Sundaralingam, 1968 Wiberg, 1990 and of the CH_2-CH-O-H(Ac) torsion in the energetics of the hydrolysis. The propanoates can show folded and extended conformations, but are not affected by the gauche effect. Acetylcarnitine vs. carnitine.

Anti conformers of N-CH_2-CH-OH(Ac) account for nearly 50% of the population of acetylcarnitine but only 1% for carnitine. The CH_2-CH-CH_2-COO^- torsion angle always prefers *gauche* + (*g*+) in carnitine and *gauche* - (*g*-) in acetylcarnitine, so folded conformations comprise 100% of the populations. We can explain this preference by Coulombic attraction between the negatively charged carboxylate and the positively charged tetramethylammonium moiety: the *gauche* conformation allows the closest approach of the charged centers.

Given that the distance between the charged centers does not change much because the conformation is always folded, we expect only a small change in the dipole moment when hydrolyzing acetylcarnitine to carnitine (the dipole moments depend on charge separation). The results of the calculations confirm this suspicion; the global minimum in acetylcarnitine has a dipole moment of 12.15 D, and the global minimum in carnitine a dipole moment of 12.74 D. The hydroxyl group in carnitine could hydrogen bond to the carboxylate. A distance of 2.1 Å separates a carboxylate oxygen from the hydroxylic proton. This indicates a weak hydrogen bond. Acetylcholine vs. choline.

The calculations reproduce the gauche effect: in both cases, the N-CH_2-CH-OH(Ac) torsion angle prefers a *gauche* conformation. The *gauche*/*anti* energy gap in choline is 1.76 kcal/mol, but in acetylcholine is only 0.28 kcal/mol. Conformers with the N-CH_2-CH-OH(Ac) torsion angle as *anti* make up about 15% of the population in acetylcholine compared to the 0.01% in choline. Differences in the inductive effects of a hydroxylic oxygen vs. an ester oxygen might explain the difference, given that the gauche effect relates to the electronegativity of the atoms X and Y that form the fragment X-C-C-Y. Conjugation of the ester oxygen with the carbonyl group can decrease the inductive effect exerted on the carbon. Such effect does not appear in the hydroxylic oxygen.

The dipole moments have a good correlation with stability: in both cases the global minimum has the lowest dipole moment, 5.9 D in acetycholine and 2.34 D in choline. Acetoxypropanoate vs. hydroxypropanoate.

Acetoxypropanoate prefers a folded conformation Note. in gas phase. This means that torsion B prefers a *gauche* conformation, but this should not be construed as an example of gauche effect because carboxylates do not have an inductive effect strong enough to cause gauche effect. Juaristi, 1995 3-Hydroxypropanoate shows equal proportions of *g*+ and *anti*. Hydrogen bonding between the carboxylate and the hydroxyl group seems to favor the *anti* conformation. The expected dipole moment decreases from 6.8 D to 5.4 D upon hydrolysis. We defined torsion angle B in the propanoates as H-C-C-COO^-, taking the pro-R hydrogen. We did this to keep consistency with the terms "folded" and "extended", and to yield an easier comparison of the torsions between different compounds.

Steric effects and dipole moment reduction seem to control the conformational preference: the bulkiest groups (acetoxy and carboxylate) stay *anti* to each other, and the global minimum has the lowest dipole moment in acetoxypropanoate, 6.8 D and one of the lowest in hydroxypropanoate, 5.4 D. Carnitines vs. cholines.

The N-CH_2-CH-OH(Ac) torsion is *anti* in 15% of the population of acetylcholine, while this conformation makes up approx. 50% of the population in acetylcarnitine. Torsion angles CH_2-CH-O-H(Ac) and C-O-C(O)-CH_3 show parallel behavior: CH_2-CH-O-H(Ac) prefers *g*, although in acetylcarnitine nearly 35% of the conformers have this torsion as *anti*. C-O-C(O)-CH_3 prefers *syn* (*s*) in all cases.

For carnitine vs. choline we observe no major differences in the preferred conformations: N-CH_2-CH-OH(Ac) prefers *gauche*, although carnitine shows 1% of *anti* vs. the 0.01% for choline. CH_2-CH-O-H(Ac) always prefers the *anti*. Carnitines vs. propanoates.

Acetylcarnitine has 100% of the population folded, acetoxypropanoate has 92% folded. Torsion CH_2-CH-O-H(Ac) shows some variation, mostly because of the presence of several *anti* torsion angles in acetylcarnitine. Torsion angle C-O-C(O)-CH_3 shows opposite behavior in the two molecules: E prefers *s* in acetylcarnitine and *anti* in acetoxypropanoate. However, the global minima have the "same" conformation, as long as all the torsions in acetoxypropanoate have a corresponding torsion in acetylcarnitine.

In carnitine, 99% of the population is folded, vs. only 51% in hydroxypropanoate. Ab initio results in the gas phase.

We calculated the predominant conformations, found by AM1, at the RHF/6-31G* level of theory for both the zwitterions and the cations. Calculations for the anions used the 6-31+G basis set. We conducted full optimizations in the gas phase (see tables). In the following tables, the conformer designated as "1" is the global minimum by AM1, and "2" is the conformer next in energy above the global minimum. Table AM1 vs 6-31G* (gas) Compound δE AM1 (kcal/mol) δE HF/6-31G* (kcal/mol) δE MP2 (kcal/mol) μ AM1 (D) μ HF/6-31G* (D) μ MP2 (D) Acetylcarnitine 1 0.00 0.00 0.00 12.15 10.72 10.72 Acetylcarnitine 2 0.20 -0.66 0.86 12.66 12.81 12.81 Carnitine 1 0.00 0.00 0.00 12.74 12.22 12.22 Carnitine 2 0.94 -0.86 -0.50 13.42 12.54 12.54 Acetylcholine 1 0.00 0.00 0.00 5.92 6.16 6.16 Acetylcholine 2 0.45 0.55 1.83 6.20 6.95 6.95 Choline 1 0.00 0.00 0.00 2.34 1.86 1.86 Choline 2 4.89 4.46 5.76 4.10 3.64 3.64 Comparison of AM1 vs. 6-31G* calculations on carnitines and cholines in the gas phase. Comparison of AM1 vs. ab initio.

We observe several differences between the ab initio and the semiempirical results. The acetylcarnitine global minimum by AM1 is a local minimum in the HF/6-31G* hypersurface, but the inclusion of electronic correlation reverses the effect. The dipole moments calculated by HF/6-31G* follow the same trend as those calculated by AM1. Most of the ab initio dipole moments approach closely the values obtained by AM1, with one exception (Acetylcarnitine 1), where the ab initio value is nearly 1.4 D lower than the semiempirical. The difference may be due to the lack of geometric optimization, meaning that we do not have a stationary point on the HF/6-31G* hypersurface, or probably due to the adjustment in the number of surface points included in the calculation. For more details, refer to the Methods section.

Compound δE AM1 (kcal/mol) δE HF/6-31+G (kcal/mol) δE MP2 (kcal/mol) μ AM1 (D) μ HF/6-31+G* (D) μ MP2 (D) Acetoxypropanoate 1 0.00 0.00 0.00 6.68 8.41 8.41 Acetoxypropanoate 2 0.24 0.00 0.00 6.64 8.41 8.41 Hydroxypropanoate 1 0.00 0.00 0.00 5.37 5.82 5.82 Hydroxypropanoate 2 0.01 0.00 0.00 5.37 5.82 5.82 Comparison of

AM1 vs 6-31+G calculations on propanoates in the gas phase.

The table shows that in the anions, correlation effects Note. The Hartree-Fock approximation does not include the Coulombic repulsion between the electrons of different spins. The Coulombic repulsion of the electrons makes the motions of the electrons depend on one another ("correlates" the motions). Inclusion of electronic correlation requires schemes that consider configuration interaction. For more details on the procedures, see the book by Szabo and Ostlund Szabo, 1996. do not exert a great influence. Given that we did not use succesively higher levels of theory in the ab initio calculations to assess convergence, we cannot guarantee that correlation effects are not likely to change with higher levels of theory. More importantly to us, we observe that the trends of the MP2 calculations are the same as that of HF. We notice that the same geometries that AM1 calculated as different in energy, are degenerate by ab initio. This may be a reflection of the numerous convergence problems found when using AM1 on these anions. Conformational analyses including the effect of solvent.

We calculated the enthalpies of formation and dipole moments of acetylcarnitine, carnitine, acetylcholine, choline, 3-acetoxypropanoate and 3-hydroxypropanoate including the effect of solvent. We used full optimization in MOPAC93 using the COSMO solvent model, while the ab initio calculations involved single points at the RHF/6-31G* level of theory employing the solvent model developed by Tomasi. Miertus, 1982, Miertus, 1981

The following tables gather the semiempirical results:

- Acetylcarnitine in water.
- Carnitine in water.
- Acetylcholine in water.
- Choline in water.
- 3-Acetoxypropanoate in water.
- 3-Hydroxypropanoate in water.

Acetylcarnitine vs. carnitine

The N-CH_2-CH-OH(Ac) torsion remains fairly constant, although we still see a slight favoring of the *anti* conformation in acetylcarnitine: conformers with the N-CH_2-CH-OH(Ac) torsion angle *anti* make up almost 9% of the population in aceytlcarnitine, while in carnitine they account for less than 4%.

Regarding the CH_2-CH-CH_2-COO^-, the extended conformation constitutes 39% of the population, almost as much as the 43% of the folded. In carnitine we see the situation reversed, with the extended predominating over the folded (61% vs. 27% respectively). Differences in solvation can explain this reversal, as solvation differences relate to polarity: as the distance between the charged centers in the molecule differs between the folded and the extended, we expect the calculated dipole moments to differ as well. In acetylcarnitine, the folded has a dipole moment of 26.67 D vs. the 29.90 D of the extended. In carnitine, the folded conformation has a dipole moment of 23.89 D vs. the 29.17 D of the extended.

There is little support for hydrogen bonding between the carboxylate and the hydroxyl groups in carnitine. In the global minimum (extended conformer), the carboxylic oxygen closest to the hydroxylic proton is 3.8 Å away from it. The only conformer showing a O-H···O distance adequate for hydrogen bonding (2.8 Å) accounts for < 4% of the population. Acetylcholine vs. choline.

Anti conformers of N-CH_2-CH_2-OH(Ac) make up about 4% of the population in acetylcholine. In choline, these conformers account for more than 9% of the population. Differential solvation might hold the key to this reversal in the conformational preference: the global minimum in acetylcholine (N-CH_2-CH-OAc *g*-) has a dipole moment of 10.85 D, while the *anti* conformation of N-CH_2-CH-OAc has a dipole moment of 9.24 D, a difference of 1.6 D. In choline, on the other hand, the global minimum (N-CH_2-CH-OH *g*-) has a dipole moment of 5.25 D, while the *anti* conformer has a dipole moment of 5.07 D. The difference is now less than 0.2 D. We can see that solvation stabilizes the choline conformers to an almost equal extent, while in acetylcholine, the lower polarity of the *anti*-containing

conformer increases the energy gap, by solvating more the global minimum. Acetoxypropanoate vs. hydroxypropanoate.

The H-C-C-COO- torsion prefers *g*-, although the *anti* and the *g*+ each make up about 12% of the population. The C-C-C(O)-O- torsion does not change much upon hydrolysis, although hydroxypropanoate shows a much lower percentage of *g*+. The H-C-O-H(Ac) torsion prefers *anti* in both cases. Acetoxypropanoate in solution differs from gas phase by a greater stabilization of *anti* conformations in torsions CH_2-CH-CH_2-COO^-, CH_2-CH-O-H(Ac) and C-O-C(O)-CH_3. *Anti* conformers of these torsion angles have the highest dipole moments in the gas phase ($10 > \mu < 14$), so solvation reduces the energy gap to the point that the global minimum in solution accounts only for 0.06% of the population in the gas phase. The population of 3-hydroxypropanoate in solution differs from that in the gas phase because of a lower presence of the extended conformer. The dipole moment decreases from 16.07 D in acetoxypropanoate to 8.93 D in hydroxypropanoate. Carnitines vs. cholines.

Both acetylcarnitine and acetylcholine show gauche effects in the N-CH_2-CH-OAc torsion. The CH_2-CH-O-Ac torsion angle is *g*- in both global minima, but in acetylcarnitine it shows a greater population of *anti*. The CH-O-C(O)-CH_3 torsion angle is *syn*, with only one high energy conformer in acetylcarnitine that shows it in *anti*. The main difference between carnitine and choline is due to the chirality of carnitine: the N-CH_2-CH-OH(Ac) torsion angle prefers the *g*- over the *g*+, while choline shows equal populations of *g*+ and *g*-. The CH_2-CH-O-H torsion angle is always *anti* in choline, but it prefers *g*- in carnitine. Carnitines vs. propanoates.

In general, the carnitines show a greater proportion of *anti* torsions than the propanoates. The conformer that corresponds to the global minimum in acetoxypropanoate, accounts for 0.01% of the population in acetylcarnitine. *Anti* torsion CH_2-CH-CH_2COO^- comprises 50% of the population in acetylcarnitine, 60% in carnitine, 23% in acetoxypropanoate and 48% in hydroxypropanoate. Ab initio results including solvent.

We compare AM1/COSMO vs. 6-31G*/Tomasi in the following table

Compound Acetylcarnitine folded Acetylcarnitine extended Carnitine extended Carnitine folded Acetylcholine 1 Acetylcholine 2 Choline 1 Choline 2 δE AM1/COSMO 0.00 0.10 0.00 0.60 0.00 0.15 0.00 0.94 δE 6-31G*/Tomasi 0.00 5.24 0.00 -4.63 0.00 2.05 0.00 0.82 μ AM1/COSMO 26.7 29.9 29.2 23.9 10.9 9.4 5.3 5.1 μ 6-31G*/Tomasi 26.7 29.5 28.9 23.6 10.4 9.0 5.0 4.7 Comparison of AM1 vs. 6-31G* calculations on carnitines and cholines in water. table Compound Acetoxypropanoate 1 Acetoxypropanoate 2 Hydroxypropanoate 1 Hydroxypropanoate 2 δE AM1/COSMO 0.00 0.18 0.00 0.10 δE 6-31+G/Tomasi 0.00 0.90 0.00 1.51 μ AM1/COSMO 17.4 14.65 9.2 9.1 μ 6-31+G/Tomasi 18.65 15.67 9.92 9.81 Comparison of AM1 vs. 6-31+G calculations on propanoates in water.

The 6-31G* calculations were single points on the geometries optimized by AM1/COSMO. We wanted to assess the ability of the combination AM1/COSMO to reproduce the change in dipole moment when going from gas phase to solution. The gas phase results indicate the need for inclusion of correlation effects. We found such optimization prohibitively long, and the full conformational search by ab initio is at present beyond the computational resources available to us. Thermochemical calculations from semiempirical results.

We can calculate the expected enthalpies of hydrolysis. (See table.)

Compound Acetylcarnitine Acetylcholine Acetoxypropanoate AM1 -7.43 -3.06 -4.02 Exp. unbuffered H_2O -4.63 -3.20 n.a. Exp. buffered pH=7.0 -14.67 -13.00 n.a. Comparison of δH_{hydr} (kcal/mol) calculated at ε=78.3 vs. calorimetric values. From the previous table, we observe that the semiempirical results for the carnitines agree moderately well with the experimental values in unbuffered solution. The results for the cholines show good agreement with the experimental values.

The expectation values for both dipole moments and solvation energies, calculated by using Boltzmann's equation are displayed in the following table.

Compound Acetylcarnitine Carnitine Acetylcholine Choline Acetoxypropanoate Hydroxypropanoate Acetic acid Water μ (D) 27.90 27.12 9.89 4.79 2.65 exp. 16.07 8.93 6.40 2.22 $\delta H°_{solv}$ (kcal/mol) -64.76 -62.35 -59.30 -54.87 -94.54 -90.06 -17.02 -12.7 exp. -9.22 -9.98 exp. Expectation values for Dipoles (μ) and Enthalpies of Solvation ($\delta H°_{solv}$)

The variation in the enthalpies of solvation parallels that in the dipole moments: a smaller decrease in dipole moment upon hydrolysis (0.78 D for acetylcarnitine vs. 5.1 D for acetylcholine and 7.1 D in acetoxypropanoate) corresponds to a smaller decrease in enthalpy of solvation (-2.41 kcal/mol in acetylcarnitine vs. -4.43 kcal/mol for acetylcholine and -4.48 kcal/mol in acetoxypropanoate).

The calculated Boltzmann factors (F) for the conformers indicate that the N-CH_2-CH-OH(Ac) torsion prefers *g*- (>90%) for both acetylcarnitine and carnitine, thus we focus mostly on the CH_2-CH-CH_2-COO^- torsion: AM1 shows that in acetylcarnitine 37% of the population is extended, and 41% of the population is folded. The values for carnitine are 57% extended and 18% folded. As acetylcarnitine loses its acetyl group through hydrolysis, the carnitine backbone goes from folded to extended. Such conformational change implies a change in the dipole moment, reflected by the AM1 calculations. The expectation values for the dipole moments of these compounds are gathered in the table

We can highlight the results stated above for acetylcarnitine in the following figure: fig.highlight.gif, 4.852KB Changes in population and dipole moments upon hydrolysis.

We cannot draw a similar figure for acetylcholine and 3-acetoxypropanoate because of the lack of the methylenecarboxylate group, but we present the differences in expectation values for the enthalpies of solvation of the three acetates in the following figure: fig.solvation.gif, 4.823KB Differences in the energies of solvation for acetylcarnitine, acetylcholine and 3-acetoxypropanoate. The values between brackets are expectation values calculated using the complete Boltzmann populations. The upper values are enthalpies of hydration in kcal/mol, while the lower values are the expectation values for the dipole moments in Debyes.

We see that the dipole moment stays nearly constant for the carnitines (change <0.8 D). For the cholines, the dipole moment suffers a reduction of about 5.0 D, while for the propanoates the dipole reduction amounts to approximately 7.0 D. These lower polarities in choline and hydroxypropanoate imply an additional work (of desolvation) that consumes part of the free energy available from these reactions. Change in free energy measures the work obtainable from a process; thus, *the hydrolysis of acetylcholine yields a lower available work than that of acetylcarnitine because part of the free energy change in acetylcholine hydrolysis is spent desolvating the product (lower polarity choline).* We could apply a similar argument to acetoxypropanoate, but we cannot compare against experiment due to lack of experimental data.

Summary: Changes in polarity coupled to conformational changes can influence deeply the thermodynamics of reactions through differential solvation. Electroneutrality does not guarantee small solvation effects. Calculations have to account for the presence of charged centers, together with the influence in molecular polarity that such centers exert, to understand correctly the thermodynamics of charged systems. Modeling of tetrahedral intermediate: preliminary results.

We modeled the tetrahedral intermediate suggested by Gandour Gandour, 1985 to see the geometry of the preferred conformation. Because the attack of the sulfide on the carbonyl group generates a chiral center, we considered both diastereomers generated by the (*R*) configuration of carnitine (*R,R*) and (*R,S*) in GB/SA water. These results are preliminary, because we looked only for the global minimum, not concerning ourselves with finding all the conformers within 3.0 kcal/mol.

The conformational searches yielded the following global minima: fig.RSWat.gif, 0.807KB Global minimum for (*R,S*) tetrahedral intermediate in GB/SA water. RSWat.wrl, 16.938KB 3D Model of the *R,S* tetrahedral intermediate in GB/SA water. fig.RRWat.gif, 0.801KB Global minimum for (*R,R*) tetrahedral intermediate in GB/SA water. RRWat.wrl, 17.048KB 3D Model of the *R,R* tetrahedral intermediate in GB/SA water.

We then determined the RMS deviations after least-squares fit to the global minima obtained from the conformational searches for the phosphonate rings. The results are displayed in the table below:

Diastereomer *R,S R,R* Unsubstituted ring. 0.438, 0.685 0.619, 0.600 *Cis*-substituted ring. 0.384, 0.809 0.716, 0.548 *Trans*-substituted ring. 0.767, 0.822 0.931, 1.017 Dimethyl substituted ring. 0.322, 0.834 0.731, 0.537 RMS deviation after least-squares fitting of global minimum of rings to global minimum of intermediate in GB/SA water.

The first value in each cell corresponds to the fitting of the *oxo* oxygen on the phosphorus to the negatively charged oxygen (for the *R,S* isomer) or the methyl group on the TI (for the *R,R* isomer) in the tetrahedral intermediate. The second value corresponds to the matching of the *oxo* oxygen on the phosphorus to the sulfur atom in the intermediate (for both diastereomers). This is equivalent to saying that both halves of the ring compounds were used in the fit. The atoms used were: fig.fitTI.gif, 1.511KB Atom pairs used in the least squares fit between the phosphonate rings and the tetrahedral intermediate. The *oxo* oxygen on the phosphorus could be matched to any of the atoms marked with asterisks. For more details, see the Methods section.

The greater RMS values obtained when matching oxygen to sulfur atom should not be discarded offhand. S-C bonds (1.85 Å) are longer than C=O bonds (1.46 Å), so the difference influences significantly the final RMS value.

The following table displays the RMS values for the second most populated conformation in GB/SA water and the global minimum of the TI. The first value in each cell corresponds to the fitting of the *oxo* oxygen on the phosphorus to the methyl group on the TI, unless specified otherwise. The second value on each cell corresponds to the matching of the *oxo* oxygen on the phosphorus to the sulfur atom in the intermediate (in all cases).

Diastereomer *R,S R,R* Unsubstituted ring. 0.471, 0.630 0.975, 1.009 *Cis*-substituted ring. 0.740, 0.935 0.975, 1.011 *Trans*-substituted ring. 0.388, 0.747 0.652, 0.577 Dimethyl substituted ring. 1.201, 1.032 1.097, 1.092 RMS deviation after least-squares fitting of second most populated conformer of ring to global minimum of intermediate in GB/SA water.

To give us an idea of the best possible fit, we did a least-squares fitting of the tetrahedral center in the intermediate to dimethyl methylphosphonate. If we match the *oxo* group on phosphorus to the negatively charged oxygen in the intermediate, the RMS value is 0.227. If we match the *oxo* oxygen to the sulfur atom on the intermediate, the RMS value is 0.203. We note that the conformation around the tetrahedral center matched the *g+,a* conformer of dimethyl methylphosphonate, which is not a stationary point either by ab initio, or by AMBER*. The fit included only the heavy atoms around the phosphorus, not including the carbons attached to the oxygens. Effects of heteroatoms on conformational stability.

Here follows a general exposition of the changes in conformational behavior induced by the introduction of heteroatoms, according to the following scheme:

- General effects of introduction of heteroatoms.
- The anomeric effect.
- The gauche effect.

General effects of introduction of heteroatoms.

The first difference between hydrocarbon rings and their hetero-substituted analogs resides in the different bond lengths and bond angles involving the heteroatoms. Shorter distances, such as those of C-N and C-O bonds, increase the van der Waals repulsion among substituents in the ring. Longer distances between substituents, as those provided by C-P and C-S bonds, relieve van der Waals repulsions. Heteroatoms differ from carbon in the number of substituents they can bond to. This difference affects directly the energies of eclipsing interactions within the ring.

Differences in electronegativity introduce dipolar bonds, and the orientation of the resulting dipoles can change the relative stabilities within a series of conformers (*e.g.*, in side-by-side dipoles, antiparallel orientation reduces Coulombic repulsions, yielding a lower energy than a parallel orientation). In general, dipoles interact to yield the smallest possible total dipole. The lowest energy conformers tend to have the smallest dipole moments. Note. However, Perrin Perrin, 1995 has shown two counterexamples to the commonly accepted assertion that the conformer with the *largest* dipole moment is always the *least* stable. Polar solvents better stabilize conformers of greater polarity

as compared to the least polar ones. Given that the solvation of a molecule depends strongly on its polarity, solvation affects the energy gap between conformations possessing opposing dipoles and the ones containing parallel dipoles, (see p.747 on Eliel, Wilen and Mander's book Eliel, 1994). As different atoms have orbitals with different energies, accounting for stereoelectronic factors, such as orbital overlap, can help understand the conformations of heterocycles. The anomeric effect provides the best known case of such an interaction.

Consideration of the lone pairs present on certain heteroatoms requires an interaction model. The debate centers on the best description of the lone pairs density: as unhybridized n_σ and n_p orbitals, or as sp^3 hybrids. Although equivalent in many respects, the models differ in the directionality of the lone pairs. sp^3-Hybridized orbitals are directionally equivalent, while the unhybridized orbitals are not. Each model requires different spatial dispositions for optimal overlap. Laing has compiled theoretical and experimental evidence Laing, 1987 supporting the nonequivalence of the lone pairs. Kirby Kirby, 1983 has discussed the differences that arise between the two models, concluding that both are equivalent energetically speaking, so the choice of a particular description is done better on a per case basis. The anomeric effect.

This review follows the main lines of a similar one in the book by Juaristi and Cuevas. Juaristi, 1995 Edward Edward, 1955 Chu, 1959 reported on the axial preference of an alkoxy substituent in pyranoses, instead of the equatorial orientation one would expect from comparison with hydrocarbon systems. This behavior received the designation of anomeric effect. Later experimental results pointed to the existence of a similar phenomenon in compounds other than sugars, calling this effect the generalized anomeric effect. The generalized anomeric effect appears whenever a molecule possesses a fragment with the formula: R-Z-X-Y, where R is an alkyl group or hydrogen, X is an atom of intermediate electronegativity (C, Si, P, S among others), Y is an atom of stronger electronegativity than X (usually O, N or halogen (Hal)) and Z is an atom with lone pairs. By the previous criteria, we can suggest several common molecular fragments expected to show an anomeric effect: **R-O-C-O**, R-O-C-N, R-O-C-S, R-O-C-Hal, R-N-C-O, R-N-C-Hal, **R-S-C-O**, **R-O-P-O**, R-O-P-N and R-O-P-Hal among others.

In addition to the marked axial preference of oxygenated substituents on pyranose rings, some researchers report Lemieux, 1969 that polar solvents preferentially stabilize the more polar conformer (equatorial). The anomeric effect results in altered bond lengths and bond angles, specifically, the axial bond is shorter than usual, while the equatorial bond is longer. An electronic model, proposed early by Edward Edward, 1955 suggests that the repulsive interaction between the ring dipole and nearly parallel polar bonds in the equatorial conformer constitute the dominating forces in the preference for the axial position. Juaristi Juaristi, 1955 has criticized Edward's hypothesis on the grounds that it cannot explain the variations on bond lengths and angles. Juaristi favors a stereoelectronic interpretation suggested by Altona. Altona, 1963 Romers, 1969 The stereoelectronic hypothesis attributes the anomeric effect to mixing of the nonbonding electrons on oxygen with the antiperiplanar antibonding σ^* orbital in C-Y, involving a stereoelectronic interaction of type n_Z ----> $\sigma^*_{C\text{-}Y}$. Hyperconjugation (no-bond/double-bond resonance) can help us visualize the effect of the electron transfer involved in this interaction. Kirby Kirby, 1983 expressed this as "there is a stereoelectronic preference for conformations in which the best donor lone pair is antiperiplanar to the best acceptor bond." fig.anomeric.gif, 1.774KB Orbital and hyperconjugation description of the anomeric effect. The gauche effect.

Polar factors can markedly bias a conformation, such as in the case of the well-known gauche effect. Sundaralingam, 1968 The gauche effect is the preference, usually 1-2 kcal/mol, that 1,2-disubstituted ethanes show for the *gauche* conformation, as opposed to the *anti* conformation preferred by butane. Wolfe Wolfe, 1972 has described it as:

> "(. . .)when electron pairs or polar bonds are placed on adjacent pyramidal atoms, *syn*- or *anti*-periplanar orientations are disfavoured energetically with respect to that structure which contains the maximum number of *gauche* interactions."

Based on steric grounds, the *anti* conformation has greater stability. The gauche effect shows up in molecules containing the unit: X-C-C-Y, where X and Y are groups more electronegative than carbon (N, O or halogen). Wolfe rationalized the gauche effect by postulating that nuclear-electron attraction between X and Y dominated over nuclear-nuclear and electron-electron repulsions. Baddeley preferred to extend Altona's explanation of the anomeric effect, arguing that the gauche effect arises from σ ---> σ^* orbital interactions that stabilize the *gauche* conformation. This

interaction implies a no-bond/double-bond resonance model. Dionne and St-Jacques Dionne, 1987 used Baddeley's argument to justify the preference for the twist-boat conformation in 3-substituted-1,5-benzodioxepines in CHF_2Cl. Based on calculated bond paths, Wiberg and Murcko Wiberg, 1990 have suggested that the gauche effect originates in "bent" bonds, due to the greater electronegativity of the 1,2 substituents. This model implies a destabilization of the *anti* conformer, as opposed to the stabilization of the *gauche* conformer suggested by hyperconjugation.
Conformational analysis of heterocycles. Six-membered rings.

The conformational analysis of compounds containing six-membered rings has been a favorite topic for organic research; thus, we have not attempted an exhaustive coverage of the literature. This section only summarizes the background needed for an understanding of the conformational behavior described in this dissertation. The interested reader can find the fundamentals in the excellent textbook by Eliel, Wilen and Mander Eliel, 1994 while some finer points regarding conformational interconversion between chair and non-chair conformers are covered by Kellie and Riddell, Kellie 1974 and Anderson. Anderson, 1974

We can assign steric energies to any substituent attached to a six-membered ring. These steric energies are usually additive, a scheme that aids in the estimation of conformational stabilities. However, geminal substitution tends to break simple additivity: one group interferes with the free rotation of its geminal neighbor so the optimal conformation of a substituent may change when adding a geminal neighbor.

Weiser *et al.* Weiser, 1996 employed MM3(92) to study the conformational behavior of polyalkylated cyclohexanes, focusing mostly on how substituents affect the chair/twist-boat energy gap. They determined that

> (. . .) two methyls and two isopropyl groups are sufficient for rendering the twist-boat form the minimum energy conformation (. . .)

and determined *cis,trans,trans*-1,2-diisopropyl-3,4-dimethylcyclohexane; *cis,syn,cis*-1,2-diisopropyl-4,5-dimethylcyclohexane and *cis,syn,cis*-1,4-diisopropyl-2,5-dimethylcyclohexane as the less crowded cyclohexanes that prefer a twist-boat (0.8 kcal/mol lower in energy than the chair).

For geminally substituted cyclohexanes, the magnitudes of the energy gaps calculated by MM3 were: cyclohexane, 6.2 kcal/mol; Aped, 1992 1,1-dimethylcyclohexane, 5.7 kcal/mol; 1,1,3,3-tetramethylcyclohexane, 5.0 kcal/mol.

Mursakulov *et al.* Mursakulov, 1984 used MM2 to study 2-substituted-1,1-dimethylcyclohexanes. They found that *gem* substitution flattens the ring. They also found a "negligibly small" amount of twist-boat in 1,1,2-trimethylcyclohexane (4.6 kcal/mol higher in energy than the chair). All these calculations simulated gas phase. Dalling's Dalling, 1967 NMR results in solution, indicate an appreciable contribution of the twist-boat.

Kolossváry and Guida Kolossváry, 1993 did a comprehensive conformational search on cyclohexane using MM2*. MM2* is the modification of the MM2 force field included in the package MacroModel. Some of their results are gathered in the table below.

Conformation Chair Twist-boat Boat Half-chair MM3(92) 0.00 6.2 n.d.* n.d.* MM2* 0.00 5.35 6.45 10.51
Comparison of relative energies in the gas phase (kcal/mol) of cyclohexane conformations. *not determined

Sieburth Sieburth, 1994 analyzed crystal structures and molecular mechanics evidence on cyclohexene-like cyclohexanes and observed a correlation between the internal bond angles and the preference for a boat over a half-chair. He concluded that partially flattened cyclohexanes prefer a boat conformation when the average value of the internal bond angles approaches 114°. As the same average approaches 117.5°, the half-chair becomes preferred.
Eight-membered rings.

Note. We discuss the behavior of eight-membered heterocycles by using cyclooctane as a reference structure. A note on nomenclature is in order: Hendrickson developed the most generally employed nomenclature for cyclooctane conformations. Hendrickson, 1964 His system visualizes the conformations of cyclooctane as formed by cyclohexane components. Anet Anet, 1974 prefers the scheme suggested by Roberts Anderson, 1969 because Hendrickson's scheme leaves the S conformer without an appropriate name. For that reason, we prefer Roberts's naming scheme throughout

4

this dissertation. The naming of the S_4 conformer is the only difference between Hendrickson's and Roberts's schemes.

Molecular mechanics calculations in the gas phase show that the conformational hypersurface of cyclooctane has at least ten possible stationary points. Hendrickson, 1964 Hendrickson, 1967 Kolossváry, 1993 We can split these conformers into three families: chair-chair, boat-boat and boat-chair. We depict the conformers of cyclooctane by the usual perspective drawings and by their Weiler plots Ounsworth, 1987 as Weiler plots are specially clear bidimensional representations of ring conformation. Weiler plots depict the internal torsion angles of a ring in the form of a radar plot. We took all the values of the torsions from Hendrickson's paper to use in the "standard" Weiler plots. Hendrickson, 1967

Chair-chair.

- fig.crown.gif, 3.852KB **Crown** (D_{4d})
- fig.cc.gif, 2.539KB Chair-chair, **CC** (C_{2v})
- fig.tcc.gif, 2.446KB Twist-chair-chair, **TCC** (D_2)
- fig.tc.gif, 2.500KB Twist-chair, **TC** (C_{2v})
- fig.c.gif, 2.416KB Chair, **C** (C_{2h})

Boat-chair.

- fig.bc.gif, 2.304KB Boat-chair, **BC** (C_s)
- fig.tbc1.gif, 2.639KB fig.tbc-1.gif, 2.601KB Twist-boat-chair, **TBC** (C_2)

Boat-boat.

- fig.bb.gif, 2.486KB Boat-boat, **BB** (D_{2d})
- fig.tb.gif, 2.426KB Twist-boat, **TB** (S_4)
- fig.b.gif Boat, **B** (D_{2d})

Most calculations indicate BC as the global minimum in cyclooctane. Bixon, 1967 Hendrickson, 1967 Allinger, 1968 Kolossváry, 1993 This agrees with X-ray structural determinations of substituted cyclooctane rings, where the BC conformation predominates. Wiberg constitutes the exception, Wiberg, 1965 finding the BC 0.25 kcal/mol higher in energy than the TCC. After reviewing dynamic NMR, X-ray and computational results for cyclooctanes, Anet Anet, 1974 concluded that

> (. . .) most 'simple' cyclooctanes, including ketones and heterocyclic analogues, exist predominantly in BC conformations.

Reports differ, though, in the energetic ranking of other conformers. The latest results by Kolossváry and Guida, Kolossváry, 1993 who employed the MM2* Allinger, 1997 force field, indicated the TCC approximately 1.0 kcal/mol above the BC. Other researchers have reported the TCC form as 1.7 Hendrickson, 1967, 1.89 Bixon, 1967, -0.25 Wiberg, 1965 and 2.20 Anet, 1971 kcal/mol higher in energy than the BC.

The crown is another conformation thought to be significantly populated in cyclooctane. Again, we find differences in the reported energies relative to the BC: 2.8 Hendrickson, 1967, 3.62 Bixon, 1967, 0.26 Wiberg, 1965 and 2.09 Anet, 1971 kcal/mol higher in energy than the BC. Kolossváry did not report finding the crown conformer.

Anet and Yavari Anet, 1972 studied oxocane (fig.oxo.gif, 0.414KB), 1,3-dioxocane (fig.dioxo.gif, 0.411KB), 1,3,6-trioxocane (fig.trioxo.gif, 0.420KB), 1,3,5,7-tetraoxocane (fig.tetraoxo.gif, 0.432KB), by ^{1}H NMR. 1,3-dioxocane showed a single BC conformation, while the two other compounds showed a mixture of two conformations. The authors could not identify positively the conformations, but they argued for a TCC or a crown, in equilibrium with a

distorted BC. They reasoned that transannular repulsions between the oxygen atoms would destabilize the BC conformers.

Dale *et al.* Dale, 1972 studied by ^{1}H NMR the conformational behavior in $CDCl_3$ and $CHFCl_2$ of 1,3,5,7-tetraoxocane, 2,2- or 6,6-disubstituted-1,3,6-trioxocanes and 2,2,6,6-tetrasubstituted-1,3-dioxocanes, including 2,2-dimethyl-1,3-dioxocane (fig.22dioxo.gif, 0.516KB), 6,6-dimethyl-1,3-dioxocane (fig.66dioxo.gif, 0.530KB) and 2,2,6,6-tetramethyl-1,3-dioxocane (fig.2266dioxo.gif, 0.573KB). Their findings led them to conclude that incorporation of a 1,3-dioxa moiety does not suffice to favor the BB over the BC, but geminal substitution at position 6 is also necessary. Geminal substitution on the 2 position had little effect on determining the preferred conformer.

Armarego reviewed extensively the stereochemistry of heterocyclic compounds. Armarego, 1977 He showed that oxocanes, in general, prefer a BC conformation, sometimes with substantial amount of the crown. Special substitution patterns, such as in 2,4,6,8-tetrakis(trischloromethyl)-1,3,5,7-tetraoxocane can bias the global minimum to the crown form. Thiocanes also prefer the BC, but the crown form is destabilized, as compared to oxocanes.

Riddell discussed briefly the conformational behavior of eight-membered rings, both saturated and heterocyclic. Riddell, 1980 Based on X-ray data, he concluded that, in general, heterocyclic eight-membered rings adopt either a crown or a BC conformation. Both conformations are generally regarded as the most populated conformations in cyclooctane.

Moore and Anet reviewed the dynamics of hydrocarbon and heteroatom-substituted eight-membered rings. Moore, 1984 The BC conformer predominated in oxocane, according to NMR data, although the position of the oxygen was not well-defined, opening the possibility for several BC conformations coexisting in solution. The crown conformer constituted a minor part of the population.

Quin thoroughly reviewed conformational analyses of medium-sized heterocycles. Quin, 1988 1,3,6-Dioxaza- and 1,3,6-dioxaphospha-2-oxide phosphocanes preferred to crystallize as crowns. In 2-oxo-1,3,6-trioxaphosphocane a CC conformation predominated at room temperature, as determined by ^{31}P NMR. In 1,3-dioxa-6-thia-2-phosphocane the most abundant conformer was the crown.

In their review of nitrogen heterocycles, Alder and White conclude that azacanes with one nitrogen atom prefer the BC. Alder, 1988 Nevertheless, additional heteroatoms give rise to a preference for other conformations, such as in the case of the explosive HMX. HMX prefers a CC global minimum. fig.hmx.gif, 0.823KB Structure of explosive HMX.

Kolossváry and Guida Kolossváry, 1993 did a comprehensive conformational search on cyclooctane. They reported the energetic ranking as follows: BC, 0.00; TCC, 0.96; CC, 1.14; TBC (minimum), 1.67; TBC (saddle), 2.80; TB, 3.13; BB, 3.56; C, 7.50 kcal/mol.

In summary, eight-membered rings prefer a BC conformer as global minimum, but heteroatom substitution can shift the preference towards a member of the chair-chair family or to a BB conformer. Conformational analyses of morpholinium rings.

Previous modeling results from our group Savle, 1997 on the following compound fig.savle97.gif, 0.583KB 2-(Hydroxymethyl)-2,4,4-trimethylmorpholinium studied by Savle *et al.* pointed to a predominant chair conformation, the same as in solid state. The calculations also showed that twist-boat conformations accounted for approximately 14% of the total population. To support this finding and to gain a better understanding of the conformational behavior of these rings, we analyzed by computational methods the conformational behavior of:

1. 1,1-dimethylcyclohexane in the gas phase
2. (*R*)-1,1,3-trimethylcyclohexane in the gas phase
3. 1,1,3,3-tetramethylcyclohexane in the gas phase
4. (*R*)-1-ethyl-1,3,3-trimethylcyclohexane in the gas phase

as a reference framework to understand:

1. 4,4-dimethylmorpholinium in the gas phase and in solution
2. (*S*)-2,4,4-trimethylmorpholinium in the gas phase and in solution
3. 2,2,4,4-tetramethylmorpholinium in the gas phase and in solution
4. (*R*)-2-hydroxymethyl-2,4,4-trimethylmorpholinium in the gas phase and in solution

respectively. Modeling in the gas phase.

We tried to get a complete picture of the energy hypersurface by means of MonteCarlo conformational searches. We chose MonteCarlo instead of Grid Search because the number of torsion angles involved made the Grid Search less efficient. For more details about the procedures, see the Methods section. Conformational energies always refer to the global minimum as 0.00 kcal/mol, unless specified otherwise.

The following figure summarizes the nomenclature we use for cyclohexane conformers: fig.hexConfs.gif, 3.085KB Labeling of substituent positions in cyclohexane. Cyclohexanes.

1,1-Dimethylcyclohexane yielded five minima: a chair (global minimum) and four twist-boats (pairs at 5.09 and 6.12 kcal/mol). Introducing *gem* substitutents in a chair destabilizes it by worsening 1,3-diaxial interactions, both because of the greater volume of the methyl group and because of Allinger buttressing, where an equatorial substituent pushes its axial neighbor into closer proximity with the other 1,3 axial substituents. As the chair constitutes our zero-energy reference, we can only *deduce* the changes in stability of the chair after analyzing the behavior of other higher-energy conformers.

We find a boat at 6.51 kcal/mol. We observe a smaller chair/boat energy gap than in cyclohexane: 6.95 kcal/mol. This boat has the methyl groups on an in-plane carbon so this increases the strain due to eclipsing interactions with the hydrogens on the adjacent in-plane carbon, and possibly with the hydrogens on the in-plane carbon connected through the out-of-plane carbon. We have now the first indication of a destabilized chair: *if* the increase in 1,3-diaxial strain in the chair is greater than the increase due to 1,2 and 1,3 eclipsing strain, the resulting destabilization of the chair yields a smaller energy-gap. A second boat appears at 9.99, a much greater energy gap than in cyclohexane. This boat has the methyl substituents in bowsprit-flagpole positions. The crowding of a methyl group with the flagpole hydrogen can account for almost 3 kcal/mol of conformational energy.

The hypersurface shows four twist-boats, two enantiomeric pairs at 5.09 and 6.12 kcal/mol. The pair at 5.09 has the *gem* substitution on an in-plane carbon. Again, we find a smaller energy gap than the 5.82 kcal/mol in cyclohexane. We can apply an argument similar to the one used for the boats: a greater destabilization of the chair than of the twist-boat, to explain the reduced gap. The twist-boats at 6.12 have flagpole-flagpole interactions strong enough to destabilize this conformer even more than the chair. Apparently, flagpole-flagpole interactions are at least 2 kcal/mol stronger than the 1,3-diaxial. We can justify this by pointing out that 1,3-diaxial interactions involve mostly changes in torsion angles, while flagpole-flagpole interactions involve compression of bonds. Bonds have usually much stiffer potentials and narrower energy wells than torsions.

Six half-chairs determine three distinguishable barriers to chair/twist-boat interconversion with values of 10.98, 11.91 and 12.12 kcal/mol. All these values are close to the 11.25 kcal/mol found in cyclohexane. Both 1,3-diaxial as well as eclipsing interactions are still at work within the appropriate substitution patterns. On the other hand, flagpole-flagpole interactions are eliminated, because there is only one out-of-plane carbon. This eliminates one of the sources of strong destabilization.

Trimethylcyclohexane shows eight minima: two chairs (0.00 and 3.61 kcal/mol) and six twist-boats. 1,3-Diaxial interactions (worsened by Allinger buttressing) raise the chair to 3.61 kcal/mol. The lowest energy boat appears at 6.68 kcal/mol, slightly higher than the lowest boat in dimethylcyclohexane (6.51), but still lower than the 6.95 kcal/mol in cyclohexane. This boat has 1,3(in-plane) diaxial interactions with one of the *gem* methyls. The third methyl group is in the equatorial orientation on one in-plane carbon. At this energy, this boat splits the twist-boats in two triads. The first three twist-boats have the third methyl group either in bowsprit or in equatorial orientation, thus reducing van der Waals interactions. The other three have the methyl group in flagpole or axial orientation, so van der Waals repulsions increase. This increased repulsion affects the bond angles: when the methyl group is equatorial, the H_{ax}-C-R bond

angle approaches 109° very closely. When the same methyl group is axial, the H_{ax}-C-R bond angle approaches 112°, being "pushed out" by the bulk of the methyl group. Higher in energy than these twist-boats, we find three boats. All have 1,3-diaxial methyl-methyl interactions, or methyl-hydrogen flagpole interactions.

Trimethylcyclohexane shows four half-chairs, three of them with energies close to the half-chair in cyclohexane: 11.22, 11.57 and 11.83 vs. 11.25. The first two half-chairs show a small energetic difference between the pseudoaxial and pseudoequatorial positions in the half-chair when the *gem* substituents are on the out-of-plane carbon, about 0.35 kcal/mol. The fourth chair has an energy of 17.05, and vibrational analysis characterized it as a higher-order saddle point. This half-chair has 1,3-diaxial methyl-methyl repulsions, justifying its high energy.

1,1,3,3-Tetramethylcyclohexane shows the effects of crowding substituents, now in a 1,1,3,3 di*gem* pattern. We see only one chair as the global minimum. The bond angles indicate strain due to 1,3-diaxial repulsions: the Me_{ax}-C-C angles are 113.3°, compared to the 109.2° of the H_{ax}-C-C angles. The change in the bond angles also affects the torsions according to the equation reported by Romers *et al.* Romers, 1969:

$$\cos(\omega) = -\cos(\theta)/(1+\cos(\theta))$$

where ω is the torsion angle, and θ is the adjacent bond angle. Measuring the torsion adjacent to the 113.3° angle yields a value of 46.8°; the value calculated with the equation is 49.1°. We can attribute the deviation to the uncommon steric crowding produced by the 1,1,3,3 di*gem* substitution pattern which induces severe 1,3-diaxial stress.

After the chair, we find four twist-boats in enantiomeric pairs. The first pair shows up at 3.93 kcal/mol and the second at 4.75. Both values, 3.93 and 4.75, are lower than the 5.82 kcal/mol gap in cyclohexane. In the first one, all the methyl groups are on in-plane carbons, the second pair has two methyls in bowsprit-flagpole positions. We infer that the reduction of the gap has to do with the severe strain present in the chair, although the twist-boats have strain as evidenced by the flatter torsions found. The average of the (absolute) values of the torsions in the cyclohexane twist-boat is 42.8°. The same average in tetramethylcyclohexane comes out as 39.8° and 37.3°.

Two boats, corresponding to the two pairs of twist-boats, have energies of 5.23 and 6.57 kcal/mol. Again, the highest energy boat has flagpole-equatorial methyl-methyl interactions, increasing its energy over the boat with axial-axial methyl-methyl interactions.

At first sight, (*R*)-1-ethyl-1,3,3-trimethylcyclohexane shows a very complex energy hypersurface, due to the additional degree of freedom introduced by the ethyl group. We can formally generate this hypersurface by splitting each conformer of 1,1,3,3-tetramethylcyclooctane into a family of three conformers, because of the three positions the ethyl group can take (*g*+, *g*- and *anti*). Closer examination reveals that some families are missing a member, namely, the one with the ethyl group pointing inside the ring.

All the minima within 3.5 kcal/mol above the global minimum are exclusively chairs. The first saddle point comes at 3.72 kcal/mol, and it involves rotation of the ethyl group. After that, we find a series of twist-boats, differing in most cases only in the ethyl torsion. The first ten twist-boats are spread over a range from 4.10 kcal/mol to 4.92 kcal/mol. With an average of 4.52 kcal/mol, the chair/twist-boat energy gap is somewhat greater than the 4.34 kcal/mol in 1,1,3,3-tetramethylcyclohexane, in agreement with a greater strain produced by the ethyl group. The first boat appears at 5.33 kcal, higher than its corresponding conformer in 1,1,3,3-tetramethylcyclohexane at 5.23 kcal/mol. 1,1,3,3-tetramethylcyclohexane has another boat at 6.57 kcal/mol, the corresponding conformer here shows up at 6.77 kcal/mol. The lowest energy chair in 1,1,3,3-tetramethylcyclohexane has an energy of 8.09 kcal/mol; the corresponding stationary point in this molecule is at 8.29.

To summarize, destabilization of the chair plays heavily in the determination of the chair/twist-boat energy gap because of the presence of six 1,3-diaxial interactions in the chair. Geminal substitution increases the diaxial strain due to Allinger buttressing. Flagpole-flagpole interactions in twist-boats account for more of the increase in strain energy than diaxial interactions. Flagpole-flagpole interactions in boats are stronger than both eclipsing and axial interactions on the in-plane carbons. Flagpole-axial interactions dominate the stability of the half-chairs, followed by eclipsing and 1-3 diaxial interactions. Our results agree with those obtained by Weiser *et al.* Weiser, 1996 who employed the

MM3(92) force field. This agreement gives us confidence in the ability of AMBER* to model crowded systems.

Cyclohexanes have helped us develop a picture of the changes in energy and strain due to steric effects. In the following sections we use the insights obtained from the analysis of these hydrocarbons as a framework for the inclusion of steric effects due to heteroatom substitution, dipolar effects and the effects of solvation. Morpholinium rings.

4,4-Dimethylmorpholinium yielded five minima: one chair (global minimum) and four twist-boats grouped in two degenerate pairs with energies equal to 4.51 and 7.12 kcal/mol, respectively. A boat at 5.38 kcal/mol separates these pairs. The other two twist-boats interconvert through a boat at 7.55 kcal/mol. The half-chairs at 10.80 and 11.11 can collapse to the chair or to any of the two twist-boats at 4.51. The half-chair at 10.80 kcal/mol has a plane of symmetry that passes through the N and the O, so it provides a symmetric path for chair-chair interconversion or for the generation of the lowest energy twist-boats. The half-chairs at 11.11 can collapse to any of the lowest energy twist-boats, but they are distorted as compared to the half-chair at 10.80. They represent asymmetric paths for chair-chair interconversion or for the generation of the twist-boats.

Comparing dimethylcyclohexane vs. 4,4-dimethylmorpholinium, one change is the lowering of the energy of one of the cyclohexane boats, from 9.99 to 5.38 kcal/mol. This corresponds to the boat having the methyl groups in bowsprit-flagpole positions. Crowding with the nearby hydrogen strains the dimethylcyclohexane molecule. Dimethylmorpholinium, having an oxygen atom that eliminates the hydrogen atoms at position 4, relieves that strain. The other boat in dimethylmorpholinium (7.55 kcal/mol) corresponds to the boat at 6.51 kcal/mol in dimethylcyclohexane. These conformers have the methyl substituents on one in-plane carbon. These methyl groups eclipse the adjacent pair of hydrogens so, the greater bulk of the methyl groups, together with the shorter C-N bond, increases the strain by steric hindrance. The asymmetric half-chairs do not have analogs in dimethylcyclohexane, but in the symmetric ones we observe only small changes to lower energies. We can ascribe them to the loss of the hydrogen atoms opposite to the nitrogen, relieving flagpole-flagpole, axial, and eclipsing interactions.

Conformer Dimethylcyclohexane 4,4-Dimethylmorpholinium chair 0.00 0.00 twist-boat 5.09 4.51 twist-boat 5.09 4.51 twist-boat 6.12 7.12 twist-boat 6.12 7.12 boat 6.51 7.55 boat 9.99 5.38 half-chair 10.98 10.80 half-chair 10.98 NA half-chair 11.19 11.11 half-chair 11.19 11.11 half-chair 12.12 11.67 half-chair 12.12 NA Comparison of morpholinium vs. dimethylcyclohexane in the gas phase.

Trimethylmorpholinium shows a total of eight minima: two chairs (the global minimum and a chair at 4.73 kcal/mol), and six twist-boats. The global minimum is a chair, followed by a twist boat at 4.49 kcal/mol. This twist-boat has the non-*gem* methyl group in equatorial. The lower destabilization of the global minimum can justify the greater energy gap here. Another chair, now with the non-*gem* methyl group axial, shows up at 4.73 kcal/mol. A combination of increased 1,3-diaxial repulsions due to bulkier groups held closer by the shorter C-N and C-O bonds can explain this higher energy (Let us not forget the lower strain present in the global minimum). The lowest energy boat appears at 7.55 kcal/mol with the non-*gem* methyl in bowsprit and the *gem* substituents on an in-plane carbon. The shape is somewhat distorted from an ideal boat, leaving the equatorial *gem* methyl in an orientation closer to axial and distorting the H_{ax}-C-C angles from the ideal 109.5°, making them as open as 111°. The lowest energy half-chair is at 10.91 kcal/mol. As with dimethylmorpholinium, we find several asymmetric half-chairs. The presence of a boat at 11.68 kcal/mol is very noticeable, as the highest energy boat we have found so far.

Drawing a comparison of trimethylmorpholinium and trimethylcyclohexane we see that the second chair is destabilized, going from 3.61 to 4.73 kcal/mol. We can ascribe part of this increased energy gap to a less strained global minimum. From the study of cyclohexanes we learned that 1,3-diaxial interactions could justify the reduced energy gaps found. Since morpholinium compounds lack a pair of hydrogens, that reduces the total number of 1,3-diaxial contacts from six to four, thus reducing the strain introduced by substituents on the ring. A similar observation comes from the boat at 10.09 in trimethylcyclohexane, which goes as low as 5.35 kcal/mol in the trimethylmorpholinium. The loss of flagpole-flagpole crowding helps this lowering of the energy. Additionally, even though this structure does not have any elements of symmetry because of its chirality, the ring conformation is the same as we found in dimethylmorpholinium (with the heteroatoms split by a mirror plane). Given that none of the methyl substituents on the ring have any heteroatoms, the dipolar picture approaches very closely that of

dimethylmorpholinium. This results in a reduction of the overall dipole moment due to a symmetric disposition of the dipoles.

Trimethylcyclohexane Trimethylmorpholinium Chair 0.00 0.00 Chair 3.61 4.73 Twist-boat 5.10 7.04 Twist-boat 6.14 4.49 Twist-boat 6.28 6.84 Boat 6.68 7.55 Twist-boat 7.44 4.89 Twist-boat 7.63 9.06 Twist-boat 8.53 5.37 Boat 10.09 5.35 Half-chair 11.22 10.91 Half-chair 11.57 11.11 Half-chair 11.83 12.22 Boat 8.76 n.f.** Boat 10.52 n.f.* Boat 10.09 n.f.* Boat 10.52 n.f.* Half-chair 17.05 n.f.* Boat n.f.* 9.41 Boat n.f.* 11.68 Half-chair n.f.* 11.61 Comparison of energies of trimethylmorpholinium vs. trimethylcyclohexane in the gas phase (kcal/mol).

The gap between the first twist-boat in trimethylcyclohexane and its chair (5.10 kcal/mol) increases in the morpholinium to 7.04. Flagpole-flagpole hydrogen-hydrogen repulsion can partly justify this result, even more because the non-*gem* methyl in bowsprit forces Allinger buttressing, but examination of the internal angles of the ring reveals that they are distorted, having an average value of 111.9°.

Tetramethylmorpholinium has a two enantiomeric chairs as global minima. These enantiomers arise because the introduction of nitrogen and oxygen into the global minimum in 1,1,3,3-tetramethylcyclohexane eliminates a plane of symmetry. After the chairs we find three enantiomeric pairs of twist-boats. The energies are remarkably low if compared to the other morpholinium rings: 1.25, 1.56 and 3.93 kcal/mol vs. the lowest twist-boat at 4.51 kcal/mol in morpholinium; or the lowest twist-boat in trimethylmorpholinium at 4.49 kcal/mol. Because of the 1,3 substitution pattern, two of the twist-boat pairs have two methyl groups in bowsprit-flagpole orientations. These are the lowest energy pairs. The third pair has all methyl groups on in-plane carbons, and corresponds to the highest energy pair. We indicated above that flagpole-flagpole interactions weighed heavily among the contributions to strain, followed by diaxial and eclipsing. The lowest energy twist-boats have a methyl in flagpole, but they lack the opposite flagpole atom, leaving only 1,3-diaxial and eclipsing repulsions to induce strain. The third twist-boat pair shows flagpole-flagpole H···H contacts, plus 1,3-diaxial Me···Me contacts, therefore increasing the strain.

At 6.69 kcal/mol we find the lowest energy half-chair in all the cases analyzed so far. It shows some distortion from a perfect half-chair, and lacks strong flagpole interactions because of the absence of hydrogens on position 1,4 to the out-of-plane carbon. Higher in energy we see a pair of enantiomeric boats at 6.86 kcal/mol. These have the methyl groups on nitrogen in bowsprit-flagpole, so flagpole-flagpole interactions do not destabilize it. By analyzing the possible permutations of the substituents on the basic boat framework, we realize that another boat, with all four methyl groups on in-plane carbons, is possible. Under the conditions of our minimizations, AMBER* could not find those stationary points in the search, nor refine the gradients under acceptable cutoffs when the structures were generated by hand and increased the number of iterations for the minimization routine (Full Matrix Newton Raphson) to 2000. **This is probably the first indication of a significant shortcoming in this model chemistry.** After this result, we consider that the results obtained at higher energies may be less reliable, so we mention only the presence of three more half-chairs, one of them classified as a multiple maximum by AMBER* although there are no methyl rotations that could justify the additional imaginary frequencies.

We can contrast tetramethylmorpholinium vs. tetramethylcyclohexane. About half of the stationary points found in morpholinium have a cyclohexane analog. Most of the conformers lose strain in the morpholinium analog, due to the loss of 1,3-diaxial or flagpole interactions. There are only two cases of more highly strained morpholinium analogs: the boat at 6.57 kcal/mol in the cyclohexane rises to 6.86 kcal/mol in the morpholinium, and the enantiomeric half-chairs that go from 8.25 to 8.73 kcal/mol. Both increases correspond to increased eclipsing interactions brought about by the shorter C-N bonds. The presence of so many conformers without an analog, casts some doubt on the ability of AMBER* to model such **highly crowded, charged** systems.

Conformer Tetramethylcyclohexane Tetramethylmorpholinium Chair 0.00 0.00 Twist-boat 4.75 1.25 & 1.56 Twist-boat 4.75 1.25 & 1.56 Boat 6.57 6.86 Half-chair 8.09 6.98 Half-chair 8.25 8.73 Half-chair 8.25 8.73 Half-chair 9.60 6.69 Twist-boat 3.93 n.f.* Twist-boat 3.93 n.f.* Boat 5.23 n.f.* Half-chair 14.07 n.f.* Half-chair 14.07 n.f.* Twist-boat n.f.* 3.93 Twist-boat n.f.* 3.93 Half-chair n.f.* 13.32 Comparison of energies of tetramethylcyclohexane vs. tetramethylmorpholinium in the gas phase (kcal/mol).

The introduction of a hydroxymethyl group complicates the hypersurface of the molecule, by adding the degrees of

freedom, in the -CH_2-CH_2-O-H fragment. Additionally, the new N-CH-CH_2-OH fragment shows a gauche effect. Given the risks involved in modeling such crowded systems uncovered by the results on tetramethylmorpholinium, we content ourselves with discussing only the lowest energy conformers, namely, those within 3.0 kcal/mol above the global minimum.

In (*R*)-2-hydroxymethyl-2,4,4-trimethylmorpholinium, the global minimum is a chair. Within 3.0 kcal/mol we observe a mixture of chairs and twist-boats. Comparing ethyltrimethylcyclohexane vs. hydroxymethyl trimethylmorpholinium shows the effects of polar influences on conformation. These comparisons take into account seven torsions: the six internal torsions of the ring and the torsion of the bond that connects the ethyl group to the ring because we cannot compare the C-C-O-H torsion to the C-C-CH_2-H. The table shows many changes in the energetic ranking of the conformers, the most noticeable of which is the change in global minimum. Both conformations are chairs, but they differ in the orientation of the ethyl/hydroxymethyl substituent. The ethyl prefers an *anti* conformation, while the hydroxymethyl prefers *gauche*. Some conformers show substantial stabilization by the presence of heteroatoms, like in the case of a twist-boat at 7.00 kcal/mol in the cyclohexane. The morpholinium analog has an energy of 2.18 kcal/mol. The gauche effect comes into play here: a *gauche* ethyl group has a much higher energy than a *gauche* hydroxymethyl subject to gauche effect. Most conformers in this morpholinium ring are highly distorted, and the identification of analog pairs was difficult.

Conformer Ethyltrimethylcyclohexane (Hydroxymethyl)trimethylmorpholinium Chair 0.00 2.19 Chair 0.35 1.77 Chair 0.74 1.60 Chair 0.74 0.81 Chair 1.64 0.00 Twist-boat 4.10 2.20 Twist-boat 4.83 2.13 Twist-boat 5.23 1.14 Twist-boat 5.39 2.71 Twist-boat 7.00 2.18 Twist-boat n.f.* 1.20 Chair n.f.* 2.01 Twist-boat n.f.* 2.35 Chair n.f.* 2.56 Chair n.f.* 2.73 Comparison of energies of ethyltrimethylcyclohexane vs. (hydroxymethyl)trimethylmorpholinium in the gas phase (kcal/mol).

In summary, morpholinium rings follow the same general trends regarding steric interactions uncovered by the study of hydrocarbon systems, but the shorter bond lengths associated with heteroatoms increase steric crowding. In analyzing these conformational energies one has to take into consideration the reduced number of diaxial or flagpole interactions, due to the absence of substituents on atoms like oxygen. Dipole-dipole interactions do not seem to play an important role in the gas phase. We might have pushed AMBER* over its limit of applicability by modeling this highly crowded, charged species. Modeling in GB/SA water.

MacroModel does not calculate dipole moments, but all calculations including solvent report a "Solvation" component. We use this term in lieu of a dipole moment. The table for dimethylmorpholinium in water displays all the minima found including GB/SA water. The comparison between gas phase and water

Conformer Energy in the gas phase Energy in GB/SA water δH_{solv} Chair 0.00 0.00 -56.66 Twist-boat 4.51 4.92 -55.35 Boat 5.38 5.93 -54.91 Twist-boat 7.12 6.66 -57.52 Boat 7.55 7.23 -57.06 Half-chair 10.80 10.66 -56.22 Half-chair 11.11 11.07 -56.47 Conformational and solvation energies (kcal/mol) of dimethylmorpholinium in the gas phase and GB/SA water. shows the differences brought about by solvation. The chair is the global minimum, two twist-boats have energies of 4.92 kcal/mol, having increased its energy by 0.41 kcal/mol from the 4.51 it had in the gas phase. The other pair has an energy of 6.66 kcal/mol. Solvation has stabilized these structures by 0.46 kcal/mol from their 7.12 kcal/mol in the gas phase. The energy gap between the twist-boats has decreased from 2.61 kcal/mol to 1.74 kcal/mol. The difference in solvation is 2.17 kcal/mol, which explains, at least qualitatively, the difference. One of the boats, at 5.38 kcal/mol in the gas phase, has an energy of 5.93 in solution. The energetic ranking in solution follows closely that in the gas phase, although the highest energy half-chair (pair) in solution does not show up in the gas phase. The saddle points have among the highest solvation terms in the set of conformers, to the exception of the first boat. The first boat has the nitrogen and the oxygen in out-of-plane positions; thus they are part of a plane of symmetry of the molecule. This symmetric arrangement makes for a partial cancellation of the dipoles, thereby reducing the overall molecular dipole moment, and yielding the smallest δH_{solv}.

Trimethylmorpholinium in water shows eight minima, two chairs and six twist-boats. The chairs follow the same energetic ranking as in the gas phase. So do most of the twist-boats. There is only one crossover in the ranking, as the twist-boat at 6.84 kcal/mol in the gas phase increases its energy to 7.54 kcal/mol in water, while the one at 7.04 is

lowered to 6.63 kcal/mol by solvation. The solvation terms fit that behavior, given that the twist-boat at 6.63 kcal/mol in water has a solvation term equal to -56.08 kcal/mol, while the destabilized twist-boat has a solvation equal to -53.50. This destabilized twist-boat does not have any elements of symmetry because of its chirality, but the ring conformation is the same as we found in dimethylmorpholinium in solution (with the heteroatoms in out-of-plane positions). Thus the dipolar picture approaches closely that of dimethylmorpholinium. This results in a reduction of the overall dipole moment due to a symmetric disposition of the dipoles and in one of the lowest solvation terms in the table.

Conformer Energy in the gas phase Energy in GB/SA water δH_{solv} Chair 0.00 0.00 -55.27 Twist-boat 4.49 4.87 -53.97 Chair 4.73 4.88 -54.98 Twist-boat 4.89 5.36 -53.66 Boat 5.35 5.86 -53.52 Twist-boat 5.37 5.76 -54.12 Twist-boat 6.84 7.54 -53.50 Twist-boat 7.04 6.63 -56.08 Boat 7.55 12.57? -55.59 Twist-boat 9.06 8.87 -55.59 Boat 9.41 n.f.* ---- Half-chair 10.91 10.84, 14.93 -54.76 Half-chair 11.11 n.f.* ---- Half-chair 11.61 n.f.* ---- Boat 11.68 n.f.* ---- Half-chair 12.22 n.f.* ---- Boat n.f.* 7.33 -55.54 Half-chair n.f.* 11.15 -55.02 Half-chair n.f.* 18.28 -55.73 Conformational and solvation energies (kcal/mol) of trimethylmorpholinium in the gas phase and GB/SA water.

In tetramethylmorpholinium, all the stationary points we found had their corresponding structure in the gas phase. They keep the same energetic ranking as in the gas phase. We found two chairs (0.00 kcal/mol) and three pairs of enantiomeric twist-boats. The saddle points, however, deviate from the calculated behavior in the gas phase. One boat and two half-chairs could not be found, despite repeated attempts with increased energy windows (perhaps one more of the difficulties AMBER* has coping with charged, crowded molecules?). The boats have energies of 4.18 and 6.67 kcal/mol and the half-chairs have energies of 6.47 and 9.95 kcal/mol.

Conformer Energy in the gas phase Energy in GB/SA water δH_{solv} Chair 0.00 0.00 -53.71 Chair 0.00 0.00 -53.71 Twist-boat 1.25 1.63 -52.40 Twist-boat 1.25 1.63 -52.40 Twist-boat 1.56 2.07 -52.23 Twist-boat 1.56 2.07 -52.23 Twist-boat 3.93 3.67 -54.27 Twist-boat 3.93 3.67 -54.27 Half-chair 6.69 6.47* -53.57 Boat 6.86 6.67 -53.85 Boat 6.86 6.67* -53.85 Half-chair 6.98 n.f.* ---- Half-chair 8.73 n.f.* ---- Half-chair 13.32 n.f.* ---- Conformational and solvation energies (kcal/mol) of tetramethylmorpholinium in the gas phase and GB/SA water.

(*R*)-2-Hydroxymethyl-2,4,4-trimethylmorpholinium in water has a chair as the global minimum. The global minimum has the C-C-CH_2-O-H fragment in *g*-,*g*+. There are two chairs within 1 kcal/mol above the global minimum. One differs only in the conformation of the C-C-CH_2-O-H fragment: *g*+,*g*-. The other one is a conformational diastereomer with the ring torsion angles as "mirror images" of those in the global minimum. That chirality, plus that due to the chiral center already present in the molecule, give rise to diastereomers. The O-C-C-C torsion is *anti* in a few high energy (>4.9 kcal/mol) instances. The C-C-O-H torsion prefers a *gauche* conformation, which probably helps hydrogen bonding to the oxygen in the ring. The first conformer with an *anti* C-C-O-H is 3.20 kcal/mol above the global minimum. We cannot see a simple correlation between the solvation energy of the conformer and the torsions in the ring or those of the hydroxymethyl group. We found a total of 43 conformations, as in the gas phase. See appendix for full listing of results

Conformer Energy in the gas phase Energy in GB/SA water δH_{solv} Chair 0.00 0.00 -59.59 Chair 0.81 0.81 -56.84 Twist-boat 1.14 2.62 -54.83 Twist-boat 1.20 n.f.* ---- Chair 1.60 0.86 -59.57 Chair 1.77 n.f.* ---- Chair 2.01 4.42 -52.24 Twist-boat 2.13 1.45 -58.46 Twist-boat 2.18 n.f.* ---- Chair 2.19 4.95 -53.66 Twist-boat 2.20 1.79 -58.51 Twist-boat 2.35 1.90 -58.34 Chair 2.63 3.20 -55.44 Twist-boat 2.71 n.f.* ---- Chair 2.73 Twist-boat 3.66 n.f.* ---- Twist-boat 3.90 6.63 -53.15 Twist-boat 4.06 4.57 -57.10 Twist-boat 4.11 7.24 -52.68 Twist-boat 4.32 7.88 -52.85 Boat 4.45 n.f.* ---- Conformational and solvation energies (kcal/mol) of (hydroxymethyl)trimethylmorpholinium in the gas phase and GB/SA water. Conformational analyses of 2-oxo-1,3,6-dioxazaphosphacinium rings.

We analyzed by molecular mechanics the conformational behavior of:

1. Cyclooctane in the gas phase.
2. 1,1,5,5-tetramethylcyclooctane in the gas phase.
3. 1,1,3,5,5-pentamethylcyclooctane in the gas phase.
4. 1,1,3,3,5,5-hexamethylcyclooctane in the gas phase.

as a reference frame to understand:

1. 6,6-dimethyl-2-oxo-1,3,6-dioxazaphosphacinium in the gas phase and in solution.
2. *cis*-4,6,6-Trimethyl-2-oxo-1,3,6-dioxazaphosphacinium in the gas phase and in solution.
3. *trans*-4,6,6-Trimethyl-2-oxo-1,3,6-dioxazaphosphacinium in the gas phase and in solution.
4. 4,4,6,6-Tetramethyl-2-oxo-1,3,6-dioxazaphosphacinium in the gas phase and in solution.

Modeling in the gas phase.

As previously indicated for the six-membered ring molecules, we repeated MonteCarlo runs until the searches converged. For details about the setup, refer to the Methods section. All energies refer to the global minimum as 0.00 kcal/mol unless specified otherwise. Cyclooctanes.

In cyclooctane we find 8 out of the ten conformations normally regarded as stationary points and which we have described previously in the review of the literature. We only miss the crown and the CC. The BC is the global minimum, in agreement with most of the previous determinations. After this, the TCC is the most populated, with an energy of 0.83 kcal/mol in the gas phase. Two kinds of TBC come at 1.77 kcal/mol (minimum) and at 2.88 kcal/mol (saddle). The TB shows up at 3.63 kcal/mol, a BB at 4.86, a C at 7.76. The TC is at 8.47 and the B at 10.55 kcal/mol. The AMBER* ordering agrees fairly well with that of Kolossváry and Guida Kolossváry, 1993 giving us confidence in the ability of AMBER* to model these rings.

Conformer BC TCC TCC' TBC TBC' TBC TBC' Structure fig.bc0O.gif, 0.249KB bc.wrl, 9.668KB fig.tcc10O.gif, 0.257KB tcc1.wrl, 9.651KB fig.tcc-10O.gif, 0.280KB tcc1.wrl, 9.651KB fig.tbc10O.gif, 0.311KB tbc1.wrl, 9.649KB fig.tbc-10O.gif, 0.307KB tbc2.wrl, 9.654KB fig.tbc10O.gif, 0.311KB tbc3.wrl, 9.667KB fig.tbc-10O.gif, 0.307KB tbc4.wrl, 9.667KB AMBER* (kcal/mol) 0.00 0.83 0.83 1.77 1.77 2.88 2.88 MM2* (kcal/mol) 0.00 0.96 0.96 1.67 1.67 2.80 2.80 Conformers of cyclooctane within 3.0 kcal/mol of global minima in the gas phase.

In 1,1,5,5-tetramethylcyclooctane the BCs are global minima with the methyl groups in positions 2 and 6. The introduction of two 1,5-*gem*-dimethyl groups lowers the symmetry, so we describe two different, enantiomeric BCs. See the appendix for a full description of the naming and numbering system used for *all* conformers. After the BC follows a lowered TCC (0.39 kcal/mol, possibly an indication of a destabilized BC) with methyl groups in 1,5. Now the TCC is followed by a 1,5 TB, not a TBC as in cyclooctane. The 1,5 TB is now only 0.45 kcal/mol higher in energy than the BC, as does the 3,7 TB, instead of the 3.63 kcal/mol it showed in cyclooctane. The 2,6 and 4,8 BB have an energy gap of 0.84, much smaller than 4.86 the BB showed in cyclooctane. A 1,5 CC appears at 1.12 kcal/mol. On the other hand, the 1,5 TBC has increased to 2.17 kcal/mol from the original 1.77 in cyclooctane.

Conformer 2,2,6,6-BC 2,2,6,6-BC' 1,1,5,5-TCC 1,1,5,5-TCC' 1,1,5,5-TB 1,1,5,5-TB' 2,2,6,6-BB 2,2,6,6-BB' 1,1,5,5-CC 1,1,5,5-TBC 1,1,5,5-TBC' Structure fig.bc14O.gif, 0.301KB bc14O.wrl, 14.058KB fig.bc24O.gif, 0.301KB bc24O.wrl, 14.074KB fig.tcc14O.gif, 0.365KB tcc14O.wrl, 14.027KB fig.tcc24O.gif, 0.357KB tcc24O.wrl, 14.082KB fig.tb14O.gif,0.435KB tb14O.wrl, 14.069KB fig.tb24O.gif, 0.427KB tb24O.wrl, 14.143KB fig.bb14O.gif, 0.430KB bb14O.wrl 14.000KB fig.bb24O.gif, 0.435KB bb24O.wrl, 14.195KB fig.cc4O.gif, 0.324KB cc4O.wrl, 14.201KB fig.tbc14O.gif, 0.377KB tbc14O.wrl, 14.084KB fig.tbc24O.gif, 0.379KB tbc24O.wrl, 14.084KB AMBER* (kcal/mol) 0.00 0.00 0.39 0.39 0.45 0.45 0.84 0.84 1.12 2.17 2.17 Conformers of tetramethylcyclooctane within 3.0 kcal/mol of global minima in the gas phase.

In 1,1,3,5,5-pentamethylcyclooctane the global minimum is formed by a pair of enantiomeric BCs, followed at 0.43 kcal/mol by two enantiomeric TCCs. The barrier for TCC-TCC' interconversion is very low, 1.49 kcal/mol (CC). We then find a set of TBs at 1.55 and 1.59 kcal/mol, two BCs and two TBCs. These results continue the pattern started with 1,1,5,5-tetramethylcyclooctane: the BCs prefer to carry the *gem* substituents in positions 2 and 6 (sometimes 4 and 8), while the methyl group prefers positions 4*e* and, sometimes, 2*e*. Only in high energy cases we find the substituents in positions 1, 3 or 7. Apparently, this positions suffer strong axial-axial or flagpole-axial interactions. The TCC carries the substituents on positions 1, 3 and 5; as the CC does. Positions 2, 3, 6 and 7 are subject to stronger axial-axial repulsions. Note The absence of substitution patterns in carbons 4 and 8 may well be an artifact of the procedure to name the conformers.

Conformer 2,2,4,6,6-BC 2,2,4,6,6-BC' 1,1,3,5,5-TCC 1,1,3,5,5-TCC' 1,1,3,5,5-CC 2,2,4,6,6-TB 2,2,4,6,6-TB' 1,1,3,5,5-TB 1,1,3,5,5-TB' 2,4,4,8,8-BC 2,4,4,8,8-BC' 1,1,5,5,7-TBC 1,1,5,5,7-TBC' 2,4,4,8,8-BC 2,4,4,8,8-BC' 2,2,4,6,6-BB 1,1,3,5,5-TBC 1,1,3,5,5-TBC' Structure fig.bc15O.gif, 0.364KB bc15O.wrl, 15.236KB fig.bc25O.gif, 0.365KB bc25O.wrl, 15.183KB fig.tcc15O.gif, 0.381KB tcc15O.wrl, 15.302KB fig.tcc25O.gif, 0.405KB tcc25O.wrl, 15.238KB fig.cc5O.gif, 0.334KB cc5O.wrl, 15.181KB fig.tb15O.gif, 0.435KB tb15O.wrl, 15.190KB fig.tb25O.gif, 0.459KB tb25O.wrl, 15.177KB fig.tb35O.gif, 0.481KB tb35O.wrl, 15.126KB fig.tb45O.gif, 0.489KB tb45O.wrl, 15.168KB fig.bc35O.gif, 0.402KB bc35O.wrl, 15.291KB fig.bc45O.gif, 0.405KB bc45O.wrl, 15.037KB fig.tbc15O.gif, 0.394KB tbc15O.wrl, 15.276KB fig.tbc25O.gif, 0.389KB tbc25O.wrl, 15.220KB fig.bc55O.gif, 0.434KB bc55O.wrl, 15.179KB fig.bc65O.gif, 0.435KB bc65O.wrl, 15.200KB fig.bb5O.gif, 0.489KB bb5O.wrl, 15.165KB fig.tbc35O.gif, 0.396KB tbc35O.wrl, 15.116KB fig.tbc45O.gif, 0.392KB tbc45O.wrl, 15.141KB Energy (kcal/mol) 0.00 0.00 0.43 0.43 1.49 1.55 1.55 1.59 1.59 1.65 1.65 1.92 1.92 2.09 2.09 2.34 2.61 2.61 Conformers of pentamethylcyclooctane within 3.0 kcal/mol of global minima in the gas phase.

The TB has a slight preference by 2,4 and 6 closely followed by 1,3 and 5. The single methyl group prefers the equatorial orientation in all cases and only in higher energy structures, (> 5.5 kcal/mol) do we find it in axial. TBC prefers a pattern 1,3,5, although a 2,6,8 pattern is also possible (2,2,6,6,8*e*). A saddle TBC shows a 2,2,4*e*,6,6 pattern. We did not name structures higher than 8.35 kcal/mol. Most of them show great distorsion, and neither by use of the Weiler plots nor direct examination of the structure could we assign them a name. We think it better to assign them a number, rather than trying to force a fit into our preconceived notions. We shall look back on them only if needed to understand the behavior of the systems that concern us.

1,1,3,3,5,5-Hexamethylcyclooctane shows a pair of TBs as global minima. The interconversion barrier, through a BB, is 0.82 kcal/mol. The BCs are now 1.21 kcal/mol higher in energy than the TBs. The TB prefers to carry its substituents in positions 2,4 and 6. The BC prefers positions 2,4, and 8; and 2,4, and 6. The TBC at 5.99 kcal/mol, prefers substitution on carbons 2,4 and 8. The conformational picture is somewhat simpler than that of 1,1,3,5,5-pentamethylcyclooctane because 1,1,3,3,5,5-hexamethylcyclooctane does not have an equatorial/axial option available as in the pentamethyl substituted ring. As we examine conformations higher in energy, we find many highly distorted structures difficult to name. The distortions seem to depend heavily on the number of substituents so, at present, we cannot see any trends emerging from the ordering of these conformers.

Conformer 1,1,3,3,5,5-TB 1,1,3,3,5,5-TB' 2,2,4,4,8,8-BB 2,2,4,4,8,8-BC 2,2,4,4,8,8-BC' Structure fig.tb16O.gif, 0.511KB tb16O.wrl, 16.172KB fig.tb26O.gif, 0.515KB tb26O.wrl, 16.226KB fig.bb6O.gif, 0.449KB bb6O.wrl, 16.350KB fig.bc16O.gif, 0.439KB bc16O.wrl, 16.189KB fig.bc26O.gif, 0.441KB bc26O.wrl, 16.221KB Energy (kcal/mol) 0.00 0.00 0.82 1.21 1.21 Conformers of hexamethylcyclooctane within 3.0 kcal/mol of global minima in the gas phase.

BCs accomodate substituents preferentially on an equatorial 2,4,6 pattern; a 2,4,8 pattern introduces more strain than a 2,4,6. Substituents on atom 1 can orient either as bowsprit or flagpole. The flagpole orientation suffers close contacts with the axial substituents on atoms 4 and 6. Axial substituents on atoms 2, 3, 7 and 8 produce strong axial-axial interactions among themselves. The most sterically unhindered positions are 1*b* and *equatorial* 2, 3, 4, 5, 6, 7 and 8. A 1,3,5 pattern becomes highly strained when adding *gem* substituents: in tetramethylcyclooctane, the 1,5 is 5.27 kcal/mol higher in energy than the 2,6; in pentamethylcyclooctane, the 1,3,5 pattern is 5.42 kcal/mol higher in energy than the 2,4,6 and 3.77 kcal/mol higher than the 2,4,8. We could not find this pattern in hexamethylcyclooctane.

TBs prefer a 2,4,6 pattern over a 1,3,5. Because of the high symmetry of the conformation, all the positions have similar steric hindrances. We see that in tetramethylcyclooctane the lowest energy TB is a 1,5; in pentamethylcyclooctane the preferred TB is a 2,4,6 followed closely by a 1,3,5 (0.4 kcal/mol gap); while in hexamethylcyclooctane the lowest TB is a 2,4,6. The TB/BC energy gap starts at 3.63 kcal/mol in cyclooctane, in tetramethylcyclooctane is only 0.45 kcal/mol; increases to 1.55 kcal/mol in pentamethylcyclooctane and becomes -1.21 kcal/mol in hexamethylcyclooctane. The best explanation for the decrease in the TB/BC gap when going from cyclooctane to tetramethylcyclooctane consists of destabilization of the BC. This argument also explains the increase in energy in the TBC conformers.

The TBCs prefer positions 1,3,5 for the substituents. Positions 2,3,6 and 7 generate some axial-flagpole repulsions with the flagpoles on carbons 1 and 4. The bowsprit orientations on atoms 1 and 5 present little steric hindrance, because they are directed away from the ring, so the justification for the preference on these positions becomes clear. The smallest TBC/BC energy gap in cyclooctane is 1.77 kcal/mol. This increases to 2.17 kcal/mol in tetramethylcyclooctane, goes down to 1.92 kcal/mol in pentamethylcyclooctane and then increases to 4.78 kcal/mol in hexamethylcyclooctane.

To summarize, the conformations of substituted cyclooctanes are very sensitive to the positioning of the substituents on the ring. As the conformation of the ring skeleton becomes less symmetric, the sensitivity to positioning of the substituents increases, *e. g.*, the BC and TBC are more sensitive to the position of the substituents than the TCC or the C. More extended conformers, like the C or the TC, are less affected than more crowded conformers, like the TB or BB. As the number of *gem* substituent groups increases, the TB/BC energy gap tends to decrease until, with three *gem* dimethyl groups in a 1,3,5 pattern, the stabilities switch and the TB becomes the global minimum.

The positions with least steric hindrance are: 2, 4, 6 in the BC (the absence of 8 is an artifact of the rules used to name the conformers); 1 and 5, followed by 3, in the TCC; 2 and 6 in the TBC, although 1 and 5 are not much more hindered; all the positions in the TB are nearly equivalent in terms of steric hindrance; the TC prefers 1 and 3 (5 and 7 are equivalent to 1 and 3 respectively). Dioxazaphosphacinium rings.

The conformational search on the unsubstituted phosphonate ring in the gas phase 6,6-dimethyl-2-oxo-1,3,6-dioxazaphosphacinium showed that the global minimum is a pair of enantiomeric BCs with the nitrogen on position 2 and the phosphorus on 6. Note. The results reported by Dale *et al.* Dale, 1972 show that 6,6-disubstituted-1,3-dioxocanes prefer the BB as the global minimum. Given the close analogy of this skeleton to that of 6,6-dimethyl-2-oxo-1,3,6-dioxazaphosphacinium, we wonder what are the reasons for this discrepancy. We defer this until we discuss the effects of solvation on the conformations of this ring. Dale carried out his determinations in $CDCl_3$ and $CHFCl_2$. Our results including water solvation *may* compare better. The more voluminous methyl group, compared to the *oxo* oxygen, prefers the least hindered equatorial position, as one would expect. Putting the methyl groups in any other position carries a very high energetic cost: the 1*b*,5,5 BC increases the energy 7.52 kcal/mol, 2*a*,6,6 increases the energy to 10.12 kcal/mol, while a 3*e*,7,7 pattern raises the energy to 11.18 kcal/mol. In these three cases, unfavorable 1,3-diaxial interactions are responsible for most of the increase in energy. We could not find examples of BCs with a 1*f*,5,5 or a 3*a*,7,7 substitution pattern.

As in the cyclooctanes, we found a minimum TBC and a saddle point TBC. The TBC (min) has an energy of 2.37 kcal/mol, compared to the 2.17 kcal/mol in tetramethylcyclooctane. The TBC (saddle) has an energy of 6.70 kcal/mol, compared to the 6.33 kcal/mol in tetramethylcyclooctane.

Two other conformers have energies within 3.0 kcal/mol above the global minimum: TB (pair at 2.55) and TC (2.75). This differs appreciably from tetramethylcyclooctane, which shows the TB at 0.45 and the TC at 4.42 kcal/mol.

Conformer 2,2,6,6-BC 2,2,6,6-BC' 2,2,6,6-TBC 2,2,6,6-TBC' 1,1,5,5-TB 1,1,5,5-TB' 3,3,7,7-TC Structure fig.bc1P2.gif, 0.451KB bc1P2.wrl, 13.665KB fig.bc2P2.gif, 0.434KB bc2P2.wrl, 13.653KB fig.tbc2P2.gif, 0.460KB tbc2P2.wrl, 13.697KB fig.tbc1P2.gif, 0.461KB tbc1P2.wrl, 13.678KB fig.tb1P2.gif, 0.522KB tb1P2.wrl, 13.780KB fig.tb2P2.gif, 0.516KB tb2P2.wrl, 13.732KB fig.tcP2.gif, 0.477KB tcP2.wrl, 13.635KB Energy (kcal/mol) 0.00 0.00 2.37 2.37 2.55 2.55 2.75 Conformers of dioxazaphosphacinium within 3.0 kcal/mol of global minima in the gas phase.

cis-4,6,6-Trimethyl-2-oxo-1,3,6-dioxazaphosphacinium in the gas phase also shows a BC as the global minimum, but its conformational heterogeneity is much lower than that of the unsubstituted ring. Pentamethylcyclooctane has BCs as global minima, but the similarity ends there. Pentamethylcyclooctane shows a TCC at 0.43 kcal/mol (a reduced TCC/BC gap that we previously ascribed to destabilization of the BC), while this phosphorus ring has its lowest TCC at 5.59 kcal/mol. The CC originally at 1.49 kcal/mol in pentamethyl, now appears at 5.70 kcal/mol. The first TB in pentamethyl has increased from 1.55 to 4.10 kcal/mol. The second TB has gone from 1.59 to 5.59 kcal/mol. The TBC starting at 1.92 is now 4.94 kcal/mol above the global minimum.

Conformer 2,2,4,6,6-BC' 1,3,3,7,7-TC Structure fig.bcP3.gif, 0.525KB bcP3.wrl, 14.873KB fig.tcP3.gif, 0.504KB

tcP3.wrl, 14.910KB Energy (kcal/mol) 0.00 2.89 Conformers of *cis*-methyl dioxazaphosphacinium within 3.0 kcal/mol of global minimum in the gas phase.

trans-4,6,6-Trimethyl-2-oxo-1,3,6-dioxazaphosphacinium in the gas phase shows a distorted TBC as the global minimum. Its conformational heterogeneity is much higher than that of the *cis* ring: the *cis* ring has only two conformers within 3.0 kcal/mol above the global minimum (inclusive), while the *trans* ring has seven. Both have fewer conformers than pentamethylcyclooctane, which has eight pairs of conformational enantiomers and two saddle points, all within 3.0 kcal/mol above the global minimum (inclusive). We find a BC (0.20 kcal/mol), two TCs (1.43 and 2.49), two TBs (1.50 and 2.84 kcal/mol) and another TBC (2.01 kcal/mol).

Conformer 2,2,4,6,6-TBC 2,2,6,6,8-BC 1,3,3,7,7-TC 1,1,3,5,5-TB 2,2,6,6,8-TBC 3,3,5,7,7-TC 1,1,3,5,5-TB' Structure fig.tbc1P4.gif, 0.509KB tbc1P4.wrl, 14.853KB fig.bcP4.gif, 0.517KB bcP4.wrl, 14.860KB fig.tc1P4.gif, 0.497KB tc1P4.wrl, 14.841KB fig.tb1P4.gif, 0.497KB tb1P4.wrl, 14.814KB fig.tbc2P4.gif, 0.519KB tbc2P4.wrl, 14.857KB fig.tc2P4.gif, 0.511KB tc2P4.wrl, 14.813KB fig.tb2P4.gif, 0.536KB tb2P4.wrl, 14.881KB Energy (kcal/mol) 0.00 0.20 1.43 1.50 2.01 2.49 2.84 Conformers of *trans*-methyl dioxazaphosphacinium within 3.0 kcal/mol of global minimum in the gas phase.

The results in the gas phase for 4,4,6,6-tetramethyl-2-oxo-1,3,6-dioxazaphosphacinium show a mixture of conformers. Five conformers show up within 3.0 kcal/mol above the global minimum. Now the global minimum is a TC, followed closely (0.58 kcal/mol) by a BC. In hexamethylcyclooctane, the global minimum is a TB, and the first TC has an energy of 7.26 kcal/mol. The first TB in this phosphonate ring appears at 2.58 kcal/mol and follows a TBC at 2.62, completing all the conformations within 3.0 kcal/mol.

Conformer 1,1,3,3,7,7-TC 2,2,6,6,8,8-BC 2,2,4,4,6,6-BC' 3,3,5,5,7,7-TB 1,1,3,3,5,5-TB 2,2,6,6,8,8-TBC Structure fig.tcP5.gif, 0.529KB tcP5.wrl, 15.871KB fig.bc1P5.gif, 0.530KB bc1P5.wrl, 15.785KB fig.bc2P5.gif, 0.521KB bc2P5.wrl, 15.646KB fig.tb1P5.gif,0.570KB tb1P5.wrl, 15.871KB fig.tb2P5.gif, 0.552KB tb2P5.wrl, 15.844KB fig.tbcP5.gif, 0.534KB tbcP5.wrl, 15.826KB Energy (kcal/mol) 0.00 0.58 1.71 2.58 2.61 2.62 Conformers of dimethyl dioxazaphosphacinium within 3.0 kcal/mol of global minimum in the gas phase. Modeling in GB/SA water.

The conformational search for the 6,6-dimethyl-2-oxo-1,3,6-dioxazaphosphacinium in water showed that the global minimum is a degenerate pair of BBs. These are followed by a degenerate pair of BC conformers, at 2.52 kcal/mol. All the other conformers are higher than 3.0 kcal/mol. The P-O bonds are longer than C-C bonds (1.59Å vs. 1.54Å), so this helps the relief of strain. The steric requirements of the oxygens and of the methyl groups are the same in both cases.

The dipole moments measured by Dale Dale, 1972 could fit both a BC or a BB, but he could not define unambiguously the positions of the oxygens. In the BBs, the oxygens could have taken positions 1,3 or 1,7; leaving the *gem*-dimethyls in positions 2,6. Our results agree with Dale's: in the BBs, the oxygens take positions 1,3 and 1,7 and the *gem* groups (dimethyl and methyl-oxo) are in 2,6. In the BCs at 2.52 kcal/mol (the only ones significantly populated at room temperature) the oxygens occupy positions 5,7 and the *gem* groups take 2,6.

Conformer 2,2,6,6-BB 4,4,8,8-BB 2,2,6,6-BC 2,2,6,6-BC' Structure fig.bb1PW2.gif, 0.489KB bb1PW2.wrl, 13.903KB fig.bb2PW2.gif, 0.457KB bb2PW2.wrl, 13.751KB fig.bc1PW2.gif, 0.446KB bc1PW2.wrl, 13.695KB fig.bc2PW2.gif, 0.437KB bc2PW2.wrl, 13.702KB Energy (kcal/mol) 0.00 0.00 2.52 2.52 Conformers of dioxazaphosphacinium within 3.0 kcal/mol of global minimum in water.

cis-4,6,6-Trimethyl-2-oxo-1,3,6-dioxazaphosphacinium in water shows a TB' as the global minimum. It is closely followed (0.19 kcal/mol) by a BC. The enantiomeric conformer TB appears at 1.71 kcal/mol, and the last conformer within 3.0 kcal/mol is a BC. The second BC is not the conformational enantiomer of the one at 0.19 kcal/mol.

Conformer 1,1,3,5,5-TB' 2,2,4,6,6-BC' 4,4,6,8,8-BB 2,2,4,6,6-BC Structure fig.tbPW3.gif, 0.555KB tbPW3.wrl, 14.900KB fig.bc1PW3.gif, 0.477KB bc1PW3.wrl, 14.847KB fig.bbPW3.gif, 0.524KB bbPW3.wrl, 14.764KB fig.bc2PW3.gif, 0.482KB bc2PW3.wrl, 14.796KB Energy (kcal/mol) 0.00 0.19 1.71 2.84 Conformers of *cis*-methyl dioxazaphosphacinium within 3.0 kcal/mol of global minimum in water.

trans-4,6,6-Trimethyl-2-oxo-1,3,6-dioxazaphosphacinium in water shows a BB as the global minimum another BB is at 0.49 kcal/mol. The oxygens prefer positions 1,7 and 5,7; and the *gem* groups (Me, Me and Me, oxo) are in 4,8 and 2,6. A series of BCs show up in the region from 0.89 to 4.81 kcal/mol. The BCs have 2, 4, 6 as the preferred substitution sites. There are no TBCs lower than 5.4 kcal/mol.

Conformer 4,4,6,8,8-BB 2,2,6,6,8-BB 2,2,4,6,6-BC' 2,2,6,6,8-BC Structure fig.bb1PW4.gif, 0.527KB bb1PW4.wrl, 14.854KB fig.bb2PW4.gif, 0.519KB bb2PW4.wrl, 14.818KB fig.bc1PW4.gif, 0.487KB bc1PW4.wrl, 14.860KB fig.bc2PW4.gif, 0.481KB bc2PW4.wrl, 14.924KB Energy (kcal/mol) 0.00 0.49 0.89 2.98 Conformers of *trans*-methyl dioxazaphosphacinium within 3.0 kcal/mol of global minimum in water.

The results in water for 4,4,6,6-tetramethyl-2-oxo-1,3,6-dioxazaphosphacinium show TB (global minimum) and TB' (1.47 kcal/mol) as the only conformers within the 3.0 kcal/mol window. We could not characterize the lowest energy structure as either a minimum or as a saddle point. We attribute that to the different gradient-calculation algorithms used in the minimization routine and the vibrational frequencies routine. The higher gradient calculated by the frequencies routine terminated the calculation every time we attempted to characterize the stationary point. The energy minimization yielded a gradient well below 0.05 and we did not find any eclipsing methyl groups, nor torsions with values approaching 0° that could make it a saddle point, so we designate it as a minimum. We believe this intuitive supplementation of the results of this model chemistry is justified, because not including the global minimum could render our reasoning without a good foundation.

Conformer 1,1,5,5,7,7-TB' 1,1,5,5,7,7-TB Structure fig.tb1PW5.gif, 0.583KB tb1PW5.wrl, 15.969KB fig.tb2PW5.gif, 0.601KB tb2PW5.wrl, 15.815KB Energy (kcal/mol) 0.00 1.47 Conformers of dimethyl dioxazaphosphacinium within 3.0 kcal/mol of global minimum in water.

This ring shows conformational homogeneity, with only two conformers within 3.0 kcal/mol above the global minimum (inclusive).

Now we can compare our results to those by Dale. Dale, 1972 Dale found that 6,6-disubstituted-1,3-dioxocanes prefer BB as the global minimum. The unsubstituted dioxazaphosphacinium ring prefers BB *in solution*, but in the gas phase it prefers BC. The *cis*-substituted ring prefers a TB in solution and a BC in the gas phase; the *trans*-substituted ring has a BB in solution and a TBC in the gas phase; while the dimethyl substituted ring prefers a TB in solution and a TC in the gas phase. Solvation plays heavily in determining the preferred conformation: the unsubstituted ring global minimum in the gas phase (BC) is destabilized in solution by 2.52 kcal/mol. The *cis*-substituted ring BC in the gas phase is destabilized by 0.19 kcal/mol. In the *trans*-substituted ring, the gas-phase TBC could not be found in solution. The gas-phase TC found for the dimethyl-substituted ring, shows up 7.51 kcal/mol higher than the global minimum in solution. Dale's finding of a BB as minimum, could be due to a true BB minimum, such as in *trans*-methyl dimethyldioxazaphosphacinium, or to a pair of rapidly interconverting TBs, which could be the case in the dimethyl substituted ring, although the searches we performed did not find the saddle point for such a transformation. Modeling of phosphonates. Modeling of phosphorus species.

Many researchers have tried conformational analysis of phosphorus species by computational means, and they have used the full range of computational approaches: molecular mechanics, semiempirical and ab initio. The following sections review the diverse attempts at modeling molecules containing phosphorus (V). This review emphasizes mostly those efforts to *develop* modeling methods for phosphorus, as opposed to the *application* of methods already developed. Ab initio methods.

Ewig and van Wazer calculated phosphinic, phosphonic and phosphoric acids using STO-3G, 3-21G and 4-31G basis sets with *d* functions added on phosphorus. Ewig, 1985 Later, the same authors studied methyl phosphinate, dimethyl phosphonate and trimethyl phosphate Van Wazer, 1986 employing STO-3G, 3-21G and 4-31G with *d* functions on phosphorus.

Denmark and Cramer studied *P*-allylphosphonic diamide the RHF/3-21G(*) level. Denmark, 1990 They found good agreement with data from X-ray for both bond lengths and bond angles, but they point out that inclusion of polarization functions would correct for possible structural artifacts, such as an artificially planar nitrogen attached to

the phosphorus.

Thatcher and Campbell recommend 3-21+G(*) basis set for modeling of phosphates and phosphonates, based on the need for *d* orbitals and diffuse functions to describe properly the electronic density. Thatcher, 1993

Liang *et al.* used 3-21G*, 6-31G* and 6-31+G* basis sets to calculate geometries of dimethyl phosphate and methylpropyl phosphate anions. Liang, 1993 They showed that 3-21G* (this basis set includes *d* orbitals for first and second row atoms) overestimates some bond lengths and the vibrational frequencies agree only qualitatively with those determined by 6-31G* and 6-31+G* basis sets. Their basis set of choice was 6-31G*, given the excellent agreement between its results and those of 6-31+G*, although they did not compare the quality of the charges.

Cramer *et al.* studied phosphorus (V)-substituted methyl anions with full geometry optimization using 3-21G(*). Cramer, 1994 They preferred 3-21G(*) (this basis set contains a set of six *d* orbitals for second row atoms but no *d* orbitals for first row atoms) because of the computational costs involved in using more extended basis sets, although they stressed the qualitative validity of the hypersurfaces calculated.

Landin *et al.* Landin, 1986 studied dimethyl phosphate anion and 2-ammonioethanol at the Hartree-Fock level using 3-21G, and 3-21G(*) basis sets for full geometry optimization, followed by single point calculations with 6-31G* and 6-31+G* basis sets. The most stable conformation had both O-CH_3 in syn-clinal (+sc) orientation. They reported differences in the charges calculated with 6-31G* and 6-31+G* basis sets, with the phosphorus atom suffering the greatest change in the charge when including polarization functions. Semiempirical methods.

Gorenstein *et al.* modeled phosphate esters at the CNDO/2 level including *d* orbitals. The results compared favorably to those of a PCILO calculation, and to an ab initio calculation using a minimal Slater-type orbital basis set without *d* orbitals. Gorenstein, 1976 They compared their calculated bond distances and bond angles against X-ray data and found good agreement. Based on Gorenstein's conclusions, Van der Veken and Herman reported conformational analysis of dimethyl methylphosphonate at the CNDO/2 level including *d* orbitals. van der Veken, 1977

Koch and Anders compared MP2(full)/6-31+G*//MP2(full)/6-31+G*, MNDO and PM3 calculations on lithiophosphonates. Koch, 1995 PM3 reproduced well the energetic ranking of the conformers produced by ab initio, while MNDO failed. The suitability of PM3 to model organolithium species was confirmed, but it underestimated the bond lengths around the phosphorus atom.

Landin *et al.* Landin, 1995 found PM3 inadequate to model dimethyl phosphate anion, a result of an underestimation of dipole-dipole interactions which in turn, related to an underestimation of charge separation by the PM3 Hamiltonian. A Fourier analysis of the coefficients for the C-O-P=O torsion indicated that the coefficient associated with the anomeric effect was less important than the one associated with the dipole-dipole interactions, although none could be neglected due to a third coefficient that coupled both effects. Molecular mechanics methods.

Plyamovatyi *et al.* modeled dimethyl phosphate anion by a molecular mechanics scheme that emphasized interactions between unshared electron pairs. The results of their suggested molecular mechanics scheme reproduced the global minimum determined experimentally better than an ab initio calculation using the STO-3G basis set. Plyamovatyi, 1977a, Plyamovatyi, 1977b, Plyamovatyi, 1990, Plyamovatyi, 1993

Weiner *et al.* developed a molecular mechanics force field (AMBER) that could model phosphates. Weiner, 1986 The molecular mechanics parameters were determined by fitting them to experimental geometries. The starting points were experimentally-determined force constants (from IR and Raman) and bond angles (from X-ray).

Mikolajczyk *et al.* studied 2-phosphoryl and 2-thiophosphoryl-1,3-heteroanes by molecular mechanics. Mikolajczyk, 1989 The potential energy function included nonbonded interactions, torsional energy, angle deformations and lone pair interactions. They concluded that hyperconjugation did not play an important role in determining the conformational stabilities of 2-substituted-1,3-dithianes

Fox, Bowen, and Allinger extended their MM3 force field to include alkylphosphines. Fox, 1992 As starting points for their parametrization, they used structural parameters from electron diffraction and microwave spectroscopy. The

resulting parameters modeled structures, vibrational spectra, moments of inertia and dipole moments fairly accurately.

Jin, Benesch, and Weaver developed MM2 parameters for modeling of lipids (MM2(Lipid) force field) by taking structures of phospholipids calculated by AM1. Jin, 1994 They observed good agreement between their results and those obtained by Ewig and Van Wazer using ab initio approaches. Ewig, 1985 Van Wazer, 1986 They showed, however, that AM1 overestimated the barriers to rotation. This overestimation reduced the reliability of their torsional parameters. Development of AMBER* parameters for phosphonates.

We suggest three levels of molecular properties that molecular mechanics (MM) should reproduce:

1. Atomic connectivities.
2. Torsion angles.
3. Energetic ranking of conformers.

If we want to believe the result of any computation, we need to ensure that it can reproduce accurately bond lengths and bond angles, otherwise we can discard its results offhand. The accurate reproduction of torsion angles implies a good representation of the intramolecular interactions, such as van der Waals repulsions and electrostatic effects, just to mention the most important. A correct ranking of the conformers means a proper accounting of the relative weights that correspond to the intramolecular forces. From these criteria, we can propose three ways to measure how well MM reproduces molecular properties:

1. Absolute differences in bond lengths and angles between the MM values and the reference values.
2. RMS deviation after least-squares fit of the MM geometry to the reference geometry.
3. Comparison of MM conformational energies against reference energies.

As reference values one can take either experimental information (X-ray data) or high level ab initio calculations. In the particular case of the energetic ranking of the conformers, one is usually limited to high level ab initio calculations, given the experimental difficulties involved in determining conformational populations in the gas phase. To see the details of the development process see the corresponding subsection in Methods. Calculations on dimethyl methylphosphonate.

The following figures show the molecular mechanics curves with the best fit to the ab initio curves. fig.pc.gif, 3.795KB Fit of AMBER* phosphonate parameters for P-C bond stretch to 6-31+G* curve. fig.po.gif, 3.817KB Fit of AMBER* phosphonate parameters for P-O bond stretch to 6-31+G* curve.

We took the P=O bond length from the ab initio results. The starting point for the fitting of the stretching force constant was the one found for the phosphonate P=O bond. fig.opo.gif, 3.991KB Fit of AMBER* phosphonate parameters for O-P-O bond angle to 6-31+G* curve. fig.cp2o.gif, 4.142KB Fit of AMBER* phosphonate parameters for C-P=O bond angle to 6-31+G* curve.

Dimethyl methylphosphonate has a total of six bond angles around the phosphorus: C-P=O, O-P-O, 2 O-P=O and 2 C-P-O. We included parameters only for C-P=O and O-P-O because adding parameters for the other bond angles gave rise to erratic behavior in the calculated geometries. Cross-coupling of the bond angle terms may be part of the reason. The simple functions used in AMBER* may not represent adequately such coupling. fig.hcpo.gif, 4.349KB Fit of AMBER* phosphonate parameters for H-C-P=O torsion angle to 6-31+G* curve. fig.copo.gif, 4.789KB Fit of AMBER* phosphonate parameters for C-O-P-O torsion angle to 6-31+G* curve.

The AMBER* H-C-P=O torsion potential very closely matches the ab initio curve. The C-O-P-O torsion potential from AMBER* has problems reproducing the very flat part of the ab initio] potential where the C-O bond eclipses the P=O bond. It also introduces an error close to 0.5 kcal/mol in the energy of the minima where the C-O bond is *gauche* to the singly bonded oxygens.

The results in the table show that our AMBER* parameters reproduce ab initio bond lengths with a maximum deviation of 0.002 Å, and bond angles with a maximum deviation of 1.1°. MM2* has maximum deviations of 0.037Å and 10.9° respectively. MMX shows maximum deviations of 0.062Å and 8.9°, while the maximum errors in UFF

predictions amounted to 0.111Å and 6.4° respectively. MM2* and MMX overestimated the P-C bond length, with values greater than 1.83Å. The prediction of UFF was as good as ours (1.799Å vs. 1.797Å). MM2*, MMX and UFF overestimated the P-O bond length, with MM2* getting the closest value (1.605Å) to the ab initio (1.590Å). Our parameters predicted 1.588Å. The smallest error by MM2*, MMX and UFF in the P=O length predictions was 0.02Å. Our modified AMBER* matched the ab initio result within 0.001 Å. In the predictions of the bond angles our modified AMBER* correctly reproduced all the ab initio trends, while MM2 and UFF predict standard tetrahedral angles, with little correlation to the ab initio results. MMX did remarkably well, predicting correctly the trends and most values, although the O-P-O angle resembles more a phosphine-like C-P-C angle. For the full listing of the predicted values for the different bond lengths and angles used in the evaluation, see the table of predicted bond lengths and angles for dimethyl methylphosphonate.

6-31+G* AMBER* ε=1.0 MM2* MMX UFF P-C 1.798 1.797 1.835 1.860 1.799 P-O 1.590 1.588 1.605 1.622 1.701 P=O 1.455 1.455 1.470 1.479 1.510 O-P-O 104.8 105.1 107.8 96.7 109.1 O=P-C 115.9 116.3 105.8 114.3 109.5 O-P-C 104.3 105.2 115.2 109.2 109.1 O=P-O 113.3 112.1 106.1 113.1 110.1 Predicted bond lengths and angles of dimethyl methylphosphonate.

The RMS deviations in the least-squares fits do not reveal major differences in the quality of the predictions. Our AMBER* parameters performed *marginally better* than the other force fields. AMBER* yields RMS values between 0.10 and 0.15, while the other force fields produced values between 0.10 and 0.25, but the difference is probably not significant. See the table of RMS fits of molecular mechanics to ab initio geometries for a full comparison of the RMS values produced by all the force fields.

g-,g- g+,g+ g-,g+ g-,a a,g+ AMBER* ε=1.0 0.140 0.141 0.135 0.102 0.102 MM2* 0.187 0.187 0.240 0.192 0.192 MMX 0.111 0.104 0.250 0.129 0.128 UFF 0.669 0.169 0.174 0.166 0.160 RMS fit of molecular mechanics to ab initio geometries.

Ab initio reveals only five minima in the conformational hypersurface of dimethyl methylphosphonate. (Our repeated attempts to locate the missing four conformers failed, when all our input structures collapsed to conformers already found.) The table of relative conformational energies shows that AMBER* using constant dielectric closely reproduces the energetic ranking of the minima found by ab initio. The greatest error resides in the energies of the *g-*, *a* and *a*, *g+* conformers, which AMBER* predicts 0.4 kcal/mol higher than ab initio. AMBER* found two more saddle points than ab initio. We believe this is a manifestation of the less-than-perfect match of our parameters to the ab initio results. Note.

The results tabulated, refer to the following conformers: fig.confs.gif, 4.000KB Conformers of dimethyl methylphosphonate.

6-31+G* AMBER* ε=1.0 AMBER*(default) MM2* MMX UFF g-,g- 0.00 0.00 0.08 2.01 0.00 0.00 g+,g+ 0.00 0.00 0.08 2.01 0.00 0.00 g-,g+ 0.14 0.12 n.f.* 4.07 0.68 0.11 g+,g- n.f.* 0.16* 0.00 4.70 0.46 n.f.* g-,a 2.75 3.17 2.15 0.00 0.39 7.58 a,g+ 2.75 3.17 2.15 0.00 0.38 7.58 a,g- n.f.* n.f.* 1.99 2.32 0.64 n.f.* g+,a n.f.* n.f.* 1.99 2.32 0.61 n.f.* a,a n.f.* 7.41* 6.86 3.70 n.f.* n.f.* Relative conformational energies (kcal/mol) Saddle point. *not found We want to illustrate the importance of dealing properly with the electrostatics: use of the default (distance-dependent) dielectric treatment of electrostatics, completely scrambles the energetic ranking of the conformers, *e.g.*, the global minima have now a relative energy of 0.08 kcal/mol, the minimum found at 0.14 kcal/mol by ab initio is found at 0.12 kcal/mol by the constant dielectric treatment, while the distance-dependent failed to find it as a stationary point. Two structures that are not part of the hypersurface (a,g- and g+,a) either by ab initio or AMBER* with constant dielectric, were found by the distance-dependent dielectric treatment at 1.99 kcal/mol. A constant dielectric was the proper choice to develop the parameters because the ab initio results were calculated assuming a vacuum, so the dielectric permittivity of the medium stayed constant. In the version of AMBER included in MacroModel, Weiner, 1986 the parameters fit *experimental* values so the authors found that a distance-dependent dielectric gave a better fit because of its emulation of polarization effects.

MM2* found degenerate pairs, but its energetic ranking differs from that by ab initio. MM2* finds *g-,a* and *a,g+* as global minima. MMX found the same global minima as ab initio and nearly degenerate pairs of conformers, but the

conformational energies span a narrow range. The hypersurface is, thus, very flat. The hypersurface contains two minima not found by ab initio. UFF found the same global minima as ab initio and the energetic ranking is qualitatively the same, but the conformational energies are much higher than the ab initio predictions. We looked repeatedly for the *g*+,*g*- conformer without success. fig.profile.gif, 4.658KB Comparison of molecular mechanics C-O-P=O torsion profiles vs. ab initio.

Our computational results agree with the experimental work by Katolichenko *et al.* Katolichenko, 1973 who used IR spectroscopy and measurements of dipole moments, and detected two major conformers: gauche-trans (*a*,*g*- and *g*+,*a* by our notation) and gauche-gauche (*g*+,*g*+, *g*-,*g*+, *g*+,*g*-, and *g*-,*g*+). They deduced the presence of the gauche-trans by elimination of other conformers due to dipole moment considerations. The difference in energy found between the gauche-trans and the gauche-gauche was less than 0.5 kcal/mol. Comparison vs. crystal structures.

After developing the parameters, we tested them against our molecule of interest and several crystal structures to see how well could they reproduce results in the condensed phase. The structures were retrieved from the Cambridge Crystallographic Data File (CCDF) Allen, 1977 and their codenames are: ZAYSIB (zaysib.wrl, 13.587KB), Kumaravel, 1995 CEGXUH (cegxuh.wrl, 15.784KB), Day, 1984 FELSOE (felsoe.wrl, 23.386KB), Nastopoulos, 1987 DUKSOR (duksor.wrl, 15.993KB) and Bentrude, 1986 DUMLEC (dumlec.wrl, 26.911KB). Dyrbusch, 1986 We looked for structural variety, always accounting for the limitations of our parameters:

- No P-C(sp^2) fragments.
- No P-C(*sp*) fragments.
- No P-O-C(*sp*).
- No charges on the oxygens.

We chose only one structure from several reported by Nastopoulos Nastopoulos, 1987 because including several molecules of the same structural type could bias the evaluation by giving a greater relative weight to a particular kind of functionality. fig.phosp.gif, 0.591KB First crystal structure used for comparison (ZAYSIB). fig.crystals.gif, 4.624KB Additional crystal structures used in the comparison.

The table of molecular mechanics vs. X-ray displays the results of the tests against crystal structures.

P-C P-O P=O O-P-O O=P-C O-P-C O=P-O X-ray 1.797 1.574 1.461 104.2 114.8 106.2 112.7 6-31+G* 1.798 1.590 1.455 104.8 115.9 104.3 113.3 AMBER* ε=1.0 1.798 1.592 1.455 103.7 117.9 106.5 110.6 MM2* 1.833 1.592 1.466 100.3 108.5 114.4 109.4 MMX 1.869 1.620 1.479 98.7 114.3 108.7 112.6 UFF 1.830 1.707 1.512 109.6 109.5 110.1 108.7 Comparison of Molecular Mechanics results vs. X-ray.

We observe the same trends as from the comparison against ab initio. Ab initio does show some discrepancies with the crystal structures. Two of the most intriguing are the longer P-O bond predicted by ab initio (1.590Å ab initio vs. 1.574Å X-ray), and the shorter P=O bond (1.455Å ab initio vs. 1.461Å X-ray). We can only suggest a few reasons for these differences: a) correlation effects not included in the calculations, b) crystal packing forces affecting the experimental values or c) a combination of a) and b). Regarding the inclusion of correlation, calculations by Koch and Anders Koch, 1995 on methylphosphonic acid at the HF/6-31+G* and MP2/6-31+G* levels show that electronic correlation *increases* both bond lengths: P=O (1.460Å by HF to 1.494Å by MP2) and P-O (1.596Å by HF to 1.629Å by MP2) so we find it difficult to justify the differences on these grounds. Note. MP2 is known to overestimate corrections in bond lengths when the basis set used is too small Szabo, 1996 and the effect is more pronounced on multiply bonded species. One could expect, then, to see a greater increase in the P=O length than in the P-O length. The P=O bond increases 0.034Å, while the P-O increases 0.033Å. Most likely, only a calculation using a larger basis set (and probably more terms in the Møller-Plesset expansion) can settle the issue of the appropriateness of the basis set used. Crystal packing forces become unlikely candidates after realizing that all the molecules used for testing crystallize in different systems. AMBER* reproduces fairly closely the deficiencies shown by HF/6-31+G* in the predicted bond lengths (maximum deviation of 0.018Å) and in the bond angles (maximum deviation of 3.1°). MM2* overestimates the P-C and P-O bond lengths by 0.035Å at the most, while the greatest deviation from the experimental bond angles amounts to 8°. MMX fits well the angles, but it overestimates P-C and P-O lengths by as much as 0.07Å. UFF has the greatest errors in bond lengths (maximum deviation of 0.13Å) and has little predictive value for the

angles, as they cluster around 109.5°.

Gas phase AMBER* MM2* MMX *Water* AMBER* MM2* MMX ZAYSIB 0.603 0.167 0.086 0.086 0.160 0.084 CEGXUH 0.241 0.416 0.013 0.474 0.417 0.013 FELSOE 0.602 0.602 0.034 0.476 0.557 0.032 DUKSOR 0.862 0.631 0.713 0.656 0.575 0.681 DUMLEC 0.445 0.446 0.056 0.502 0.433 0.284 RMS values of MM vs. X-ray including all heavy atoms.

The RMS values including all heavy atoms show that MMX yields best fits both in the gas phase and in water. AMBER* produces a low RMS value only for ZAYSIB in water, but we note that some torsion angles far from the phosphonate group change after minimization. MM2* yields RMS values close to those by AMBER*. Differences in torsion angles dominate RMS values, so changes in torsion angles not controlled by our parameters can give a wrong idea of the quality of the fit.

Gas phase AMBER* MM2* MMX *Water* AMBER* MM2* MMX ZAYSIB 0.445 0.170 0.097 0.078 0.159 0.087 CEGXUH 0.240 0.287 0.262 0.281 0.294 0.011 FELSOE 0.176 0.182 0.150 0.157 0.186 0.013 DUKSOR 0.039 0.094 0.058 0.046 0.099 0.055 DUMLEC 0.347 0.286 0.213 0.280 0.280 0.251 RMS values of MM vs. X-ray including phosphonate heavy atoms only.

If we include only the phosphonate atoms, we observe a much improved fit in the AMBER* results for water. MM2* has values slightly higher than those by AMBER* both in the gas phase and water. MMX consistently yields very low RMS values in the gas phase and water.

The low RMS values obtained by MMX are misleading because MMX provides a very flat hypersurface, as evidenced in the table and in the profiles. This means that the starting geometry changes very little. Methods. General methods and software. Molecular mechanics.

We employed the package MacroModel v.5.0 for Silicon Graphics workstations. All the conformational searches used the AMBER* force field and MonteCarlo sampling routine with Normal setup and Full Matrix Newton Raphson (FMNR) minimization with line search disabled. All the stationary points obtained were characterized as minima or saddle points by using the MTEST utility (calculation of vibrational frequencies) available in MacroModel. All the saddle points showed only one imaginary frequency and the minima had only real frequencies.

FMNR with line search disabled requires substantial storage resources and accumulates many structures with high gradients which render them meaningless chemically; however, the author opted for this algorithm due to its extreme speed (even when including solvent effects) and because of the *good ability of the algorithm to find saddle points*. Polak-Ribiere Conjugate Gradient (PRCG) and Oren-Spedicato Variable Metric (OSVM) are not likely to converge to saddle points. TCNG can converge to saddle points, but its speed makes it less convenient than FMNR, while Steepest Descent (SD) is a mediocre gradient minimizer. SD requires a postprocessing step of the structures it generates by some algorithm able to reduce the gradients under acceptable cutoffs. For a better discussion of the relative merits of the different minimization algorithms available in MacroModel, see the MacroModel Manual. The spurious structures are easily filtered out by cutting and pasting only the structures with gradients <0.05.

The AMBER* calculations in water used the GB/SA solvent model. In all cases we calculated the vibrational frequencies of the conformations to characterize them as minima or as saddle points. The morpholinium rings and the cyclohexanes used the default distance-dependent dielectric.

When using PCMODEL v.4.0 we used all the default settings. When including the effect of water the dielectric constant was set to 78.3. PCMODEL uses the MMX force field. We also used PCMODEL as a front end for MOPAC 6.0 and MOPAC93. Gajewski, 1991 Semiempirical calculations.

We used MOPAC 6.0 Stewart, 1990 and MOPAC93 for the semiempirical calculations. We chose AM1 as the Hamiltonian in all cases. The solvent model COSMO Klamt, 1993 employed a dielectric constant of 78.3. All the structures were minimized (sometimes requiring an Intrinsic Reaction Coordinate calculation) until a vibrational analysis showed absence of imaginary frequencies. The optimizations in the gas phase used the Broyden-Fletcher-Golfarb-Shannon (BFGS) minimization routine, reducing all the gradient norms under 0.01. The minimizations in

solution benefitted from using Eigenvector Following (EF), to lower all the gradient norms under 0.3. Ab initio calculations.

All the ab initio computations were done using Gaussian94 Gaussian, Inc. In those cases where the structure corresponded to a stationary point, the vibrational frequencies were calculated to confirm the absence of imaginary frequencies, for the minima, or the presence of just one imaginary frequency, for the saddle points. We chose single points for the carnitine calculations after finding out that full optimization including solvent effects was prohibitively expensive, and only a supercomputer could tackle such calculations. Acetylcarnitine calculations. Conformational search strategy by molecular mechanics.

We performed a grid search with the following guidelines:

1. We allowed three initial values, 60°, -60° and 180° (*g*+, *g*- and *a* respectively) for the following torsions: N-CH_2-CH-OH(Ac), CH_2-CH-CH_2COO^-, and CH_2-CH-O-H(Ac)
2. We used initial values of 0° and 180° (*s* and *a* conformations) for the CH-O-C(O)-CH_3torsion angle.
3. We used initial values of 90° and 180° for the CH-CH_2-C(O)-O^- torsion angle
4. No initial values were given to torsions containing symmetric tops, like those for methyl groups and $(CH_3)_3N^+$-CH_2, but they were left free for optimization.

The previous conditions yielded 108 conformers for acetylcarnitine, 54 for carnitine, 27 for acetylcholine and 9 for choline. All input geometries were fully optimized in the gas phase (AM1) and with solvent (AM1/COSMO). We also calculated water and acetic acid. Conformational populations.

Boltzmann factors (F) were calculated by the following formula:
$F(c)=\exp(-\delta H_f/RT)/\sigma i(\exp(-\delta H_f/RT))$
where:

$F(c)$
: Boltzmann factor corresponding to conformer c

δH_f
: Heat of formation,

R
: Gas constant

T
: Temperature.

Heats of formation that included the contributions of individual conformers were calculated with the following equation:
$\delta H_{ftot} = \sigma i\ (F(c))(\delta Hf(c_i))$
where:

δH_{ftot}
: Heat of formation over all conformers

$F(c_i)$
: Boltzmann factor for conformer i

$\delta Hf(c_i)$
: Heat of formation for conformer i

Semiempirical calculations on carnitines, cholines and propanoates.

The first route card we tried was:

AM1 NOXYZ NOINTER PRECISE

but the most effective route card used for the carnitines in the gas phase was:

AM1 NOINTER T=3600.00 EF LET DDMIN=0.0

The cholines required a different route card:

AM1 CHARGE=+1 GNORM=0.01 GEO-OK EF LET DDMIN=0.0 NOINTER T=3600.00

The acetoxypropanoates used:

AM1 CHARGE=-1 GEO-OK GNORM=0.5 NOXYZ NOINTER NOLOG T=3600.00 XYZ

The hydroxypropanoates used:

AM1 CHARGE=-1 GNORM=0.5 T=3600.00 GEO-OK NOXYZ NOINTER NOLOG

The inclusion of solvent required the following route card for carnitines:

AM1 NOINTER T=3600.00 EPS=78.3 PRECISE EF LET DDMIN=0.0

while the carnitines needed more care with the gradient norm:

AM1 T=3600.00 EF LET DDMIN=0.0 EPS=78.3 GNORM=0.01 NOINTER PRECISE

The acetylcholines used:

AM1 CHARGE=+1 GNORM=0.01 GEO-OK EF LET DDMIN=0.0 EPS=78.3 NOINTER T=3600.00

and the cholines:

AM1 CHARGE=+1 GNORM=0.01 GEO-OK EPS=78.3 EF LET DDMIN=0.0 NOINTER T=3600.00

The propanoates used:

AM1 CHARGE=-1 EPS=78.3 GNORM=0.5 NOXYZ NOINTER NOLOG T=3600.00

The hydroxypropanoates used:

AM1 CHARGE=-1 EPS=78.3 T=3600.00 GNORM=0.5 NOXYZ NOINTER NOLOG

To simplify, a general route card would be:

AM1 CHARGE=(charge) EPS=78.3 EF LET DDMIN=0.0 T=(time) PRECISE + GNORM=X.XXXX GEO-OK NOXYZ NOINTER NOLOG XYZ

AM1 CHARGE=(charge) EPS=78.3
: Specify Hamiltonian, charge on the system and solvent dielectric constant.

EF LET DDMIN=0.0 T=(time)
: Minimization options: eigenvector following, let the heat of formation increase, take the smallest possible step for the trust radius. Specify a time long enough to complete the optimization.

PRECISE
: (optional) Tighten up criteria in case the final gradients are >2.0. Adjust (time) appropriately. Sometimes (not always) MOPAC prints out a message to indicate this keyword is needed.

GNORM=X.XXXX
(optional) Tighten up the gradient norm criterion to finish the minimization to <X.XXXX (0.01 < X.XXXX < 2.0). Use this keyword in case PRECISE is unable to reduce the gradients <2.0.
GEO-OK
(optional) Some distorted input geometries may require this keyword. MOPAC prints out a message whenever this keyword is needed.
NOXYZ NOINTER NOLOG
(preferred) Keywords to reduce the size of the output files: do not print cartesian coordinates, do not print interatomic distances, suppress log trail if possible.
XYZ
(optional) Last resort for difficult minimization cases: perform optimization in cartesian coordinates.

Ab initio calculations on carnitines, cholines and propanoates.

In gas phase, the output geometries after full optimization by AM1 were used as input for Gaussian94. We used the following route card:

```
#rhf 6-31G* opt freq scf=direct maxdisk=10000000 geom=(nodistance, noangle)
```

for the carnitines and the cholines. For the propanoates we used:

```
#rhf 6-31+G opt freq scf=direct maxdisk=10000000 geom=(nodistance, noangle)
```

notice that the only difference resides in the choice of basis set. The MP2 calculations had the following route cards:

```
#rhf mp2 6-31g* scf=direct maxdisk=10000000 geom=(nodistance, noangle)
```

for the carnitines and the cholines, and

```
#rhf mp2 6-31+g scf=direct maxdisk=10000000 geom=(nodistance, noangle)
```

for the propanoates.

In solvent, the output geometries after full optimization by AM1/COSMO (ε=78.3) were used as input for single point calculations including the Tomasi solvent model. The route card was:

```
#rhf 6-31G* scrf=Tomasi scf=direct maxdisk=10000000 geom=(noangle, nodistance)
```

for the carnitines and the cholines. The propanoates used:

```
#rhf 6-31+G scrf=Tomasi scf=direct maxdisk=10000000 geom=(noangle, nodistance)
```

Again, the only difference resides in the choice of basis set. The acetylcarnitines used `78.3 100`, the carnitines used `78.3 200`, the acetylcholines used `78.5 128`, the cholines used `78.3 200`, the acetoxypropanoates and hydroxypropanoates used `78.3 128`. The value `78.5` for the acetylcholines was the product of attempts at eliminating oscillatory behavior of the wavefunction. The choice of the number of points per sphere was governed by the possibility to achieve convergence in the wavefunction. In every case we started with the default value of "200" and reduced the number of points until the program could achieve self-consistency. According to the Gaussian94 manual, the number of points per sphere has to be a number in the series #points = $2(n^2)$ where "n" is a positive integer. Conformational search in six-membered rings.

An average of 15,000 structures were generated for each compound to achieve convergence. The criterion for convergence was that one 2,000-structure run failed to generate any new conformers after examination of a minimum of 10,000 structures. The energy window was 35.8 kcal/mol above the global minimum (150 kJ/mol). The default distance-dependent dielectric constant was used for the calculations in the gas phase. Conformational search and analyses in eight-membered rings.

For the eight-membered rings, an average of 130,000 structures for each compound were generated and minimized until convergence was achieved. The criterion for convergence was that one 15,000-structure run failed to produce any new conformers after examination of a minimum of 100,000 structures. All the calculations in the gas phase were done specifying constant dielectric treatment of the electrostatics, instead of the default distance-dependent dielectrics.

The conformations were named by comparing the structures to perspective drawings of cyclooctane conformers. In difficult cases (distorted structures), recourse to Weiler plots usually afforded a fast identification of the conformer. AMBER* parametrization of phosphonates.

We followed the procedure described by Hopfinger and Pearlstein. Hopfinger, 1984 All the points for the parametrization of dimethylmethylphosphonate were calculated at the RHF/6-31+G* level of theory. 6-31G* can easily match the 6-31+G* geometries, the reason for the choice of 6-31+G* was our desire to generate high-quality charges for the inclusion of solvation effects. Landin *et al.* Landin, 1995 found appreciable differences in the charges calculated by 6-31G* and 6-31+G* in their calculations. We calculated seven points, taken at 0.1 Å steps, for each of the P-C, and P-O bonds stretchings. For the C-P=O, and O-P-O bond angles, we calculated 15 points with 1° separation. The H-C-P=O and C-O-P-O torsions each required 36 points, at 10° steps, to parametrize the full rotation. We used the optimized values of the bond lengths and angles as first guesses for the parameters. The parameters were then adjusted by trial and error, judging "by eye" the best fit to the ab initio curves.

In the evaluation of the RMS fits, we used the least-squares fit utility provided in each MM program. Only heavy atoms were included in the fitting. We used the program Babel v.1.1 Babel, v.1.1 for the translation of structures between the different file formats required by each program.

Cerius^2 v.2.0, which employs the Universal Force Field (UFF) Castonguay, 1992 Rappé, 1992 Rappé, 1993 was used only for comparison purposes in the calculations on dimethyl methylphosphonate. We set the phosphorus atom type to P_3+5, disabled "Automatic Atom Typing". Enabled "Update Charges" by the QEq charge equilibration scheme Rappé, 1991 every 50 iterations. Selected "Grid Search" varying both C-O-P=O torsions from -150° to 130° with 30° steps, minimizing each conformer. We disabled restraining of the torsions and kept unique conformers within 100.00 kcal/mol above the current minimum. Least-squares fit of phosphonate rings to tetrahedral intermediate.

First, we fit only the N-C-C-O atom pairs, to determine the atoms that corresponded best to the *oxo* on the phosphorus, and the corresponding methyl groups on the quaternary nitrogens. After that, we repeated the least-squares fitting including all the atoms pairs described in the figure. Hardware.

PCMODEL v.4.0, MacroModel v.5.0, Cerius^2 v.2.0, MOPAC 6.0 and MOPAC93 ran on a Silicon Graphics Indigo^2 Extreme with 96 MB of RAM, R4400 CPU and R4010 FPU, under IRIX 5.3. Gaussian94 (serial version) ran on an IBM SP2 equipped with 14 nodes, 128 MB/node of RAM and 2 GB/node of scratch space, running under AIX 3.2/4.0 and LoadLeveler as a batch process controller. Conclusions. Summary

One goal of our research is determine what are the conformations and configurations of the tetrahedral intermediates in carnitine acyl transfers. So far, the approach has been experimental, by designing conformationally constrained analogues of the tetrahedral intermediates. To make the approach cost-effective, we need reliable modeling methods to guide the choice of the next generation of inhibitors. The modeling methods developed in this dissertation fulfill that need for the most part.

This dissertation addressed two additional questions:

- Why does acetylcarnitine have such a high free energy of hydrolysis?
- What are the conformations of our heterocyclic moieties that could best fit the tetrahedral intermediate for acetylcarnitine-CoA exchange?

Acetylcarnitine reaches its high energy of hydrolysis by drawing from the solvation energy. The coupling between solvation energy, dipole moment and conformational change, supplies the necessary energy from the solvation term to yield a free energy of hydrolysis that compares to that of AcCoA. The high-energy status of acylcarnitine makes

possible an exchange equilibrium with CoA (K_{eq} = 0.6), that minimizes the energy consumed by processes other than the transport through the cell membrane.

From the preliminary results for the modeling of the tetrahedral intermediate, shown in the table in chapter 3, we see the RMS fits of the dioxazaphosphacinium rings to the intermediate. The most promising candidates are both boat-boat conformers that correspond to the *R,S* diastereomer of the tetrahedral intermediate. The *cis*-substituted ring and the dimethyl-substituted ring yield the closest fit to the *R,S* tetrahedral intermediate. These fits should be considered as one parameter in a quantitative structure-activity relationship for the inhibitory potency of the inhibitors already developed by our group. This will help in the prediction of the next generation of inhibitors. The morpholinium rings should receive a similar treatment.

- Upon hydrolysis, the zwitterion of acetylcarnitine keeps a nearly constant dipole moment thanks to the influence of conformational flexibility on the positioning of the charged centers. This keeps the solvation energy nearly constant, leaving more chemical energy available to be released.
- Conformational change can act as a mechanism for the storage of chemical energy.
- In morpholinium rings, the conformational preference in aqueous media obeys more the increased steric interactions due to the shorter C-N and C-O bonds than the differences in dipole moment.
- *Gem* substitution in morpholinium rings can help control the relative stabilities of the chair and the twist-boat.
- Addition of substituents in a 1,1,3,3-di*gem* pattern on dioxazaphosphacinium rings can favor a twist-boat global minimum over a boat-chair conformation.
- Differences in polarity in dioxazaphosphacinium rings override steric effects, when methyl groups are involved, in determining the preferred conformation in aqueous solution.
- We have developed parameters for accurate modeling of neutral dialkyl alkylphosphonates by molecular mechanics (AMBER*). We used three measures of the goodness of fit when testing against ab initio results and crystal structures, and found our parameters more reliable than other commonly used force fields (MM2*, MMX and UFF)

Future work.

Based on the results obtained from the acetylcarnitine hydrolysis, the aqueous modeling of the heterocycles including a methylenecarboxylate should pay attention to the influence of the dipole moments. In the dioxazaphosphacinium rings, there will be two sources of polarity: the dipoles due to the C-O-P=O torsions, and the dipole due to the zwitterion. How will the conformational preference of the rings be affected by the presence of the zwitterion?. Answering such question will require careful attention to the charge set used in the calculation. It may be desirable to determine a new charge set for the methylenecarboxylate-substituted ring, at the HF/6-31+G* level of theory using the CHelpG scheme, to ensure that the charge set found in this dissertation is still applicable (see the file BondPC.txt for the output from the CHelpG calculation). After all, changing from a cation to a neutral species will likely affect the charge distribution in the molecule. In addition, unless newer versions of MacroModel provide utilities for the calculation of the dipole moment, it will be necessary to supplement the MacroModel results with some other modeling package. Single-point calculations on the AMBER*-optimized geometries, using the AM1 Hamiltonian in MOPAC93, would provide an appropriate starting point.

- Improved modeling of the transition structure for the acetyl exchange between acetylcarnitine and CoA by:
    1. Modeling by semiempirical (or ab initio) methods, including a solvent model.
    2. Determination of molecular mechanics parameters specific to the sulfur found in the molecule (from ab initio).
    3. Molecular mechanics modeling including longer chains in place of the acetyl group.
- Modeling of the morpholinium rings including a methylenecarboxylate, both in the gas phase and solution.
- Modeling of the phosphonate rings including a methylenecarboxylate, both in the gas phase and solution.

Alder, R. W.; White, J. M. Conformational Analysis of Medium-Sized Rings; Glass, R. S.; VCH Publishers, Inc.: *New York, 1988, 97-150 Allen, F. H.; Bellard, S.; Brice, M .D.; Cartwright, B. A.; Doubleday, A.; Higgs, H.; Hummelink, T.; Hummelink-Peters, B. G.; Kennard, O.; Motherwell, W. D. S.; Rodgers, J. R.; Watson, D. G. Acta Crystallogr., Sect. B 1977, B35, 2331-2339 Allinger, N. L.; Hirsch, J. A.; Miller, M.; Tyminski, J. J.; van Catledge, F.*

A. J. Am. Chem. Soc. 1968, 90, 1199-1210 Allinger, N. L.; Yuh, Y. H.; Lii, J.-J. J. Am. Chem. Soc. 1977, 99, 8127-8134 Altona, C.; Knobler, C.; Romers, C. Acta Crystallogr. 1963, 16, 1217-1225 Anderson, J. E.; Glazer, E. D.; Griffith, D. L.; Knorr, R.; Roberts, J. D. J. Am. Chem. Soc. 1969, 91, 1386-1395 Anderson, J. E. Topics in Current Chemistry. Dynamic Chemistry; Springer-Verlag:
Berlin, 1974, 139-168 Anderson, R. C.; Balestra, M.; Bell, P. A.; Deems, R. O.; Fillers, W. S.; Foley, J. E.; Fraser, J. D.; Mann, W. R.; Rudin, M.; Vilhauer, E. B. J. Med. Chem. 1995, 38, 3448-3450 Anet, F. A. L; Anet, R. Det. Org. Struct. Phys. Methods; 1971, 5 344-420 Anet, F. A. L; Degen, P. J. J. Am. Chem. Soc. 1972, 94, 1390-1392 Anet, F. A. L. Topics in Current Chemistry. Dynamic Chemistry; Springer-Verlag:
Berlin, 1974, 169-220 Aped, P.; Allinger, N. L. J. Am. Chem. Soc. 1992, 114, 1-16 Armarego, W. L. F. Stereochemistry of Heterocyclic Compounds; Taylor, E. C.; Weisberger, A. John Wiley & Sons:
New York, 1977 Walters, P.; Stahl, M. Babel, v.1.1
University of Arizona, Tucson, AZ 85721, 1994 Ben-Naim, A. Solvation Thermodynamics Plenum Press:
New York, 1987, p 81 Bentrude, W. G.; Sopchik, A. E.; Bajwa, G. S.; Setzer, W. N.; Sheldrick, W. S. Acta Crystallogr., Sect. C 1986, C42, 1027-1029 Bieber, L. L.; Dai, G.; Chung, C. Current Concepts in Carnitine Research A. Lee Carter; CRC Press:
Boca Raton, 1992, 7-18 Bixon, M. Lifson, S. Tetrahedron 1967, 23, 769-784 Burton, K. Biochem. J. 1954, 59, 44-46 Castonguay, L. A.; Rappé, A. K. J. Am. Chem. Soc. 1992, 114, 5832-5842 Colucci, W. J.; Gandour, R. D.; Mooberry, E. A. J. Am. Chem. Soc. 1986, 108, 7141-7147 Colucci, W. J.; Gandour, R. D. Bioorg. Chem. 1988, 16, 307-334 Chase, J. F. A.; Tubbs, P. K. Biochem. J. 1969, 111, 225-235 Chu, N.-J. Ph.D. Thesis; University of Ottawa 1959 Cramer, C. J.; Denmark, S. E.; Miller, P. C.; Dorow, R. L.; Swiss, K. A.; Wilson, S. R. J. Am. Chem. Soc. 1994, 116, 2437-2447 Cramer, C. J.; Truhlar, D. G. Reviews in Computational Chemistry; Lipkowitz, K. B.; Boyd, D. B; VCH Publishers:
New York, 1995, 1-72 Dale, J.; Ekeland, T.; Krane, J. J. Am. Chem. Soc. 1972, 94, 1389-1390 Dalling, D. K.; Grant, D. M. J. Am. Chem. Soc. 1967, 89, 6612-6622 Day, R. O.; Bentrude, W. G.; Yee, K. C.; Setzer, W. N.; Dieters, J. A.; Holmes, R. R. J. Am. Chem. Soc. 1984, 106, 103-106 Denmark, S. E.; Cramer, C. J. J. Org. Chem. 1990, 55, 1806-1813 Derrick, J. P.; Ramsay, R. R. Biochem. J. 1989, 262, 801-806 Dionne, P.; St-Jacques, M. J. Am. Chem. Soc. 1987, 109, 2616-2623 Dyrbusch, M.; Egert, E. Acta Crystallogr., Sect. C 1986, C42, 1235-1237 Edward, J. T. Chem. Ind. 1955, 1102-1104 Eliel, E. L.; Wilen, S. H.; Mander, L. N. Stereochemistry of organic compounds; Wiley-Interscience:
New York, 1994 Eistetter, K.; Wolf, H. P. O. J. Med. Chem. 1982, 25, 109-113 Ewig, C. S.; Van Wazer, J. R. J. Am. Chem. Soc. 1985, 107, 1965-1971 Fox, P. C.; Bowen, J. P.; Allinger, N. L. J. Am. Chem. Soc. 1992, 114, 8536-8544 Friedman, S.; Fraenkel, G. Arch. Bioch. Biophys. 1955, 59, 491-501 Fritz, I. B.; Schultz, S. K.; Srere, P. A. J. Biol. Chem. 1963, 238, 2509-2517 Fritz, I. B.; Schultz, S. K.; J. Biol. Chem. 1965, 240, 2188-2192 Gajewski, J. J. Gilbert, K. E. McKelvey, J. Adv. Mol. Mod.; Liotta, D.; JAI Press, Inc.:
Greenwich, 2, 1990, 65-92 Gandour, R. D.; Colucci, W. J.; Fronczek, F. R. Bioorg. Chem. 1985, 13, 197-208 Gandour, R. D.; Colucci, W. J.; Stelly, T. C.; Brady, P. S.; Brady, L. J. Biochem. Biophys. Res. Commun. 1986, 138, 735-741 Gandour, R. D.; Colucci, W. J.; Stelly, T. C.; Brady, P. S.; Brady, L. J. Arch. Bioch. Biophys. 1988, 267, 515-520 Gandour, R. D.; Blackwell, M.; Colucci, W. J.; Chung, C.; Bieber, L.; Ramsay, R. R.; Brass, E. P.; Fronczek, F. R. J. Org. Chem. 1992, 57, 3426-3431 Gandour, R. D.; Leung, O.-T.; Greway, A. T.; Ramsay, R. R.; Bhaird, N. N.; Fronczek, F. R.; Bellard, B. M.; Kumaravel, G. J. Med. Chem. 1993, 36, 237-248 Gaussian 94, Revision C.2, Frisch, M. J.; Trucks, G. W.; Schlegel, H. B.; Gill, P. M. W.; Johnson, B. G.; Robb, M. A.; Cheeseman, J. R.; Keith, T.; Petersson, G. A.; Montgomery, J. A.; Raghavachari, K.; Al-Laham, M. A.; Zakrzewski, V. G.; Ortiz, J. V.; Foresman, J. B.; Cioslowski, J.; Stefanov, B. B.; Nanayakkara, A.; Challacombe, M.; Peng, C. Y.; Ayala, P. Y.; Chen, W.; Wong, M. W.; Andres, J. L.; Replogle, E. S.; Gomperts, R.; Martin, R. L.; Fox, D. J.; Binkley, J. S.; Defrees, D. J.; Baker, J.; Stewart, J. P.; Head-Gordon, M.; Gonzalez, C.; Pople, J. A. Gaussian, Inc.,
Pittsburgh PA, 1995 George, P.; Witonsky, R. J.; Trachtman, M.; Wu, C.; Dorwart, W.; Richman, L.; Richman, W.; Shuryah, F.; Lentz, B. Biochim. Biophys. Acta 1970, 223, 1-15 Hayes, D. M.; Kenyon, G. L.; Kollman, P. A. J. Am. Chem. Soc. 1978, 100, 4331-4340 Hendrickson, J. B. J. Am. Chem. Soc. 1964, 86, 4854-4866 Hendrickson, J. B. J. Am. Chem. Soc. 1967, 89, 7036-7043 Hopfinger, A. J.; Pearlstein, R. A. J. Comput. Chem. 1984, 5, 486-499 Jencks, W. P.; Cordes, S.; Carriuolo, J. J. Biol. Chem. 1960, 235, 3608-3614 Jenkins, D. L.; Griffith, O. W. J. Biol. Chem. 1985, 260, 14748-14755 Jenkins, D. L.; Griffith, O. W. Proc. Natl. Acad. Sci. U.S.A. 1986, 83, 290-294 Jin, A. Y.; Benesch, L. A.; Weaver, D. F. Can. J. Chem. 1994, 72, 1596-1604 Stewart, J. J. P. MOPAC: a General Molecular Orbital Package Quant. Chem. Prog. Exch. 1990 10:86 Juaristi, E.; Cuevas, G. The Anomeric Effect CRC Press:
Boca Raton, 1995 Kanamaru, T.; Shinagawa, S.; Asai, M.; Okazaki, H.; Sugiyama, Y.; Fujita, T.; Iwatsuka, H.;

Yoneda, M. Life Sci. 1985, 30, 217-223 Katolichenko, V. I.; Egorov, Y. P.; Boronikov, Y. Y.; Golik, G. A. Zh. Obshch. Khim. 1973, 43, 2475-2490 Kellie, G. M.; Riddell, F. G. Topics in Stereochemistry; Eliel, E. L. Allinger, N. L. John Wiley & Sons:
New York, 8, 1974, 225-270 Kirby, A. J. The Anomeric Effect and Related Stereoelectronic Effects at Oxygen; Springer Verlag:
Berlin, 1983, p 77 Klamt, A. Shüürman, G. J. Chem. Soc. Perkin Trans. 2 1993, 799-805 Koch, R.; Anders, E. J. Org. Chem. 1995, 60, 5861-5866 Kolossváry, I. Guida, W. C. J. Am. Chem. Soc. 1993, 115, 2107-2119 Kumaravel, G.; a' Bhaird, N. N.; Fronczek, F. R.; Ramsay, R. R.; Ashendel, C. L.; Gandour, R. D. Bioorg. Med. Chem. Lett. 1994, 4, 883-886 Kumaravel, G.; Gandour, R. D.; Acta Crystallogr., Sect. C 1995, C51, 1919-1921 Laing, M. J. Chem. Ed. 1987, 64, 124-128 Landin, J.; Pascher, I.; Cremer, D. J. Phys. Chem. 1995, 99, 4471-4485 Lemieux, R. U.; Pavia, A. A.; Martin, J. C.; Watanabe, K. A. Can. J. Chem. 1969, 47, 4427-4439 Liang, C.; Ewig, C. S.; Stouch, T. R.; Hagler, A. T. J. Am. Chem. Soc. 1993, 115, 1537-1545 Marsh, F. J.; Weiner, P.; Douglas, J. E.; Kollman, P. A.; Kenyon, G. L.; Gerlt, J. A. J. Am. Chem. Soc. 1980, 102, 1660-1665 Maurel, P.; Galzigna, L. Biophys. J. 1971, 11, 550-557 Miertus, S.; Scrocco, E.; Tomasi, J. Chem. Phys. 1981, 55, 117-129 Miertus, S.; Tomasi, J. Chem. Phys. 1982, 65, 239-245 Müller, D. M.; Strack, E. Hoppe-Seyler's Z. Physiol. Chem. 1973, 354, 1091-1096 Mursakulov, I. G.; Svyatkin, V. A; Samoshin, V. V.; Palyulin, V. A.; Zefirov, N. S. Zh. Org. Khim. 1984, 20, 80-88 PCMODEL v.4.0 Serena Software, IN Perrin, C. L.; Young, D. B. Tet. Lett. 1995, 36, 7185-7188 Pierlik, J. R.; Guynn, R. W. J. Biol. Chem. 1975, 250, 4445-4450 Riddell, F. G. The Conformational Analysis of Heterocyclic Compounds; Academic Press:
London, 1980 Thatcher, G. R. J.; Campbell, A. S. J. Org. Chem. 1993, 58, 2272-2281 Tutwiler, G. F.; Brentzel, H. J.; Kiorpes, T. C. Proc. Soc. Exp. Biol. Med. 1985, 178, 288-296 Moore, J. A.; Anet, F. A. L. Comprehensive Heterocyclic Chemistry; Katritzki, A. R.; Rees, C. W. Pergamon Press Ltd.:
Oxford, 1984, 697-707 Gorenstein, D. G.; Kar, D.; Luxon, B. A.; Momii, R. K. J. Am. Chem. Soc. 1976, 98, 1668-1673 van der Veken, B. J.; Herman, M. A. J. Mol. Struct. 1977, 42, 161-170 Mikolajczyk, M.; Graczyk, P.; Kabachnik, M. I.; Baranov, A. P. J. Org. Chem. 1989, 54, 2859-2861 Nastopoulos, V.; Germain, G.; Kallistis, J.; Voliotis, S. Acta Crystallogr., Sect. C 1987, C43, 245-249 Ounsworth, J. P.; Weiler, L. J. Chem. Ed. 1987, 64, 568-572 Plyamovatyi, A. Kh.; Dashevskii, V. G.; Kabachnik, M. I. Dokl. Akad. Nauk SSSR 1977, 234, 1100-1103 Plyamovatyi, A. Kh.; Dashevskii, V. G.; Kabachnik, M. I. Dokl. Akad. Nauk SSSR 1977, 235, 124-127 Plyamovatyi, A. Kh.; Vandyukova, I. I.; Shagidullin, R. R.; Vizel, A. O. Izv. Akad. Nauk SSSR, Ser. Khim. 1990, 1577-1584 Plyamovatyi, A. Kh.; Vandyukova, I. I.; Shagidullin, R. R.; Zhur. Obshch. Khim. 1994, 64, 232-235 Quin, L. D. Conformational Analysis of Medium-Sized Heterocycles; Glass, R. S.; VCH Publishers, Inc.:
New York, 1988, 181-216 Rappé, A. K.; Goddard-III, W. A. J. Phys. Chem. 1991, 95, 3358-3363 Rappé, A. K.; Casewit, C. J.; Colwell, K. S.; Goddard-III, W. A.; Skiff, W. M. J. Am. Chem. Soc. 1992, 114, 10024-10035 Rappé, A. K.; Colwell, K. S. Inorg. Chem. 1993, 32, 3438-3450 Romers, C.; Altona, C.; Buys, H. R.; Havinga, E. Topics in Stereochemistry; E. L. Eliel; N. L. Allinger; Wiley-Interscience:
New York, 4 1969, 39-97 Saeed, A.; McMillin, J. B.; Wolkowicz, P. E.; Brouillette, W. J. Arch. Biochem. Biophys. 1993, 305, 307-312 Saeed, A.; McMillin, J. B.; Wolkowicz, P. E.; Brouillette, W. J. J. Med. Chem. 1994, 37, 3247-3251 Savle, P. S.; Medhekar, R. A.; Kelley, E. L.; May, J. G.; Watkins, S. F.; Fronzcek, F. R.; Quinn, D. M.; Gandour, R. D. Chem. Res. Toxicol. in press. Shinagawa, S.; Kanamaru, T.; Harada, S.; Asai, M.; Okazaki, H. J. Med. Chem. 1987, 30, 1458-1463 Sieburth, S. McN. J. Chem. Soc., Chem. Commun. 1994, 1663-1664 Sun, G.; Savle, P. S.; Gandour, R. D.; a' Bhaird, N. N.; Ramsay, R. R.; Fronczek, F. R. J. Org. Chem. 1995, 60, 6688-6695 Sundaralingam, M. Nature 1968, 217, 35-37 Szabo, A.; Ostlund, N. S. Modern Quantum Chemistry: Introduction to Advanced Electronic Structure Theory; Dover Publications, Inc.:
Mineola, NY, 1996 370-378 Tipton, K. F.; Chase, J. F. A.; Biochem. J. 1969, 115, 517-521 Van Wazer, J. R.; Ewig, C. S. J. Am. Chem. Soc. 1986, 108, 4354-4360 Venkatraghavan, V.; Smith, D. J. Arch. Biochem. Biophys. 1983, 220, 193-199 Weiner, S. J.; Kollman, P. A.; Nguyen, D. T.; Case, D. A. J. Comp. Chem. 1986, 7, 230-252 Weiser, J.; Golan, O.; Fitjer, L.; Biali, S. E. J. Org. Chem. 1996, 61, 8277-8284 Wiberg, K. B. J. Am. Chem. Soc. 1965, 87, 1070-1078 Wiberg, K. B.; Murcko, M. A.; Laidig, K. E.; MacDougall, P. J. J. Phys. Chem. 1990, 94, 6956-6959 Wilson, B.; Georgiadis, R.; Bartmess, J. E. J. Am. Chem. Soc. 1991, 113, 1762-1766 Wolfe, S.; Acc. Chem. Res. 1972, 5, 102-111 Wolfenden, R. Nature 1969, 223, 704-705 Wolfenden, R.; Liang, Y.-L. J. Biol. Chem. 1988, 263, 8022-8026 Wolfenden, R.; Liang, Y.-L. Bioorg. Chem. 1989, 17, 486-489 Naming and numbering scheme for cyclooctane conformers. Boat-chair family.

We have tried to keep the scheme simple and, primarily, to make it easy to draw a particular conformer from the

name. BC has a C_s point group. In general, as soon as substituents are introduced in the ring, the point group becomes C_1 unless the substituents happen to lie in the carbons split by the mirror plane that defines C_s symmetry. Thus, in the general case, we can distinguish two enantiomeric BC conformers, one \ "left-oriented" and one "right-oriented" fig.chiralBCs.gif, 1.640KB "Left-oriented" and "right-oriented" BCs We denote the "left-oriented" version by BC, while the "right-oriented" is BC'. The numbers on the carbons follow a specular relationship to the numbers in the conformational enantiomer.

To name a particular conformer, we keep the numbering fixed. We do follow the chemical convention of always trying to assign the lowest possible numbers, within the constraint that the positions of fixed number positions. Thus, if the substitution pattern allows it, the choice between BC and BC' depends on which one yields the lowest numbers. We define completely the position of a substituent by choosing the appropriate letter among the following:

e
: equatorial

a
: axial

b
: bowsprit

f
: flagpole

i
: isoclinal

according to the following scheme (we have left some of the positions unlabeled for the sake of clarity in the drawing): fig.BCtags.gif, 0.939KB Labels for the orientations of substituents in BC

The point group of TBC is C_2. This is a disymmetric group and allows for chiral shapes. We can therefore distinguish two conformers, one "twisted to the right" and one "twisted to the left". We designate the one "twisted to the left" as TBC, and the "twisted to the right" as TBC'. See the scheme: fig.chiralTBCs.gif, 1.689KB "Left-oriented" and "right-oriented" TBCs The labels for the orientation are as follows: fig.TBCtags.gif, 1.257KB Labels for the orientations of substituents in TBC Chair-chair family.

The CC has a C_{2v} point group. Its shape is slightly elliptical (when seen from the z axis). It has four sets of isochronous carbons (same NMR signal by symmetry). C_{2v} is not a chiral point group so we only have: fig.CCtags.gif, 0.846KB CC numbering and labeling scheme. The numbering starts on one carbon along the major axis of the ellipse.

The Crown is a very high-symmetry conformer, with a D_{4d} point group. All the carbons are undistinguishable by symmetry operations so the choice of any particular carbon to start the numbering is immaterial. The Crown is actually a special case of the CC , but we give the numbering and labels for substituents for the sake of completeness. The introduction of substituents is bound to perturb the high symmetry of the molecule, rendering it as a CC. We do not have any examples of crowns in our results, and we do not find any crown conformers among substituted cyclooctanes, although some authors have referred to CCs as crowns in the past. fig.crowntags.gif, 0.941KB Crown.

The TCC has a D_2 point group. This is a disymmetric group, so we find two enantiomers. The numbering and the names follow this scheme: fig.TCCtags.gif, 1.751KB TCC numbering and labeling scheme.

The TC has a C_{2h} point group. The numbering and the names follow this scheme: fig.TCtags.gif, 1.593KB TC numbering and labeling scheme.

The C has a C_{2h} point group. The numbering and labeling are as follows: fig.Ctags.gif, 0.971KB C numbering and labeling scheme. Boat-boat family.

Boat. fig.Btags.gif, 0.944KB B numbering and labeling scheme. Boat-boat. fig.BBtags.gif, 0.997KB BB numbering and

labeling scheme. Twist-boat. fig.TBtags.gif, 1.700KB TB numbering and labeling scheme. Rules for naming hetero-substituted cyclooctanes.

- *Keep the numberings assigned to the conformations of cyclooctane fixed.*
- *Keep the orientation descriptors, such as equatorial and axial, assigned to the conformations of cyclooctane fixed.*
- *Find out the numbers that correspond to the heteroatoms within the ring.*
- *In case there is more than one way to read the numbers that correspond to the heteroatoms, e. g. 2P-6N in BC vs. 4N-8P in BC', choose the locant set that assigns the lowest numbers.*
- *If the numbers are the same and they just switch positions, e. g., 1N-5P in TBC vs. 1P-5N in TBC', the atom with the highest priority by Cahn-Ingold-Prelog rules gets the lowest number.*
- *If it is not clear which locant set assigns the lowest numbers e.g., 1,4,5,6 or 1,2,7,8 then the locant set that assigns the lowest number to the highest priority atom (CIP rules) is chosen. In the previous locant sets, if the highest priority atom can be either 2 or 4, then the locant set 1,2,7,8 should be chosen, despite the 7,8 being higher than 5 and 6.*
- *Read the numbers that correspond to the substituents on the ring.*
- *List the substituents on the ring preceded by the numbers and an appropriate prefix to indicate the number of times the substituent appears.*
- *Attach to the numbers the abbreviation of the appropriate orientational descriptor.*
- *For substituents on isoclinal positions, specify the R or S configuration of the atom.*

By the previous rules the name for the following conformer: fig.example.gif, 0.827KB Example conformer. is 1,1,5e,8,8-pentamethyl-5a-oxo-1N-4,6-diO-5P-TBC. Software standards used.

This document is encoded in Electronic Theses and Dissertations Markup Language (ETDML) using etd.dtd v.1.1. Non-ASCII characters are encoded in Unicode v.2.0. All the figures are GIF87a (Data type: unsigned char, Dimension order: interleaved, Color model: color index, Coordinate space: upper-left, Minimum: 0, Maximum: 255). The virtual reality models (.wrl files) are encoded in VRML 1.0.*

*The SGML parser used to check this document was "nsgmls" included as part of the package SP v.1.0.1 by James Clark. The word processor was "jot", a utility provided in IRIX 5.3. ISIS/Draw v.1.2 was used for all the chemical drawings. The figures were generated either by using the "snapshot" utility provided in IRIX 5.3 to make a *.rgb image file, which was later converted to GIF87a by "movieconvert", another image processing utility provided in IRIX 5.3; or by saving the image as a Microsoft *.bmp file, which was later converted to GIF87a by LView for Windows v.3.1. The *.wrl files were generated by saving the molecule in PDB format from MacroModel, and then translating with the program pdb2vrml using the "-stick" flag. All the conversions between chemical file formats were done using Babel v.1.1.*

Mention of a given program or brand name does not imply endorsement by Virginia Polytechnic Institute and State University or any of its departments. Chemical files included.

For each VRML model I have included the corresponding file in PDB format (found in the PDB directory). I have also included all the consolidated output files from the conformational searches in macromodel format. README: Notes on the creation of a dissertation in ETD-ML. ETD-ML source encoding.

This the first ETD-ML ETD ever to be submitted. As a hint for future ETD-ML authors, we have made the encoding for this ETD available in its source format.

- *ETD-ML source*

The whole document is structured, with left-indentation corresponding to the logical subdivisions:

```
No spaces for a chapter,
    4 spaces for a section,
        8 spaces (tab) for a subsection,
```

```
            12 spaces (tab + 4) for a block and
                16 spaces (2 tabs) for a subblock.
```

Links, floating matter, footnotes and tables are not indented. That is to allow an easier construction of a list of tables and list of figures by a reformatter (so far, I am the "reformatter" for those lists, I use the UNIX command "grep" and pipe the output to a file, so I have to keep all the text of the captions in the same line).

Greek letters are symbolyzed by their "{name}" to allow them to show up in the HTML version (there is no provision for greek characters in HTML 2.0). The "{name}" should be substituted by the Unicode number. Note: micro and mu are expressed by the same greek letter, but micro is a prefix in the SI system, while mu may have many other meanings. I considered them as separate entities to allow for a "smart" reformatter or search engine that could take that into account.

The entities chemname, casnum and chemform are included only to help in the search of chemical names, Chemical Abstracts Registry Numbers and chemical formulas, respectively. Virtual Reality Modeling Language (VRML).

The three dimensional figures are VRML 1.0 models. The way to incorporate them into a formatted document depends on the technology available and the effect desired by the formatter. VRML figures can be shown as hyperlinks (in HTML) by means of an anchored reference, such as:

```
(caption text)
]]>
```

This is what I did in the HTML version of my dissertation, because of the computational overhead involved in loading and displaying literally hundreds of little VRML viewers in the same page. Anyway, the VRML models are still encoded as:

```
(caption text)
]]>
```

so the reformatter has to make the decision about displaying them as an anchored reference or as an embedded VRML viewer window, e.g., a smart reformatter could choose to display some of the 3D models as anchored references and embed the others.

The virtual reality viewer can also be embedded in a HTML homepage by means of the following code:

```
    (caption text)
]]>
```

It is strongly recommended that the "type" parameter be present. This helps the browser correctly handle the

rendering of the image. In the future, it may be necessary to change the x-world/x-vrml type to the definitive MIME type declaration (probably "world/vrml"). So far, "x-world/x-vrml" is an experimental MIME type (thus the "x-" prefix), although it is recognized by most browsers.

These VRML files were succesfully viewed using CosmoPlayer and Live3D. PDB files can be converted to VRML using the script pdb2vrml, available from:

- *http://www.pc.chemie.th-darmstadt.de/vrml/pdb2vrml.html*

Chemical Markup Language (CML).

Markup coding of chemical information is still in its infancy. There is a beginning in CML v.1.0 (Chemical Markup Language). You can find all there is to know about CML at (as of June, 1997):

- *http://www.venus.co.uk/omf/cml-1.0/intro.html*

If the URL doesn't work, a Web search specifying "Chemical Markup Language" or "Open Molecule Foundation" should yield some relevant hits.

*Attempting a "merge" of CML coding into ETD-ML coding was beyond the resources (mostly time) available to this writer, although it is clearly the best way to go. Future customizations of the ETD-ML for chemistry should allow for elements encoded in CML. Anyway, since so far there is no accepted standard format for encoding molecular structures I decided to store the structures as VRML models and in PDB format. The PDB format files are not referred to *at any point* in the text of the dissertation, they are kept only because they are the actual results obtained from the modeling and, therefore, contain more chemical information than VRML files. PDB is not even a de facto standard, but it is widely used and it is better than XYZ coordinates because it preserves the connectivities between the atoms (XYZ readers have to make educated guesses about how atoms are connected and about the bond orders). Babel, PDB, Chime.*

It is possible to use Babel, together with the PDB files and a Netscape plug-in called Chime (available without cost from MDL, Inc.), to yield a fancier rendering of the molecules. Use Babel to transform the PDB files to MDL's MOL format and embed the images in a HTML page using the following code:

```
    (caption text)
</embed>
```

This will result in a figure containing a 2D projection of the 3D structure. Clicking on the right button of the mouse will bring up the option of 3D rendering. It also allows for real-time rotation, rendering as wires, ball and stick, sticks, VDW spheres and others. I have included the MDL molfiles. They have the extension ".mol". Chime can be downloaded from:

- *http://www.mdli.com/chemscape/chime/chime.html*

Chime can identify and render many other chemical types, such as: PDB, XYZ, MOPAC and Gaussian input, MDL's molfile and rxnfile, and EMBL nucleotide format. Only the MDL molfile format will yield the switchable 2D<->3D view.Note. NOTE: The SGI version of Chime will not work reading molfiles in a local filesystem, only through a network.

BTW, Babel can be downloaded from the software archives of the Computational Chemistry Mailing List at:

- *ftp://ccl.osc.edu/pub/chemistry/software/*

looking under the appropriate operating system. Reformatting the molecules.

If a reformatter decides to use XYZ files to visualize the molecules (after converting the PDB files to XYZ format), there is a Java applet developed by Sun Microsystems named XYZApp.class (downloadable from http://java.sun.com) that can do the job, although the rendering is somewhat primitive.

A minimum code to embed XYZApp.class in a HTML document is:

```
]]>
```

It is necessary to have Matrix3D.class to be able to run XYZApp.class. Footnotes.

All the footnotes are referred to as "Note."s. It would be desirable to have a reformatter that used more standard designations: superscript arabic numbers (Journal of American Chemical Society-style), or a standard sequence of characters (such as the ones specified in the journals "Science" or the "Proceedings of the National Academy of Sciences of the USA") Notes on MOL notation substitution.

*The following table contains only GIF images and VRML models. Substituting the extension "mol" instead of the "wrl" will access the MDL molfiles, displayable with Chime. It will also be necessary to move the *.mol files out of the MOL directory.In that case, the GIF images will be unnecessary, because molfiles in Chime yield both 2D and 3d views. This is likely to require human intervention, because a reformating script would have to be *really* smart to accomodate all these changes. The caption is all in one line to make it easier to use a utility like "grep" when gathering a "List of Tables." See table. README.TXT: Files in this ETD.*

```
Rosas.tar.gz can be gunzipped to yield a tarred file that contains all
the files of my dissertation.  When untarred, the whole thing takes about
6.5MB.  The following is a list of all the files included (total of 457,
not including directories):

The version of gzip was 1.2.4.

dissertation:
total 1166
-rw-r--r--    1 rosas    user      320242 Jul  3 17:30 diss.etd
-rw-r--r--    1 rosas    user         243 Jun 17 13:16 README.TXT
drwxr-xr-x    4 rosas    user        1024 Jun 17 11:17 carnitine
drwxr-xr-x    3 rosas    user         512 Jun 17 11:09 cyclohexane
drwxr-xr-x    5 rosas    user        3072 Jun 17 11:04 cyclooctane
-rw-r--r--    1 rosas    user       13594 Mar 11 03:09 etd.dtd
drwxr-xr-x    4 rosas    user         512 Jun 17 11:31 methylphosp
drwxr-xr-x    3 rosas    user         512 Jun 17 11:10 morpholinium
drwxr-xr-x    5 rosas    user        3072 Jun 17 11:21 phosphacinium
drwxr-xr-x    2 rosas    user        1024 Jun 17 11:26 reviews

dissertation/carnitine:
total 247
drwxr-xr-x    2 rosas    user         512 Jun 17 11:17 MOL
drwxr-xr-x    2 rosas    user         512 Jun 17 11:17 PDB
-rw-r--r--    1 rosas    user       16959 May 17 11:46 RRGas.wrl
-rw-r--r--    1 rosas    user       17048 May 17 11:47 RRWat.wrl
-rw-r--r--    1 rosas    user       17017 May 17 11:48 RSGas.wrl
-rw-r--r--    1 rosas    user       16938 May 17 11:51 RSWat.wrl
-rw-r--r--    1 rosas    user        1967 May  1 12:32 TableAcCarnAM1Gas.html
-rw-r--r--    1 rosas    user        4961 May  1 12:33 TableAcCarnAM1Wat.html
-rw-r--r--    1 rosas    user        1781 May  1 12:33 TableAcCholAM1Gas.html
-rw-r--r--    1 rosas    user        2935 May  1 12:34 TableAcCholAM1Wat.html
-rw-r--r--    1 rosas    user        1949 May  1 12:34 TableCarnAM1Gas.html
-rw-r--r--    1 rosas    user        3251 May  1 12:34 TableCarnAM1Wat.html
-rw-r--r--    1 rosas    user        1203 May  1 12:34 TableCholAM1Gas.html
-rw-r--r--    1 rosas    user        1172 May  1 12:35 TableCholAM1Wat.html
```

```
-rw-r--r--    1 rosas    user        4805 May  1 12:36 TableOAcPrAM1Gas.html
-rw-r--r--    1 rosas    user        3950 May  1 12:36 TableOAcPrAM1Wat.html
-rw-r--r--    1 rosas    user        3356 May  1 12:37 TableOHPrAM1Gas.html
-rw-r--r--    1 rosas    user        2896 May  1 12:37 TableOHPrAM1Wat.html
-rw-r--r--    1 rosas    user         801 May 17 11:29 fig.RRWat.gif
-rw-r--r--    1 rosas    user         807 May 17 11:36 fig.RSWat.gif
-rw-r--r--    1 rosas    user         608 Feb  8 23:41 fig.extended.gif
-rw-r--r--    1 rosas    user        1511 May 18 12:47 fig.fitTI.gif
-rw-r--r--    1 rosas    user         510 May 22 14:17 fig.folded.gif
-rw-r--r--    1 rosas    user        4852 Apr  1 00:25 fig.highlight.gif
-rw-r--r--    1 rosas    user        2491 Apr  1 12:51 fig.hydrolysis1.gif
-rw-r--r--    1 rosas    user        4823 Apr  3 18:56 fig.solvation.gif
-rw-r--r--    1 rosas    user         731 May  5 21:15 fig.torsions.gif

dissertation/carnitine/MOL:
total 24
-rw-r--r--    1 rosas    user        2679 May 27 13:56 RRGas.mol
-rw-r--r--    1 rosas    user        2679 May 27 13:56 RRWat.mol
-rw-r--r--    1 rosas    user        2679 May 27 13:56 RSGas.mol
-rw-r--r--    1 rosas    user        2679 May 27 13:56 RSWat.mol

dissertation/carnitine/PDB:
total 40
-rw-r--r--    1 rosas    user        4620 May 17 11:41 RRGas.pdb
-rw-r--r--    1 rosas    user        4620 May 17 11:41 RRWat.pdb
-rw-r--r--    1 rosas    user        4620 May 17 11:41 RSGas.pdb
-rw-r--r--    1 rosas    user        4620 May 17 11:42 RSWat.pdb

dissertation/cyclohexane:
total 68
drwxr-xr-x    2 rosas    user         512 Jun 17 11:10 MOD
-rw-r--r--    1 rosas    user        1545 Jan 30 14:16 TableCyclohGas.html
-rw-r--r--    1 rosas    user        3660 May  1 13:49 TableDiMeCyclohGas.html
-rw-r--r--    1 rosas    user       15426 May  1 14:11 TableEtTriMeCyclohGas.html
-rw-r--r--    1 rosas    user        3913 May  1 14:03 TableTetraMeCyclohGas.html
-rw-r--r--    1 rosas    user        4378 May  1 14:02 TableTriMeCyclohGas.html
-rw-r--r--    1 rosas    user        3085 Mar  8 23:56 fig.hexConfs.gif

dissertation/cyclohexane/MOD:
total 813
-rw-r--r--    1 rosas    user        9431 Jun 17 11:09 CyclohexGas.out
-rw-r--r--    1 rosas    user       37811 Jun 17 11:09 DiMeCyclohexGas.out
-rw-r--r--    1 rosas    user       51129 Jun 17 11:09 TetMeCyclohexGas.out
-rw-r--r--    1 rosas    user       70920 Jun 17 11:09 TriMeCyclohexGas.out
-rw-r--r--    1 rosas    user      246240 Jun 17 11:09 TriMeEtCyclohexGas.out

dissertation/cyclooctane:
total 1331
drwxr-xr-x    2 rosas    user         512 Jun 17 11:04 MOD
drwxr-xr-x    2 rosas    user         512 Jun 17 10:02 MOL
drwxr-xr-x    2 rosas    user        1024 Jun 17 10:02 PDB
-rw-r--r--    1 rosas    user       10455 May  1 14:28 Table4MeCyclooctGas.html
-rw-r--r--    1 rosas    user       27249 May  1 14:28 Table5MeCyclooctGas.html
-rw-r--r--    1 rosas    user       19927 May 15 11:11 Table6MeCyclooctGas.html
-rw-r--r--    1 rosas    user        6936 May  1 14:30 TableCycloctGas.html
-rw-r--r--    1 rosas    user       14000 May 15 15:18 bb14O.wrl
-rw-r--r--    1 rosas    user       14195 May 15 15:31 bb24O.wrl
-rw-r--r--    1 rosas    user       15165 May 16 15:18 bb5O.wrl
-rw-r--r--    1 rosas    user       16350 May 16 22:21 bb6O.wrl
-rw-r--r--    1 rosas    user        9668 May 15 14:02 bc.wrl
-rw-r--r--    1 rosas    user       14058 May 15 15:17 bc14O.wrl
-rw-r--r--    1 rosas    user       15236 May 16 15:26 bc15O.wrl
-rw-r--r--    1 rosas    user       16189 May 16 22:29 bc16O.wrl
-rw-r--r--    1 rosas    user       14074 May 15 15:22 bc24O.wrl
-rw-r--r--    1 rosas    user       15183 May 16 15:27 bc25O.wrl
-rw-r--r--    1 rosas    user       16221 May 16 22:24 bc26O.wrl
-rw-r--r--    1 rosas    user       15291 May 16 15:37 bc35O.wrl
-rw-r--r--    1 rosas    user       15037 May 16 15:39 bc45O.wrl
-rw-r--r--    1 rosas    user       15179 May 16 15:43 bc55O.wrl
-rw-r--r--    1 rosas    user       15200 May 16 15:44 bc65O.wrl
-rw-r--r--    1 rosas    user       14201 May 15 15:33 cc4O.wrl
-rw-r--r--    1 rosas    user       15181 May 16 15:32 cc5O.wrl
-rw-r--r--    1 rosas    user         997 Mar 12 14:05 fig.BBtags.gif
-rw-r--r--    1 rosas    user         939 Mar 12 02:34 fig.BCtags.gif
-rw-r--r--    1 rosas    user         944 Mar 12 13:59 fig.Btags.gif
-rw-r--r--    1 rosas    user         846 Mar 12 12:30 fig.CCtags.gif
-rw-r--r--    1 rosas    user         971 Mar 12 13:48 fig.Ctags.gif
-rw-r--r--    1 rosas    user        1257 Mar 12 11:37 fig.TBCtags.gif
-rw-r--r--    1 rosas    user        1700 Mar 12 16:24 fig.TBtags.gif
-rw-r--r--    1 rosas    user        1751 Mar 12 12:46 fig.TCCtags.gif
-rw-r--r--    1 rosas    user        1593 Jun 13 15:25 fig.TCtags.gif
```

```
-rw-r--r--    1 rosas    user         430 May 14 21:50 fig.bb14O.gif
-rw-r--r--    1 rosas    user         435 May 14 21:49 fig.bb24O.gif
-rw-r--r--    1 rosas    user         489 May 15 11:04 fig.bb5O.gif
-rw-r--r--    1 rosas    user         449 May 15 14:18 fig.bb6O.gif
-rw-r--r--    1 rosas    user         249 May 14 20:01 fig.bc0O.gif
-rw-r--r--    1 rosas    user         301 May 14 21:23 fig.bc14O.gif
-rw-r--r--    1 rosas    user         364 May 14 22:15 fig.bc15O.gif
-rw-r--r--    1 rosas    user         439 May 15 14:21 fig.bc16O.gif
-rw-r--r--    1 rosas    user         301 May 14 21:20 fig.bc24O.gif
-rw-r--r--    1 rosas    user         365 May 14 22:37 fig.bc25O.gif
-rw-r--r--    1 rosas    user         441 May 15 14:20 fig.bc26O.gif
-rw-r--r--    1 rosas    user         402 May 14 23:20 fig.bc35O.gif
-rw-r--r--    1 rosas    user         405 May 14 23:24 fig.bc45O.gif
-rw-r--r--    1 rosas    user         434 May 15 10:58 fig.bc55O.gif
-rw-r--r--    1 rosas    user         435 May 15 11:01 fig.bc65O.gif
-rw-r--r--    1 rosas    user         324 May 14 21:54 fig.cc4O.gif
-rw-r--r--    1 rosas    user         334 May 14 22:52 fig.cc5O.gif
-rw-r--r--    1 rosas    user        1640 Mar 12 02:09 fig.chiralBCs.gif
-rw-r--r--    1 rosas    user        1689 Mar 12 02:47 fig.chiralTBCs.gif
-rw-r--r--    1 rosas    user         941 Mar 12 12:16 fig.crowntags.gif
-rw-r--r--    1 rosas    user         823 May 14 16:07 fig.hmx.gif
-rw-r--r--    1 rosas    user         435 May 14 21:32 fig.tb14O.gif
-rw-r--r--    1 rosas    user         435 May 14 22:58 fig.tb15O.gif
-rw-r--r--    1 rosas    user         511 May 15 11:18 fig.tb16O.gif
-rw-r--r--    1 rosas    user         427 May 14 21:34 fig.tb24O.gif
-rw-r--r--    1 rosas    user         459 May 14 23:04 fig.tb25O.gif
-rw-r--r--    1 rosas    user         515 May 15 11:21 fig.tb26O.gif
-rw-r--r--    1 rosas    user         481 May 14 23:07 fig.tb35O.gif
-rw-r--r--    1 rosas    user         489 May 14 23:17 fig.tb45O.gif
-rw-r--r--    1 rosas    user         307 May 14 20:42 fig.tbc-10O.gif
-rw-r--r--    1 rosas    user         311 May 14 20:29 fig.tbc10O.gif
-rw-r--r--    1 rosas    user         377 May 14 21:57 fig.tbc14O.gif
-rw-r--r--    1 rosas    user         394 May 15 10:38 fig.tbc15O.gif
-rw-r--r--    1 rosas    user         379 May 14 21:59 fig.tbc24O.gif
-rw-r--r--    1 rosas    user         389 May 15 10:41 fig.tbc25O.gif
-rw-r--r--    1 rosas    user         396 May 15 10:49 fig.tbc35O.gif
-rw-r--r--    1 rosas    user         392 May 15 10:51 fig.tbc45O.gif
-rw-r--r--    1 rosas    user         280 May 14 20:19 fig.tcc-10O.gif
-rw-r--r--    1 rosas    user         257 May 14 20:03 fig.tcc10O.gif
-rw-r--r--    1 rosas    user         365 May 14 21:27 fig.tcc14O.gif
-rw-r--r--    1 rosas    user         381 May 14 22:44 fig.tcc15O.gif
-rw-r--r--    1 rosas    user         357 May 14 21:28 fig.tcc24O.gif
-rw-r--r--    1 rosas    user         405 May 14 22:48 fig.tcc25O.gif
-rw-r--r--    1 rosas    user       14069 May 15 15:25 tb14O.wrl
-rw-r--r--    1 rosas    user       15190 May 16 15:33 tb15O.wrl
-rw-r--r--    1 rosas    user       16172 May 16 22:26 tb16O.wrl
-rw-r--r--    1 rosas    user       14143 May 15 15:28 tb24O.wrl
-rw-r--r--    1 rosas    user       15177 May 16 15:34 tb25O.wrl
-rw-r--r--    1 rosas    user       16226 May 16 22:27 tb26O.wrl
-rw-r--r--    1 rosas    user       15126 May 16 15:35 tb35O.wrl
-rw-r--r--    1 rosas    user       15168 May 16 15:36 tb45O.wrl
-rw-r--r--    1 rosas    user        9649 May 15 14:02 tbc1.wrl
-rw-r--r--    1 rosas    user       14084 May 15 15:37 tbc14O.wrl
-rw-r--r--    1 rosas    user       15276 May 16 15:40 tbc15O.wrl
-rw-r--r--    1 rosas    user        9654 May 15 14:04 tbc2.wrl
-rw-r--r--    1 rosas    user       14084 May 15 15:38 tbc24O.wrl
-rw-r--r--    1 rosas    user       15220 May 16 15:41 tbc25O.wrl
-rw-r--r--    1 rosas    user        9667 May 15 14:04 tbc3.wrl
-rw-r--r--    1 rosas    user       15116 May 16 15:45 tbc35O.wrl
-rw-r--r--    1 rosas    user        9667 May 15 14:05 tbc4.wrl
-rw-r--r--    1 rosas    user       15141 May 16 15:46 tbc45O.wrl
-rw-r--r--    1 rosas    user        9651 May 15 14:05 tcc1.wrl
-rw-r--r--    1 rosas    user       14027 May 15 15:23 tcc14O.wrl
-rw-r--r--    1 rosas    user       15302 May 16 15:29 tcc15O.wrl
-rw-r--r--    1 rosas    user       14082 May 15 15:24 tcc24O.wrl
-rw-r--r--    1 rosas    user       15238 May 16 15:31 tcc25O.wrl

dissertation/cyclooctane/MOD:
total 1177
-rw-r--r--    1 rosas    user       56619 Jun 17 11:03 CycloocTotGas.out
-rw-r--r--    1 rosas    user      190512 Jun 17 11:03 HexMeCycloocTotGas.out
-rw-r--r--    1 rosas    user      171493 Jun 17 11:03 PentMeCycloocTotGas.out
-rw-r--r--    1 rosas    user      183139 Jun 17 11:03 TetMeCycloocTotGas.out

dissertation/cyclooctane/MOL:
total 138
-rw-r--r--    1 rosas    user        2697 May 27 13:56 bb5O.mol
-rw-r--r--    1 rosas    user        2901 May 27 13:56 bb6O.mol
-rw-r--r--    1 rosas    user        2698 May 27 13:56 bc15O.mol
-rw-r--r--    1 rosas    user        2902 May 27 13:56 bc16O.mol
-rw-r--r--    1 rosas    user        2698 May 27 13:56 bc25O.mol
```

```
-rw-r--r--    1 rosas    user         2902 May 27 13:56 bc26O.mol
-rw-r--r--    1 rosas    user         2698 May 27 13:56 bc35O.mol
-rw-r--r--    1 rosas    user         2698 May 27 13:56 bc45O.mol
-rw-r--r--    1 rosas    user         2698 May 27 13:56 bc55O.mol
-rw-r--r--    1 rosas    user         2698 May 27 13:56 bc65O.mol
-rw-r--r--    1 rosas    user         2697 May 27 13:56 cc5O.mol
-rw-r--r--    1 rosas    user         2698 May 27 13:56 tb15O.mol
-rw-r--r--    1 rosas    user         2902 May 27 13:56 tb16O.mol
-rw-r--r--    1 rosas    user         2698 May 27 13:56 tb25O.mol
-rw-r--r--    1 rosas    user         2902 May 27 13:56 tb26O.mol
-rw-r--r--    1 rosas    user         2698 May 27 13:56 tb35O.mol
-rw-r--r--    1 rosas    user         2698 May 27 13:56 tb45O.mol
-rw-r--r--    1 rosas    user         2699 May 27 13:56 tbc15O.mol
-rw-r--r--    1 rosas    user         2699 May 27 13:56 tbc25O.mol
-rw-r--r--    1 rosas    user         2699 May 27 13:56 tbc35O.mol
-rw-r--r--    1 rosas    user         2699 May 27 13:56 tbc45O.mol
-rw-r--r--    1 rosas    user         2699 May 27 13:56 tcc15O.mol
-rw-r--r--    1 rosas    user         2699 May 27 13:56 tcc25O.mol

dissertation/cyclooctane/PDB:
total 347
-rw-r--r--    1 rosas    user         2899 May 15 11:28 BC.pdb
-rw-r--r--    1 rosas    user         2899 May 15 11:32 TBC1.pdb
-rw-r--r--    1 rosas    user         2899 May 15 11:31 TBC2.pdb
-rw-r--r--    1 rosas    user         2899 May 15 11:34 TBC3.pdb
-rw-r--r--    1 rosas    user         2899 May 15 11:35 TBC4.pdb
-rw-r--r--    1 rosas    user         2899 May 15 11:27 TCC1.pdb
-rw-r--r--    1 rosas    user         4197 May 15 14:56 bb14O.pdb
-rw-r--r--    1 rosas    user         4197 May 15 14:57 bb24O.pdb
-rw-r--r--    1 rosas    user         4550 May 16 15:04 bb5O.pdb
-rw-r--r--    1 rosas    user         4865 May 16 21:49 bb6O.pdb
-rw-r--r--    1 rosas    user         4197 May 15 14:52 bc14O.pdb
-rw-r--r--    1 rosas    user         4550 May 16 14:57 bc15O.pdb
-rw-r--r--    1 rosas    user         4865 May 16 21:49 bc16O.pdb
-rw-r--r--    1 rosas    user         4197 May 15 14:52 bc24O.pdb
-rw-r--r--    1 rosas    user         4550 May 16 14:57 bc25O.pdb
-rw-r--r--    1 rosas    user         4865 May 16 21:50 bc26O.pdb
-rw-r--r--    1 rosas    user         4550 May 16 15:01 bc35O.pdb
-rw-r--r--    1 rosas    user         4550 May 16 15:01 bc45O.pdb
-rw-r--r--    1 rosas    user         4550 May 16 15:04 bc55O.pdb
-rw-r--r--    1 rosas    user         4550 May 16 15:04 bc65O.pdb
-rw-r--r--    1 rosas    user         4197 May 15 14:57 cc4O.pdb
-rw-r--r--    1 rosas    user         4550 May 16 14:58 cc5O.pdb
-rw-r--r--    1 rosas    user         4197 May 15 14:55 tb14O.pdb
-rw-r--r--    1 rosas    user         4550 May 16 14:59 tb15O.pdb
-rw-r--r--    1 rosas    user         4865 May 16 21:47 tb16O.pdb
-rw-r--r--    1 rosas    user         4197 May 15 14:55 tb24O.pdb
-rw-r--r--    1 rosas    user         4550 May 16 14:58 tb25O.pdb
-rw-r--r--    1 rosas    user         4865 May 16 21:48 tb26O.pdb
-rw-r--r--    1 rosas    user         4550 May 16 15:00 tb35O.pdb
-rw-r--r--    1 rosas    user         4550 May 16 14:59 tb45O.pdb
-rw-r--r--    1 rosas    user         4197 May 15 14:57 tbc14O.pdb
-rw-r--r--    1 rosas    user         4550 May 16 15:02 tbc15O.pdb
-rw-r--r--    1 rosas    user         4197 May 15 14:58 tbc24O.pdb
-rw-r--r--    1 rosas    user         4550 May 16 15:02 tbc25O.pdb
-rw-r--r--    1 rosas    user         4550 May 16 15:05 tbc35O.pdb
-rw-r--r--    1 rosas    user         4550 May 16 15:05 tbc45O.pdb
-rw-r--r--    1 rosas    user         4197 May 15 14:53 tcc14O.pdb
-rw-r--r--    1 rosas    user         4550 May 16 14:57 tcc15O.pdb
-rw-r--r--    1 rosas    user         4197 May 15 14:55 tcc24O.pdb
-rw-r--r--    1 rosas    user         4550 May 16 14:58 tcc25O.pdb

dissertation/methylphosp:
total 271
drwxr-xr-x    2 rosas    user          512 Jun 17 11:15 Abinitio
drwxr-xr-x    2 rosas    user          512 Jun 17 11:31 PDB
-rw-r--r--    1 rosas    user        15784 Mar 15 02:53 cegxuh.wrl
-rw-r--r--    1 rosas    user        15993 Mar 15 02:53 duksor.wrl
-rw-r--r--    1 rosas    user        26911 Mar 15 02:54 dumlec.wrl
-rw-r--r--    1 rosas    user        23386 Mar 15 02:54 felsoe.wrl
-rw-r--r--    1 rosas    user         4000 May 19 10:18 fig.confs.gif
-rw-r--r--    1 rosas    user         4789 May 13 14:31 fig.copo.gif
-rw-r--r--    1 rosas    user         4142 May 13 14:31 fig.cp2o.gif
-rw-r--r--    1 rosas    user         4624 May 13 16:04 fig.crystals.gif
-rw-r--r--    1 rosas    user         4349 May 13 14:31 fig.hcpo.gif
-rw-r--r--    1 rosas    user         3991 May 13 14:31 fig.opo.gif
-rw-r--r--    1 rosas    user         3795 May 13 14:31 fig.pc.gif
-rw-r--r--    1 rosas    user         3817 May 13 14:31 fig.po.gif
-rw-r--r--    1 rosas    user         4658 Jun 12 15:27 fig.profiles.gif
-rw-r--r--    1 rosas    user        13587 Mar 15 02:54 zaysib.wrl
```

```
dissertation/methylphosp/Abinitio:
total 303
-rw-r--r--    1 rosas    user       17096 Jun 17 11:14 AngleCP2O.txt
-rw-r--r--    1 rosas    user       19003 Jun 17 11:14 AngleOPO.txt
-rw-r--r--    1 rosas    user       12499 Jun 17 11:14 BondPC.txt
-rw-r--r--    1 rosas    user        9487 Jun 17 11:14 BondPO.txt
-rw-r--r--    1 rosas    user        1958 Jun 17 11:14 CP1O2angle.txt
-rw-r--r--    1 rosas    user       10562 Jun 17 11:14 CP1Oangle.txt
-rw-r--r--    1 rosas    user       59929 Jun 17 11:14 TorCOPO.txt
-rw-r--r--    1 rosas    user       21441 Jun 17 11:14 TorHCPO.txt
-rw-r--r--    1 rosas    user        1014 Jun 17 11:14 diMephopGM.txt

dissertation/methylphosp/PDB:
total 54
-rw-r--r--    1 rosas    user        4491 Mar 15 02:48 cegxuh.pdb
-rw-r--r--    1 rosas    user        4308 Mar 15 02:48 duksor.pdb
-rw-r--r--    1 rosas    user        7539 Mar 15 02:49 dumlec.pdb
-rw-r--r--    1 rosas    user        6677 Mar 15 02:49 felsoe.pdb
-rw-r--r--    1 rosas    user        3508 Mar 15 02:47 zaysib.pdb

dissertation/morpholinium:
total 113
drwxr-xr-x    2 rosas    user         512 Jun 17 11:12 MOD
-rw-r--r--    1 rosas    user        3762 May  1 14:18 TableDiMeMorpholGas.html
-rw-r--r--    1 rosas    user        3635 May  1 14:20 TableDiMeMorpholWat.html
-rw-r--r--    1 rosas    user       13510 May 11 17:36 TableMeOHMorpholGas.html
-rw-r--r--    1 rosas    user       13489 May  1 14:24 TableMeOHMorpholWat.html
-rw-r--r--    1 rosas    user        3031 May  1 13:46 TableMorpholGas.html
-rw-r--r--    1 rosas    user        3655 May  1 14:13 TableMorpholWat.html
-rw-r--r--    1 rosas    user        4232 May  1 14:22 TableSMeMorpholGas.html
-rw-r--r--    1 rosas    user        4452 May  1 14:23 TableSMeMorpholWat.html
-rw-r--r--    1 rosas    user         607 Apr  3 12:04 fig.MeOHtags.gif
-rw-r--r--    1 rosas    user         497 Apr  3 11:42 fig.Morphtags.gif
-rw-r--r--    1 rosas    user         539 Apr  3 11:47 fig.StriMetags.gif
-rw-r--r--    1 rosas    user         440 Mar  4 16:34 fig.morph.gif
-rw-r--r--    1 rosas    user         583 May 19 12:25 fig.savle97.gif
-rw-r--r--    1 rosas    user         527 Apr  3 11:57 fig.tetraMetags.gif

dissertation/morpholinium/MOD:
total 1830
-rw-r--r--    1 rosas    user       58800 Jun 17 11:11 DiMeMorphGas.out
-rw-r--r--    1 rosas    user       76314 Jun 17 11:11 DiMeMorphWat.out
-rw-r--r--    1 rosas    user      384203 Jun 17 11:11 MeOHMorphGas.out
-rw-r--r--    1 rosas    user      224436 Jun 17 11:11 MeOHMorphWat.out
-rw-r--r--    1 rosas    user       34813 Jun 17 11:11 MorphGas.out
-rw-r--r--    1 rosas    user       43515 Jun 17 11:11 MorphWat.out
-rw-r--r--    1 rosas    user       55895 Jun 17 11:11 SMeMorphGas.out
-rw-r--r--    1 rosas    user       57159 Jun 17 11:11 SMeMorphWat.out

dissertation/phosphacinium:
total 1575
drwxr-xr-x    2 rosas    user         512 Jun 17 11:07 MOD
drwxr-xr-x    2 rosas    user         512 Jun 17 10:00 MOL
drwxr-xr-x    2 rosas    user        1024 Jun 17 10:00 PDB
-rw-r--r--    1 rosas    user       21169 May  1 14:35 TableCisMedioxPGas.html
-rw-r--r--    1 rosas    user       22816 May  1 14:35 TableCisMedioxPWat.html
-rw-r--r--    1 rosas    user       28178 May  1 14:36 TableDiMePGas.html
-rw-r--r--    1 rosas    user       41551 Jun 17 10:52 TableDiMePWat.html
-rw-r--r--    1 rosas    user       20393 May 10 11:24 TableDioxPGas.html
-rw-r--r--    1 rosas    user       30599 May  8 20:27 TableDioxPWat.html
-rw-r--r--    1 rosas    user       29038 May  1 14:40 TableTransMedioxPGas.html
-rw-r--r--    1 rosas    user       37001 Jun 17 11:00 TableTransMedioxPWat.html
-rw-r--r--    1 rosas    user       13903 May 16 20:25 bb1PW2.wrl
-rw-r--r--    1 rosas    user       14854 Jun 13 10:44 bb1PW4.wrl
-rw-r--r--    1 rosas    user       13751 May 16 20:27 bb2PW2.wrl
-rw-r--r--    1 rosas    user       14818 May 16 21:40 bb2PW4.wrl
-rw-r--r--    1 rosas    user       14764 May 16 21:38 bbPW3.wrl
-rw-r--r--    1 rosas    user       13665 May 26 11:18 bc1P2.wrl
-rw-r--r--    1 rosas    user       15785 Jun 13 10:45 bc1P5.wrl
-rw-r--r--    1 rosas    user       13695 May 16 20:28 bc1PW2.wrl
-rw-r--r--    1 rosas    user       14847 May 16 21:36 bc1PW3.wrl
-rw-r--r--    1 rosas    user       14860 May 16 21:37 bc1PW4.wrl
-rw-r--r--    1 rosas    user       13653 May 16 22:40 bc2P2.wrl
-rw-r--r--    1 rosas    user       15785 Jun 16 15:47 bc2P5.wrl
-rw-r--r--    1 rosas    user       13702 May 16 20:32 bc2PW2.wrl
-rw-r--r--    1 rosas    user       14796 May 16 21:36 bc2PW3.wrl
-rw-r--r--    1 rosas    user       14924 May 16 21:37 bc2PW4.wrl
-rw-r--r--    1 rosas    user       14873 May 16 22:55 bcP3.wrl
-rw-r--r--    1 rosas    user       14860 Jun 13 10:47 bcP4.wrl
-rw-r--r--    1 rosas    user         489 May 16 10:42 fig.bb1PW2.gif
-rw-r--r--    1 rosas    user         527 May 16 11:34 fig.bb1PW4.gif
```

```
-rw-r--r--   1 rosas    user         457 May 16 10:42 fig.bb2PW2.gif
-rw-r--r--   1 rosas    user         519 May 16 11:29 fig.bb2PW4.gif
-rw-r--r--   1 rosas    user         524 May 16 11:21 fig.bbPW3.gif
-rw-r--r--   1 rosas    user         451 May 15 16:02 fig.bc1P2.gif
-rw-r--r--   1 rosas    user         530 May 16 14:38 fig.bc1P5.gif
-rw-r--r--   1 rosas    user         446 May 16 10:45 fig.bc1PW2.gif
-rw-r--r--   1 rosas    user         477 May 16 11:15 fig.bc1PW3.gif
-rw-r--r--   1 rosas    user         487 May 16 11:39 fig.bc1PW4.gif
-rw-r--r--   1 rosas    user         434 May 15 16:05 fig.bc2P2.gif
-rw-r--r--   1 rosas    user         521 May 16 14:37 fig.bc2P5.gif
-rw-r--r--   1 rosas    user         437 May 16 10:47 fig.bc2PW2.gif
-rw-r--r--   1 rosas    user         482 May 16 11:14 fig.bc2PW3.gif
-rw-r--r--   1 rosas    user         481 May 16 11:44 fig.bc2PW4.gif
-rw-r--r--   1 rosas    user         525 May 16 13:58 fig.bcP3.gif
-rw-r--r--   1 rosas    user         517 May 16 14:06 fig.bcP4.gif
-rw-r--r--   1 rosas    user         695 Mar 25 01:16 fig.cis.gif
-rw-r--r--   1 rosas    user         728 Mar 25 01:25 fig.diMeP.gif
-rw-r--r--   1 rosas    user         827 Apr  3 14:05 fig.example.gif
-rw-r--r--   1 rosas    user         591 Feb  8 23:03 fig.phosp.gif
-rw-r--r--   1 rosas    user         670 Mar 18 22:59 fig.phospTab.gif
-rw-r--r--   1 rosas    user         522 May 16 13:39 fig.tb1P2.gif
-rw-r--r--   1 rosas    user         497 May 16 14:11 fig.tb1P4.gif
-rw-r--r--   1 rosas    user         570 May 16 14:44 fig.tb1P5.gif
-rw-r--r--   1 rosas    user         583 May 16 13:21 fig.tb1PW5.gif
-rw-r--r--   1 rosas    user         516 May 16 13:37 fig.tb2P2.gif
-rw-r--r--   1 rosas    user         536 May 16 14:28 fig.tb2P4.gif
-rw-r--r--   1 rosas    user         552 May 16 14:48 fig.tb2P5.gif
-rw-r--r--   1 rosas    user         601 May 16 13:24 fig.tb2PW5.gif
-rw-r--r--   1 rosas    user         555 May 16 11:07 fig.tbPW3.gif
-rw-r--r--   1 rosas    user         461 May 15 16:13 fig.tbc1P2.gif
-rw-r--r--   1 rosas    user         509 May 16 14:02 fig.tbc1P4.gif
-rw-r--r--   1 rosas    user         460 May 15 16:11 fig.tbc2P2.gif
-rw-r--r--   1 rosas    user         519 May 16 14:17 fig.tbc2P4.gif
-rw-r--r--   1 rosas    user         534 May 16 14:51 fig.tbcP5.gif
-rw-r--r--   1 rosas    user         497 May 16 14:08 fig.tc1P4.gif
-rw-r--r--   1 rosas    user         511 May 16 14:20 fig.tc2P4.gif
-rw-r--r--   1 rosas    user         477 May 16 13:46 fig.tcP2.gif
-rw-r--r--   1 rosas    user         504 May 16 13:51 fig.tcP3.gif
-rw-r--r--   1 rosas    user         529 May 16 14:31 fig.tcP5.gif
-rw-r--r--   1 rosas    user         730 Mar 25 01:12 fig.trans.gif
-rw-r--r--   1 rosas    user       13780 May 16 22:50 tb1P2.wrl
-rw-r--r--   1 rosas    user       14814 Jun 13 10:47 tb1P4.wrl
-rw-r--r--   1 rosas    user       15871 Jun 13 10:49 tb1P5.wrl
-rw-r--r--   1 rosas    user       15969 May 16 21:42 tb1PW5.wrl
-rw-r--r--   1 rosas    user       13732 May 16 22:53 tb2P2.wrl
-rw-r--r--   1 rosas    user       14881 Jun 13 10:50 tb2P4.wrl
-rw-r--r--   1 rosas    user       15844 Jun 13 10:50 tb2P5.wrl
-rw-r--r--   1 rosas    user       15815 May 16 21:43 tb2PW5.wrl
-rw-r--r--   1 rosas    user       14900 May 16 21:36 tbPW3.wrl
-rw-r--r--   1 rosas    user       13678 May 16 22:42 tbc1P2.wrl
-rw-r--r--   1 rosas    user       14853 May 16 23:00 tbc1P4.wrl
-rw-r--r--   1 rosas    user       13697 May 16 22:41 tbc2P2.wrl
-rw-r--r--   1 rosas    user       14857 Jun 13 10:52 tbc2P4.wrl
-rw-r--r--   1 rosas    user       15826 Jun 13 10:53 tbcP5.wrl
-rw-r--r--   1 rosas    user       14841 Jun 13 10:54 tc1P4.wrl
-rw-r--r--   1 rosas    user       14813 Jun 13 10:57 tc2P4.wrl
-rw-r--r--   1 rosas    user       13635 May 16 22:54 tcP2.wrl
-rw-r--r--   1 rosas    user       14910 May 16 22:57 tcP3.wrl
-rw-r--r--   1 rosas    user       15871 Jun 13 10:56 tcP5.wrl

dissertation/phosphacinium/MOD:
total 2564
-rw-r--r--   1 rosas    user      117723 Jun 17 11:05 CisMeDioxTotGas.out
-rw-r--r--   1 rosas    user      127314 Jun 17 11:06 CisMedioxTotWat.out
-rw-r--r--   1 rosas    user      157966 Jun 17 11:05 DiMeTotGas.out
-rw-r--r--   1 rosas    user      234647 Jun 17 11:06 DiMetotalWat.out
-rw-r--r--   1 rosas    user      120205 Jun 17 11:05 DioxTotGas.out
-rw-r--r--   1 rosas    user      208927 Jun 17 11:06 DioxTotWat.out
-rw-r--r--   1 rosas    user      173618 Jun 17 11:05 TransMeDioxTotGas.out
-rw-r--r--   1 rosas    user      170490 Jun 17 11:06 TransMeDioxTotWat.out

dissertation/phosphacinium/MOL:
total 139
-rw-r--r--   1 rosas    user        2019 May 27 13:56 bb1PW2.mol
-rw-r--r--   1 rosas    user        2223 May 27 13:56 bb1PW4.mol
-rw-r--r--   1 rosas    user        2019 May 27 13:56 bb2PW2.mol
-rw-r--r--   1 rosas    user        2223 May 27 13:56 bb2PW4.mol
-rw-r--r--   1 rosas    user        2222 May 27 13:56 bbPW3.mol
-rw-r--r--   1 rosas    user        2018 May 27 13:56 bc1P2.mol
-rw-r--r--   1 rosas    user        2019 May 27 13:56 bc1PW2.mol
-rw-r--r--   1 rosas    user        2223 May 27 13:56 bc1PW3.mol
```

```
-rw-r--r--   1 rosas    user        2223 May 27 13:56 bc1PW4.mol
-rw-r--r--   1 rosas    user        2018 May 27 13:56 bc2P2.mol
-rw-r--r--   1 rosas    user        2019 May 27 13:56 bc2PW2.mol
-rw-r--r--   1 rosas    user        2223 May 27 13:56 bc2PW3.mol
-rw-r--r--   1 rosas    user        2223 May 27 13:56 bc2PW4.mol
-rw-r--r--   1 rosas    user        2221 May 27 13:56 bcP3.mol
-rw-r--r--   1 rosas    user        2221 May 27 13:56 bcP4.mol
-rw-r--r--   1 rosas    user        2018 May 27 13:56 tb1P2.mol
-rw-r--r--   1 rosas    user        2222 May 27 13:56 tb1P4.mol
-rw-r--r--   1 rosas    user        2427 May 27 13:56 tb1PW5.mol
-rw-r--r--   1 rosas    user        2018 May 27 13:56 tb2P2.mol
-rw-r--r--   1 rosas    user        2222 May 27 13:56 tb2P4.mol
-rw-r--r--   1 rosas    user        2427 May 27 13:56 tb2PW5.mol
-rw-r--r--   1 rosas    user        2222 May 27 13:56 tbPW3.mol
-rw-r--r--   1 rosas    user        2019 May 27 13:56 tbc1P2.mol
-rw-r--r--   1 rosas    user        2019 May 27 13:56 tbc2P2.mol
-rw-r--r--   1 rosas    user        2223 May 27 13:56 tbc2P4.mol
-rw-r--r--   1 rosas    user        2222 May 27 13:56 tbcP4.mol
-rw-r--r--   1 rosas    user        2222 May 27 13:56 tc1P4.mol
-rw-r--r--   1 rosas    user        2222 May 27 13:56 tc2P4.mol
-rw-r--r--   1 rosas    user        2017 May 27 13:56 tcP2.mol
-rw-r--r--   1 rosas    user        2221 May 27 13:56 tcP3.mol

dissertation/phosphacinium/PDB:
total 285
-rw-r--r--   1 rosas    user        3508 May 16 15:56 bb1PW2.pdb
-rw-r--r--   1 rosas    user        3823 May 16 21:17 bb1PW4.pdb
-rw-r--r--   1 rosas    user        3508 May 16 15:57 bb2PW2.pdb
-rw-r--r--   1 rosas    user        3823 May 16 21:18 bb2PW4.pdb
-rw-r--r--   1 rosas    user        3823 May 16 21:16 bbPW3.pdb
-rw-r--r--   1 rosas    user        3508 May 16 21:51 bc1P2.pdb
-rw-r--r--   1 rosas    user        4138 Jun 12 15:32 bc1P5.pdb
-rw-r--r--   1 rosas    user        3508 May 16 15:58 bc1PW2.pdb
-rw-r--r--   1 rosas    user        3823 May 16 21:15 bc1PW3.pdb
-rw-r--r--   1 rosas    user        3823 May 16 21:18 bc1PW4.pdb
-rw-r--r--   1 rosas    user        3508 May 16 21:51 bc2P2.pdb
-rw-r--r--   1 rosas    user        4138 Jun 12 15:32 bc2P5.pdb
-rw-r--r--   1 rosas    user        3508 May 16 15:58 bc2PW2.pdb
-rw-r--r--   1 rosas    user        3823 May 16 21:16 bc2PW3.pdb
-rw-r--r--   1 rosas    user        3823 May 16 21:19 bc2PW4.pdb
-rw-r--r--   1 rosas    user        3823 May 16 21:56 bcP3.pdb
-rw-r--r--   1 rosas    user        3823 May 16 21:58 bcP4.pdb
-rw-r--r--   1 rosas    user        3508 May 16 21:54 tb1P2.pdb
-rw-r--r--   1 rosas    user        3823 May 16 22:03 tb1P4.pdb
-rw-r--r--   1 rosas    user        4138 Jun 12 15:32 tb1P5.pdb
-rw-r--r--   1 rosas    user        4138 May 16 21:20 tb1PW5.pdb
-rw-r--r--   1 rosas    user        3508 May 16 21:53 tb2P2.pdb
-rw-r--r--   1 rosas    user        3823 May 16 22:05 tb2P4.pdb
-rw-r--r--   1 rosas    user        4138 Jun 12 15:32 tb2P5.pdb
-rw-r--r--   1 rosas    user        4138 May 16 21:20 tb2PW5.pdb
-rw-r--r--   1 rosas    user        3823 May 16 21:15 tbPW3.pdb
-rw-r--r--   1 rosas    user        3508 May 16 21:52 tbc1P2.pdb
-rw-r--r--   1 rosas    user        3508 May 16 21:52 tbc2P2.pdb
-rw-r--r--   1 rosas    user        3823 May 16 22:03 tbc2P4.pdb
-rw-r--r--   1 rosas    user        3823 May 16 21:57 tbcP4.pdb
-rw-r--r--   1 rosas    user        4138 Jun 12 15:33 tbcP5.pdb
-rw-r--r--   1 rosas    user        3823 May 16 21:59 tc1P4.pdb
-rw-r--r--   1 rosas    user        4138 Jun 12 15:31 tc1P5.pdb
-rw-r--r--   1 rosas    user        3823 May 16 22:04 tc2P4.pdb
-rw-r--r--   1 rosas    user        3508 May 16 21:55 tcP2.pdb
-rw-r--r--   1 rosas    user        3823 May 16 21:56 tcP3.pdb

dissertation/reviews:
total 105
-rw-r--r--   1 rosas    user         573 Feb 21 00:20 fig.2266dioxo.gif
-rw-r--r--   1 rosas    user         516 Feb 21 00:20 fig.22dioxo.gif
-rw-r--r--   1 rosas    user         530 Feb 21 00:20 fig.66dioxo.gif
-rw-r--r--   1 rosas    user         740 Mar 15 01:07 fig.HAC.gif
-rw-r--r--   1 rosas    user         595 Feb 26 01:18 fig.aminocarn.gif
-rw-r--r--   1 rosas    user         842 Feb 26 01:56 fig.anderson951.gif
-rw-r--r--   1 rosas    user         980 May 14 10:02 fig.anderson952.gif
-rw-r--r--   1 rosas    user        1774 Mar  4 15:45 fig.anomeric.gif
-rw-r--r--   1 rosas    user        2302 Feb 10 16:10 fig.b.gif
-rw-r--r--   1 rosas    user        2486 Feb 10 16:09 fig.bb.gif
-rw-r--r--   1 rosas    user        2304 Feb 10 16:09 fig.bc.gif
-rw-r--r--   1 rosas    user        2416 Feb 10 16:10 fig.c.gif
-rw-r--r--   1 rosas    user        2539 Feb 10 16:10 fig.cc.gif
-rw-r--r--   1 rosas    user        3852 Mar  3 14:56 fig.crown.gif
-rw-r--r--   1 rosas    user         411 May 14 11:36 fig.dioxo.gif
-rw-r--r--   1 rosas    user        2362 Feb 23 00:42 fig.fritz63.gif
-rw-r--r--   1 rosas    user        1231 May 22 14:09 fig.gandour93.gif
```

```
-rw-r--r--    1 rosas    user         2714 Apr 15 11:30 fig.hydrolysis2.gif
-rw-r--r--    1 rosas    user          743 May 14 10:00 fig.kumaravel94.gif
-rw-r--r--    1 rosas    user          414 May 14 11:35 fig.oxo.gif
-rw-r--r--    1 rosas    user          581 Feb 26 01:21 fig.saeed93.gif
-rw-r--r--    1 rosas    user          585 Mar  4 16:39 fig.saeed94.gif
-rw-r--r--    1 rosas    user         1157 Apr 15 10:24 fig.sun95.gif
-rw-r--r--    1 rosas    user         2426 Feb 10 16:11 fig.tb.gif
-rw-r--r--    1 rosas    user         2601 Feb 10 16:20 fig.tbc-1.gif
-rw-r--r--    1 rosas    user         2639 Feb 10 16:10 fig.tbc1.gif
-rw-r--r--    1 rosas    user         2500 Feb 10 16:11 fig.tc.gif
-rw-r--r--    1 rosas    user         2446 Feb 10 16:11 fig.tcc.gif
-rw-r--r--    1 rosas    user          432 May 14 11:34 fig.tetraoxo.gif
-rw-r--r--    1 rosas    user          420 May 14 11:36 fig.trioxo.gif
```

Víctor was born in Monterrey, México, on February 24th, 1969. Due to his father's job, the family alternated residence between Monterrey and México City, to finally settle down in Monterrey. There Víctor pursued his B.S. in Industrial Chemistry at UANL and, after graduation, held his first job as a Quality Control chemist. Having decided that his chemical skills required (substantial) polishing, he joined the PhD program at Louisiana State University in Baton Rouge, LA. At LSU he joined Professor Gandour's research group, while thoroughly enjoying the Cajun and Creole heritage of the land (Mardi Gras included). Little he suspected that he would later be transferring to Virginia Tech, following his advisor. While at Virginia Tech, he decided that computers were fun and chemistry was fun so putting them together would be fun[2]. Thus he turned his interests to Computational Chemistry, to finally get his Ph.D. as a Computational Bioorganic Chemist.